University of South-Eastern Norway

Nima Janatian

Real-time Optimization and Control for Oil Production under Uncertainty

Dissertation for the degree of Ph.D
Process, Energy and Automation

Faculty of Technology, Natural Sciences and Maritime Studies

University of
South-Eastern Norway

Nima Janatian

Real-time Optimization and Control for Oil Production under Uncertainty

A PhD dissertation in
Process, Energy and Automation Engineering

Faculty of Technology, Natural Sciences and Maritime Studies
University of South-Eastern Norway
Porsgrunn

Doctoral dissertations at the University of South-Eastern Norway no. 179

ISSN: 2535-5244 (print)
ISSN: 2535-5252 (online)

ISBN: 978-82-7206-822-5 (print)
ISBN: 978-82-7206-823-2 (online)

Print: University of South-Eastern Norway

"There are no solutions. There are only trade-offs."

Thomas Sowell, *A Conflict of Visions: Ideological Origins of Political Struggles*

Preface

"This thesis is submitted as a partial fulfillment of the requirements for the degree of Philosophiae Doctor (PhD) at the University of South-Eastern Norway (USN). It encapsulates my three-year journey of research, exploration, and collaboration aimed at contributing to the field of dynamic optimization under uncertainty."

This endeavor was undertaken as part of a larger project (Project Number: 308817), "Digital wells for optimal production and drainage - DigiWell," funded by The Norwegian Research Council, Equinor ASA, and USN. DigiWell involved a collaborative effort of several researchers from reputable academic and industrial institutions, aiming to develop new methods, algorithms, and tools for oil production with maximized profit and minimum energy consumption under uncertain information.

My doctoral research within the DigiWell project has been devoted to addressing the complex challenge of short-term optimization for oil production under the presence of uncertainty. On a broader scale, I was eager to participate in the ongoing research trend of addressing the challenges of dynamic optimization under uncertainty, a domain that has yet to realize its full potential in practical applications.

The PhD research was carried out at the Department of Electrical Engineering, Information Technology and Cybernetics at USN in the period from September 2020 to September 2023. Beyond the academic and research aspects, this journey has provided me with opportunities for personal and professional growth. The collaborative environment within the Norwegian research community and the supportive atmosphere at USN have been instrumental throughout this endeavor.

Porsgrunn, 12th October 2023
Nima Janatian

Acknowledgments

I extend my deepest gratitude to all those who have played pivotal roles in my doctoral journey. First and foremost, I would like to express my profound appreciation to my main supervisor, Associate Professor Roshan Sharma, for taking me on as his PhD student and granting me the opportunity to explore this incredible journey. His guidance, expertise, and patience have been invaluable throughout this research endeavor, and his trust in my capabilities provided me with the necessary confidence to make mistakes and learn from them. Beyond academic guidance, I have acquired critical thinking and problem-solving skills under his mentorship. I consider myself fortunate to have had Roshan by my side, guiding me and shaping my path.

I would also like to express my sincere gratitude to my co-supervisor, Professor Carlos Pfeiffer, for his valuable support, guidance, and his willingness to provide assistance throughout this research journey. My thanks extend to Professor Bernt Lie, the project leader of DigiWell and several other projects. His well-established reputation among the industrial communities in Telemark, along with his active role in leading industry-oriented projects, has provided priceless opportunities for the growth and development of the young generations, including me, at USN over the years. I also gratefully acknowledge the financial support from DigiWell, which is financed by the Research Council of Norway, Equinor ASA, and USN.

I have been fortunate to have had the privilege of working alongside several dedicated and knowledgeable researchers and engineers in DigiWell. I would like to express my gratitude to Robert Aasheim and Kjetil Fjalestad from Equinor for the insights they shared through several fruitful discussions we have had during our status meetings. Their extensive experience in the oil production industry and their patience in answering even the simplest questions were invaluable in building my understanding of oil production processes and short-term optimization. I also heartfully appreciate Stein Krogstad from Sintef for introducing me to reservoir modeling and simulation and guiding me through The MATLAB Reservoir Simulation Toolbox (MRST). His character, alongside his profound knowledge and expertise, was a source of inspiration for me throughout our collaboration.

The acknowledgments would not be complete without mentioning my friends, who have set the bar high in terms of what I expect from friendship. In addition to long-standing friends that have been spread all over the world, I made new ones here in Norway who

have touched my life in various ways. I refrain from naming individuals as the list can extend indefinitely, but their contributions to my character are undeniable.

Finally, I must acknowledge my family for their unconditional love, support, and encouragement throughout my entire life, although words cannot fully convey my sincere and heartfelt gratitude and appreciation. I am always indebted to them, especially to my sister Nasim, who has consistently provided support during various chapters of my life and lent an open ear for sharing moments of both joy and despair. Last but not least, I am deeply thankful to Mercedeh, who has enriched my life with her love and her remarkable ability to brighten my days with her presence.

Summary

The practical use of model-based optimization depends significantly on the accuracy of the model in use. This is because the presence of uncertainty can introduce a mismatch between the model and the real plant, which may eventually lead to suboptimal or even infeasible solutions due to constraint violations in cases where fulfillment of the constraints is strictly required.

The existing robust methods for addressing the presence of uncertainty are known to be overly conservative, meaning they sacrifice optimality to a relatively great extent in order to achieve robustness. This is not ideal because the conservativeness or sacrifice of optimality implies the optimization has not been exploited to its full potential. Therefore, besides the complexity of the robust methods, the trade-off between optimality and robustness is a main challenge for this category of methods. On the other hand, the other approaches for reducing conservativeness can potentially lead to constraint violation, at least temporarily, meaning that the robust characteristics will be lost.

Accordingly, this thesis covers real-time optimization and control strategies tailored for short-term oil production processes, addressing the challenges imposed by the presence of uncertainty. Particularly, the research has been devoted to investigating the applicability of the existing methods for short-term oil production optimization under uncertainty and a further improvement in the existing method in order to reduce the conservativeness without losing the robust fulfillment of constraint and imposing extra computational complexity to the methods.

Two oil production methods, namely gas lift and electrical submersible pump lifting method, have been taken into account as case studies. The research mostly leaned toward the dynamic optimization formulated for short-term production from gas lift oil fields. The well-established methods within the domain of robust model predictive control, as well as an adaptive MPC framework with moving horizon estimation, have been investigated thoroughly. The knowledge acquired in these investigations is further employed to propose a robust method within the robust category that decreases the conservativeness without imposing extra complexity and losing the robustness. This has been done particularly by using the output error in directly modifying the boundaries of the active constraints.

The dynamic formulation for the second case study, the ESP-lifted field, is proven to be challenging even in the deterministic case. Therefore, the scenario-based framework is

used along with the steady-state model to formulate the robust approach for the ESP-lifted system. The use of the steady-state model enabled us to consider a longer horizon and assess the effect of uncertainty in the oil price as well as the uncertainty in the well parameters. The results demonstrated that the uncertainty in the oil price is not influential over the short-term horizon.

In summary, this thesis provides a comprehensive insight into the challenges associated with real-time optimization and control under uncertainty in the domain of short-term oil production. The research outcomes collectively emphasize the importance of accounting for uncertainty within the oil well characteristics. The thesis also offers insights into methods that can enhance efficiency, robustness, and operational safety in oil production processes.

Contents

List of Figures

List of Tables

Nomenclature

Acronyms	**Explanation**
DAE	Differential and Algebraic Equations
DMC	Dynamic Matrix Control
DPO	Daily Production Optimization
DRTO	Dynamic Real-Time Optimization
ESP	Electrical Submersible Pump
GPC	Generalized Predictive Control
LQR	Linear Quadratic Regulator
MAC	Model Algorithmic Control
MHE	Moving Horizon Estimation
MIMO	Multi-Input Multi-Output
MINLP	Mixed Integer Nonlinear Programming
MPC	Model Predictive Control
NPV	Net Present Value
ODE	Ordinary Differential Equation
OCP	Optimal Control Problem
PLC	Programmable Logic Controller
QDMC	Quadratic Dynamic Matrix Control
QP	Quadratic Programming
RTO	Real-Time Optimization
SISO	Single-Input Single-Output
SMPC	Stochastic Model Predictive Control
SQP	Sequential Quadratic Programming
SRTO	Steady-state Real-Time Optimization
TES	Total Energy Supply
VSD	Variable Speed Drive

Symbols	**Explanation**
A_{a}	Annulus cross-section area
A_{t}	Tubing cross-section area
C_v	Valve opening characteristic
f	Frequency of ESP
H_{esp}	Head developed by ESP
$L_{\mathrm{a\_tl}}$	Total length of annulus

$L_{\text{a\_vl}}$	Vertical length of annulus
$L_{\text{t\_tl}}$	Total length of tubing above injection point
$L_{\text{t\_vl}}$	Vertical length of tubing above injection point
$L_{\text{r\_vl}}$	Vertical length of tubing below injection point
m_{ga}	Mass of lift gas in annulus
m_{gt}	Mass of gas in the tubing above the injection point
m_{lt}	Mass of liquid in the tubing above the injection point
M	Molar mass
p_{a}	Pressure of gas in annulus downstream the gas lift choke valve
p_{ainj}	Pressure upstream of the gas injection valve in the annulus
p_{tinj}	Pressure downstream of the gas injection valve in the tubing
p_{m}	Gathering manifold pressure
p_{bh}	Bottomhole pressure
p_{wh}	Wellhead pressure
p_{r}	Reservoir pressure
q_l	Average volumetric flow rate in the well
q_{tr}	Average volumetric flow rate in transportation line
q_r	Volumetric flow rate from reservoir into well
q_c	Volumetric flow rate through production choke valve
q_o	Volumetric flow rate of total produced oil
q_w	Volumetric flow rate of total produced water
w_{ga}	Mass flow rate of gas injected into annulus
w_{ginj}	Mass flow rate of gas injected from annulus into tubing
w_{gr}	Mass flow rate of gas from reservoir into well
w_{gp}	Mass flow rate of gas phase through production choke valve
w_{lr}	Mass flow rate of liquid from reservoir into well
w_{lp}	Mass flow rate of liquid phase through production choke valve
w_{glp}	Total mass flow rate through the production choke valve
PI	Productivity index
WC	Water cut
GOR	Gas to oil ratio
BHP_{esp}	ESP brake horsepower
β	Bulk modulus of the reservoir fluid
Δp_f	Frictional pressure drop in the pipe
Δp_{bp}	Pressure gradient by booster pump
ρ_{w}	Density of water
ρ_{o}	Density of oil
ρ_{ga}	Average density of gas in the annulus
ρ_{m}	Density of multiphase mixture in tubing above injection point
ρ_{l}	Average density of the liquid phase
ρ_{tr}	Density of the fluid in transportation line

1 Introduction

1.1 Background

In a world with ever-increasing demand for energy and limited available resources, it is crucial to manage and plan resources in an efficient manner to obtain as much as possible from a given resource. In this sense, mathematical optimization is a powerful tool that can utilize the mathematical representation of the system (which is known as *model*) to maximize the benefits or minimize the costs. However, a key challenge in this endeavor is that in real-life scenarios, perfect knowledge of the system model does not exist. Therefore, the uncertainty is essential to be considered. This becomes even more important and also more challenging when considering that processes are under a wide variety of constraints arising from operating conditions, product specifications, and safety limits. Accordingly, optimization under uncertainty is a growing field that has attracted much attention in recent years. There are, however, significant challenges in implementing many of these approaches. Some methods are overly conservative, which means they sacrifice optimality to satisfy the constraints under the uncertainty, while others are computationally extremely expensive. Nonlinearity in system dynamics and scaling for large problems are the other challenges, to name a few. A detailed review of different approaches for optimization under uncertainty and their strengths and weaknesses are given in Section 3.1.

According to data from the International Energy Agency [1], as depicted in Figure 1.1, oil still remained the predominant source in the global and European total energy supply. This substantial contribution to the total energy supply boosts the significance of optimization in the oil industry because, in such a large-scale business, even minor improvements in efficiency can have significant impacts. Consequently, engineers and researchers put considerable effort into extracting the last droplets of oil from the reservoir and also into minimizing the cost of reaching this goal. However, oil production is not exempt from the difficulties associated with implementing model-based optimization. The unavoidable forms of uncertainty linked to oil production, alongside the critical importance of safety and operational constraints, make optimization under uncertainty a highly relevant topic for oil production. Therefore, this thesis is focused on the application of optimization under uncertainty for oil production.

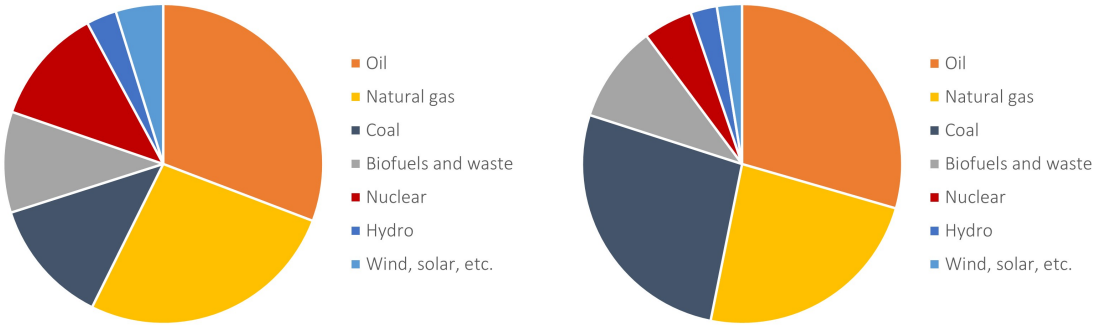

(a) Europe (b) World

Figure 1.1: Total energy supply (TES) by source 2020.

1.2 Optimization in Oil Industry

Developing an oil field asset requires scheduling and making several decisions, which makes it a perfect application for mathematical optimization. However, these decisions should be taken over different horizons that span an extremely wide range of time, from seconds to many years. In addition to extreme differences between time horizons, these decisions are expected to be taken in order to follow different objectives, which may even be conflicting. Hence, it is prohibitively challenging, if not impossible, to define a universal optimization problem that encompasses all the different objectives over all the different horizons.

Instead, it is widespread in the process control community to organize the decisions in a multi-level control hierarchy. This hierarchical structure consists of different decision-making layers with different time scales that separate various objectives according to their relevant time scale and enable the appropriate decisions to be taken to optimize the corresponding objective. The flow of information in these hierarchies is such that the upper layers provide setpoints to the layer beneath, while the lower layers report any difficulties encountered in achieving these targets, as detailed in [2] under the title of *plantwide control*.

Figure 1.2 illustrates the control hierarchy within the oil industry, adopted from [3]. Within this framework, most of the decisions made for licensing, exploration, development, and decommissioning are classified as *Asset Management* decisions. The impact of these decisions is noticeable over the lifetime of the field, and the required data to make these decisions takes several months to acquire.

The *Reservoir Management* layer corresponds to the long-term horizon, ranges from several months to a couple of years, and mainly aims to improve the field recovery factor. The decisions such as water and gas injection into the reservoir for pressure support, production policies, and the exact location of new wells to be drilled are classified within

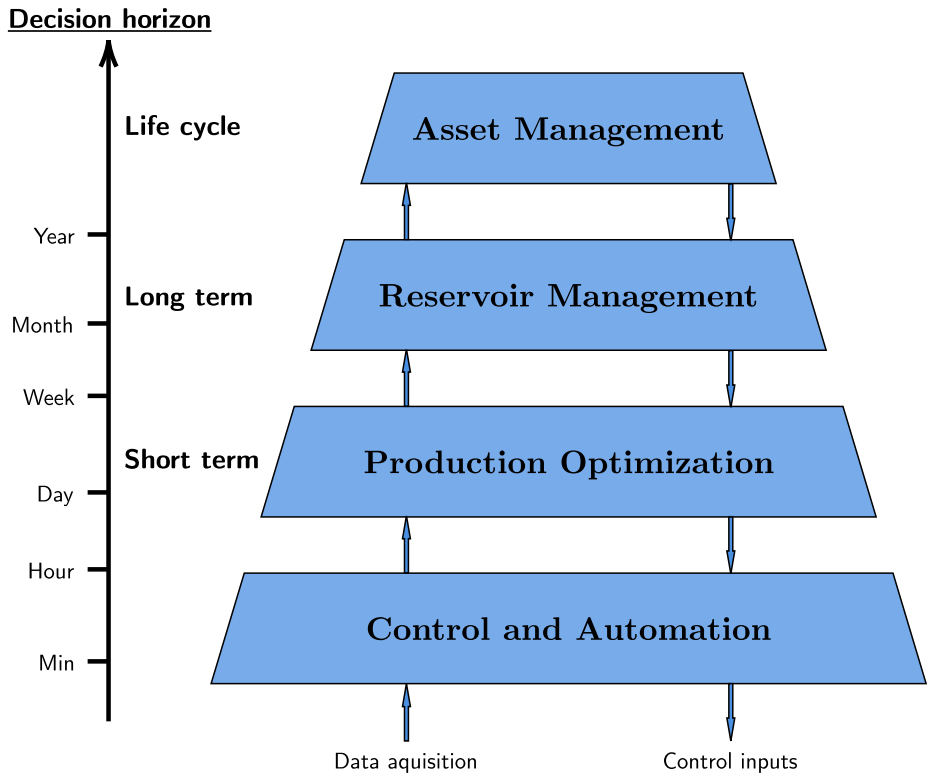

Figure 1.2: Multi-level control hierarchy in oil industry.

this category. As the title of reservoir management suggests, the dynamic of the reservoir plays a crucial role in these decisions, whereas the well response is assumed to be immediate as its dynamic is significantly faster than the reservoir.

Production Optimization or *Real-time Optimization* which is the main focus of this thesis, corresponds to decisions and objectives with short-term horizons ranging from a couple of hours to a week. The decisions such as well-separator routing configurations, controller tunings, and facilities operational set-points are classified within this decision-making layer, and their main goal is to optimize the utilization of the facilities; see [4] for a comprehensive review. The decision-making tools for real-time production optimization often rely on well models and consider capacity constraints of the surface facilities while disregarding the reservoir dynamics because its dynamics are too slow within this horizon and can be considered constant.

The *Control and Automation* layer primarily deals with regulatory tasks, such as keeping a stable operation, tracking setpoints, damping oscillations, and rejecting disturbances. The required decisions must be taken within the fastest time scale spanning from seconds to hours. This layer is also equipped with emergency shutdown mechanisms to prevent operations in unsafe conditions.

The aforementioned hierarchical structure with different time scales allows skipping the overwhelming computational challenges of the joint-model optimization approach by tackling each problem separately and simplifying the other problems in different time scales, as the different time scales are usually associated with different physical components of the process. In this way, when solving a short-term oil production optimization problem, the decision support tools may use an appropriate model of the well while the other parts of the process with different time scales are lumped into simplified algebraic equations or constraints.

1.3 Research Objectives and Scope

The wide range of ongoing difficulties for modeling, simulation, and optimization of short-term oil production under uncertainty is the primary motivation behind this research work. The reviewed literature in Chapter 3 exhibits a vital knowledge gap in the area of real-time optimization for short-term oil production under the presence of uncertainty, whereas long-term production optimization under uncertainty has been studied extensively. So, this research particularly aims to address this knowledge gap by extending the previous work [5] done at the Telemark University College (now USN) and explicitly handling the uncertainty in short-term oil production optimization. In a broad context, the purpose of this research is to make a contribution to the field of optimization under uncertainty by investigating the well-established approaches of optimization under uncertainty and the potential for enhancing them. Within the given context, the overarching research question can be formulated as:

> *How can short-term production optimization in the oil industry be effectively managed while the uncertainty is also taken into account?*

This primary research question is too broad and complex to answer; therefore, it is further decomposed into three smaller and more manageable research questions encompassing three different aspects of the problem. To be more specific, three research questions that arise in this regard and required to be addressed are outlined as follows:

1. *How to develop or improve the existing simple mechanistic models of short-term oil production suitable for use in real-time optimization?*
   An appropriate answer to this question requires an understanding of the oil production mechanisms. It should be clearly known what is the difference between short-term and long-term oil production and which physical components of an oil production system are relevant in order to develop a model for short-term production. Furthermore, the developed model is required to be accurate to capture the dynamics of the process, while it should also be simple to be used in optimization and control. This question has been pursued in papers A, E, and F.

2. *How to identify the source of uncertainty in the model and the optimization problem?*
   The uncertainty can appear in the optimization problem in various forms, such as the physical parameters of the production model or the uncertainty in the oil market. The importance of this question arises from the fact that the presence of uncertainty in an optimization problem becomes challenging when the effect of uncertainty is significant. Otherwise, it can be simply overlooked if the uncertainty has no effect on the objective function or constraints. Therefore, it is crucial not only to identify which parameters include uncertainty but also it is important to realize which parameters should be considered to contain uncertainty and which parameters have no/less effect and can be neglected. This question has been pursued in papers A and E.

3. *How to formulate the real-time optimization problem for short-term oil production under the presence of uncertainty to achieve optimal profitability and fulfillment of the constraints?*
   This question probably captures the most fundamental essence of the previously mentioned overarching research question, and it has been the subject of investigation in papers B, C, D, E, and F. To address this question, one must grasp the distinction between steady-state and dynamic real-time optimization. Additionally, a thorough comprehension of the current methodologies for handling the presence of uncertainty in the optimization problem is required. The challenges, strengths, and weaknesses of the methods should be clearly understood in order to identify the potential for these methods for further improvement or developing a novel method.

Therefore, the scope of this research work is limited to *Short-term Production Optimization*, meaning that it exclusively focuses on the models, objectives, decisions, and constraints that are within the short-term horizons. Although the term "*short-term*" may occasionally be omitted for simplicity, it should be noted that throughout this thesis, production optimization always refers to short-term production unless otherwise specified. Comprehensive and detailed information about short-term production optimization is presented further in Chapter 2. Nevertheless, to clarify the boundaries of the considered problem in this thesis, it is worthwhile to mention that mathematical models of the production wells and surface constraints are the most relevant ingredients within the domain of short-term production optimization, whereas the reservoir dynamic (which has time scales of months), long-term objectives (such as the net present value), and decisions (such as injection into the reservoir) that fall under the subject of reservoir management are beyond the scope of this thesis.

Moreover, this study solely concentrates on production wells with two artificial lifting methods, namely the gas lift and the Electrical Submersible Pump lifting methods. These production mechanisms are explained thoroughly in the process description provided in Chapter 2. Furthermore, among the different approaches for handling the uncertainty in the optimization problem, which are comprehensively reviewed in Chapter 3, this thesis

only considers the robust and adaptive approaches. Finally, the last point of distinction lies in the choice between utilizing either a dynamic or steady-state model of the wells for optimization. While both steady-state and dynamic models are utilized in this thesis, the primary emphasis during the research is placed on dynamic optimization under uncertainty.

The aforementioned research questions are pursued and investigated in different papers generated during this study. Each paper corresponds to one or more research questions. This correspondence and the scope of each paper are summarized in Table 1.2.

Table 1.2: Scope of the resulted papers and their contribution to research questions.

Paper	Lift Method	Approach	Model	Research Questions
A	Gas Lift	Deterministic	Dynamic	1 & 2
B	Gas Lift	Robust	Dynamic	3
C	Gas Lift	Adaptive	Dynamic	3
D	Gas Lift	Robust	Dynamic	3
E	ESP Lift	Robust	Steady State	1 & 2 & 3
F	ESP Lift	Robust	Steady State	1 & 3

1.4 Challenges and Contributions

In the domain of optimization under uncertainty, the critical scientific challenges revolve around achieving robust performance, required computational expenses, and ensuring stability. Although none of these challenges are inherently more important than the others, this research solely makes contributions to the first two challenges. This is because the first two challenges are mostly associated with the practical implementation aspects of the methods and are more in line with the ultimate goal of the project, while the third challenge predominantly deals with theoretical aspects, such as the establishment of mathematical proofs for closed-loop stability.

The challenge of robust performance arises from the fact that under the presence of uncertainty, the constraints in the optimization problem may be violated due to the mismatch between the prediction model and the real process. On the other hand, the methods for ensuring robust fulfillment of the constraints are inherently conservative, meaning they sacrifice optimality in order to achieve robustness. The conflicting relationship between the robustness and conservativeness of the methods is a big challenge for industrial processes. Moreover, these methods are typically complex, and their computational costs for real-time implementation are prohibitively high, which highlights the second challenge. This challenge becomes more severe in the case of dynamic optimization, while steady-state optimizations typically have less computational cost. This study addresses

these two challenges by investigating the established methods of real-time optimization under uncertainty with application to short-term oil production and then by improving the existing methods to be applicable to the considered case study.

A particularly novel aspect of this project is to improve the existing robust method for handling the uncertainty in dynamic optimization, which reduces the conservativeness significantly while not imposing extra complexity on the existing method. Although this has been developed based on the special characteristics of a specific case study, it can be easily generalized to be applicable to a class of systems with the same features. Accordingly, the other contributions of this work include:

- Minor improvements in modeling for the artificial lifting oil field to be suitable for use in real-time optimization problems.
- Describing the major sources of uncertainties with such simplified models and handling these uncertainties during real-time optimization.
- Extensive investigation of the existing frameworks and methods to find an implementable solution for online optimization under the presence of uncertainty.
- Improve the existing robust method for dynamic optimization under uncertainty without imposing extra complexity.

1.5 List of Publications

Throughout the research period, a total of six articles were written as follows. Out of these, five articles have been published in peer-reviewed journals and conference proceedings, while one article has been submitted to a journal and is currently under review.

- **Paper A: Model based control and analysis of gas lifted oil field for optimal operation.**
  Published in *Proceeding of The First SIMS EUROSIM Conference on Modelling and Simulation, SIMS EUROSIM 2021, and 62nd International Conference of Scandinavian Simulation Society, SIMS 2021*, September 21-23, Virtual Conference, Finland, 2021.
  Authors: Nima Janatian, Kushila Jayamanne, and Roshan Sharma.
- **Paper B: Multi-stage scenario-based MPC for short term oil production optimization under the presence of uncertainty.**
  Published in *Journal of Process Control*, Volume 118, October 2022.
  Authors: Nima Janatian and Roshan Sharma.

- **Paper C: A reactive approach for real-time optimization of oil production under uncertainty.**
  Published in *Proceeding of 2023 American Control Conference (ACC)*, May 31 - June 2, San Diego, CA, USA, 2023.
  Authors: Nima Janatian and Roshan Sharma.

- **Paper D: A robust model predictive control with constraint modification for gas lift allocation optimization.**
  Published in *Journal of Process Control*, Volume 128, August 2023.
  Authors: Nima Janatian and Roshan Sharma.

- **Paper E: Short-term production optimization for Electric Submersible Pump lifted oil field with parametric uncertainty.**
  Published in *IEEE Access*, Volume 11, September 2023.
  Authors: Nima Janatian and Roshan Sharma.

- **Paper F: Investigating the performance of robust daily production optimization against a coupled well–reservoir model.**
  Submitted to *Modeling, Identification and Control*, October 2023.
  Authors: Nima Janatian, Stein Krogstad, and Roshan Sharma.

1.6 Outline of Thesis

The outcomes of this research are published in six peer-reviewed scientific papers that are self-contained. The first part of this dissertation, Part I: Synopsis, integrates these independent papers into a unified framework that shows how each paper answers the research questions and contributes to the central objective. The synopsis comprises six chapters:

Chapter 1 provides a brief background to the research, highlighting the pivotal role of optimization in oil production. The research objectives and scope are defined, giving readers a clear understanding of the study's boundaries. Additionally, the inherent challenges and the original contributions offered by this research are outlined, providing a roadmap for the reader.

Chapter 2, deals with the short-term production optimization in the context of the oil industry. The two production mechanisms are chosen as the case studies are introduced, giving the reader a clear understanding of the model, objective function, and the constraints involved in short-term optimization. Furthermore, the chapter introduces the description of uncertainty within this research.

Chapter 3 presents an extensive literature review exploring the different approaches to addressing uncertainty in optimization problems. This exploration includes a review of robust, stochastic, and adaptive optimization approaches. Furthermore, the chapter covers existing modeling and optimization techniques employed specifically within the domain of oil production.

Chapter 4 forms the theoretical foundation of the thesis, elucidating both the established methods and the contributions made during the research. From open-loop optimal control to different robust and adaptive methods, this chapter equips the reader with a comprehensive understanding of the methods supplemented with an illustrative example that compares all the methods in a unified framework.

Chapter 5 provides a summary of the research papers generated throughout the journey. Each paper's motivations, results, and conclusions are encapsulated, presenting a concise yet informative overview of the research's academic contributions and development over the past three years.

Finally, Chapter 6 completes the Synopsis by concluding the findings and their implications. The chapter also looks forward, outlining potential directions for future research within the realm of optimization in oil production under uncertainty.

The subsequent Part II: Scientific Papers, includes the full papers associated with the research, building the backbone of this thesis.

2 Short-term Production Optimization

This chapter provides detailed information about *Short-term Production Optimization* in the oil industry, which has been sometimes referred to as Daily Production Optimization (DPO) or Real-Time Optimization (RTO) as well [6], [7]. It also illustrates the interactions between this decision-making layer and its upper and lower layers according to the hierarchical structure described in Section 1.2. This chapter also introduces the two artificial lift methods that have been studied in this dissertation. These methods include the gas lift method, which has been employed as the case study in papers A, B, C, and D, and the ESP lift method, which has been utilized in papers E and F. The process descriptions for both production methods are then followed by specific considerations of short-term production optimization in the context of that particular production method.

2.1 General Structure of Production Optimization

Like every other mathematical optimization, the main ingredients of production optimization consist of a mathematical model of the process, an objective function, and possibly constraints. However, one must not forget that these models, objectives, and constraints should have time scales ranging from hours to a week. Figure 2.1 illustrates the physical components of a typical petroleum production system, adopted from [6]. These components include producing wells, gathering facilities, manifolds, and transport pipelines.

The specific characteristics of the mathematical model of the well may vary depending on which recovery method is employed for production. This thesis exclusively concentrates on two artificial lifting methods: gas lift and ESP lifting methods. Therefore, comprehensive descriptions of these processes are provided in Sections 2.2 and 2.3, respectively. The optimization problem may be formulated as a steady-state real-time optimization (SRTO) when the steady-state version of the model is utilized in the optimization. While this is the conventional approach in the industry, there are also incentives, at least among the academic community, to frame the problem as a dynamic real-time optimization (DRTO) by using the dynamic version of the model in the optimization problem [8]. Regardless of whether it is a steady-state or dynamic optimization, the optimal decisions are typically passed to a lower-level regulatory controller to be implemented.

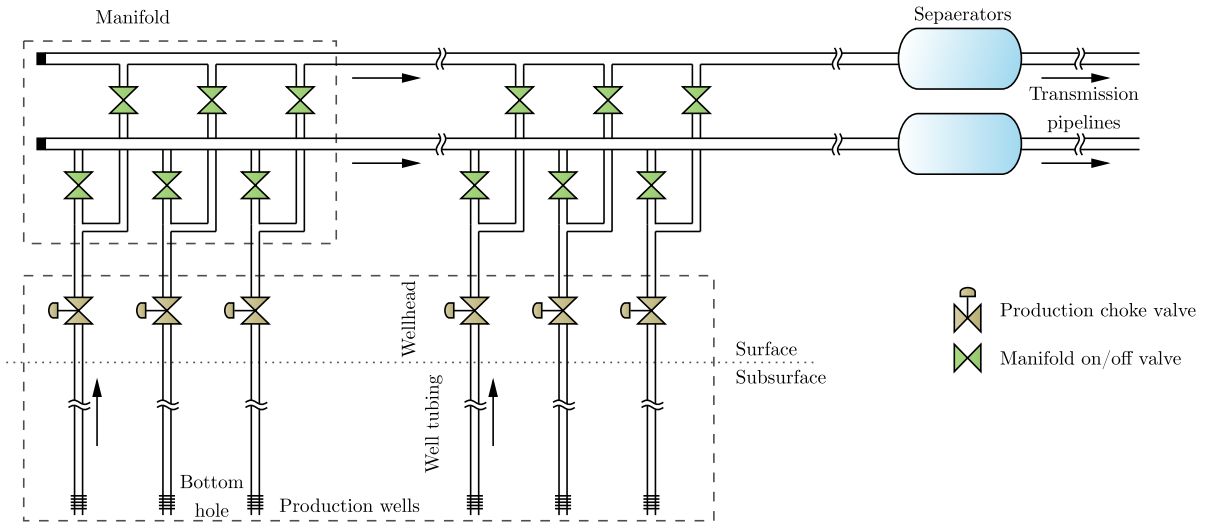

Figure 2.1: A typical petroleum production system.

Once the model is identified, it is essential to establish the objective function. Although the specific formulation of the objective function may vary depending on the situation, a shared characteristic is that it should be relevant over a short-term horizon. This implies that objectives like the net present value (NPV), which are usually meaningful for long-term perspectives, are not suitable in this context. The total production from the field and the economic objective, i.e., the revenue obtained from selling oil subtracted by the operational expenses associated with production, are the two most frequently used objective functions within the short-term horizon. The particular costs that appear in the objective are also determined by the specific production method. For instance, in the gas lifting method that utilizes high-pressure gas for production, the compressor expenses constitute a significant cost, while for the ESP lifting method, the electrical consumption of the pumps is a relevant cost. It is crystal clear that the costs under consideration must be relevant over the short-term horizon. Thus, the costs associated with drilling new wells or injection into the reservoir that are relevant to long-term optimization are excluded. Alternatively, it is also possible to define the objective function as a tracking problem. However, in such scenarios, the higher-level decision-making layer should provide the required total production as a setpoint, while the short-term layer is responsible for allocating the total production among the wells and managing the remaining constraints.

The final component to complete the optimization problem is the constraints. These constraints may vary depending on the production method; however, there are some typical constraints as well. The mathematical model of the production well and network is an apparently necessary constraint that should be included. Capacity constraints are another typical operational constraint, meaning that the amount of fluid entering the

separator must honor the handling capacity of the downstream process facility. Besides, the so-called draw-down constraint is another typical constraint that prevents operation at pressures that potentially can damage the well and near-well reservoir by putting a lower limit on the bottom hole pressure of a well. An insightful overview of the basic structure of short-term production optimization can be found in [6], [9].

2.2 Production Optimization for Gas Lift System

As explained in Section 2.1, the formulation of short-term production optimization is notably influenced by the production method. Therefore, it is crucial to introduce the gas lift production method in order to identify the different specifications of the production optimization. Accordingly, the following Subsection 2.2.1 provides a comprehensive description of the process followed by short-term production optimization for such systems in Subsection 2.2.2.

2.2.1 Process Description

The gas lift mechanism is a widely recognized artificial lifting method employed to increase or revive oil production from a subsurface reservoir. Like other artificial lifting methods, the core idea behind the method is to make use of an external source to decrease the pressure at the bottom hole so the difference between the reservoir pressure and bottom-hole pressure would be enough for the fluid to flow to the surface. In the gas lift method, this can be achieved by injecting the so-called lift gas into the well, resulting in a decrease in the density of the fluid mixture in the well's tubing.

A gas-lifted oil field consists of multiple oil wells that share a common source of lift gas compressed by a compressor at the surface. Schematic representation of different components of a single oil well connected to a gas distribution pipeline has been depicted in Figure 2.2. This lift gas distribution pipeline is a long pipeline utilized for distributing the compressed lift gas among the multiple oil wells connected to it. The lift gas enters into the annulus of each well from the common gas distribution manifold. The flow rate of the lift gas to be injected is controlled by the gas lift choke valve. Subsequently, within the annulus, the high-pressure lift gas is injected into the tubing through the gas injection valve. The injection of the gas into the tubing gives rise to one or more of the following effects to occur [10].

- The injected gas mixes with the multiphase fluid (crude oil, water, and gas produced from the reservoir) at the injection point in the tubing. Due to aeration, the average density of the mixture of the liquid and the gas is reduced. Consequently, the hydrostatic pressure, which is directly influenced by the density of the fluid, drops

as the density of the liquid column in the tubing above the point of injection is reduced. Therefore, the weight of the liquid column and the bottom hole pressure of the well are also reduced.

- The injected gas is lighter than the liquid, so it rises up and expands in the tubing. The expansion of the gas pushes liquid ahead of it in the tubing above the point of injection. When the liquid in the tubing is pushed, the weight of the liquid column is then reduced, which causes the bottom-hole pressure to decrease.
- When the flow rate of the lift gas injected into the annulus is low, the lift gas accumulates in the annulus, causing the pressure at the injection point in the annulus to increase. When this pressure is sufficient enough to open the gas injection valve, the accumulated lift gas gets injected into the tubing suddenly. Large gas bubbles may be formed in the tubing, which might act as a piston to displace the liquid column above it, forming liquid slugs.

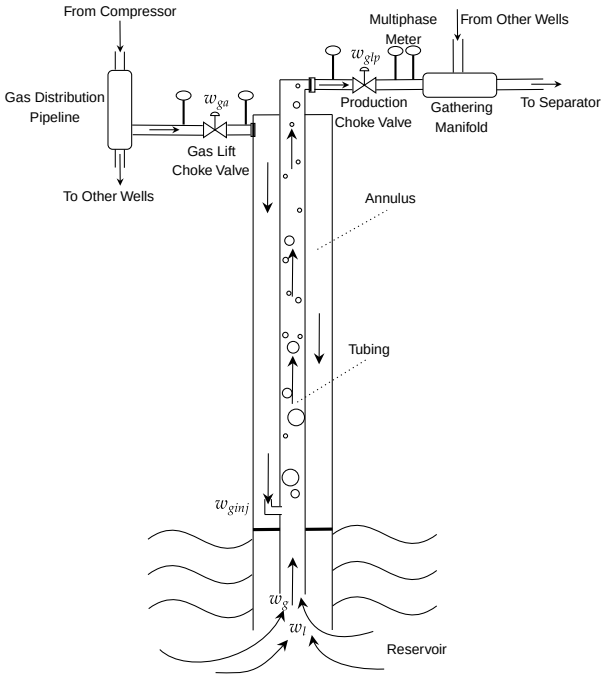

Figure 2.2: Schematic diagram of different components of a single gas lift oil well.

These three phenomena, as previously explained, collectively decrease the resistance of the tubing to liquid flow. As a result of these changes, the pressure difference between the reservoir and the bottom-hole pressure becomes sufficient to overcome all pressure losses, thus causing the liquid stream to move to the surface.

The fluid produced from the reservoir flows through the production choke valve and is collected by the gathering manifold. The production choke valve can be used to control

the flow rate of the fluid produced from the reservoir. However, in most of the cases and under normal working conditions, it is left fully opened. Many authors [11]–[13] have considered the production choke valve for stabilizing unstable gas-lifted oil wells. In this research work, the oil wells are assumed to be stable (without casing-heading instability), and hence, the production choke valves in the gas-lifted oil field have not been used for the purpose of control and optimization. The valve that is used to inject the lift gas from the annulus into the tubing is an orifice venturi valve. The critical flow is always maintained in the orifice venturi valves, and the gas injection rate is constant and independent of any fluctuations in tubing pressure. This prevents heading and gas lift instability and results in increased production. The gathering manifold also collects the fluid from other oil wells. The fluid is then transported to the separation facility, where they are separated into their respective constituents. The gas is recycled for future use in the lifting process.

The mathematical model of the process can be developed using first-principle techniques, as presented in Appendix A. The differential equations of the model are obtained from the mass balances of each phase. The algebraic equations are mostly density models, pressure models, flow models, etc., which are obtained from equations of states, valve equations, and other first principal modeling techniques. The gas lift model employed in papers A, B, C, and D as a case study is based on the previous work in USN [5] with minor modifications. These modifications include:

- In the previous work, the reservoir was assumed to contain pure oil, meaning no gas and water were produced from the reservoir. This assumption has been substituted with a more realistic one. Therefore, the reservoir in the current work contains a mixture of crude oil, water, and gas.
- The gas distribution pipeline was modeled in the previous work, and an external controller was supposed to maintain constant pressure in the manifold, which was not directly related to the problem of optimal distribution of the lift gas. Therefore, this work simplifies the model by neglecting the manifold and considering the mass flow rate of injection lift gas into the annulus as the control input.

2.2.2 Short-term Optimization

After establishing an understanding of the gas lift mechanism, it becomes straightforward to clarify the approach to short-term production optimization for the gas-lifted oil field examined in papers A, B, C, and D. To this end, it is essential to recognize that the inflow characteristics of the wells are different, and oil wells from a field are not equally capable of production. This means if the same amount of lift gas is injected into different wells, it is unlikely that they will produce at equivalent rates. Furthermore, the available resources for production, which in this case is the amount of compressed lift gas, are finite. Therefore, the short-term production optimization within the context of gas-lifted

fields aims to calculate the optimal distribution of a limited supply of lift gas among the production wells to maximize the benefit from production.

The aforementioned objective implemented in papers A, B, and D simply as maximization of the total oil production from the field while the use of gas lift is also introduced in the objective function to penalize excessive lift-gas utilization. Paper C, on the other hand, maximizes the profit from the field; therefore, the objective function includes the total revenue from selling produced oil subtracted by the costs associated with the separator and compressor. The specific

Apart from the model equations, which obviously should be incorporated into the problem, the process is subjected to two operational constraints. First, the total injected lift gas into the wells should not exceed the total available lift gas. Next, the total produced fluid should not exceed the maximum handling capacity of the separator. Consequently, the role of short-term production optimization can be interpreted in two distinct manners, depending on which constraint is currently active. First, for a given separator capacity, i.e., when the constraint on the total production is active, it minimizes the use of lift gas. While, for a given amount of lift gas, i.e., when the constraint on the available lift gas is active, it maximizes the production.

2.3 Production Optimization for ESP Lift System

Similar to the gas lift system, optimizing production in an ESP-lifted oil field requires an initial grasp of the ESP lift mechanism. Consequently, the following Subsection 2.3.1 describes the process followed by short-term production optimization for ESP-lifted systems in Subsection 2.3.2.

2.3.1 Process Description

The Electrical Submersible Pump, typically called ESP, is another artificial lift method for lifting moderate to high volumes of fluid from wellbores. As the name suggests, this method employs an electrical submersible pump to generate the necessary artificial lift for production, effectively by reducing the bottom hole pressure in the wells.

An ESP-lifted oil field consists of multiple oil wells connected to a common production manifold. Each oil well is equipped with an electric submersible pump located at the bottom of the tubing string. This pump's role is to overcome the sum of pressure losses in the pipeline, allowing ESP to provide the necessary lift for transporting oil from the reservoir to the production manifold. In general, the ESP lifting method is an efficient and reliable method suited to produce high liquid volumes [14]. Each ESP is a multistage

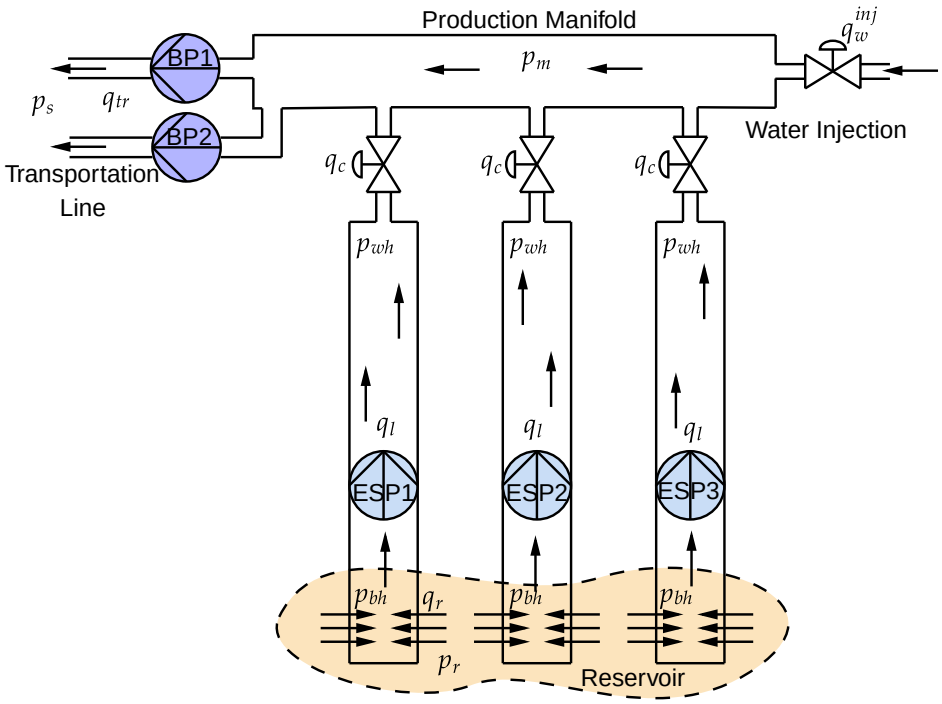

Figure 2.3: Schematic diagram of an ESP lift oil network with three oil wells.

centrifugal pump that is powered by an induction motor. A schematic representation of an ESP-lifted oil field is illustrated in Figure 2.3.

In the research work, all the oil wells are connected to the same reservoir, and it is assumed that the reservoir maintains a constant pressure, which is an admissible assumption over a short-term horizon. The reservoir contains viscous fluid, which is a mixture of both oil and water. The electrical submersible pumps (ESPs) employed in each oil well extract this fluid, which is subsequently gathered in a common production manifold. From there, it is transported over a long distance to a separation facility, where the various components of the fluid are separated.

Two parallel transportation lines demonstrated in Figure 2.3, each fitted with a booster pump, facilitate this transportation process. The booster pumps are used to increase the pressure to compensate for the pressure losses in the transportation pipelines. However, before the viscous fluid can be effectively transported over a long distance to the separation facility using the transportation pipeline, the viscosity of the reservoir fluid should be reduced to ease the transportation. If the viscosity of the fluid is not reduced, the viscous losses occurring in the transportation pipelines will be high, and the booster pumps will have to utilize more electrical power to transport the fluid. The reduction in viscosity of the reservoir fluid is achieved by introducing water injection at one end of the gathering manifold (right end in Figure 2.3). The injected water mixes with the reservoir fluid

pumped by the ESPs, and its viscosity reduces before finally being transported to the separator.

The ESP unit is submerged in the reservoir fluid at the bottom of the tubing within the oil well. To supply the necessary electrical power and frequency to the submersible motor, electric cables run from the surface down the entire length of the tubing to the motor. A Variable Speed Drive (VSD) unit located on the top side is used for changing the frequency of the AC driving the motor. The submersible motor usually lies at the bottom of the ESP unit and is cooled by the reservoir fluid flowing around it, while the pump resides on the top of the ESP unit and functions as a multistage centrifugal pump operating in a vertical orientation. Details about the design and the working principles of the motor, protector/seal, pump, and the other parts of the ESP unit fall out of the scope of this research; however, they can be found in [5].

Additionally, each oil well is equipped with a production choke valve at the wellhead. This valve serves the purpose of regulating the flow of fluid from the oil well into the production manifold.

The governing equations of the model, including oil wells, transportation lines, and production manifold, can be derived by applying mass and momentum balance to the different components of the well as presented in Appendix B. The model, which has been used as the case study in papers E and F, is adopted from [5], supplemented by subtle modifications to assumptions as follows:

- Modeling the electrical motors subsystem is neglected due to the fast response of electrical systems.
- Assumption of constant water cut in the production manifold is substituted by a more realistic one. Therefore, instead of injecting water to keep the water cut constant, which needs a perfect controller, a constant water flow is injected into the manifold. Accordingly, the water cut of the liquid phase within the manifold varies and depends on the proportion of fluid produced from production chock valves.
- Water cuts of the wells are considered to be different to draw a meaningful optimization problem.

2.3.2 Short-term Optimization

The framework for short-term production optimization for the ESP-lifted oil field, which is investigated in two last papers, E and F, closely resembles that of the gas lift system. The distinctions primarily arise from the different operational aspects of these two processes. For example, the process description for the ESP system clearly shows that the production in the ESP system crucially relies on electric pumps. Therefore, the production cost is linked to electricity consumption rather than gas compression. Nevertheless, the

underlying logic remains the same, and the objective function to be maximized consists of the desired production penalized by the costs associated with the production.

In the papers produced as part of this research, the optimization problem is formulated using an economic objective function that aims to maximize the short-term revenue from the sale of oil subtracted while accounting for operational expenses. These expenses include electricity consumption, represented by the brake horsepower in the pumps, as well as costs associated with water treatment and carbon taxation.

In addition to the objective function, the constraints in the problem also change as they stem from specific operational aspects. As expected, the separator handling capacity continues to be a pertinent constraint because the separation and downstream facilities are essential in both processes. However, instead of the available lift gas, the operation of pumps plays an essential role as a constraint. This is because the failure in pumps requires shutting down the well and replacing or repairing the ESP unit, which is a costly process. Therefore, it is crucial to ensure that the pumps operate within their safe operational window provided by the manufacturer.

To enforce the safe operation of the pump, constraints on the flow rate, head, and frequency of the pump can be incorporated into the problem formulation. Additionally, the minimum allowable pressure at the bottom hole and wellhead are the other constraints that can be included in the short-term production optimization for ESP systems.

2.4 Uncertainty in Production Optimization

The uncertainty generally manifests itself in various forms. One source of uncertainty relates to the fidelity of the model and is typically known as unmodeled dynamics. This type of uncertainty arises from missing some underlying structures or phenomena due to a lack of knowledge to capture their complex nature or due to simplifying assumptions such as approximating a system with a finite number of coordinates or state variables while the actual system is of infinite dimension. The unmodeled dynamics, in its simplest case, may appear as additive or multiplicative exogenous disturbances in state equations. A second form of uncertainty appears in terms of measurement noise or error due to challenging operating conditions (like very high pressure/temperature), accuracy of the equipment, etc.

Among the other forms of uncertainty, this thesis is particularly focused on bounded parametric uncertainty, which corresponds to a lack of enough information about the exact value of the parameters. The parameters, however, are bounded between an upper and lower limit, and they may be constant or varying, which may affect the design of the controller/optimizer.

In the context of oil production optimization, gas to oil ratio (GOR), water cut (WC), and productivity index (PI) are some of the most important uncertain parameters that are considered in this study. These parameters are assumed to belong to a bounded set and without any further assumption on their distribution over the uncertainty bound, which is a standard assumption within the area of robust optimization. Furthermore, there are also some other sources of uncertainty in oil production optimization problems, such as uncertainty in oil price in the market, that are investigated in paper E.

3 Literature Review

3.1 Optimization under Uncertainty

The origin of optimal control dates back to 1697, three centuries ago, in Groningen, a university town in the north of the Netherlands. It was Johann Bernoulli, a mathematics professor at the local university during the period of 1695 to 1705, who published his solution to the brachystochrone problem [15]. Nonetheless, substantial interest in this discipline really flourished only with the advent of the computer, launched by the spectacular successes of optimal trajectory prediction in aerospace applications in the early 1960s [16].

Rooted in optimal control, model predictive control (MPC) is possibly one of the most popular modern control strategies, which has been successfully employed for many applications in the process, automotive, and aerospace industries [17]. Its popularity can mainly be attributed to its capability to effectively handle constraints and manage systems with multiple inputs and multiple outputs (MIMO). The first ideas on model predictive control can be traced back to the 1960s [18]. The receding horizon approach was proposed in [19]; however, substantial interest in this innovative approach gained momentum only later, in the 1980s, following the first publications on Model Algorithmic Control (MAC) [20], Dynamic Matrix Control (DMC) [21], [22], and a complete description on Generalized Predictive Control (GPC) [23], [24]. Dynamic Matrix Control (DMC) was primarily developed to meet the practical demands of the oil and chemical industries by tackling multivariable constrained control problems. As mentioned in [17], the success of DMC in the oil and chemical industries attracted the academic community. Therefore, early research on MPC was intended as an attempt to understand DMC.

MPC replaces the classical offline feedback control law with an online control action by solving an optimal control problem. MPC is particularly advantageous when the offline control law is difficult or impossible to obtain [25]. An excellent review paper on the history of industrial applications of MPC can be found in [17]. In spite of the inherent robustness of MPC under appropriate conditions [26]–[28], uncertainty deteriorates its performance. The need for more rigorous treatment, especially for systems that require satisfaction of stability and performance metrics under model variations [29], prompts research into robust MPC approaches.

3.1.1 Robust Approach

A conventional remedy to mitigate the influence of uncertainty is the robust approach, where the uncertainty is assumed to belong to a bounded set, and the controller is designed to guarantee robust requirements for the worst-case situation. This ensures that if any other realization within the bounded uncertainty region happens, the controller is able to handle it. The worst-case formulation, which is also known as the min–max formulation, was originally proposed in [30] and later in the context of MPC in [31]. Traditional min–max MPC formulations, similar to standard MPC, are open-loop optimizations in the sense that they solve an open-loop optimal control problem at each sampling instance. An open-loop optimization fashion does not take into account the explicit notion of feedback in the formulation of the optimization problem, although the new information will be available in the next time instance. The main drawback of open-loop optimization is that it leads to an overly conservative solution; therefore, the controller will be significantly sub-optimal, and all resources available in the process may not be fully utilized.

To address the problem of conservativeness, the notion of feedback has been explicitly introduced in the closed-loop min–max framework as in [32], [33]. This means that the optimization will be solved over control policies rather than a single control sequence. This allows the future decisions to depend directly on the future measurements. In other words, it introduces some extra degrees of freedom to the optimization problem that reduces the conservativeness. However, the general formulation that leads to dynamic programming suffers from the curse of dimensionality and will not be practically implementable. Hence, optimization over state feedback policies [34], affine policies parameterized on the uncertainty [35], [36], and deep neural network [37] have been proposed to approximate the general problem.

Tube-based MPC method is another alternative in the framework of robust approach for both linear [38] and nonlinear systems [39], [40]. The basic idea of this method is to split the control problem into two parts. First is an ancillary controller, which is responsible for maintaining the real uncertain system within an invariant set around the nominal trajectory. Second, a deterministic standard MPC with tightened constraints based on the nominal trajectory steers the bundle of trajectories (known as a tube) to the desired state. Since the invariant set can be designed offline, the method does not impose too much extra online computational cost. However, constructing such an invariant set might not be simple, especially for complicated nonlinear systems. Different modifications of the method have been presented in [41]–[44].

The main drawback of optimization over control policies is known as the curse of dimensionality. It means the general formulation of feedback optimization, leading to a dynamic program, has infinite dimensions that cannot be solved easily. Therefore, the original problem needs to be approximated. multistage scenario-based MPC, as introduced in [45], is a widely known method that approximates the optimization over control

policies by considering only finite possible realizations of uncertainty. It utilizes a scenario tree to represent the uncertainty. Considering the system's evolution in each scenario enables the method to solve the optimization problem over different control trajectories. However, multistage MPC is computationally expensive because the size of the problem grows exponentially with the length of the prediction horizon and the number of uncertainty realizations considered. Therefore, the applicability of the method is still limited. Nevertheless, effort has been made for an efficient solution to the multistage programs through parallelizable decomposition methods [46], where primal decompositions perform iterations on stages, and dual decompositions iterate on scenarios [47], [48].

3.1.2 Stochastic Approach

Although efforts have been devoted to reducing the conservativeness of robust approaches, such methods are still computationally expensive and inherently conservative. This conservativeness may be considered as an inevitable price that should be paid to guarantee the fulfillment of required performance. However, it may be more beneficial for some specific applications to let the constraints be violated minorly in order to obtain a better overall performance. Accordingly, stochastic model predictive control (SMPC) provides a probabilistic framework by the inclusion of chance constraints [49], which enables a systematic trade-off between attainable control performance and probability of constraint fulfillment in a stochastic setting [50]. Nevertheless, SMPC is challenging too. For example, it needs the probability distribution function of the uncertainty to be known a priori, which is rarely possible. The other challenge is that propagating the uncertainty through the outputs is difficult, especially for complex nonlinear systems [51]. Sample-based approaches [52], Gaussian-mixture approximations [53], and generalized polynomial chaos [54] are some examples of such complicated uncertainty propagation methods. Two relatively old but insightful overviews of the stochastic approach can be found in [51], [55].

3.1.3 Adaptive Approach

Considering the conservatism of the robust approach and the complexity of stochastic, a simple and efficient implementation of optimization under uncertainty is still required for cases where constraint violation can be tolerated to some extent. The main idea of the adaptive approach for handling uncertainty in real-time optimization is to make use of available measurements to estimate the uncertainties and then use the updated model in the optimization problem. Contrary to the robust and stochastic methods that consider the uncertainty inside the optimization problem, an adaptive approach deals with the uncertainty outside the optimization problem.

Although online state estimation algorithms have been widely used individually [56] or accompanied by MPC in an output feedback setting [57], [58], the development of an adaptive formulation to address the optimization under uncertainty has received relatively little attention and still is an open problem [59] due to difficulties in guaranteeing closed-loop stability. However, the method's non-conservative and computationally efficient characteristics made it appealing to practitioners. For example, a model adaptation based on the homotopic transition between models was proposed in [60] for an Electric Submersible Pump in a subsea environment. Besides, Moving horizon estimation has been used for state and parameter estimation along with MPC in optimal dosing of cancer chemotherapy [61] and for real-time dispatch of energy storage systems [62].

3.2 Modeling and Optimization for Oil Production

3.2.1 Production Optimization

Long-term production optimization of oil and gas fields is typically classified as reservoir management [6] and has been extensively studied under the presence of uncertainty [63]–[65]. To name a few, economic MPC has been employed in [66], [67], multi-objective optimization in [68], and Artificial Intelligence in [69], to study long-term production optimization under uncertainty. However, most of the works on short-term optimization are limited to deterministic cases where the uncertainty is overlooked– see for examples [5] and the references within. Neglecting the uncertainty, on the other hand, may lead to constraint violation and infeasibility problems, which jeopardizes the relevance of the optimal solution for implementation [70]. Therefore, considering the uncertainty in short-term production optimization is attracting more attention recently.

The uncertainty within the domain of short-term production optimization was first handled explicitly in [71] by proposing to formulate the optimization solution as a priority list between the wells. This list represents an operational strategy; thus, whenever there is spare capacity or the opposite, the priority list is applied. In another early related work in [72], the uncertainty is accounted for by iteratively changing the setpoints until the capacity constraints, which should be active, are utilized to their limits.

The use of a dynamic model for real-time optimization is another aspect that makes handling the uncertainty even more challenging. In many process control applications, real-time optimization uses nonlinear steady-state process models to compute the optimal setpoint at steady-state operation [73]. However, there are a few works on dynamic real-time optimization for short-term production while uncertainty is neglected; see [74]–[76] for instance. A discussion on static versus dynamic optimization problem formulation is provided in [77], where the hybrid RTO approach (i.e., static optimization with dynamic model adaptation) is proposed to address the expensive computation costs.

Recently, real-time process optimization under the presence of uncertainty has been studied in [48], [78] to address the challenges in this area. However, the gas to oil ratio is the only uncertain parameter considered in this work. The other parameters, such as water cut and productivity index, are assumed to be deterministic, while the water cut is the most varying (uncertain) parameter in the field. So, neglecting the water in the reservoir makes the model unrealistic.

3.2.2 Artificial Lifting Methods

Gas Lift [79] method has been extensively studied. For instance, mathematical modeling of gas-lifted oil fields has been studied before for different purposes, such as flow stabilization in [12], [80]–[82] and production optimization in [83]–[86]. Despite some minor differences in the assumptions, such as the inflow performance of oil wells and constituents of the fluid in the reservoir, all the models are derived based on mass conservation of different fluid phases in the tubing and annulus. It has been shown in [87] that these first principle models are sufficient to capture the essential dynamic behavior of the process for control purposes.

Similarly, the Electrical Submersible Lifting method [14] has been studied extensively too. A mathematical model for a single ESP oil well was developed in [88], and a linear Model Predictive Control (MPC) was designed in the Statoil Estimation and Prediction Tool for Identification and Control (SEPTIC) based on the step response model of the process. This controller was later implemented on a Programmable Logic Controller (PLC) in [89]. A Moving Horizon Estimator (MHE) was successfully implemented in [56] using the same model to estimate the flow rate and the productivity index of the well and the viscosity of the produced fluid.

A similar first principle model was derived in [90] for multiple ESP wells that share a common production manifold. The steady-state version of this model was used in [91] to develop a nonlinear optimization based on Sequential Quadratic Programming (SQP) for two optimal control strategies. The authors demonstrated that the production choke valve for each oil well has to be fully open during normal operation to maintain the optimal fluid flow rate and minimize electrical power. The same authors formulated a Mixed Integer Nonlinear Programming problem (MINLP) in [92] to calculate and identify the number of oil wells that should be used for special cases with low production demand. The dynamic version of the model was also used in [93], where the nonlinear model predictive control framework was implemented as an economic optimizer for maximizing profit. Even though the controls in this work were assumed constant throughout the prediction horizon, the length of the prediction horizon was limited to one second due to the fast dynamics of ESP and the high computational cost of a longer prediction horizon.

The research based on the model developed in [88] was pursued further, and it was shown in [94] that the linear model of an ESP lifted well varies significantly depending on the

choke opening. Therefore, a model adaptation based on the homotopic transition between models was proposed in [60], where an adaptive linear MPC strategy was implemented as a Quadratic Dynamic Matrix Control (QDMC) algorithm in order to control the pump inlet pressure, minimizing the pump power and respecting the variable's constraints. An adaptive infinite horizon MPC strategy was also implemented in [95], where the proposed control law used successive linearization of the dynamic model in [88] to update the model internally. The ESP model was used in [96] to investigate the implementation aspects of measured disturbances in MPC. The main control objective in this work was to sustain a given production rate from the well while maintaining acceptable operating conditions for the pump.

A different approach was proposed in [7], translating the optimization objectives into control objectives to avoid solving a numerical optimization problem. The proposed method was applied to a single ESP lifted well successfully to track the inlet pressure of ESP subject to constraints. Nevertheless, the method violated the constraints dynamically. Recently a high-fidelity model of a single ESP well was proposed in [97] to be used as a surrogate model for the real plant. This model was used in [98] to propose an economic-oriented MPC auto-tuning strategy with a flexible structure able to enclose different MPC formulations, different tuning requirements, online implementation, and process attributes. An Echo State Neural Network was trained in [99] to capture the dynamic model of ESP well. The trained neural network was used for two nonlinear model predictive controllers that aimed to track the bottom-hole pressure subject to constraints on control inputs, bottom-hole and well-head pressures, and liquid flows. In spite of the numerous studies on daily production optimization, such as [100]–[104] to name a few, the uncertainty has rarely been taken into account in the optimization problem explicitly.

4 Theoretical Background

This chapter presents the theoretical background of the methods used during the research. The methods are introduced in the most general way; however, a specific application of the methods may be accompanied by several assumptions that may simplify the problem or make it more challenging. Therefore, a driven Van der Pol oscillator is utilized as an illustrative example at the end of this chapter to demonstrate the various pros and cons of each method under unified circumstances. The illustrative example and the corresponding mathematical formulation and simulation result for each method are presented in Appendix C.

4.1 Optimal Control Problem

Optimal Control, as its name suggests, is a branch of control theory that aims to determine a sequence of decisions (control signals) that will cause a dynamical system (process) to satisfy the physical constraints and, at the same time, minimize (or maximize) some performance criterion [105]. The broad domain of optimal control can be categorized from different points of view into linear/nonlinear control, continuous/discrete time, finite/infinite horizon, etc. However, all these categories, in a nutshell, are nothing but a mathematical optimization problem. A mathematical statement of the optimal control problem (OCP) consists of [106]:

- A description of the system to be controlled.
- A description of the system constraints and possible alternatives.
- A description of the task to be accomplished.
- A statement of the criterion for judging optimal performance.

which correspond to the main ingredients of the mathematical optimization problem, namely, objective function, equality constraints, and inequality constraints.

The dynamic of the systems to be controlled is typically described by Ordinary Differential Equations (ODEs) or Differential and Algebraic Equations (DAEs) in a continuous-time format, resulting in an infinite-dimensional optimal control problem. Although for the special case of linear systems with a quadratic cost function, also known as linear quadratic

regulator (LQR), an analytical solution can be obtained by solving the Riccati differential equation, such analytical solutions are generally not possible for nonlinear cases. Therefore, numerical approximation methods must be employed to solve these nonlinear cases. Two distinct approaches for seeking approximate numerical solutions to these problems are the direct and indirect methods [107]. Indirect or *first optimize then discretize* methods solve the problem first by applying the optimality conditions, e.g. applying Pontryagin's minimum principle [108], and then discretizing them to obtain the solution numerically. The direct methods, however, first discretize the dynamics of the system and control inputs into a finite-dimensional nonlinear programming problem, which is then can be solved to get the numerical solution. The latter approach is also known as *first discretize then optimize* methods, include single shooting [109], [110], multiple shooting [111] and collocation on finite elements [112], [113]. It should be noted that the multiple shooting, along with the Runge–Kutta 4th order integration method, has been used throughout the entire thesis for solving optimal control problems.

The general formulation of the nonlinear optimal control problem over a finite horizon N in a discrete-time setting $\mathcal{K} = \{0, 1, \ldots, N-1\}$ that needs to be solved numerically at a given initial state x_0 is defined as follows. For ease of notation, the sequence of $\mathbf{u} \coloneqq (u(0), u(1), \ldots, u(N-1))$ and $\mathbf{x} \coloneqq (x(0), x(1), \ldots, u(N))$ are introduced, which encompass all the control and state vectors and $x(k) \in \mathbb{R}^{n_x}$, $u(k) \in \mathbb{R}^{n_u}$, and $d(k) \in \mathbb{R}^{n_d}$, represent the states, control and parameter vectors at sampling time k.

$$\min_{\mathbf{x},\mathbf{u}} \quad \sum_{k=0}^{N-1} \ell(x(k), u(k), d(k)) + V_f(x(N)) \tag{4.1a}$$

$$\text{s.t.} \quad x(0) = x_0 \tag{4.1b}$$

$$f(x(k), u(k), d(k)) = 0, \qquad \forall k \in \mathcal{K} \tag{4.1c}$$

$$g(x(k), u(k), d(k)) < 0, \qquad \forall k \in \mathcal{K} \tag{4.1d}$$

Remark 1: The OCP is conventionally posed in the form of a minimization problem, as most of the solvers are developed to minimize the cost function. However, a maximization problem can be converted into a minimization problem easily by multiplying the objective function by -1.

Remark 2: The scalar cost function in (4.1a) consists of two parts: $\ell(x(k), u(k), d(k))$, which computes the stage cost for each k and $V_f(x(N))$, which accounts for the terminal cost. The cost or objective function is the mathematical representation of the desired performance. Tracking error, economic index, or any other form of desire can be incorporated into the objective function as long as it is translated into a scaler function.

Remark 3: The equality constraints in (4.1c) typically consist of the dynamic of the system. Although, any other equality constraint that needs to be satisfied can be included. Similarly, (4.1d) can include all the inequality requirements of the system.

Remark 4: The OCP in (4.1) is an open-loop optimization problem, meaning that there is an underlying assumption that indicates all the control inputs will be implemented, and no extra information in the form of feedback is included in the problem. In other words, once the problem is initialized at the initial state x_0 and the sequence of control actions are computed, the actions will be implemented without any modification one after the other, no matter what happens to the real plant.

4.2 Model Predictive Control

Model Predictive Control (MPC) roots in optimal control in the sense that they both use the model of the system to forecast the future behavior of the system and compute the sequence of inputs by solving an open-loop optimization problem that leads to desired performance. However, the key distinction between MPC and OCP lies in how they implement the optimal decisions. As highlighted in the previous section, the solution to OCP is a sequence of decisions. It is intuitively obvious that implementing a sequence of inputs in an open-loop fashion does not effectively satisfy the required performance, and the actual plant may drift from the predicted trajectory as time passes simply because the model used for prediction is not perfect, and furthermore, unforeseen scenarios may happen, e.g. external disturbance. MPC solves this problem by re-computing the optimal decision at each sampling time. This strategy, which is known as the receding horizon strategy, suggests that only the first element of control inputs should be implemented and in the next sampling time, the optimization should be re-calculated by initializing the optimization problem at the new initial state. The concept of receding horizon, which is demonstrated in Fugure 4.1, is a simple strategy to introduce feedback into MPC and to compensate for the mismatch between the prediction and what happens in reality, at least to some extent. With more precise language, it can be said the receding horizon facilitates MPC to implement an open-loop optimal solution in a closed-loop fashion by re-initializing and solving the optimization problem repeatedly. The great advantage of MPC is that the open-loop optimization problem can be solved fast enough to allow the implementation of feedback control, which is especially true with the development of modern computing infrastructure.

The general formulation of the nonlinear model predictive control over a finite horizon N_p in a discrete-time setting $\mathcal{K} = \{0, 1, \ldots, N_p - 1\}$ that needs to be solved numerically at any given initial state x_0 is defined in (4.2), and as it is expected, it is very similar to

OCP in (4.1).

$$\min_{\mathbf{x},\mathbf{u}} \quad \sum_{k=0}^{N_p-1} \ell(x(k), u(k), d(k)) + V_f(x(N_p)) \tag{4.2a}$$

$$\text{s.t.} \quad x(0) = x_0 \tag{4.2b}$$

$$f(x(k), u(k), d(k)) = 0, \qquad \forall k \in \mathcal{K} \tag{4.2c}$$

$$g(x(k), u(k), d(k)) < 0, \qquad \forall k \in \mathcal{K} \tag{4.2d}$$

Remark 1: There is no concrete rule for the length of prediction horizon N_p. A too-short prediction horizon may make the closed-loop system unstable, whereas the open-loop system is stable.

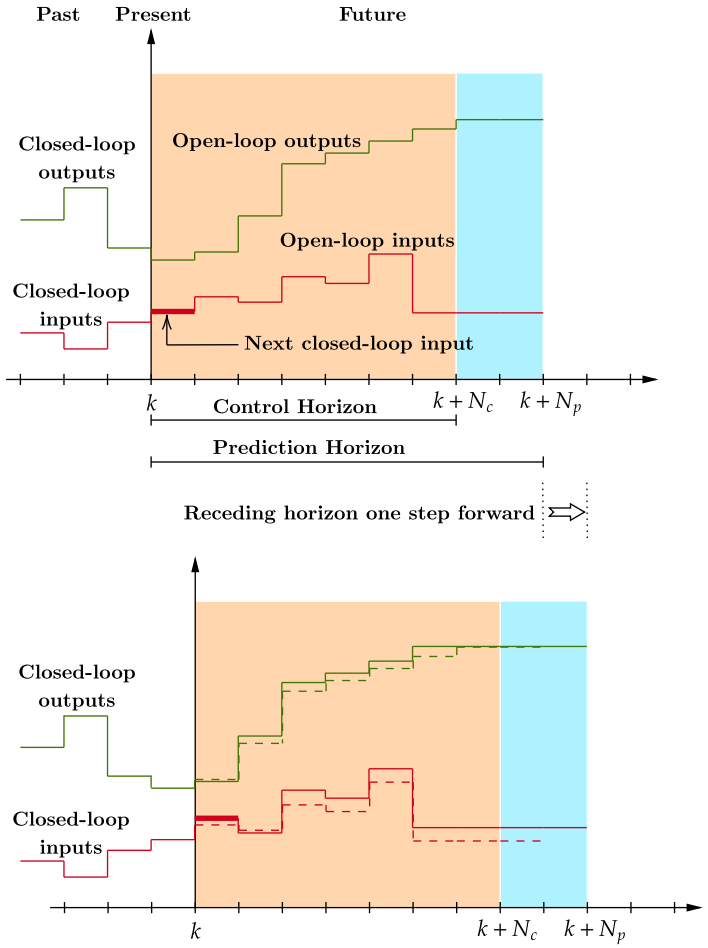

Figure 4.1: Receding horizon strategy.

4.3 Min-Max Model Predictive Control

Min-Max Model Predictive Control has been regarded as an effective robust MPC framework [31], [33]. It is robust in the sense that it can mitigate the effect of uncertainty, where the uncertainty characteristic belongs to a prescribed bounded set $\mathcal{D}$ without any extra assumption on the probability distribution function of the uncertainty. The compound term *Min-Max* arises from the fact that the method consists of two operators. The inner layer (max operator) determines the worst-case scenario, and the outer layer (min operator) minimizes the objective function corresponding to the worst-case scenario. Thus it is also known as the worst-case formulation or worst-case scenario MPC. One unified sequence of control actions applies to all scenarios, and the same constraints are enforced for every scenario, including the worst scenario.

The general formulation of the nonlinear Min-Max MPC for the bounded uncertainty $d(k) \in \mathcal{D}$ over a finite horizon N_p in a discrete-time setting $\mathcal{K} = \{0, 1, \ldots, N_p - 1\}$ that needs to be solved numerically at any given initial state x_0 is defined in (4.3).

$$\min_{\mathbf{x},\mathbf{u}} \quad \max_{\mathbf{d}} \quad \sum_{k=0}^{N_p-1} \ell(x(k), u(k), d(k)) + V_f(x(N_p)) \tag{4.3a}$$

$$\text{s.t.} \quad x(0) = x_0 \tag{4.3b}$$

$$f(x(k), u(k), d(k)) = 0, \qquad \forall d(k) \in \mathcal{D},\ \forall k \in \mathcal{K} \tag{4.3c}$$

$$g(x(k), u(k), d(k)) < 0, \qquad \forall d(k) \in \mathcal{D},\ \forall k \in \mathcal{K} \tag{4.3d}$$

Remark 1: The general formulation of nonlinear Min-Max MPC is difficult to solve, especially when the uncertainty belongs to a continuous bounded set. Therefore it is common to discretize the infinite-dimensional space of the continuous uncertainty set into finite discrete realizations. Frequently, the task can be accomplished using a scenario tree.

Remark 2: Similar to all the other robust control methods, the credibility of the Min-Max MPC is limited to the bounded range of uncertainty. Thus they are not able to compensate for the uncertainties beyond the considered bound.

Remark 3: Min-Max MPC computes a sequence of control inputs that satisfies the constraints for all the realizations of uncertainty by minimizing the worst-case value of the objective function. Thus, it often leads to overly conservative or even infeasible solutions. This shortcoming is addressed by introducing the feedback explicitly into the optimization, as it will be presented in the next section.

4.4 Multistage Model Predictive Control

Multistage MPC or Scenario-based MPC is built upon the basic scenario tree structure. The simple idea of discretizing the uncertainty into finite realizations and representing them by a discretized scenario tree not only allows us to propagate the uncertainty in time efficiently but also gives the opportunity to explicitly account for the notion of *feedback* or *recourse* and formulate the optimization problem in a closed-loop format.

The essential difference between closed-loop and open-loop optimization problems arises from the fact that an open-loop optimization does not take into account that only the first control action (which is known as *here-and-now* decision in stochastic programming terminology) is going to be implemented and the remaining control variables (which are known as *wait-and-see* decisions) will be refined as the optimization problem will be solved at the next sampling with updated information. In other words, the closed-loop optimization formulation explicitly takes future information into account and solves the problem over several control trajectories, also known as control policies. However, an open-loop formulation solves the optimization problem over one single control sequence, which makes the solution overly conservative.

Although accounting for future information that is yet to be realized might be a challenging concept to grasp, we instinctively use this strategy in our daily life. To elucidate the concept, let us consider an oversimplified example in which two hitchhikers have a one-month journey ahead, and they are willing to minimize the weight of their backpacks. Person A, with an open-loop optimization strategy, collects all items that may be required during the journey, including his heavy jacket, since the weather forecast is only valid for the next day, and he wants to ensure (robustly) that he will not be soaked. On the other hand, person B takes into account that they will spend each night in a town, and they will have access to the weather forecast and free market. So, instead of collecting each and every item, his closed-loop strategy includes: packing the necessary items for tomorrow, checking the weather forecast every day, going to the store, and trading the unnecessary items on a daily basis to fulfill the most recent requirements. As a result, person B carries a lighter backpack, while overly conservative person A performs sub-optimally.

To formulate the optimization problem, the scenario tree should be constructed as demonstrated in Figure 4.2. Note that a scenario is defined as a sequence of states from the root node to a leaf node. Let n_d be the dimensionality of the uncertain parameters vector, which is equivalent to the number of uncertain parameters, and each parameter can take m realizations; therefore, at each sampling time, the scenario tree should be forked into m^{n_d} branches. Now, for a prediction horizon with the length N_p, the total number of scenarios adds up to $N_s = (m^{n_d})^{N_p}$. As it is presented in Table 4.1, the number of scenarios grows exponentially with the number of uncertainties, as well as with the length of the prediction horizon. As a result, the computational expenses may quickly become intractable.

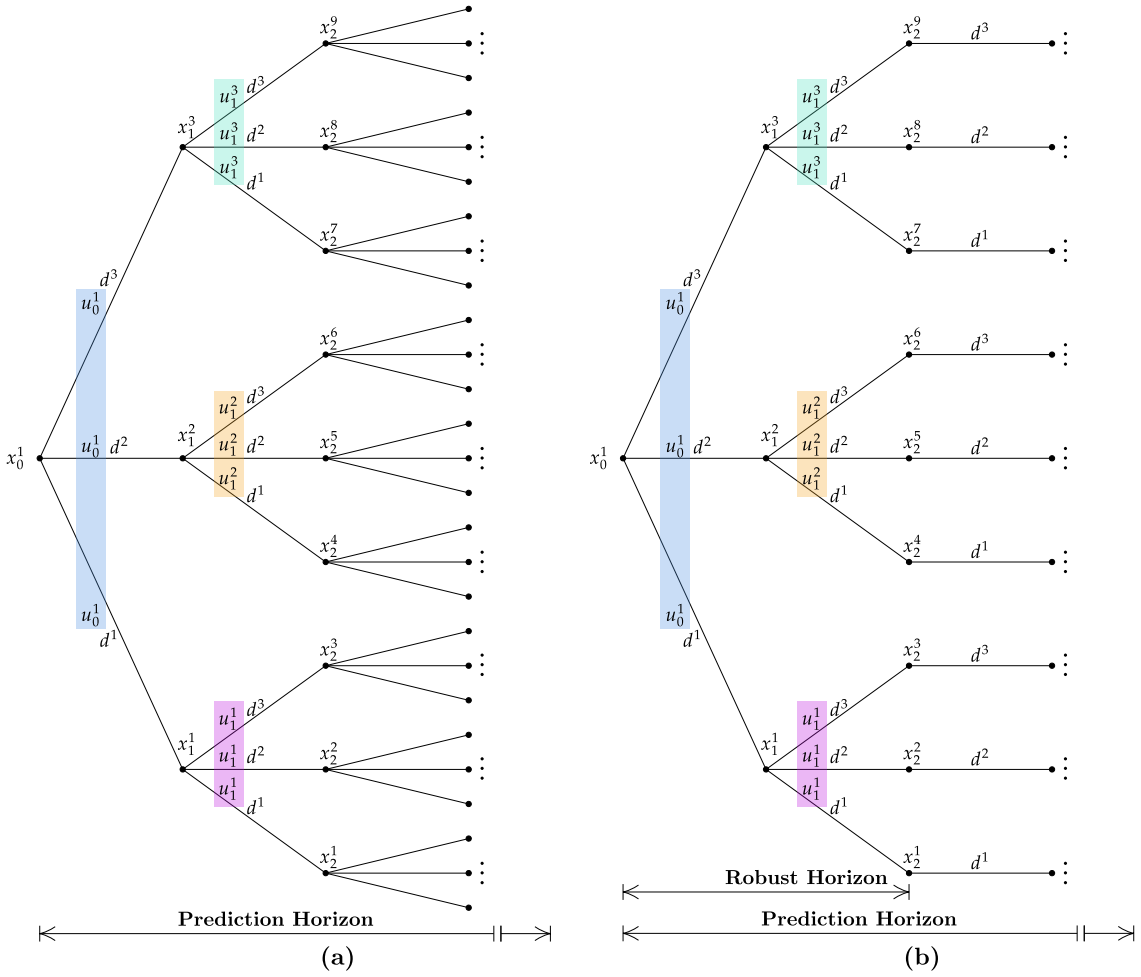

Figure 4.2: Scenario tree: (a) fully-branched, (b) with robust horizon.

An online tractable problem formulation gives rise to a concept called the robust horizon [45]. The robust horizon means that branching continues until a certain number of sampling times N_r, which is typically one or two. After that, the uncertain parameters remain at their last values in the robust horizon throughout the rest of the prediction horizon. The truncated scenario tree with robust horizon $N_r = 2$ is demonstrated in Figure 4.2, where the number of scenarios decreased from 3^{N_p} to 9.

As the scenario tree is constructed, the general formulation of the nonlinear Multistage MPC for the bounded uncertainty $d(k) \in \mathcal{D}$ represented by the discrete scenarios $\mathcal{S} = \{1, \ldots, N_s\}$, over a finite horizon N_p in a discrete-time setting $\mathcal{K} = \{0, 1, \ldots, N_p - 1\}$ that needs to be solved numerically at any given initial state x_0 is defined in (4.4).

Table 4.1: Number of scenarios assuming two realizations ($m = 2$) for each parameter.

	n_d				
N_p	**1**	**2**	**3**	**4**	**5**
1	2	4	8	16	32
2	4	16	64	256	1024
3	8	64	512	4096	32768
4	16	256	4096	65536	1048576
5	32	1024	32768	1048576	33554432
6	64	4096	262144	16777216	1073741824
7	128	16384	2097152	268435456	34359738368
8	256	65536	16777216	4294967296	1099511627776
9	512	262144	134217728	68719476736	35184372088832
10	1024	1048576	1073741824	1099511627776	1125899906842624

$$\min_{\mathbf{X},\mathbf{U}} \quad \sum_{j=1}^{N_s} \sum_{k=0}^{N_p-1} \omega^j \left(\ell \left(x^j(k), u^j(k), d^j(k) \right) + V_f(x^j(N_p)) \right) \tag{4.4a}$$

$$\text{s.t.} \quad x^j(0) = x_0, \qquad \forall j \in \mathcal{S} \tag{4.4b}$$

$$f(x^j(k), u^j(k), d^j(k)) = 0, \qquad \forall j \in \mathcal{S},\ \forall k \in \mathcal{K} \tag{4.4c}$$

$$g(x^j(k), u^j(k), d^j(k)) < 0, \qquad \forall j \in \mathcal{S},\ \forall k \in \mathcal{K} \tag{4.4d}$$

$$u^j(k) = u^p(k) \ \text{ if } \ x^j(k) = x^p(k), \qquad \forall j, p \in \mathcal{S},\ \forall k \in \mathcal{K} \tag{4.4e}$$

Remark 1: It should be noted that the optimal solution of Multistage method, as a closed-loop optimization fashion, is changed from one single control trajectory $\mathbf{u}$ in open-loop optimization to $\mathbf{U} \coloneqq (\mathbf{u}^1, \mathbf{u}^2, \ldots, \mathbf{u}^{N_s})$ that encompasses the control trajectories for all scenarios. Similarly, $\mathbf{X} \coloneqq (\mathbf{x}^1, \mathbf{x}^2, \ldots, \mathbf{x}^{N_s})$ contains all the state trajectories of the scenarios.

Remark 2: An extra set of constraints called *non-anticipativity constraint* imposed in (4.4e), that indicates the control actions $u^j(k)$ and $u^p(k)$ that are rooted from the same parent node $x^j(k) = x^p(k)$ have to be equal, regardless the number of branches. This constraint reflects the fact that in real-time decision-making, the controller is not able to anticipate the future realization of the uncertainty. Another functionality of this constraint is that it guarantees the uniqueness of the first control action that needs to be injected into the plant, as all the scenarios share the same parent node x_0.

Remark 3: Non-anticipativity of the uncertainty at the moment of making a decision should not be mistaken for the elegant idea of closed-loop optimization, which states that future decisions depend on future information. To clarify the difference, let us consider

Figure 4.2, in which the different sets of non-anticipativity constraints are highlighted by different colors. The non-anticipativity constraint implies that u_0^1 should be equal for all the scenarios as they share the same parent node x_0^1. The same argument is valid for the other sets of non-anticipativity constraints, which are highlighted by different colors. However, closed-loop optimization means that future decisions, e.g., choosing between u_1^1 or u_1^2 or u_1^3 depend on the state is propagated to which trajectory, here x_1^1 or x_1^2 or x_1^3.

Remark 4: The weight ω^j in (4.4a) represents the relative likelihood of occurring j^{th} scenario. It is common to assume equal weights for all scenarios when no extra information is available. However, if such information is accessible, the performance can be improved by tuning the weights accordingly.

Remark 5: The idea of closed-loop optimization can be incorporated into Min-Max MPC, leading to the closed-loop or feedback Min-Max MPC. In this case, the same scenario tree structure will be used with non-anticipativity constraints, and the only difference between the two methods is the objective function. Multistage MPC optimizes a weighted sum objective for all scenarios, yet closed-loop Min-Max MPC only optimizes the performance for the worst-case scenario. The difference between open-loop and closed-loop Min-Max is explained with a simple example in [33].

4.5 Adaptive Model Predictive Control with MHE

The main idea of the adaptive approach for handling uncertainty in real-time optimization is to make use of available measurements to estimate the uncertainties and then use the updated model in the optimization problem. Contrary to the robust and stochastic approaches that consider the uncertainty inside the optimization problem, the adaptive approach handles the uncertainty "*outside*" the optimization problem, i.e., the optimization problem is supplemented with an external parameter estimation block, and the optimization problem itself can be deterministic as demonstrated in Figure 4.3.

The first ingredient of the method is the Moving Horizon Estimation (MHE) algorithm, which is an optimization-based state estimation technique that estimates the states and potentially the uncertain parameters of the system based on a finite sequence of past measurements while incorporating information from the dynamic system equation. Similar to MPC, MHE makes use of a sliding horizon strategy by looking back into a moving window of past measurements and solving an optimization problem to calculate the best set of parameters and previous states that match with the past measurements and applied control inputs. A schematic visualization of the method is presented in Figure 4.4.

The optimization problem that needs to be solved numerically at each sampling time over a backward window of N_{MHE} past measurements $\mathbf{y}^m \coloneqq (y^m(0), y^m(1), \ldots, y^m(N_{\text{MHE}}-1))$ and applied control is given by:

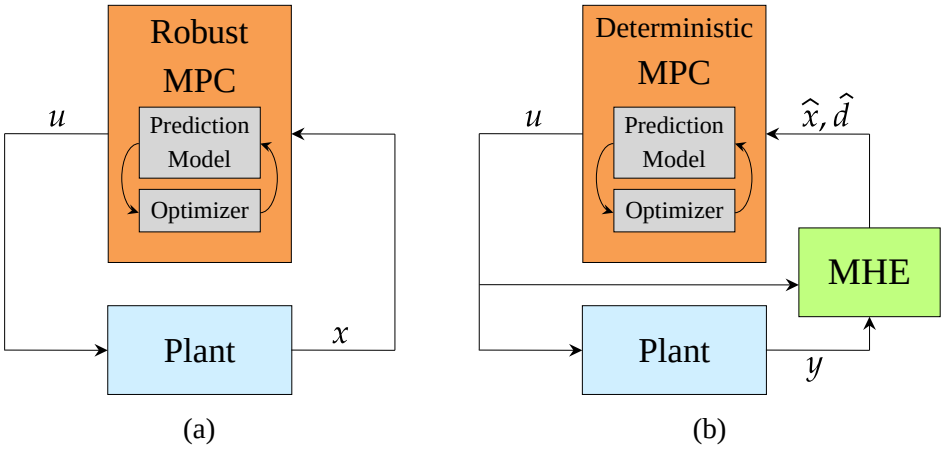

Figure 4.3: Block diagrams for (a) robust and (b) adaptive approaches.

$$\min_{\hat{x},\hat{d}} \quad 1/2\|\hat{x}(0) - x_a\|^2_{P_x} + 1/2\|\hat{d} - d_{\text{prev}}\|^2_{P_d}$$
$$+ 1/2 \sum_{k=0}^{N_{\text{MHE}}-1} \|y^m(k)) - h(\hat{x}(k)), u(k), \hat{d}(k))\|^2_{P_y} \tag{4.5a}$$
$$\text{s.t.} \quad \hat{x}(k+1) = f\left(\hat{x}(k), u(k), \hat{d}\right), \quad k = 0, ..., N_{\text{MHE}} - 1 \tag{4.5b}$$
$$g\left(\hat{x}(k), u(k), \hat{d}(k)\right) \leq 0, \quad k = 0, ..., N_{\text{MHE}} - 1 \tag{4.5c}$$
$$x_{\text{lb}} \leq \hat{x}(k) \leq x_{\text{ub}}, \quad k = 0, ..., N_{\text{MHE}} - 1 \tag{4.5d}$$
$$d_{\text{lb}} \leq \hat{d}(k) \leq d_{\text{ub}}, \quad k = 0, ..., N_{\text{MHE}} - 1 \tag{4.5e}$$

Remark 1: The decision variables of the optimization problem defined in (4.5) are $\hat{\mathbf{x}} := (\hat{x}(0), \hat{x}(1), \ldots, \hat{x}(N_{\text{MHE}}))$ that encompasses estimation of the all states over the estimation window and $\hat{d}$ which is the estimation of the parameter. The underlying assumption is that the parameter is constant over the estimation horizon.

Remark 2: The quadratic cost defined in (4.5a) consists of three terms, namely, arrival cost, change of parameter, and error between measured and computed outputs. P_x, P_d, and P_y are three corresponding weights for these three terms, respectively.

Remark 3: The arrival cost in the objective function is introduced to counteract the information loss due to the finite horizon [114]. It ensures that the initial state of the sequence is coherent with the previous estimate. Therefore, x_a, which conveys the information from the previous estimation, is equal to $\hat{x}(1)$ from the previous estimated solution.

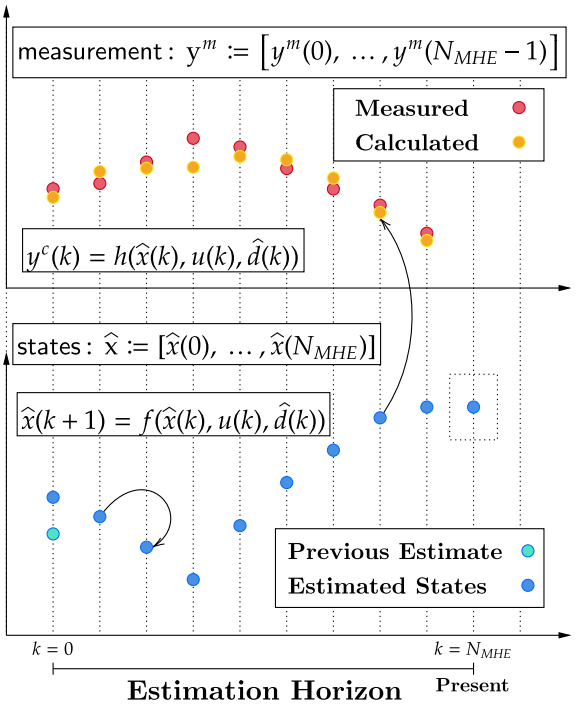

Figure 4.4: Schematic visualization of Moving Horizon Estimation method.

The second term in the cost function penalizes the error between the current and previous estimated parameters, and the third term minimizes the error between measured and computed outputs.

Remark 4: If the bounds on states and parameters are known, they can be implemented as inequality constraint as imposed in (4.5d) and (4.5e).

The estimated parameter $\hat{d}$ and state $\hat{x}(N_{\text{MHE}})$ computed by the MHE are provided to initialize the optimization problem in MPC as an estimated parameter and initial state. Therefore, adaptive MPC formulation over a finite horizon N_p in a discrete-time setting $\mathcal{K} = \{0, 1, \ldots, N_p - 1\}$ that needs to be solved numerically at any given initial (estimated) state $\hat{x}_0$ is defined in (4.6).

$$\min_{\mathbf{x},\mathbf{u}} \quad \sum_{k=0}^{N_p-1} \ell(x(k), u(k), \hat{d}(k)) + V_f(x(N_p)) \tag{4.6a}$$

$$\text{s.t.} \quad x(0) = \hat{x}_0 \tag{4.6b}$$

$$f(x(k), u(k), \hat{d}(k)) = 0, \qquad \forall k \in \mathcal{K} \tag{4.6c}$$

$$g(x(k), u(k), \hat{d}(k)) < 0, \qquad \forall k \in \mathcal{K} \tag{4.6d}$$

Remark 5: In general, the alternative estimation algorithms can be used for the estimation part. However, in comparison to more traditional state estimation methods, MHE often tends to exhibit superior performance in terms of estimation accuracy. This is especially true for nonlinear dynamical systems, which are treated rigorously in MHE. An additional advantage of MHE lies in its capacity to integrate supplementary constraints on estimated variables.

4.6 Min-Max MPC with Constraint Modification

The proposed method in this section is a modified version of the original Min–Max MPC to reduce the conservativeness of the classical Min–Max in a computationally efficient manner. Since the proposed method does not solve the optimization problem over control policies, it falls under the category of open-loop optimization; however, it decreases the conservativeness even better than the closed-loop optimization techniques such as multistage MPC. The main idea behind the method emerged after studying robust and adaptive methods for production optimization from gas-lift oil fields. Particularly, it has been observed that for the given case study, the output constraint is upper bounded, and the conservativeness arises from overestimating outputs by the controller in the prediction part. Therefore, a simple innovative method has been developed to compensate for this overestimation by modifying the active output constraint. The most important requirement of the method is that the output (constraint) should be directly measurable, which is an admissible requirement for several chemical processes since the constraints are mostly on pressures, temperatures, or flows. Therefore, the method can be generalized to be applicable to a class of systems where this requirement is fulfilled, although it has been developed based on special features of a specific case study.

The main idea is presented schematically in Figure 4.5. At the current time $k = 0$, the reachable outputs can be calculated using the prediction model and previous state and control input, which are known. Therefore, the maximum and minimum predicted/calculated outputs can be used to calculate the modification terms for the upper and lower bounds of the constraint as follows:

$$\delta_{\mathrm{L}} = \min(y^c(k)) - y^m(k) \tag{4.7a}$$

$$\delta_{\mathrm{U}} = \max(y^c(k)) - y^m(k) \tag{4.7b}$$

Accordingly, the lower and upper bounds of the constraint can be modified as presented in (4.8), where ω_s is the tuning coefficient between 0 and 1, decided by the designer. Obviously, $\omega_s = 0$ is equivalent to no modification. And the bigger $\omega_s = 1$, the more aggressive the controller would be.

$$y_{\mathrm{lb}} + \omega_s \delta_{\mathrm{L}} \leq y(k) \leq y_{\mathrm{ub}} + \omega_s \delta_{\mathrm{U}} \tag{4.8}$$

The general formulation of the method is based on traditional open-loop Min-Max MPC. As a result, when the parameters of the actual process take their worst-case realization, there will be no mismatch between the prediction and measurement; therefore, the method would be equivalent to a Min–Max MPC applied in the worst-case situation of the process. Otherwise, the mismatch between the prediction and measurement modifies the bounds of the constraint and decreases the conservatives. Therefore, the formulation of the method for the bounded uncertainty $d(k) \in \mathcal{D}$ over a finite horizon N_p in a discrete-time setting $\mathcal{K} = \{0, 1, \ldots, N_p - 1\}$ that needs to be solved numerically at any given initial state x_0 is defined in (4.9), while the modification terms are calculated using (4.7) at $k = 0$.

$$\min_{\mathbf{x},\mathbf{u}} \quad \max_{\mathbf{d}} \quad \sum_{k=0}^{N_p-1} \ell(x(k), u(k), d(k)) + V_f(x(N_p)) \tag{4.9a}$$

$$\text{s.t.} \quad x(0) = x_0 \tag{4.9b}$$

$$f(x(k), u(k), d(k)) = 0, \qquad \forall d(k) \in \mathcal{D},\ \forall k \in \mathcal{K} \tag{4.9c}$$

$$g(x(k), u(k), d(k)) < 0, \qquad \forall d(k) \in \mathcal{D},\ \forall k \in \mathcal{K} \tag{4.9d}$$

$$y_{\text{lb}} + \omega_s \delta_{\text{L}} \leq y(k) \leq y_{\text{ub}} + \omega_s \delta_{\text{U}}, \qquad \forall d(k) \in \mathcal{D},\ \forall k \in \mathcal{K} \tag{4.9e}$$

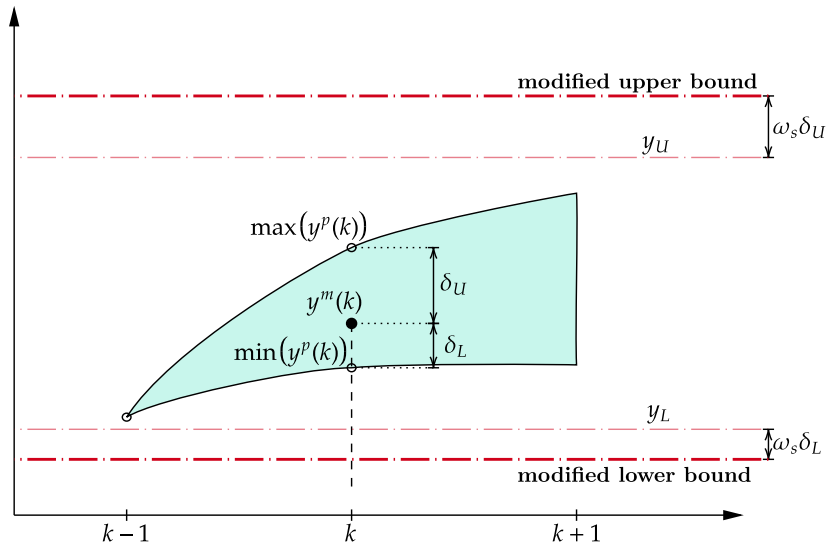

Figure 4.5: Schematic representation of employing output(constraint) measurement for modifying the bounds on the constraint.

Remark 1: Although the early version of Quadratic Dynamic Matrix Control (QDMC) [115] and more recent versions of adaptive model predictive control [60], [62] take advantage of the difference between measured and predicted outputs, the fundamental distinction between these works and the proposed method lies in the different purposes of utilization of output error. QDMC uses the error to estimate the uncertainty and then uses the

adapted model in the optimization problem, while the proposed method uses the error to modify the bounds on the constraints directly, and no estimation part exists in between. Additionally, the optimization problem in QDMC is based on the nominal (estimated) model, while the proposed method is built upon robust Min-Max MPC in which the worst-case optimization is utilized to cope with the worst-case realization of the plant.

Remark 2: It should be emphasized that the modification terms δ_{L} and δ_{U} are not slack variables, which should be calculated by the optimizer. However, they represent how much mismatch exists between the forecast model in the controller and the real process. In other words, they will be calculated at every sampling time $k = 0$ to initialize the optimization problem.

4.7 Illustrative Example

As it was promised at the beginning of this chapter, all the methods are implemented using a driven Van der Pol oscillator as an illustrative example for the sake of comparison. The mathematical formulation of the problems and the detailed information about each simulation are given in Appendix C. The objective is to maximize the output y in the first half of the simulation and minimize it in the second half with the minimum possible control effort subject to constraints on the control input and the output. The motivation for defining such an objective function is that it makes both the upper bound and lower bound of the constraint active at different times during the simulation. There is one bounded uncertain parameter p in the problem, and the simulations are implemented in three scenarios in which p takes its minimum, nominal, and maximum value.

To compare the two essential characteristics of the methods, namely robustness and conservativeness, the constrained output is plotted in Figure 4.6. Expectedly, open-loop implementation of the optimal control (OCP), which is shown in black dotted lines, demonstrates extremely poor performance when the uncertain parameter takes other realizations than the nominal value. Standard deterministic MPC in grey dashed lines (Det), nevertheless, improves this poor performance to some extent due to the receding horizon strategy. However, deterministic MPC is not robust either, meaning that the lower bound or the upper bound of the constraint would be violated, depending on whether the real value of the parameter leads to underestimating or overestimating the output.

The other non-robust method, which is adaptive MPC, is demonstrated in orange dashed lines (Ad). It can be seen that the adaptive method violates the constraints temporarily, but it adjusts itself when the estimated values of the parameters converge to their real values. However, as demonstrated in the second half of the subplot (a) and the first half of the subplot (c), deterministic MPC perpetually violates the constraints. The other advantage of adaptive MPC over deterministic MPC can be seen when the mismatch between the model and real process does not lead to constraint violation, such as in the

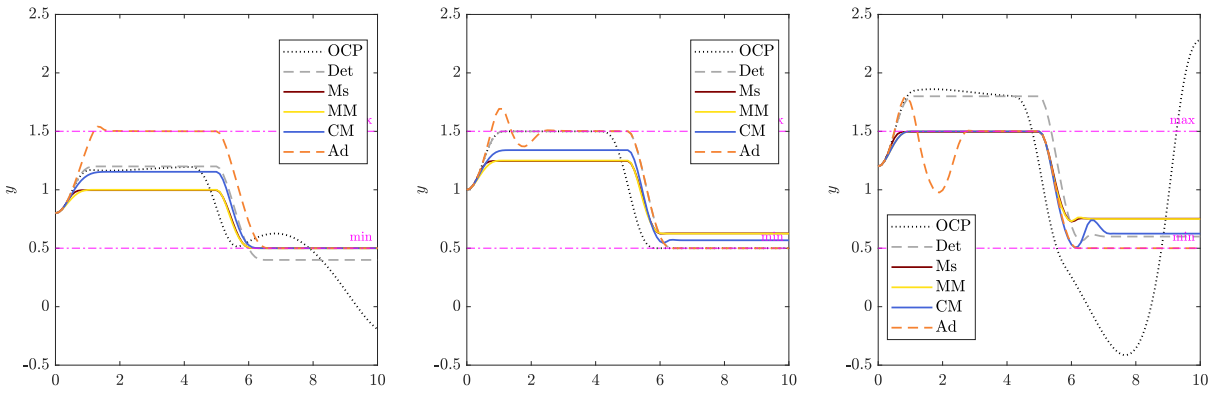

(a) $p = p_{min}$ (b) $p = p_{nom}$ (c) $p = p_{max}$

Figure 4.6: Constrained output and its upper and lower bound for three scenarios.

first half of the subplot (a) and the second half of the subplot (c). One should remember that the objective is to maximize the output in the first half of the simulation and minimize it in the second half; therefore, in these periods, adaptive MPC stands out compared to deterministic MPC in terms of optimality. In other words, it is less conservative, which is more favorable.

Multistage MPC, standard Min-Max MPC, and Min-Max with constraint modification are three methods demonstrated by maroon (Ms), yellow (MM), and blue (CM) solid lines, respectively. It can be seen that neither of these method lead to any constraint violation, which is expected as all of them belong to the category of robust approach. However, their performance is not the same from the optimality/conservativeness point of view. It can be seen that the Min-Max with constraint modification outperforms the two other methods, especially in the first half of the subplot (a) and the second half of the subplot (c).

Computational costs or speed of the methods is the third important factor in evaluating the methods. Accordingly, the execution times of the methods are plotted in Figure 4.7. It can be seen that the deterministic MPC is the simplest and fastest method. Adaptive MPC stands in the second rank as it handles the uncertainty outside the optimization problem, and the optimization problem itself is deterministic. The robust methods, on the other hand, take a longer time to solve the problem due to their complexity. Multistage MPC outperforms the standard Min-Max MPC in terms of execution time, while the execution time for standard Min-Max MPC and Min-Max with constraint modification is approximately equal. It should be mentioned that the considered toy example is a small-scale problem, whereas, for larger problems, the difference may become more significant.

To summarize, the inadequacy of deterministic MPC and the extremely poor performance of open-loop optimal control hinder them from being useful when it comes to handling uncertainty. However, it becomes apparent that among the four remaining methods, no

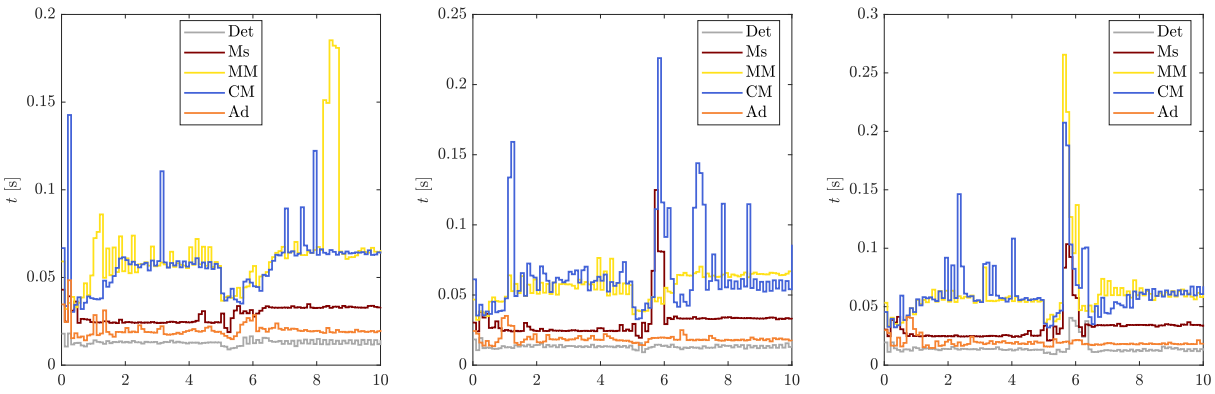

(a) $p = p_{min}$ (b) $p = p_{nom}$ (c) $p = p_{max}$

Figure 4.7: Execution time for three scenarios.

method prevails over the others in all aspects, and their relevance is highly dependent on the requirements of the specific application.

5 Summary of Papers

This chapter presents a concise review of the research outcomes, which have been previously published in peer-reviewed journals and conference papers. In an effort to avoid redundancy, this chapter refrains from duplicating the content that is already present in those publications. Instead, its focus lies in illustrating the interconnections between these works, demonstrating how the outputs of each paper naturally and logically progress into the next. The goal of this chapter is to serve as a unifying element that brings together all the different components of the research into a cohesive whole. The connection between papers and their scope is demonstrated in Figure 5.1.

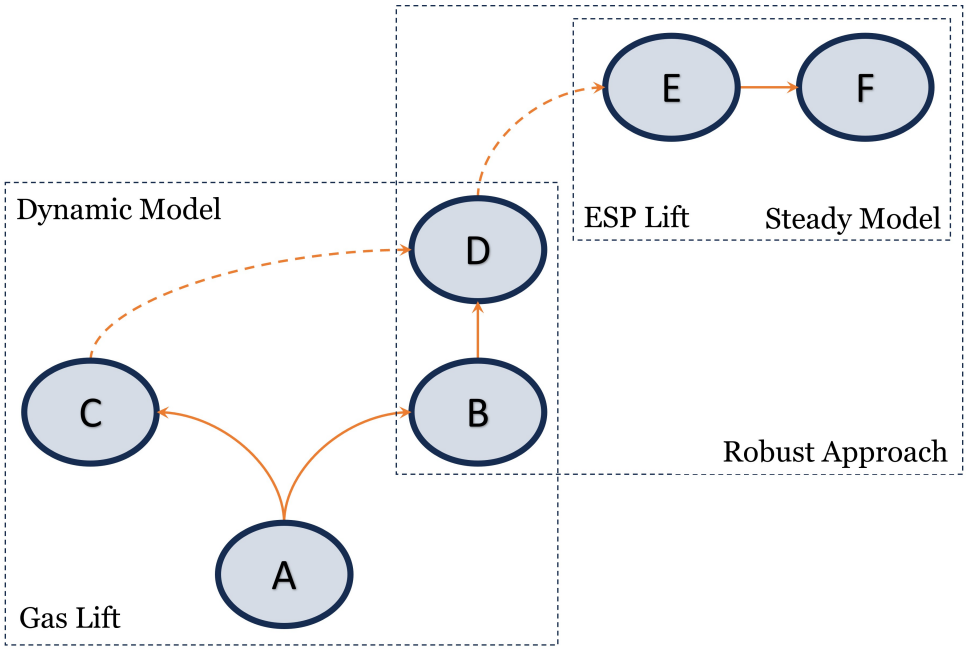

Figure 5.1: Roadmap of the papers generated throughout the journey.

5.1 Paper A: Foundation

Paper A is entitled "Model based control and analysis of gas lifted oil field for optimal operation" and was published in the proceedings of the first SIMS EUROSIM 2021 Con-

ference on Modelling and Simulation. This paper was considered to be the starting point for tackling the research objectives. More specifically, it was meant to develop the mathematical model required for optimization and control, and also to demonstrate the effect of parametric uncertainty, and finally, justify the importance of considering uncertainty in the optimization problem. The gas-lifted artificial lifting method was chosen as the case study because the industrial partner was more interested in gas-lifted oil fields.

5.1.1 Motivations

Three main objectives are pursued in this paper. First, to build a simple mechanistic model to be used in model-based optimization. The model is required to be accurate to capture the dynamics of the system, and it should be simple for being used in optimization and control. In particular, this paper aims to improve the previous model developed at USN [5] by incorporating a more realistic assumption on the composition of the fluid in the reservoir. In the previous model, it was assumed that the reservoir contained single-phase pure oil; however, paper A accounts for three-phase fluid in the reservoir, which comprises oil, water, and gas.

The second objective is to classify parameters that are both sensitive and uncertain simultaneously. It is important to identify the uncertain and sensitive parameters because if the desired output (here, total oil production from the field) is not sensitive to a parameter, the uncertainty in that parameter can be neglected, whereas if a parameter is sensitive and uncertain, it can cause problems.

The third aim of this paper is to study the effect of parametric uncertainty on the optimal distribution of lift gas between the wells in a production unit. More specifically, it is desired to demonstrate that neglecting the uncertainty in the optimization problem may lead to an infeasible solution due to constraint violations, which is a direct effect of the mismatch between the prediction model in the controller and the real plant. This justifies the necessity of considering the uncertainty in the optimization problem.

5.1.2 Result and Discussion

To fulfill the first objectives, a first principle model has been derived based on the mass balance of different phases in different components of the gas-lifted oil well. It is assumed that the reservoir contains a mixture of oil, gas, and water. It has been shown that the derived model is capable of capturing all the necessary dynamics while it is simple enough for control and optimization purposes.

It is useful to figure out which parameters have a strong/weak influence on the model output, especially under the presence of uncertainties, because the model-based control design will be more problematic and needs more care if the uncertain parameters are

sensitive as well. The variance-based global sensitivity analysis method is selected due to its valuable features such as model independence, capacity to capture the influence of the full range of variation of each input factor, and appreciation of interaction effects among input factors.

The first order and total sensitivity indices are calculated using the variance-based method introduced in [116]. A number of 136000 Monte Carlo simulations have been executed to calculate the sensitivity indices. The output of interest is the total oil production from the field, and the productivity index, gas to oil ratio, and water cut are considered to be the parameters. Both sensitivity indices show that for the considered uncertainty region, gas to oil ratio is the most sensitive/influential parameter, and productivity index and water cut stand in the second and third place, respectively. In other words, the standard controller based on the nominal model will be more robust to deviation in water cut. On the other hand, a slight deviation in the gas to oil ratio leads to a severe mismatch between the nominal and uncertain model; therefore, poor performance is expected. These interpretations are verified by simulation results and analysis.

To achieve the third goal, a deterministic nonlinear model predictive controller is designed based on the nominal values of the parameters to maximize the total oil production from the network by optimally distributing a limited amount of lift gas between several oil wells. Apart from the model equations and also the upper and lower bounds on control inputs and change of control due to the physical limitation of the actuators (valves), the process is subjected to two main operational constraints. First, the total injected lift gas needs to be equal to or less than the total available lift gas, and second, the total produced fluid should not exceed the maximum handling capacity of the separator. The first constraint is easier to handle as the uncertainty does not appear in control inputs. However, the latter constraint on the output has proven to be problematic due to the presence of uncertainty.

The controller is tested in several scenarios against the plant with nominal and uncertain parameters. Simulation results show that when the deterministic MPC is applied to the nominal model, the total oil production is increased, and all the constraints are satisfied. In the other scenarios, the same controller is applied to the models containing uncertainties to investigate whether the controller can cope with the uncertainties in the model or not. The results demonstrate that for the extreme cases where the uncertain parameters take their maximums and minimums in the uncertainty region, constraints would be violated, and severe oscillations occur that lead to instability.

5.1.3 Conclusions

This paper presents a model-based control and analysis of a gas-lifted oil field with five oil wells for optimal operation. The simulation results demonstrate that the deterministic

certainty equivalent MPC based on nominal values of parameters is capable of fulfilling the desired performance when it is applied to the model with the nominal realization of the parameters. However, if the real plant takes a different realization for uncertainty, the MPC framework fails to respect the constraints, meaning the solution is practically infeasible if the robust fulfillment of the constraints is required. This suggests that the inherent robustness of MPC is not sufficient, and the uncertainty needs to be taken into account explicitly by using the Robust, Stochastic, or Adaptive approach. Therefore, paper A leads to two separate directions to explore opportunities for further improvements. The robust approach is investigated in Paper B, and the adaptive approach is studied in Paper C.

5.2 Paper B: Robust Approach

As discussed in section 5.1, neglecting the uncertainty leads to constraint violations; therefore, the uncertainty needs to be taken into account if there is a strict requirement for respecting the constraints. As a result, this paper provides a robust framework for the short-term optimization of gas-lifted oil systems, assuming circumstances that no constraint violation can be tolerated. In a bigger picture, it is meant to scrutinize the robust methods for dynamic optimization under uncertainty in order to shed light on the pros and cons of the methods and ultimately explore the possibilities for further improvements that are at least applicable to our particular case study. Paper B is entitled "Multi-stage scenario-based MPC for short term oil production optimization under the presence of uncertainty" and was published in the Journal of Process Control.

5.2.1 Motivations

Two main objectives are followed in this paper. The first objective is to develop a multistage scenario-based control framework for the short-term optimization of a gas lift oil system that can assure robust performance under the presence of parametric uncertainties. The second objective, on the other hand, is to investigate the superiority of the developed framework compared with the other robust counterparts, such as min-max MPC, in terms of conservativeness and execution time.

Although the application of multistage MPC and its comparison to worst-case MPC was studied for gas-lifted oil fields earlier in [84], considering the water cut is a crucial difference that was neglected in previous works. The distinction from the previous work is not limited to an increase in the number of uncertain parameters and the complexity of the problem, but also, from a practical point of view, it relates to considering a more realistic assumption on modeling of the process and the optimization problem as well. More specifically, the water cut, which was neglected in the previous work, is the most

varying (uncertain) parameter. So, neglecting the water in the reservoir makes the model unrealistic. Furthermore, since the most rapid changes occur in the water cut, neglecting the water cut may totally influence the optimization problem. In addition to a more realistic model, the comprehensive analysis provided in this paper is another significant difference that contributes to gaining a better understanding of multistage MPC, open-loop, and closed-loop optimization methods and their pros and cons.

5.2.2 Result and Discussion

The first objective is pursued by designing a multistage nonlinear model predictive controller based on a scenario tree with 65 scenarios to optimally distribute a limited amount of lift gas among two oil wells while the two main constraints in the problem are robustly satisfied. The success of multistage MPC in robust fulfillment of the constraints method is demonstrated by drawing a comparison between the proposed multistage MPC and a deterministic MPC based on the nominal model. However, reducing the number of considered oil wells from 5 wells in paper A to 2 wells in this paper clearly highlights the fact that the computational cost for multistage MPC is a considerable challenge for the robust approach. Considering only one more oil well in the field would increase the number of scenarios from 65 to 513, which would make the optimization problem intractable. The comparison between the total produced oil in deterministic and multistage MPC illustrates an even more critical limitation of the robust approach, which is conservativeness. The reason that conservativeness can be even more problematic than the computational cost can be explained by considering that it is not beyond the imagination that the computation expenses may become affordable in the future as the calculation resources progress. However, conservativeness is an inherent characteristic of the robust approach and can be considered as a paying price to achieve robustness.

The superiority of the multistage MPC in terms of conservativeness is elaborated in comparison between the multistage MPC and an open-loop min-max MPC to achieve the second objective. Accordingly, a min-max MPC is designed based on the worst-case scenario open-loop optimization, which means the notion of feedback is not considered explicitly in the optimization problem, and a single control trajectory is used to calculate the objective function over all the possible scenarios. The comparison between multistage and open-loop min-max MPC demonstrates that the multistage MPC is less conservative, which means that the real power of control has been exploited, and the solution is closer to the optimal operation.

A comparison between the multistage framework and closed-loop min-max MPC depicts that the multistage method is 4 to 5 times faster in small-scale problems, while in a large-scale problem, the difference was even more noticeable. Therefore, the multistage MPC has a better performance in terms of conservativeness compared with open-loop min-max MPC and execution time compared with closed-loop min-max MPC. It should

be noted that this paper utilizes some apriori knowledge of gas lift operation in the design of open-loop min-max MPC. Particularly, it is known in advance that the worst-case situation for the constraints happens when the productivity index and gas to oil ratio take their maximum values, and the water cut takes its minimum value. Incorporating this information in the optimization problem decreases the computation costs of open-loop min-max MPC below the multistage method; however, such information is not available in general. In fact, the general case is the opposite, and multistage MPC defeats the open-loop min-max MPC in terms of execution time, as demonstrated in section 4.7.

The uncertainty description was also investigated through simulation cases where different ranges and distributions were considered in the control design. The simulations demonstrated the conservativeness will be reduced for a smaller range of uncertainty. However, one should accept the risk that the system will fail if the very rare parameter realization occurs. In other words, the worst-case realization of parameters must be considered in the scenario tree. Otherwise, the controller would not cope with the uncertainty when the worst-case realization of parameters happens. It has been shown that using a truncated uncertainty description in control design improves the conservativeness of working in nominal operational conditions, while the controller loses its robustness for the worst-case operational condition.

5.2.3 Conclusions

This paper presents the design and a vast analysis of the robust approach for the gas-lifted well system and total oil production maximization as a dynamic real-time optimization problem under the presence of parametric uncertainty. The multistage MPC and both open-loop and closed-loop versions of the min-max MPC are studied and evaluated through several simulation cases. Despite the advantages and disadvantages of one method over the other, the whole family of robust methods shares some features that are noteworthy to build a big picture and possibly make further improvements in the methods.

The promising capability of the robust approach in fulfilling the constraints under the presence of uncertainty comes at a cost. The first is the computational cost, which can become prohibitively high and make the problem intractable. The computational complexity is still an open problem for research in two directions. The first direction, from the problem formulation point of view, is to formulate the optimization problem in a way that reduces the complexity of robust optimization. The second direction is to develop more efficient numerical algorithms to reduce the execution time.

The second limitation is the conservativeness, which is common among all the robust methods. The conservativeness of robust optimization methods can be understood as the unexploited possibility for better performance, which is neglected in order to achieve a

guarantee for the satisfaction of uncertainty. Therefore, conservativeness is undesirable, and it can be considered as the opposite of optimality. This aspect is the subject of the next two papers. Paper C investigates the adaptive approach by giving up on robust satisfaction of the constraints. On the other hand, paper D improves the conservativeness of the robust method while the robustness is also preserved.

5.3 Paper C: Adaptive Approach

After justifying the necessity of considering uncertainty in paper A, paper B provided a robust framework for the short-term optimization of gas-lifted oil systems, assuming circumstances that no constraint violation can be tolerated. However, this presumption may be violable in some cases. Additionally, the robust methods are inherently conservative, and it may be more beneficial for some specific applications to let the constraints be violated minorly in order to obtain a better overall performance. Therefore, paper C is going to take the other direction and explore the adaptive approach for handling the uncertainty in the same problem, assuming the constraints may be violated dynamically, for instance, by flaring the excessive production. Paper C is entitled "A reactive approach for real-time optimization of oil production under uncertainty" and was published in the proceedings of the American Control Conference 2023.

5.3.1 Motivations

The primary motivation for paper C is to avoid the prohibitive computation and conservative solution of the robust approach by handling the uncertainty outside the optimization problem using an adaptive approach. Accordingly, this paper aims to develop a simple and efficient implementation of the optimization under uncertainty by first employing an estimation algorithm to estimate the states and uncertain parameters in real-time; and then using the estimated model to solve a certainty-equivalent MPC to maximize the monetary profit from the gas lift oil network.

5.3.2 Result and Discussion

The objective is pursued by developing a moving horizon estimation scheme that uses measurable outputs in order to estimate the states and uncertain parameters jointly. The estimation of the uncertain parameters is then fed into the optimization problem, and the optimization problem is solved as a deterministic problem. A multistage MPC is also designed for the comparison.

A comparison between the proposed adaptive framework and the multistage MPC is conducted to investigate their strengths and weaknesses. The simulations demonstrate that the adaptive approach is less conservative and more profitable. It also demonstrates that the adaptive approach is considerably faster. Despite these advantages, the adaptive method violates the constraint on the separator capacity for some periods of time. The constraint violation occurs due to lag in parameter estimation when the parameters change. Therefore, the adaptive approach is not robust to change in parameters. The simulations show that the performance of the adaptive method is highly dependent on the speed and accuracy of parameter estimation and the characteristics of the process. In other words, this method is desirable when the parameters of the plant do not change rapidly, and the constraint violation is allowed for some limited periods of time.

5.3.3 Conclusions

The main contributions of this work are twofold. First, to develop an efficient adaptive framework for optimization under uncertainty that is significantly faster than its robust counterpart. Second, developing a real-time combined state and parameter estimation algorithm that is more practical than a full state feedback setting. Simulations show that the proposed online estimation method not only addresses the uncertainty in a computationally efficient manner but also significantly reduces conservativeness. The other promising feature of the method is that it makes use of measurable outputs instead of unmeasurable states; therefore, it is more realistic from a practical perspective. However, the performance of the method deteriorates in transition periods, particularly when the system's parameters change rapidly. Nevertheless, when the estimations converge to the actual values, the adaptive MPC will be adjusted quickly to respect the constraints.

To draw a fair conclusion, it has to be said that when the uncertainty in the problem is due to unknown or slowly changing parameters and high performance is more desirable than robust fulfillment of the constraints; the adaptive approach is more profitable. On the other hand, a robust approach is preferable when the uncertainty is considerably stochastic in nature, such as random exogenous disturbances, or when the robust fulfillment of the constraint is necessary. Therefore, paper D explores the possibility of addressing the problem of conservativeness while the robust satisfaction of the constraints is still preserved.

5.4 Paper D: Improved Conservativeness

The vast analysis provided in paper B demonstrated that conservativeness, which in the context of oil production optimization can be interpreted as an unexploited possibility for more production, is an inevitable drawback of a robust approach. On the other hand, the

existing methods to reduce the conservativeness are either too computationally heavy, such as stochastic methods, or they deteriorate the robust performance, such as the adaptive approach as explored in paper C. Therefore, paper D utilizes the knowledge gained from papers B and C to provide a simple and efficient method for the short-term optimization of gas-lifted networks to mitigate the conservativeness of the robust approach while the robust fulfillment of the constraints is still preserved. Paper D is entitled "A robust model predictive control with constraint modification for gas lift allocation optimization" and was published in the Journal of Process Control.

5.4.1 Motivations

The primary motivation of this paper is to address the problem of conservativeness in the robust approach. It has been observed earlier in paper B that for the given gas lift oil field case study, the output constraint (separator capacity) is upper bounded, and the conservativeness arises from overestimating output by the controller in the prediction part. Therefore, paper D aims to provide a simple innovative method to compensate for this overestimation by modifying the active output constraint in the worst-case MPC formulation. The most important requirement of the method is that the output (constraint) should be directly measurable, which is a valid assumption for the total flow from the field.

The proposed method in this paper is based on the worst-case realization of the uncertainties with constraint modification. More specifically, the mismatch between measured and predicted output is used directly to modify the active constraint in the optimization problem. Since the design is based on the worst-case situation, there will be no mismatch between the prediction and measurement when the worst-case realization of the uncertainty occurs. Under such conditions, the method reduces to traditional min–max MPC. However, for the other realizations of uncertainty, the constraint modification leads to a higher production rate and thus results in a less conservative operation.

5.4.2 Result and Discussion

Although the output error was employed in the early versions of predictive control [115] and later in more recent versions of adaptive model predictive control [60], the fundamental distinction between the proposed method of this paper and previous works lies in the role of measurements. Despite the adaptive approach, which makes use of output error to estimate the uncertainty and utilizes the estimated values of uncertainty in the optimization problem, in the proposed method of this paper, the output error is used directly to reconstruct the boundary on constraints in the optimization problem, meaning the method does not contain any estimation algorithm. Paper C demonstrated that in an adaptive approach, the constraints can be violated dynamically during the transient

periods due to the lag in the parameter estimation step. However, the proposed method of this paper does not estimate the parameters. Instead, the measurement is used to modify the constraint boundaries directly. The second major difference is that contrary to the adaptive approach, the optimization problem in the proposed method is based on the worst-case realization of the uncertainty, which enables this method to fulfill the constraints robustly for all the realizations of uncertainty within the considered bounded set.

Additionally, a multistage MPC and open-loop min-max MPC are designed to demonstrate the promising advantages of the proposed novel method over other robust methods. All the competing methods are applied to a gas-lifted oil field with two oil wells in three simulation cases. It has been shown that when the uncertain parameters of the process take their worst-case realizations, all three methods are able to satisfy the constraints, i.e., all methods are robust within the uncertainty region. However, when the uncertain parameters take other realizations, the proposed method is significantly less conservative than min–max and multistage methods; therefore, the proposed method is superior to both min–max and multistage methods because it preserves the robust performance and reduces the conservativeness significantly. The simulation results also demonstrate that the complexity of the method is at the level of min–max MPC, and for this specific case study, it is considerably more straightforward and more efficient than multistage MPC.

5.4.3 Conclusions

This paper presents a novel approach for implementing a robust real-time optimization framework under the presence of parametric uncertainty. Several simulation cases demonstrate that the conservativeness, which is an inevitable drawback of a robust control approach, is decreased significantly. While, contrary to adaptive approach, the robust satisfaction of the constraints is preserved. The other promising advantage of the proposed method is that it does not increase the complexity of the standard robust methods such as min-max MPC.

It should be mentioned that although some apriori knowledge about the process has been used to simplify the min–max MPC which may not be available in general; however, the method at least does not impose any further complexity on the original min–max formulation. While on the contrary, multi-stage MPC introduces too much complexity with less reward in terms of conservativeness. The other limitation of the method is that it requires the active constraints to be measurable, which is an admissible requirement for several chemical processes since the constrained outputs are mostly pressures, temperatures, or flows. Therefore, the method can be generalized to be applicable to a class of systems where this requirement is fulfilled, although it has been developed based on special features of a specific case study.

This paper sums up the work on the gas lift oil field as the case study. Paper D is also the last paper in this dissertation that utilizes the dynamic model in real-time optimization. In the next two papers, E and F, the ESP-lifted oil field is used as the case study. More specifically, paper E makes use of the steady-state version of the ESP model in the optimization problem to investigate other aspects of the uncertainty, such as the uncertainty in oil price. Finally, paper F focuses on testing similar algorithms against a more sophisticated representation of the plant.

5.5 Paper E: Daily Production Optimization

Paper E investigates the problem of daily production optimization for an Electric Submersible Pump lifted oil field with three oil wells under the presence of uncertainty. Despite the efforts in papers B and C to address the real-time optimization under uncertainty and despite the minor improvement in paper D for the gas lift case study, some challenges still remained. First and foremost, the computational cost of using the dynamic model in real-time optimization is extremely high. The longest possible prediction horizon in papers A to D could not exceed ten minutes. However, the prediction horizon in daily production optimization typically ranges from a few hours to a couple of days. Additionally, considering the ESP-lifted oil field as the new case study made this problem even more challenging because the fast dynamics in ESP-lifted wells require a shorter sampling time, meaning that the computations have to be executed even faster. Therefore, the steady-state model of the system has been used in a robust optimization framework. This paper is entitled "Short-term production optimization for Electric Submersible Pump lifted oil field with parametric uncertainty" and was published in IEEE Access.

5.5.1 Motivations

Two main objectives are pursued in this paper. The first objective is to investigate the daily production optimization from an ESP oil field with multiple oil wells, considering the parameter uncertainty. This requires using the steady-state version of the previous model developed at USN [5] with minor modifications. ESP-lifted oil field adds different types of constraints in the optimization problem, e.g., the operational envelope of ESPs. The scenario-based robust optimization framework is employed to fulfill these constraints for all the realizations of uncertain parameters. The second objective, on the other hand, is to exploit the potential provided by the steady-state model and scenario-based framework to study the different forms of uncertainty. Particularly, the uncertainty in the oil price and the uncertainty in well flow parameters are investigated to evaluate their influence on the optimization problem.

5.5.2 Result and Discussion

To improve the mathematical model from previous work [5], the assumption of constant water cut in the production manifold is substituted by a more realistic one. Therefore, instead of injecting water to keep the water cut constant, which needs a perfect controller, a constant flow of water is injected into the manifold. Accordingly, the water cut of the liquid phase within the manifold varies and depends on the proportion of fluid produced from production chock valves. It has been shown that using the dynamic model of the plant in the optimization problem is too computationally expensive, even in a deterministic case. Accordingly, the fairly long prediction horizon of DPO is divided into segments, and the plant is considered to operate at a possibly new steady-state over each segment. Therefore, the piecewise steady-state model of the plant is used as the prediction model to determine the future of the system over each segment. The daily production optimization is formulated as successive scenario-based optimization problems in a receding horizon fashion to address the constraint fulfillment under the presence of uncertainty.

The accomplishment of the proposed method and the necessity of considering uncertainty is demonstrated by a comparison between the deterministic optimization based on the nominal model and the scenario-based optimization applied to a plant containing uncertainty. It has been shown that scenario-based optimization for daily production optimization yields a robust solution and safe operation of the ESP pump and also satisfaction of other operational constraints.

Additionally, two simulation cases are proposed to study the effect of uncertainty on the oil price. The first simulation compares the optimization under constant oil prices and also varying oil prices with uncertainty. The results demonstrate that although the absolute values of income for the two cases are different (due to differences in oil prices), the amount of produced fluid for the two cases is identical, meaning that uncertainty in oil prices does not influence the optimal solution itself. The second simulation, whereby the oil price drops significantly low, demonstrates that the optimizer works properly and decreases the production to the minimum allowed production when producing from the field is not profitable anymore. On the other hand, the investigation of the range of considered uncertainty in well flow parameters reveals that contrary to the oil price, the uncertainty related to the well characteristics is significantly important, and the net profit from a field can be increased by reducing the uncertainty in well flow parameters.

5.5.3 Conclusions

Paper E employs the scenario-based optimization method to address the daily production optimization for an ESP-lifted oil field under parametric uncertainty. This paper yields two key findings. Firstly, utilizing scenario-based optimization effectively manages

uncertainty in daily production optimization. This is crucial because deviating from optimal pump operation reduces their lifespan and entails costly repairs. Secondly, while price uncertainty can be disregarded in short-term optimization, it is vital to account for uncertainties in well characteristics. This implies an intuitive and yet interesting conclusion, that is, the economic objective would be translated to achieving either maximum or minimum production, depending on whether the production is profitable or not.

5.6 Paper F: Combined Well-Reservoir Model

Paper F is entitled "Investigating the performance of robust daily production optimization against a combined well–reservoir model," and it is under review in the Modeling, Identification and Control journal. This paper extends the daily production optimization problem for an ESP lift oil field under the presence of uncertainty, investigated in paper E, by incorporating a more sophisticated representation of the actual plant in order to facilitate the implementation of the method in real-life applications. Although both papers E and F make use of a simple linear well flow model with productivity index and water cut in the optimization problem, the distinction between the two works lies in the inclusion of a more advanced plant model in this work to accurately portray the actual process. To this end, a reservoir model is combined with the well model in a simple and efficient way to represent the real process. Particularly, instead of testing the optimization algorithm against the same linear model with different parameters, a combined well-reservoir model is tailored to evaluate the performance of the optimization algorithm.

5.6.1 Motivations

The primary objective of this paper is to develop a combined well-reservoir model to test the robust optimization algorithm against a more realistic representation of the actual process. Therefore, further adjustments in the model developed in paper E is required. In this paper, the ESP frequency and desired production rate are the inputs to the plant. The production rate is fed into the reservoir model as well controls, while the true response of the reservoir is utilized alongside the pump frequency in the well model to compute the other outputs such as wellhead pressure and head of the pump, etc. Employing this straightforward combined model instead of a well model with synthetic varying parameters makes it possible to benefit from a more accurate representation of the plant by capturing the variation of uncertainty interactively in accordance with the dynamic of the reservoir and its history.

5.6.2 Result and Discussion

In order to achieve the objectives, the steady-state model of the ESP wells was combined with the reservoir model in a simple and efficient way. Therefore, although the optimization algorithms themselves are based on top-side well models, their performance was evaluated against a more sophisticated model in which the uncertain parameters change interactively in accordance with the dynamic of the reservoir and its history rather than randomly. The simulation results demonstrate that the robust method is able to cope with the uncertainty and fulfill all the constraints while neglecting the uncertainty in the optimization problem leads to constraint violation on wellhead pressures.

5.6.3 Conclusions

This paper utilizes the scenario-based optimization framework to address the robust fulfillment of the constraint in daily production optimization for an ESP-lifted oil field under parametric uncertainty. Additionally, it presented a simple combined well–reservoir model to analyze the performance of the method in a more realistic setting. Thus, it contributes to two major aspects: First, incorporating the explicit notion of uncertainty in daily production optimization, and second, investigating the performance of the method against a more sophisticated representation of the real process.

6 Conclusion and Perspective

This chapter provides a brief summary of the research conducted over the past three years. Since the research outcomes have been published in scientific papers that contain explicit conclusions, the intention here is to offer a global perspective on the work and to recap the key findings and contributions. Subsequently, the future perspective outlines the potential directions for future endeavors within this particular field.

6.1 Conclusion

This thesis covers different methods for short-term oil production optimization under parametric uncertainty. The ultimate goal in production optimization is to maximize the total production or economic return from the field over a short-term horizon by adjusting the decision variables. However, introducing uncertainty into the problem, which is an unavoidable factor for actual implementation, may lead to a constraint violation, i.e., the optimal solution becomes unimplementable if the violated constraint is a hard constraint.

On the other hand, the existing methods for counteracting the negative effect of uncertainty have some challenges, too. The robust methods are inherently conservative, meaning they sacrifice optimality in order to guarantee the fulfillment of constraints. Therefore, making a trade-off between these two conflicting desires, optimality and robustness, is a common challenge for all constrained optimizations under uncertainty, including short-term oil production optimization. The other challenge, which is especially severe for large-scale nonlinear dynamical cases, is that the computational cost of such methods is prohibitively high; therefore, the real-time implementation of such methods is really limited. This research contributes to addressing these challenges by particularly considering short-term production optimization for two oil production methods, namely gas lift and ESP lifting method.

The dynamic optimization under uncertainty is investigated in papers A to D using the gas lift oil field as the case study. In paper A, the mechanistic model of the gas lift system is developed to be used in dynamic optimization by including three-phase (oil-water-gas) fluid. Although developing such a model is not a novel task, its application for dynamic real-time optimization, to the best of our knowledge, is new. This paper also demonstrates

the problems that occur by neglecting uncertainty and justifies the necessity of considering uncertainty.

In paper B, the applicability of the existing robust methods is investigated by applying several robust methods such as multistage MPC, open-loop, and closed-loop min-max MPC. The vast analysis demonstrated that although the methods are capable of guaranteeing the robust fulfillment of the constraints, the price for this achievement is still high. The conservativeness of the existing methods, which in the context of the gas-lifted system can be interpreted as an unexploited capacity for more production, is still a big issue. On the other hand, the computational cost does not allow for considering more than two wells, which does not seem realistic. Therefore, in an overall judgment, real-life implementation of the existing methods for short-term production optimization in gas lift oil fields is under serious doubt.

Alternatively, the applicability of the adaptive approach is explored in paper C. It has been demonstrated that the adaptive approach has more potential to be exploited in real applications. Firstly, the computational cost is hugely cheaper than the robust method. Secondly, it is less conservative, meaning that it is capable of producing more oil than the robust method. Finally, it has a more realistic structure because the states in the gas-lift system, the masses in control volumes, are not measurable. Since the adaptive method is equipped with an estimation block, contrary to the robust method, it only relies on measurable pressures. However, these valuable features come at a cost, and that is loss of robustness, which means the constraint would be violated dynamically during the transition periods; therefore, if the constraint violation is not an option, the method cannot be implemented.

The investigations in paper B demonstrated that the conservativeness of the robust method arises from the fact that the prediction model in the controller overestimates the production. On the other hand, it has been seen in paper C that the measurement can successfully be utilized in order to decrease the conservativeness. Consequently, these two conclusions are employed to reduce the conservativeness of the robust method while the robustness is preserved. This has been accomplished in paper D, particularly by modifying the constraint in traditional min-max MPC. The novel proposed method in this paper, which contributes to the field of dynamic optimization under uncertainty, can be classified between robust and adaptive approaches because, instead of estimating the uncertain parameters, the method uses the measurements to modify the constraint in the optimization problem directly. Despite the success of the proposed method in reducing the conservativeness of the robust methods without imposing extra computational costs, the costs are still prohibitively high for real-life applications in short-term oil production optimization.

Figure 6.1 demonstrates a qualitative comparison of the aforementioned methods in terms of execution speed and optimality. From a general perspective, the multistage MPC stands superior to traditional min-max MPC as it outperforms min-max MPC in terms of both

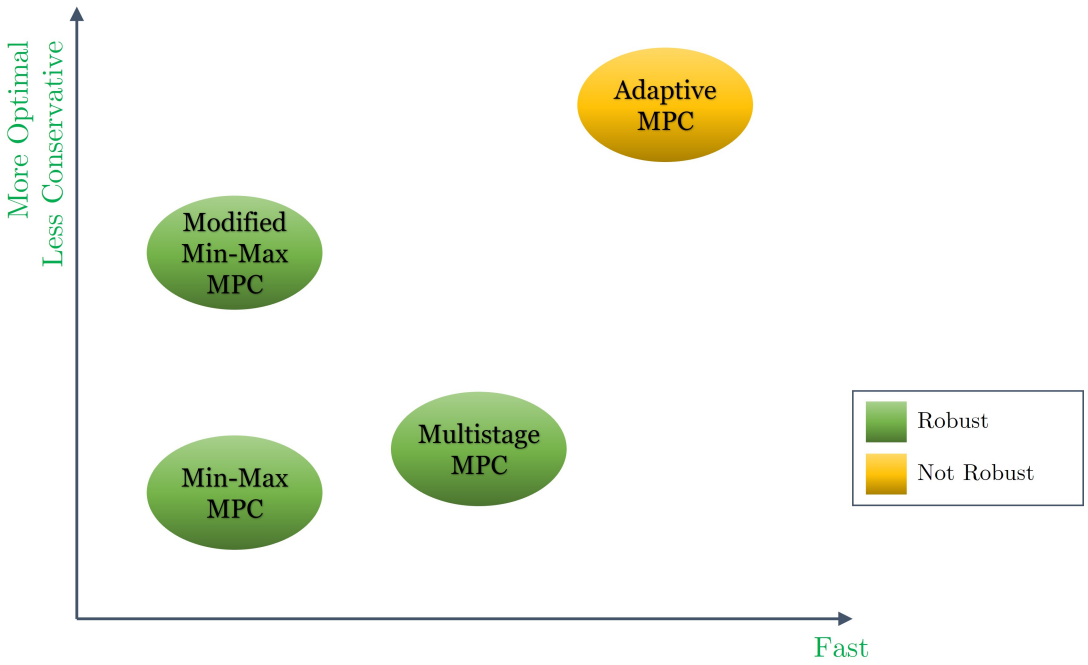

Figure 6.1: Qualitative comparison of methods in terms of speed and optimality/conservativeness.

speed and optimality. However, the remaining three methods have their pros and cons. The adaptive method, which is the fastest and the least conservative method, is not robust, i.e., it fails in cases where the constraints must be strictly respected. On the other hand, each one of the two remaining methods wins the competition in one aspect. Thus, in cases where the bottleneck is the execution time, multistage MPC would be more beneficial. Nevertheless, in cases where the optimality is more preferred, modified min-max MPC would surpass its robust counterparts.

Despite the occasional constraint violations that occur in the adaptive approach, it has the highest chance among the assessed methods for actual implementation in the gas lift oil field as a particular case study. This is because the computational costs for the robust methods are too high. Moreover, the adaptive approach is significantly better in terms of optimality/conservativeness, and it does not rely on unmeasurable states.

The mechanistic model of the ESP system, developed in paper E, clearly shows that formulating the production optimization for the ESP-lifted oil field as a dynamic optimization problem is not tractable. Therefore, the focus of the subsequent two papers, E and F, shifted from dynamic optimization to steady-state optimization.

It has been shown that the robust scenario-based optimization method can be accompanied by the steady-state version of the model to address the presence of parametric uncertainty successfully. The proposed framework is further used to investigate the importance of different types of uncertainty, including the well characteristics and oil price.

It has been shown that contrary to the physical characteristics of the wells, the uncertainty in oil price in the short term is not a significant factor for production optimization. In other words, short-term production optimization greedily maximizes production unless the oil price drops drastically to the point that the economic return from the field becomes negative. Since such a sharp drop in oil price conventionally does not occur over a short time, it is reasonable to neglect the uncertainty in oil price in favor of achieving a reduction in the computational cost.

Finally, paper F develops a more realistic representation of the plant to assess the robust scenario-based framework in a more challenging setup. The combined well-reservoir model developed in this paper is solely used to test the robust framework, while the optimization is yet based on a simple steady-state version of well model. Testing the robust scenario-based framework against the proposed model of this paper, in which the uncertain parameters change interactively in accordance with the dynamic of the reservoir rather than randomly, demonstrates that the scenario-based method can be applied in real applications.

6.2 Future Perspective

Despite the efforts that have been devoted to addressing the challenges of optimization under uncertainty and despite the contributions that have been made through this research work, there are many aspects for further improvement. This can be divided into two separate directions from industrial and academic perspectives, which are further explained hereby.

The computational complexity of the dynamic methods investigated in this thesis made it clear that, at least in the near future, steady-state optimization continues to remain the dominant approach for short-term production optimization in the oil industry. Therefore, from a practical point of view, it is more rewarding to invest in steady-state optimization rather than dynamic optimization under uncertainty. Instead, the resources can be allocated to quantify and reduce the uncertainties by using data assimilation techniques, although such methods heavily rely on the availability of required data.

The other possibility is using a self-optimizing control strategy [117], [118] to avoid solving rigorous optimization problems numerically and instead translate the optimization objectives into control objectives and track the control objectives using classical feedback control; however, handling the constraints remains a challenge that is yet to be addressed.

Extremum Seeking Control[119], as a model-free control technique, is yet another effective alternative that can adapt in real-time to optimize key performance metrics such as

production rate without relying on a precise mathematical model of the system. By introducing controlled perturbations and leveraging feedback mechanisms, the extremum seeking control can mitigate the impact of uncertainty, and thereby potentially enhancing the overall efficiency and profitability of short-term oil production processes.

Despite the limitations of industrial implementation of dynamic real-time optimization under uncertainty, it remains an intriguing topic for further academic research as well. Investigation of numerical algorithms for increasing the speed of the methods is almost always an open challenge and can be explored further as a potential research direction. Machine Learning algorithms and Reinforcement Learning for approximating the optimization problem are the other possible directions that have acquired a great deal of attention recently.

Bibliography

[1] 'Energy statistics data browser.' (2022), [Online]. Available: https://www.iea.org/data-and-statistics/data-tools/energy-statistics-data-browser.

[2] S. Skogestad, 'Plantwide control: The search for the self-optimizing control structure,' *Journal of process control*, vol. 10, no. 5, pp. 487–507, 2000.

[3] B. Foss, 'Process control in conventional oil and gas fields—challenges and opportunities,' *Control Engineering Practice*, vol. 20, no. 10, pp. 1058–1064, 2012.

[4] H. P. Bieker, O. Slupphaug and T. A. Johansen, 'Real-time production optimization of oil and gas production systems: A technology survey,' *SPE Production & Operations*, vol. 22, no. 04, pp. 382–391, 2007.

[5] R. Sharma, 'Optimal operation of gas lifted and esp lifted oil fields: An approach based on modeling, simulation, optimization and control,' PhD Dissertation, Telemark University College, Porsgrunn, Norway, 2014.

[6] B. Foss, B. R. Knudsen and B. Grimstad, 'Petroleum production optimization–a static or dynamic problem?' *Computers & Chemical Engineering*, vol. 114, pp. 245–253, 2018.

[7] D. Krishnamoorthy, K. Fjalestad and S. Skogestad, 'Optimal operation of oil and gas production using simple feedback control structures,' *Control Engineering Practice*, vol. 91, p. 104 107, 2019.

[8] A. Willersrud, L. Imsland, S. O. Hauger and P. Kittilsen, 'Short-term production optimization of offshore oil and gas production using nonlinear model predictive control,' *Journal of Process Control*, vol. 23, no. 2, pp. 215–223, 2013.

[9] B. Grimstad, B. Foss, R. Heddle and M. Woodman, 'Global optimization of multiphase flow networks using spline surrogate models,' *Computers & Chemical Engineering*, vol. 84, pp. 237–254, 2016.

[10] A. P. I. P. Department, *Gas Lift: (book 6 of the Vocational Training Series)* (Vocational training series). American Petroleum Institute, 1984. [Online]. Available: https://books.google.no/books?id=gJe8HAAACAAJ.

[11] L. Imsland, 'Topics in nonlinear control.: Output feedback stabilization and control of positive systems,' 2002.

[12] G. O. Eikrem, L. Imsland and B. Foss, 'Stabilization of gas lifted wells based on state estimation,' *IFAC Proceedings Volumes*, vol. 37, no. 1, pp. 323–328, 2004.

[13] O. M. Aamo, G. O. Eikrem, H. Siahaan and B. Foss, 'Observer design for gas lifted oil wells,' in *Proceedings of the 2004 American control conference*, IEEE, vol. 2, 2004, pp. 1552–1557.

[14] G. Takacs, *Electrical submersible pumps manual: design, operations, and maintenance*. Gulf professional publishing, 2017.

[15] H. J. Sussmann and J. C. Willems, '300 years of optimal control: From the brachystochrone to the maximum principle,' *IEEE Control Systems Magazine*, vol. 17, no. 3, pp. 32–44, 1997.

[16] R. Sargent, 'Optimal control,' *Journal of Computational and Applied Mathematics*, vol. 124, no. 1-2, pp. 361–371, 2000.

[17] S. J. Qin and T. A. Badgwell, 'A survey of industrial model predictive control technology,' *Control engineering practice*, vol. 11, no. 7, pp. 733–764, 2003.

[18] C. E. Garcia, D. M. Prett and M. Morari, 'Model predictive control: Theory and practice—a survey,' *Automatica*, vol. 25, no. 3, pp. 335–348, 1989.

[19] A. I. Propoi, 'Use of lp methods for synthesizing sampled-data automatic systems',' *Automation and Remote Control*, vol. 24, pp. 837–844, 1963.

[20] J. Richalet, A. Rault, J. Testud and J. Papon, 'Model predictive heuristic control: Applications to industrial processes,' *Automatica*, vol. 14, no. 5, pp. 413–428, 1978.

[21] C. R. Cutler and B. Ramaker, 'Dmc-a computer control algorithm,' in *AIChE Annual Meeting, Houston*, 1979.

[22] C. R. Cutler and B. L. Ramaker, 'Dynamic matrix control?? a computer control algorithm,' in *joint automatic control conference*, 1980, p. 72.

[23] D. W. Clarke, C. Mohtadi and P. S. Tuffs, 'Generalized predictive control—part i. the basic algorithm,' *Automatica*, vol. 23, no. 2, pp. 137–148, 1987.

[24] D. W. Clarke, C. Mohtadi and P. S. Tuffs, 'Generalized predictive control—part ii extensions and interpretations,' *Automatica*, vol. 23, no. 2, pp. 149–160, 1987.

[25] D. Q. Mayne, J. B. Rawlings, C. V. Rao and P. O. Scokaert, 'Constrained model predictive control: Stability and optimality,' *Automatica*, vol. 36, no. 6, pp. 789–814, 2000.

[26] G. De Nicolao, L. Magni and R. Scattolini, 'On the robustness of receding-horizon control with terminal constraints,' *IEEE Transactions on Automatic Control*, vol. 41, no. 3, pp. 451–453, 1996.

[27] S. Yu, M. Reble, H. Chen and F. Allgöwer, 'Inherent robustness properties of quasi-infinite horizon nonlinear model predictive control,' *Automatica*, vol. 50, no. 9, pp. 2269–2280, 2014.

[28] D. A. Allan, C. N. Bates, M. J. Risbeck and J. B. Rawlings, 'On the inherent robustness of optimal and suboptimal nonlinear mpc,' *Systems & Control Letters*, vol. 106, pp. 68–78, 2017.

[29] A. Bemporad and M. Morari, 'Robust model predictive control: A survey,' *Robustness in identification and control*, pp. 207–226, 1999.

[30] H. Witsenhausen, 'A minimax control problem for sampled linear systems,' *IEEE Transactions on Automatic Control*, vol. 13, no. 1, pp. 5–21, 1968.

[31] P. J. Campo and M. Morari, 'Robust model predictive control,' in *1987 American control conference*, IEEE, 1987, pp. 1021–1026.

[32] J. H. Lee and Z. Yu, 'Worst-case formulations of model predictive control for systems with bounded parameters,' *Automatica*, vol. 33, no. 5, pp. 763–781, 1997.

[33] P. O. Scokaert and D. Q. Mayne, 'Min-max feedback model predictive control for constrained linear systems,' *IEEE Transactions on Automatic control*, vol. 43, no. 8, pp. 1136–1142, 1998.

[34] A. Bemporad, 'Reducing conservativeness in predictive control of constrained systems with disturbances,' in *Proceedings of the 37th IEEE Conference on Decision and Control (Cat. No. 98CH36171)*, IEEE, vol. 2, 1998, pp. 1384–1389.

[35] J. Lofberg, 'Approximations of closed-loop minimax mpc,' in *42nd IEEE International Conference on Decision and Control (IEEE Cat. No. 03CH37475)*, IEEE, vol. 2, 2003, pp. 1438–1442.

[36] P. J. Goulart, E. C. Kerrigan and J. M. Maciejowski, 'Optimization over state feedback policies for robust control with constraints,' *Automatica*, vol. 42, no. 4, pp. 523–533, 2006.

[37] J. A. Paulson and A. Mesbah, 'Approximate closed-loop robust model predictive control with guaranteed stability and constraint satisfaction,' *IEEE Control Systems Letters*, vol. 4, no. 3, pp. 719–724, 2020.

[38] D. Q. Mayne, M. M. Seron and S. Raković, 'Robust model predictive control of constrained linear systems with bounded disturbances,' *Automatica*, vol. 41, no. 2, pp. 219–224, 2005.

[39] D. Q. Mayne and E. C. Kerrigan, 'Tube-based robust nonlinear model predictive control,' *IFAC Proceedings Volumes*, vol. 40, no. 12, pp. 36–41, 2007.

[40] D. Q. Mayne, E. C. Kerrigan, E. Van Wyk and P. Falugi, 'Tube-based robust nonlinear model predictive control,' *International journal of robust and nonlinear control*, vol. 21, no. 11, pp. 1341–1353, 2011.

[41] P. Falugi and D. Q. Mayne, 'Getting robustness against unstructured uncertainty: A tube-based mpc approach,' *IEEE Transactions on Automatic Control*, vol. 59, no. 5, pp. 1290–1295, 2013.

[42] S. V. Raković, W. S. Levine and B. Açikmese, 'Elastic tube model predictive control,' in *2016 American Control Conference (ACC)*, IEEE, 2016, pp. 3594–3599.

[43] X. Lu and M. Cannon, 'Robust adaptive tube model predictive control,' in *2019 American Control Conference (ACC)*, IEEE, 2019, pp. 3695–3701.

[44] J. Köhler, R. Soloperto, M. A. Müller and F. Allgöwer, 'A computationally efficient robust model predictive control framework for uncertain nonlinear systems,' *IEEE Transactions on Automatic Control*, vol. 66, no. 2, pp. 794–801, 2020.

[45] S. Lucia, T. Finkler and S. Engell, 'Multi-stage nonlinear model predictive control applied to a semi-batch polymerization reactor under uncertainty,' *Journal of process control*, vol. 23, no. 9, pp. 1306–1319, 2013.

[46] J. R. Birge and F. Louveaux, *Introduction to stochastic programming*. Springer Science & Business Media, 2011.

[47] D. Krishnamoorthy, B. Foss and S. Skogestad, 'A distributed algorithm for scenario-based model predictive control using primal decomposition,' *IFAC-PapersOnLine*, vol. 51, no. 18, pp. 351–356, 2018.

[48] D. Krishnamoorthy, B. Foss and S. Skogestad, 'A primal decomposition algorithm for distributed multistage scenario model predictive control,' *Journal of Process Control*, vol. 81, pp. 162–171, 2019.

[49] A. T. Schwarm and M. Nikolaou, 'Chance-constrained model predictive control,' *AIChE Journal*, vol. 45, no. 8, pp. 1743–1752, 1999.

[50] T. A. N. Heirung, J. A. Paulson, J. O'Leary and A. Mesbah, 'Stochastic model predictive control—how does it work?' *Computers & Chemical Engineering*, vol. 114, pp. 158–170, 2018.

[51] A. Mesbah, 'Stochastic model predictive control: An overview and perspectives for future research,' *IEEE Control Systems Magazine*, vol. 36, no. 6, pp. 30–44, 2016.

[52] Y. Ma, J. Matuško and F. Borrelli, 'Stochastic model predictive control for building hvac systems: Complexity and conservatism,' *IEEE Transactions on Control Systems Technology*, vol. 23, no. 1, pp. 101–116, 2014.

[53] F. Weissel, M. F. Huber and U. D. Hanebeck, 'Stochastic nonlinear model predictive control based on gaussian mixture approximations,' in *Informatics in Control, Automation and Robotics: Selected Papers from the International Conference on Informatics in Control, Automation and Robotics 2007*, Springer, 2009, pp. 239–252.

[54] A. Mesbah, S. Streif, R. Findeisen and R. D. Braatz, 'Stochastic nonlinear model predictive control with probabilistic constraints,' in *2014 American control conference*, IEEE, 2014, pp. 2413–2419.

[55] D. Mayne, 'Robust and stochastic model predictive control: Are we going in the right direction?' *Annual Reviews in Control*, vol. 41, pp. 184–192, 2016.

[56] B. J. Binder, A. Pavlov and T. A. Johansen, 'Estimation of flow rate and viscosity in a well with an electric submersible pump using moving horizon estimation,' *IFAC-PapersOnLine*, vol. 48, no. 6, pp. 140–146, 2015.

[57] D. A. Copp and J. P. Hespanha, 'Nonlinear output-feedback model predictive control with moving horizon estimation,' in *53rd IEEE conference on decision and control*, IEEE, 2014, pp. 3511–3517.

[58] D. A. Copp, R. Gondhalekar and J. P. Hespanha, 'Simultaneous model predictive control and moving horizon estimation for blood glucose regulation in type 1 diabetes,' *Optimal Control Applications and Methods*, vol. 39, no. 2, pp. 904–918, 2018.

[59] D. Q. Mayne, 'Model predictive control: Recent developments and future promise,' *Automatica*, vol. 50, no. 12, pp. 2967–2986, 2014.

[60] P. d. A. Delou, J. P. de Azevedo, D. Krishnamoorthy, M. B. de Souza Jr and A. R. Secchi, 'Model predictive control with adaptive strategy applied to an electric submersible pump in a subsea environment,' *IFAC-PapersOnLine*, vol. 52, no. 1, pp. 784–789, 2019.

[61] T. Chen, N. F. Kirkby and R. Jena, 'Optimal dosing of cancer chemotherapy using model predictive control and moving horizon state/parameter estimation,' *Computer methods and programs in biomedicine*, vol. 108, no. 3, pp. 973–983, 2012.

[62] D. A. Copp, T. A. Nguyen and R. H. Byrne, 'Adaptive model predictive control for real-time dispatch of energy storage systems,' in *2019 American Control Conference (ACC)*, IEEE, 2019, pp. 3611–3616.

[63] A. Capolei, L. H. Christiansen and J. B. Jørgensen, 'A novel approach for risk minimization in life-cycle oil production optimization,' in *Computer Aided Chemical Engineering*, vol. 40, Elsevier, 2017, pp. 157–162.

[64] A. Capolei, L. H. Christiansen and J. B. Jørgensen, 'Risk minimization in life-cycle oil production optimization,' *arXiv preprint arXiv:1801.00684*, 2018.

[65] A. Codas, K. G. Hanssen, B. Foss, A. Capolei and J. B. Jørgensen, 'Multiple shooting applied to robust reservoir control optimization including output constraints on coherent risk measures,' *Computational Geosciences*, vol. 21, pp. 479–497, 2017.

[66] A. Capolei, B. Foss and J. B. Jørgensen, 'Profit and risk measures in oil production optimization,' *IFAC-PapersOnLine*, vol. 48, no. 6, pp. 214–220, 2015. DOI: 10.1016/j.ifacol.2015.08.034.

[67] K. G. Hanssen, A. Codas and B. Foss, 'Closed-loop predictions in reservoir management under uncertainty,' *SPE Journal*, vol. 22, no. 5, pp. 1585–1595, 2017. DOI: 10.2118/185956-PA.

[68] B. Chen, R.-M. Fonseca, O. Leeuwenburgh and A. C. Reynolds, 'Minimizing the risk in the robust life-cycle production optimization using stochastic simplex approximate gradient,' *Journal of Petroleum Science and Engineering*, vol. 153, pp. 331–344, 2017.

[69] Z. Guo and A. C. Reynolds, 'Robust life-cycle production optimization with a support-vector-regression proxy,' *Spe Journal*, vol. 23, no. 06, pp. 2409–2427, 2018.

[70] A. Ben-Tal and A. Nemirovski, 'Robust solutions of linear programming problems contaminated with uncertain data,' *Mathematical programming*, vol. 88, pp. 411–424, 2000.

[71] H. P. Bieker, O. Slupphaug and T. A. Johansen, 'Well management under uncertain gas/or water/oil ratios,' in *SPE Digital Energy Conference and Exhibition*, SPE, 2007, SPE–106 959.

[72] S. M. Elgsæter, O. Slupphaug and T. A. Johansen, 'A structured approach to optimizing offshore oil and gas production with uncertain models,' *Computers & chemical engineering*, vol. 34, no. 2, pp. 163–176, 2010.

[73] D. Krishnamoorthy, 'Novel approaches to online process optimization under uncertainty: Addressing the limitations of current industrial practice,' PhD Dissertation, Norwegian University of Science and Technology, Trondheim, Norway, 2019.

[74] A. Codas, E. Jahanshahi and B. Foss, 'A two-layer structure for stabilization and optimization of an oil gathering network,' *IFAC-PapersOnLine*, vol. 49, no. 7, pp. 931–936, 2016.

[75] R. Sharma, K. Fjalestad and B. Glemmestad, 'Optimization of lift gas allocation in a gas lifted oil field as non-linear optimization problem,' *Modeling, Identification and Control*, vol. 33, no. 1, pp. 13–25, 2012.

[76] R. Sharma and B. Glemmestad, 'On generalized reduced gradient method with multi-start and self-optimizing control structure for gas lift allocation optimization,' *Journal of Process Control*, vol. 23, no. 8, pp. 1129–1140, 2013.

[77] D. Krishnamoorthy, B. Foss and S. Skogestad, 'Steady-state real-time optimization using transient measurements,' *Computers & Chemical Engineering*, vol. 115, pp. 34–45, 2018.

[78] D. Krishnamoorthy, S. Skogestad and J. Jäschke, 'Multistage model predictive control with online scenario tree update using recursive bayesian weighting,' *18th European Control Conference (ECC)*, pp. 1443–1448, 2019. DOI: 10.23919/ECC.2019.8795839.

[79] G. Takacs, *Gas Lift Manual*. Tulsa, OK: PennWell Corporation, 2005.

[80] F. C. Diehl, C. S. Almeida, T. K. Anzai *et al.*, 'Oil production increase in unstable gas lift systems through nonlinear model predictive control,' *Journal of Process Control*, vol. 69, pp. 58–69, 2018.

[81] O. M. Aamo, G. Eikrem, H. Siahaan and B. A. Foss, 'Observer design for multiphase flow in vertical pipes with gas-lift—-theory and experiments,' *Journal of process control*, vol. 15, no. 3, pp. 247–257, 2005.

[82] L. Sinegre, N. Petit and P. Ménégatti, 'Predicting instabilities in gas-lifted wells simulation,' in *2006 American Control Conference*, IEEE, 2006, 8–pp.

[83] R. Sharma, K. Fjalestad and B. Glemmestad, 'Modeling and control of gas lifted oil field with five oil wells,' *the 52nd International Conference of Scandinavian Simulation Society*, pp. 47–59, 2011.

[84] D. Krishnamoorthy, B. Foss and S. Skogestad, 'Real-time optimization under uncertainty applied to a gas lifted well network,' *Processes*, vol. 52, no. 4, 2016. DOI: 10.3390/pr4040052.

[85] D. Krishnamoorthy, B. Foss and S. Skogestad, 'Gas lift optimization under uncertainty,' in *Computer Aided Chemical Engineering*, vol. 40, Elsevier, 2017, pp. 1753–1758.

[86] A. J. Peixoto, D. Pereira-Dias, A. F. Xaud and A. R. Secchi, 'Modelling and extremum seeking control of gas lifted oil wells,' *IFAC-PapersOnLine*, vol. 48, no. 6, pp. 21–26, 2015.

[87] E. Jahanshahi and S. Skogestad, 'Simplified dynamic models for control of riser slugging in offshore oil production,' *Oil and Gas Facilities*, vol. 3, no. 06, pp. 080–088, 2014.

[88] A. Pavlov, D. Krishnamoorthy, K. Fjalestad, E. Aske and M. Fredriksen, 'Modelling and model predictive control of oil wells with electric submersible pumps,' in *2014 IEEE Conference on Control Applications (CCA)*, IEEE, 2014, pp. 586–592.

[89] B. J. T. Binder, D. K. M. Kufoalor, A. Pavlov and T. A. Johansen, 'Embedded model predictive control for an electric submersible pump on a programmable logic controller,' in *2014 IEEE Conference on Control Applications (CCA)*, IEEE, 2014, pp. 579–585.

[90] R. Sharma and B. Glemmestad, 'Modeling and simulation of an electric submersible pump lifted oil field,' *International Journal of Petroleum Science and Technology*, vol. 8, no. 1, pp. 39–68, 2014.

[91] R. Sharma and B. Glemmestad, 'Optimal control strategies with nonlinear optimization for an electric submersible pump lifted oil field,' 2013.

[92] R. Sharma and B. Glemmestad, 'Mixed integer nonlinear optimization for esp lifted oil field and improved operation through production valve choking,' *International Journal of Modeling and Optimization*, vol. 4, no. 6, p. 465, 2014.

[93] R. Sharma and B. Glemmestad, 'Nonlinear model predictive control for optimal operation of electric submersible pump lifted oil field,' in *Proceedings of the IASTED International Conference on Modelling, Identification and Control*, 2014, pp. 229–236.

[94] D. Krishnamoorthy, E. M. Bergheim, A. Pavlov, M. Fredriksen and K. Fjalestad, 'Modelling and robustness analysis of model predictive control for electrical submersible pump lifted heavy oil wells,' *IFAC-PapersOnLine*, vol. 49, no. 7, pp. 544–549, 2016.

[95] B. A. Santana, R. M. Fontes, L. Schnitman and M. A. Martins, 'An adaptive infinite horizon model predictive control strategy applied to an esp-lifted oil well system,' *IFAC-PapersOnLine*, vol. 54, no. 3, pp. 176–181, 2021.

[96] B. J. T. Binder, T. A. Johansen and L. Imsland, 'Improved predictions from measured disturbances in linear model predictive control,' *Journal of Process Control*, vol. 75, pp. 86–106, 2019.

[97] E. Costa, O. de Abreu, T. d. O. Silva, M. Ribeiro and L. Schnitman, 'A bayesian approach to the dynamic modeling of esp-lifted oil well systems: An experimental validation on an esp prototype,' *Journal of Petroleum Science and Engineering*, vol. 205, p. 108 880, 2021.

[98] R. M. Fontes, D. D. Santana and M. A. Martins, 'An mpc auto-tuning framework for tracking economic goals of an esp-lifted oil well,' *Journal of Petroleum Science and Engineering*, vol. 217, p. 110 867, 2022.

[99] J. P. Jordanou, I. Osnes, S. B. Hernes, E. Camponogara, E. A. Antonelo and L. Imsland, 'Nonlinear model predictive control of electrical submersible pumps based on echo state networks,' *Advanced Engineering Informatics*, vol. 52, p. 101 553, 2022.

[100] M. Mohammadzaheri, R. Tafreshi, Z. Khan, M. Franchek and K. Grigoriadis, 'An intelligent approach to optimize multiphase subsea oil fields lifted by electrical submersible pumps,' *Journal of Computational Science*, vol. 15, pp. 50–59, 2016.

[101] J. A. P. Mejía, L. A. Silva and J. A. P. Flórez, 'Control strategy for oil production wells with electrical submersible pumping based on the nonlinear model-based predictive control technique,' in *2018 IEEE ANDESCON*, IEEE, 2018, pp. 1–6.

[102] E. I. Epelle and D. I. Gerogiorgis, 'Mixed-integer nonlinear programming (minlp) for production optimisation of naturally flowing and artificial lift wells with routing constraints,' *Chemical Engineering Research and Design*, vol. 152, pp. 134–148, 2019.

[103] A. Hoffmann and M. Stanko, 'Short-term model-based production optimization of a surface production network with electric submersible pumps using piecewise-linear functions,' *Journal of Petroleum Science and Engineering*, vol. 158, pp. 570–584, 2017.

[104] E. R. Müller, E. Camponogara, L. O. Seman *et al.*, 'Short-term steady-state production optimization of offshore oil platforms: Wells with dual completion (gas-lift and esp) and flow assurance,' *Top*, vol. 30, no. 1, pp. 152–180, 2022.

[105] D. E. Kirk, *Optimal control theory: an introduction*. Courier Corporation, 2004.

[106] W. L. Brogan, *Modern control theory*. Pearson education india, 1991.

[107] U. M. Ascher and L. R. Petzold, *Computer methods for ordinary differential equations and differential-algebraic equations*. Siam, 1998, vol. 61.

[108] L. S. Pontryagin, *Mathematical theory of optimal processes*. Routledge, 2018.

[109] G. Hicks and W. Ray, 'Approximation methods for optimal control synthesis,' *The Canadian Journal of Chemical Engineering*, vol. 49, no. 4, pp. 522–528, 1971.

[110] R. Sargent and G. Sullivan, 'The development of an efficient optimal control package,' in *Optimization Techniques: Proceedings of the 8th IFIP Conference on Optimization Techniques Würzburg, September 5–9, 1977*, Springer, 1978, pp. 158–168.

[111] H. G. Bock and K.-J. Plitt, 'A multiple shooting algorithm for direct solution of optimal control problems,' *IFAC Proceedings Volumes*, vol. 17, no. 2, pp. 1603–1608, 1984.

[112] J. E. Cuthrell and L. T. Biegler, 'On the optimization of differential-algebraic process systems,' *AIChE Journal*, vol. 33, no. 8, pp. 1257–1270, 1987.

[113] L. T. Biegler, *Nonlinear programming: concepts, algorithms, and applications to chemical processes*. SIAM, 2010.

[114] B. Karg and S. Lucia, 'Approximate moving horizon estimation and robust nonlinear model predictive control via deep learning,' *Computers & Chemical Engineering*, vol. 148, p. 107 266, 2021.

[115] C. E. Garcia and A. Morshedi, 'Quadratic programming solution of dynamic matrix control (qdmc),' *Chemical Engineering Communications*, vol. 46, no. 1-3, pp. 73–87, 1986.

[116] A. Saltelli, M. Ratto, T. Andres *et al.*, *Global Sensitivity Analysis: The Primer*. John Wiley & Sons, 2008, ISBN: 978-0-470-72517-7.

[117] S. Skogestad, 'Near-optimal operation by self-optimizing control: From process control to marathon running and business systems,' *Computers & chemical engineering*, vol. 29, no. 1, pp. 127–137, 2004.

[118] J. Jäschke, Y. Cao and V. Kariwala, 'Self-optimizing control–a survey,' *Annual Reviews in Control*, vol. 43, pp. 199–223, 2017.

[119] K. B. Ariyur and M. Krstic, *Real-time optimization by extremum-seeking control*. John Wiley & Sons, 2003.

Appendix A

Gas Lift Model

Despite very subtle differences in notation, the equations that have been used in different papers with the same case study are the same. However, the number of wells and numerical values of parameters have changed from paper to paper according to the specific requirements and circumstances of that specific paper. Therefore, the readers are referred to each paper for the numerical values of the parameter. The gas lift model employed in papers A, B, C, and D as a case study is based on the previous work in USN [5] with minor modifications. These modifications include:

- In the previous work, the reservoir was assumed to contain pure oil, meaning no gas and water were produced from the reservoir. This assumption has been substituted with a more realistic one. Therefore, the reservoir in the current work contains a mixture of crude oil, water, and gas.
- The gas distribution pipeline was modeled in the previous work, and an external controller was supposed to maintain constant pressure in the manifold, which was not directly related to the problem of optimal distribution of the lift gas. Therefore, this work simplifies the model by neglecting the manifold and considering the mass flow rate of injection lift gas into the annulus as the control input.

Similar to [5], the other assumptions considered for simplifying the development of the model are:

- Pressure of the reservoir is assumed to be constant.
- Density of liquid is assumed to be constant and not a function of pressure and temperature.
- Loss of pressure heads due to friction in the pipes has been neglected for the purpose of control and optimization.
- Temperature of gas and oil is considered to be constant at all points in the pipelines.
- All the phases of the multiphase fluid in the tubing are considered to be evenly distributed (no slugging).

- It is assumed that flashing does not occur in any section of the oil well.

Considering the different components of a single oil well, two control volumes are needed to apply the mass balance and derive the differential equations of the systems. These two control volumes are the annulus of the well and the tubing of the well above the injection point. The three states that are required to describe the system in these control volumes are the mass of lift gas in annulus m^i_{ga}, the mass of gas in the tubing above the injection point m^i_{gt}, and the mass of liquid (mixture of oil and water) in the tubing above the injection point m^i_{lt}. The superscript i refers to the ith oil well. By applying the mass balance, three corresponding ordinary differential equations are given by:

$$\dot{m}^i_{\text{ga}} = w^i_{\text{ga}} - w^i_{\text{ginj}} \tag{A.1a}$$
$$\dot{m}^i_{\text{gt}} = w^i_{\text{ginj}} + w^i_{\text{gr}} - w^i_{\text{gp}} \tag{A.1b}$$
$$\dot{m}^i_{\text{lt}} = w^i_{\text{lr}} - w^i_{\text{lp}} \tag{A.1c}$$

Equation (A.1a) represents the mass balance of the gas in the annulus. w^i_{ga} is the mass flow rate of the injected lift gas into each well from the gas lift choke valve (control input), and w^i_{ginj} is the mass flow rate of the gas injection from the annulus into the tubing. Equation (A.1b) is derived by applying the mass balance of the gas phase in the tubing above the injection point. w^i_{gr} and w^i_{gp} are the mass flow rate of the gas from the reservoir into the well and the produced gas phase mass flow rate from the production choke valve, respectively. Finally, equation (A.1c) represents the mass balance of the liquid phase in the tubing above the injection point. w^i_{lr} and w^i_{lp} are liquid mass flow rates from the reservoir into the well and the produced liquid phase mass flow rates from the production choke valve, respectively.

In order to complete the model, the mass flow rates on the right-hand side of (A.1) should be calculated. The mass flow rate of the gas injected into the tubing from the annulus w^i_{ginj} can be calculated by:

$$w^i_{\text{ginj}} = K^i Y^i_2 \sqrt{\rho^i_{\text{ga}} \max(p^i_{\text{ainj}} - p^i_{\text{tinj}}, 0)} \tag{A.2}$$

K^i is the gas injection valve constant, p^i_{ainj} is the pressure upstream of the gas injection valve in the annulus, and p^i_{tinj} is the pressure downstream of the gas injection valve in the tubing. Y^i_2 is the gas expandability factor for the gas that passes through the gas injection valve, and it is given by:

$$Y^i_2 = 1 - \alpha_{\text{Y}} \frac{p^i_{\text{ainj}} - p^i_{\text{tinj}}}{\max\left(p^i_{\text{ainj}}, p^{\min}_{\text{ainj}}\right)} \tag{A.3}$$

ρ^i_{ga} in (A.2) is the average density of gas in the annulus, and it is given by the equation of state of the gas as:

$$\rho^i_{\text{ga}} = \frac{M(p^i_{\text{a}} + p^i_{\text{ainj}})}{2ZRT^i_{\text{a}}} \tag{A.4}$$

p^i_{a} is the pressure of lift gas in the annulus downstream of the gas lift choke valve and can be calculated as:

$$p^i_{\text{a}} = \frac{Zm^i_{\text{ga}}RT^i_{\text{a}}}{MA^i_{\text{a}}L^i_{\text{a\_tl}}} \tag{A.5}$$

p^i_{ainj} is the pressure upstream of the gas injection valve in the annulus, and it is given by:

$$p^i_{\text{ainj}} = p^i_{\text{a}} + \frac{m^i_{\text{ga}}}{A^i_{\text{a}}L^i_{\text{a\_tl}}} gL^i_{\text{a\_vl}} \tag{A.6}$$

p^i_{tinj} is the pressure downstream of the gas injection valve in the tubing and it is given by:

$$p^i_{\text{tinj}} = \frac{Zm^i_{\text{gt}}RT^i_{\text{t}}}{MV^i_G} + \frac{\rho^i_{\text{m}}gL^i_{\text{t\_vl}}}{2} \tag{A.7}$$

The volume of gas present in the tubing above the gas injection point V_G can be found by subtracting the volume of liquid present inside the tubing from the total volume of the tubing above the gas injection point as:

$$V^i_G = A^i_{\text{t}}L^i_{\text{t\_tl}} - \frac{m^i_{\text{lt}}}{\rho^i_{\text{l}}} \tag{A.8}$$

The density of the liquid phase (mixture of oil and water) ρ^i_{l} can be calculated as:

$$\rho^i_{\text{l}} = \rho_w WC^i + \rho_o(1 - WC^i) \tag{A.9}$$

w^i_{lr} is the liquid mass flow rate from the reservoir into the well

$$w^i_{\text{lr}} = PI^i \max(p_{\text{r}} - p^i_{\text{bh}}) \tag{A.10}$$

w^i_{gr} is the mass flow rate of the gas from the reservoir into the well.

$$w^i_{\text{gr}} = GOR^i w^i_{\text{lr}} \tag{A.11}$$

w^i_{gp} is the produced gas phase mass flow rate from the production choke valve.

$$w^i_{\text{gp}} = \frac{m^i_{\text{gt}}}{m^i_{\text{gt}} + m^i_{\text{lt}}} w^i_{\text{glp}} \tag{A.12}$$

And w^i_{lp} is the produced liquid phase mass flow rates from the production choke valve

$$w^i_{\text{lp}} = \frac{m^i_{\text{lt}}}{m^i_{\text{gt}} + m^i_{\text{lt}}} w^i_{\text{glp}} \tag{A.13}$$

w^i_{glp} is the total mass flow rate of all phases from the production choke valve, and it can be computed by:

$$w^i_{\text{glp}} = C_v Y^i_3 \sqrt{\rho^i_{\text{m}} \max(p^i_{\text{wh}} - p_{\text{m}}, 0)} \tag{A.14}$$

w^i_{op} is the oil compartment of the liquid produced from production choke valve w^i_{lp}, and it is given by:

$$w^i_{\text{op}} = \frac{\rho_o}{\rho_w}(1 - WC^i) w^i_{\text{lp}} \tag{A.15}$$

p^i_{wh} is the well-head pressure, respectively.

$$p^i_{\text{wh}} = \frac{Z m^i_{\text{gt}} R T^i_{\text{t}}}{M V^i_G} - \frac{\rho^i_{\text{m}} g L^i_{\text{t\_vl}}}{2} \tag{A.16}$$

And P^i_{wf} is the bottom hole pressure.

$$p^i_{\text{bh}} = p^i_{\text{tinj}} + \rho^i_{\text{l}} g L^i_{\text{r\_vl}} \tag{A.17}$$

ρ^i_{m} is the average density of multiphase mixture in the tubing above the injection point.

$$\rho^i_{\text{m}} = \frac{m^i_{\text{gt}} + m^i_{\text{lt}}}{A^i_{\text{t}} L^i_{\text{t\_tl}}} \tag{A.18}$$

Y^i_3 is the gas expandability factor for the gas that passes through the production choke valve,

$$Y^i_3 = 1 - \alpha_{\text{Y}} \frac{p^i_{\text{wh}} - p_{\text{m}}}{\max\left(p^i_{\text{wh}}, p^{\min}_{\text{wh}}\right)} \tag{A.19}$$

All the variables and parameters of the model are listed in Table A.1 and Table A.2

Table A.1: List of the states, input, and dependent variables in the model.

Symbol	Type	Description
m_{ga}	State	Mass of lift gas in annulus
m_{gt}	State	Mass of gas in the tubing above the injection point
m_{lt}	State	Mass of liquid in the tubing above the injection point
w_{ga}	Input	Mass flow rate of gas injected into annulus
w_{ginj}	Variable	Mass flow rate of gas injected from annulus into tubing
w_{gr}	Variable	Mass flow rate of gas from reservoir into well
w_{gp}	Variable	Mass flow rate of gas phase through production choke valve
w_{lr}	Variable	Mass flow rate of liquid from reservoir into well
w_{lp}	Variable	Mass flow rate of liquid phase through production choke valve
w_{glp}	Variable	Total mass flow rate through the production choke valve
p_{a}	Variable	Pressure of gas in annulus downstream the gas lift choke valve
p_{ainj}	Variable	Pressure upstream of the gas injection valve in the annulus
p_{tinj}	Variable	Pressure downstream of the gas injection valve in the tubing
p_{bh}	Variable	Bottomhole pressure
p_{wh}	Variable	Wellhead pressure
ρ_{ga}	Variable	Average density of gas in the annulus
ρ_{m}	Variable	Density of multiphase mixture in tubing above injection point
ρ_{l}	Variable	Average density of the liquid phase
V_G	Variable	Volume of the gas in the tubing above the gas injection point
Y_2	Variable	Gas expandability factor through the gas injection valve
Y_3	Variable	Gas expandability factor through the production choke valve

Table A.2: List of the parameters and constants.

Symbol	Type	Description
PI	Parameter	Productivity index
WC	Parameter	Water cut
GOR	Parameter	Gas to oil ratio
p_{r}	Parameter	Reservoir pressure
p_{m}	Parameter	Gathering manifold pressure
T_{a}	Parameter	Temperature in annulus
T_{t}	Parameter	Temperature in tubing
A_{a}	Parameter	Annulus cross-section area
A_{t}	Parameter	Tubing cross-section area
$L_{\mathrm{a\_tl}}$	Parameter	Total length of annulus
$L_{\mathrm{a\_vl}}$	Parameter	Vertical length of annulus
$L_{\mathrm{t\_tl}}$	Parameter	Total length of tubing above injection point
$L_{\mathrm{t\_vl}}$	Parameter	Vertical length of tubing above injection point
$L_{\mathrm{r\_vl}}$	Parameter	Vertical length of tubing below injection point
C_v	Constant	Valve opening characteristic
K	Constant	Gas injection valve constant
α_{Y}	Constant	Constant
M	Constant	Molar mass
Z	Constant	Gas compressibility factor
R	Constant	Universal gas constant
g	Constant	Gravity
ρ_{w}	Constant	Density of water
ρ_{o}	Constant	Density of oil

Appendix B

ESP Model

The model which has been used as the case study in papers E and F is adopted from [5], supplemented by subtle modifications to assumptions as follows:

- Modeling the electrical motors subsystem is neglected due to the fast response of electrical systems.
- Assumption of constant water cut in the production manifold is substituted by a more realistic one. Therefore, instead of injecting water to keep the water cut constant, which needs a perfect controller, a constant flow of water is injected into the manifold. Accordingly, the water cut of the liquid phase within the manifold varies and depends on the proportion of fluid produced from production chock valves.
- Water cuts of the wells are considered to be different to draw a meaningful optimization problem.

The following assumptions for simplifying the model are kept as they were in previous work [5].

- Frictional losses occurring inside the pumps due to the flow of fluid are not considered.
- The pump responds instantaneously to changes in the input parameters.
- No gas is produced from the reservoir.
- The reservoir pressure is considered to be constant.
- Distance between the production choke valve and the production manifold is neglected.

The governing equations of the model can be derived by applying mass and momentum balance to the different components of the well. The process is described by three states for each well, namely, the pressure at the bottom hole p^i_{bh}, the pressure at the wellhead p^i_{wh}, and the average volumetric flow rate of the well q^i_l, where the superscript i refers

to the i^{th} oil well. The remaining states are the pressure in the production manifold p_m and the average volumetric flow rate of the j^{th} transportation line q_{tr}^j. The corresponding differential equations are given by:

$$\dot{p}_{bh}^i = \frac{\beta}{A_r^i L_r^i}\left[q_r^i - q_l^i\right] \tag{B.1a}$$

$$\dot{p}_{wh}^i = \frac{\beta}{A_t^i L_t^i}\left[q_l^i - q_c^i\right] \tag{B.1b}$$

$$\begin{aligned}\dot{q}_l^i = &\frac{A_t^i}{\rho_l^i\left(L_r^i + L_t^i\right)}\Big[p_{bh}^i - p_{wh}^i + \rho_l^i g H_{esp}^i \\ &- \rho_l^i g(L_r^i + L_t^i) - \Delta p_{f,w}^i\Big]\end{aligned} \tag{B.1c}$$

$$\dot{p}_m = \frac{\beta}{A_m L_m}\left[\sum_{i=1}^{3} q_c^i - \sum_{j=1}^{2} q_{tr}^j + q_w^{inj}\right] \tag{B.1d}$$

$$\dot{q}_{tr}^j = \frac{A_{tr}^j}{\rho_{tr}^j L_{tr}^j}\left[p_m - p_s + \Delta p_{bp}^j - \Delta p_{f,tr}^j\right] \tag{B.1e}$$

Equation (B.1a) is derived by applying the mass balance to the lower section of the well between the ESP and the reservoir. q_r^i is the volumetric flow rate that comes from the reservoir into the well. (B.1b) is derived by applying the mass balance to the upper section of the well between the ESP and the well-head and q_c^i is the volumetric flow rate that passes through the production choke valve. (B.1c) is derived by applying the momentum balance to the entire well and H_{esp}^i and $\Delta p_{f,w}^i$ represent the produced head by ESP and frictional pressure loss in the well, respectively. Applying the mass balance to the gathering manifold yields (B.1d) in which q_w^{inj} represents the constant water injection to the manifold for decreasing the frictional loss of the transportation. Finally, (B.1e) is derived by applying the momentum balance to the transportation lines. p_s is the pressure at the separator, Δp_{bp}^j and $\Delta p_{f,tr}^j$ demonstrate the pressure gradient produced by the booster pump and the frictional loss in the transportation line, respectively.

To complete the model, the algebraic equations are required to compute the variables on the right-hand side of (B.1). Accordingly, the volumetric flow rate from the reservoir into the well q_r^i is given by:

$$q_r^i = PI^i\left(p_r - p_{bh}^i\right) \tag{B.2}$$

The volumetric flow rate that passes through the production choke valve q_c^i can be calculated by:

$$q_c^i = C_v^i\sqrt{\frac{\max(p_{wh}^i - p_m, 0)}{\rho_l^i}} \tag{B.3}$$

ρ_l^i is the density of the mixture and can be calculated based on the density of oil and water as:

$$\rho_l^i = WC^i \rho_w + (1 - WC^i)\rho_o \tag{B.4}$$

The head produced by ESP H_{esp}^i is a function of the frequency f^i and flow q_l^i of the pump and can be calculated by the performance curves of the pump which is provided by the manufacturer at characteristic reference frequency f_0 and the affinity laws of the pumps.

$$H_{esp}^i = \bar{a}_0 \left(\frac{f^i}{f_0}\right)^2 + \bar{a}_1 \left(\frac{f}{f_0}\right) q_l^i + \bar{a}_2 {q_l^i}^2 + \bar{a}_3 \left(\frac{f_0}{f}\right) {q_l^i}^3 \tag{B.5}$$

The pressure loss due to the flow of the fluid through the wells and transportation pipelines appeared in (B.1c) and (B.1e) can be calculated using Darcy-Weisbach formula and their corresponding density, length, etc., as:

$$\Delta p_f = \frac{f_D L \rho \upsilon^2}{2D_h} \tag{B.6}$$

The Darcy friction factor f_D in (B.6) can be computed by Serghides' equation, which is an approximation of the Colebrook equation used to solve for the Darcy friction factor explicitly.

$$A = -2\log_{10}\left(\frac{\epsilon/D_h}{3.7} + \frac{12}{Re}\right) \tag{B.7a}$$

$$B = -2\log_{10}\left(\frac{\epsilon/D_h}{3.7} + \frac{2.51A}{Re}\right) \tag{B.7b}$$

$$C = -2\log_{10}\left(\frac{\epsilon/D_h}{3.7} + \frac{2.51B}{Re}\right) \tag{B.7c}$$

$$f_D = \left(A - \frac{(B-A)^2}{C - 2B + A}\right)^{-2} \tag{B.7d}$$

The water cut, which is the ratio of the volumetric flow rate of water to the total volumetric flow rate, can be calculated by:

$$WC_{tr} = \frac{q_w^{inj} + \sum_{i=1}^{3} WC^i q_c^i}{q_w^{inj} + \sum_{i=1}^{3} q_c^i} \tag{B.8}$$

Accordingly, the density of the transported fluid in the transportation lines can be calculated as:

$$\rho_{tr} = WC_{tr}\rho_w + (1 - WC_{tr})\rho_o \tag{B.9}$$

The total produced oil can be calculated as:

$$q_o = \sum_{j=1}^{n_{tr}} (1 - WC_{tr}) q_{tr}^j \tag{B.10}$$

Similarly, the total produced water can be calculated as:

$$q_w = \sum_{j=1}^{n_{tr}} WC_{tr} q_{tr}^j \tag{B.11}$$

The brake horsepower of the ESP which is required in the optimization problem can be calculated as:

$$BHP_{esp}^i = \hat{a}_0 \left(\frac{f^i}{f_0}\right)^3 + \hat{a}_1 \left(\frac{f^i}{f_0}\right)^2 q_l^i + \hat{a}_2 \left(\frac{f}{f_0}\right) {q_l^i}^2 + \hat{a}_3 {q_l^i}^3 + \hat{a}_4 \left(\frac{f_0}{f}\right) {q_l^i}^4 \tag{B.12}$$

Also the minimum and the maximum allowed flow rates through the ESP can be calculated by affinity law as:

$$Q_{\min}(f^i) = \frac{f^i}{f_0} Q_{f_0,\min}^i \tag{B.13a}$$

$$Q_{\max}(f^i) = \frac{f^i}{f_0} Q_{f_0,\max}^i \tag{B.13b}$$

All the variables and parameters of the model are listed in Table B.2 and Table B.1

Table B.1: List of the states, input, and dependent variables in the model.

Symbol	Type	Description
f	Input	Frequency of ESP
p_{bh}	State	Bottomhole pressure
p_{wh}	State	Wellhead pressure
p_m	State	Gathering manifold pressure
q_l	State	Average volumetric flow rate in the well
q_{tr}	State	Average volumetric flow rate in transportation line
q_r	Variable	Volumetric flow rate from reservoir into well
q_c	Variable	Volumetric flow rate through production choke valve
q_o	Variable	Volumetric flow rate of total produced oil
q_w	Variable	Volumetric flow rate of total produced water
Δp_f	Variable	Frictional pressure drop in the pipe
H_{esp}	Variable	Head developed by ESP
BHP_{esp}	Variable	ESP brake horsepower
ρ_l	Variable	Density of the fluid in the well
ρ_{tr}	Variable	Density of the fluid in transportation line

Table B.2: List of the parameters and constants.

Symbol	Type	Description
PI	Parameter	Productivity index
WC	Parameter	Water cut
WC_{tr}	Parameter	Water cut in transportation line
p_r	Parameter	Reservoir pressure
p_s	Parameter	Separator pressure
Δp_{bp}	Parameter	Pressure gradient by booster pump
A_a	Parameter	Annulus cross-section area
A_t	Parameter	Tubing cross-section area
L_{tr}	Parameter	Total length of transportation line
L_m	Parameter	Total length of manifold
L_t	Parameter	Length of well above ESP
L_r	Parameter	Length of well below ESP
A	Parameter	Cross section area of all pipelines
D_h	Parameter	Hydraulic diameter of all pipelines
C_v	Constant	Valve opening characteristic
g	Constant	Gravity
β	Constant	Bulk modulus of the reservoir fluid
ρ_w	Constant	Density of water
ρ_o	Constant	Density of oil

Appendix C

Driven Van der Pol Oscillator

Illustrative Example

A driven Van der Pol oscillator with one uncertain parameter is chosen as a toy example to illustrate the different aspects of the methods throughout this chapter. The system is simple enough and yet capable of conveying the points that need to be illustrated. It has two states $x = [x_1, x_2]^T \in \mathbb{R}^2$, one input $u \in \mathbb{R}$, one output $y \in \mathbb{R}$, and one uncertain parameter $p \in \mathbb{R}$, which is assumed to be constant, unknown, and bounded. Phase portrait of the unforced system for three realizations of uncertainty is plotted in Figure C.1. The numerical values of the parameters and the requirements of the system are presented in Table C.1.

$$\dot{x}_1 = (p - x_2^2)x_1 - x_2 - u \tag{C.1a}$$

$$\dot{x}_2 = x_1 \tag{C.1b}$$

$$y = px_2 \tag{C.1c}$$

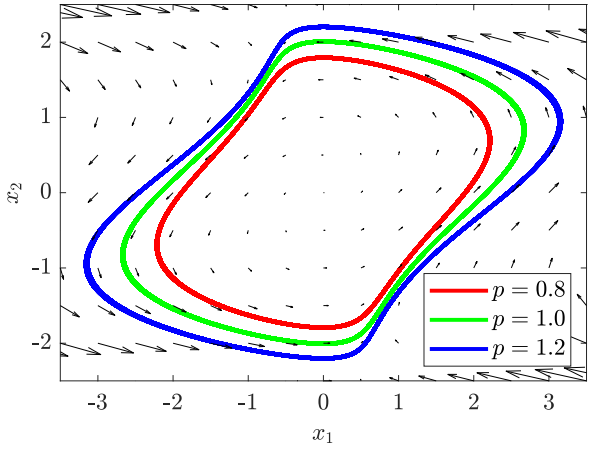

Figure C.1: Phase portrait.

Table C.1: Numerical Values of the parameters and constraints.

Parameter	Value	Description
T	10	Total simulation time
N	100	Total number of sampling times
p^{nom}	1.0	Nominal value of parameter
p^{min}	0.8	Minimum value of parameter
p^{max}	1.2	Maximum value of parameter
x_1^{min}	$-\infty$	Lower bound on first state
x_1^{max}	$+\infty$	Upper bound on first state
x_2^{min}	$-\infty$	Lower bound on second state
x_2^{max}	$+\infty$	Upper bound on second state
y^{min}	0.5	Lower bound on output
y^{max}	1.5	Upper bound on output
u^{min}	-3.0	Lower bound on control input
u^{max}	$+3.0$	Upper bound on control input
ω_y	50	Tuning weight

Optimal Control Problem

The objective function is to maximize the output y in the first half of the simulation and minimize it in the second half with the minimum possible control effort. It can be easily done by defining a function such as (C.2) that adjusts the sign of the output in the objective function. The motivation for such an objective function is that it makes both the upper bound and lower bound of the constraint active at different times during the simulation.

$$\omega(k) = \begin{cases} +1 & \text{if } k \leq 50 \\ -1 & \text{if } 50 < k \end{cases} \tag{C.2}$$

Therefore, the optimal control problem for a driven Van der Pol Oscillator can be formulated as:

$$\min_{\mathbf{x},\mathbf{u}} \quad \sum_{k=0}^{N-1} \left[-\omega(k)\omega_y y(k) + u^2(k)\right] - \omega(N)\omega_y y(N) \tag{C.3a}$$

$$\text{s.t.} \quad x(0) = [0,1]^T \tag{C.3b}$$

$$x(k+1) = f(x(k), u(k), p), \qquad k = 0, 1, \ldots, N-1 \tag{C.3c}$$

$$x_1^{min} \leq x_1(k) \leq x_1^{max}, \qquad k = 0, 1, \ldots, N \tag{C.3d}$$

$$x_2^{min} \leq x_2(k) \leq x_2^{max}, \qquad k = 0, 1, \ldots, N \tag{C.3e}$$

$$y^{min} \leq y(k) \leq y^{max}, \qquad k = 0, 1, \ldots, N \tag{C.3f}$$

$$u^{min} \leq u(k) \leq u^{max}, \qquad k = 0, 1, \ldots, N-1 \tag{C.3g}$$

In the optimal control problem defined in (C.3), scaler ω_y represents the relative importance of the output y to input u in the objective function. Moreover, the discretized dynamic of the system is implemented as the quality constraint in (C.3c). The simulation results for applying the open-loop optimal control to the plant with three different realizations of uncertainty are plotted in Figure C.2

Model Predictive Control

As discussed in chapter 4, MPC is an open-loop optimal control problem that is implemented in a receding horizon fashion. Therefore, MPC formulation is similar to the optimal control problem defined in (C.3) with two differences. First, the optimization problem is defined over a shorter horizon with the length $N_p = 10$, which slides one step forward at each time instance. Second, only the first control action is implemented and the optimization problem will be initialized with a new initial state x_0 (current state) at the next time instance. Simulation results for the MPC formulation presented in (C.4) are plotted in Figure C.3

$$\min_{\mathbf{x},\mathbf{u}} \quad \sum_{k=0}^{N_p-1} \left[-\omega(k)\omega_y y(k) + u^2(k)\right] - \omega(N)\omega_y y(N) \tag{C.4a}$$

$$\text{s.t.} \quad x(0) = x_0 \tag{C.4b}$$

$$x(k+1) = f(x(k), u(k), p), \qquad k = 0, 1, \ldots, N_p-1 \tag{C.4c}$$

$$x_1^{min} \leq x_1(k) \leq x_1^{max}, \qquad k = 0, 1, \ldots, N_p \tag{C.4d}$$

$$x_2^{min} \leq x_2(k) \leq x_2^{max}, \qquad k = 0, 1, \ldots, N_p \tag{C.4e}$$

$$y^{min} \leq y(k) \leq y^{max}, \qquad k = 0, 1, \ldots, N_p \tag{C.4f}$$

$$u^{min} \leq u(k) \leq u^{max}, \qquad k = 0, 1, \ldots, N_p-1 \tag{C.4g}$$

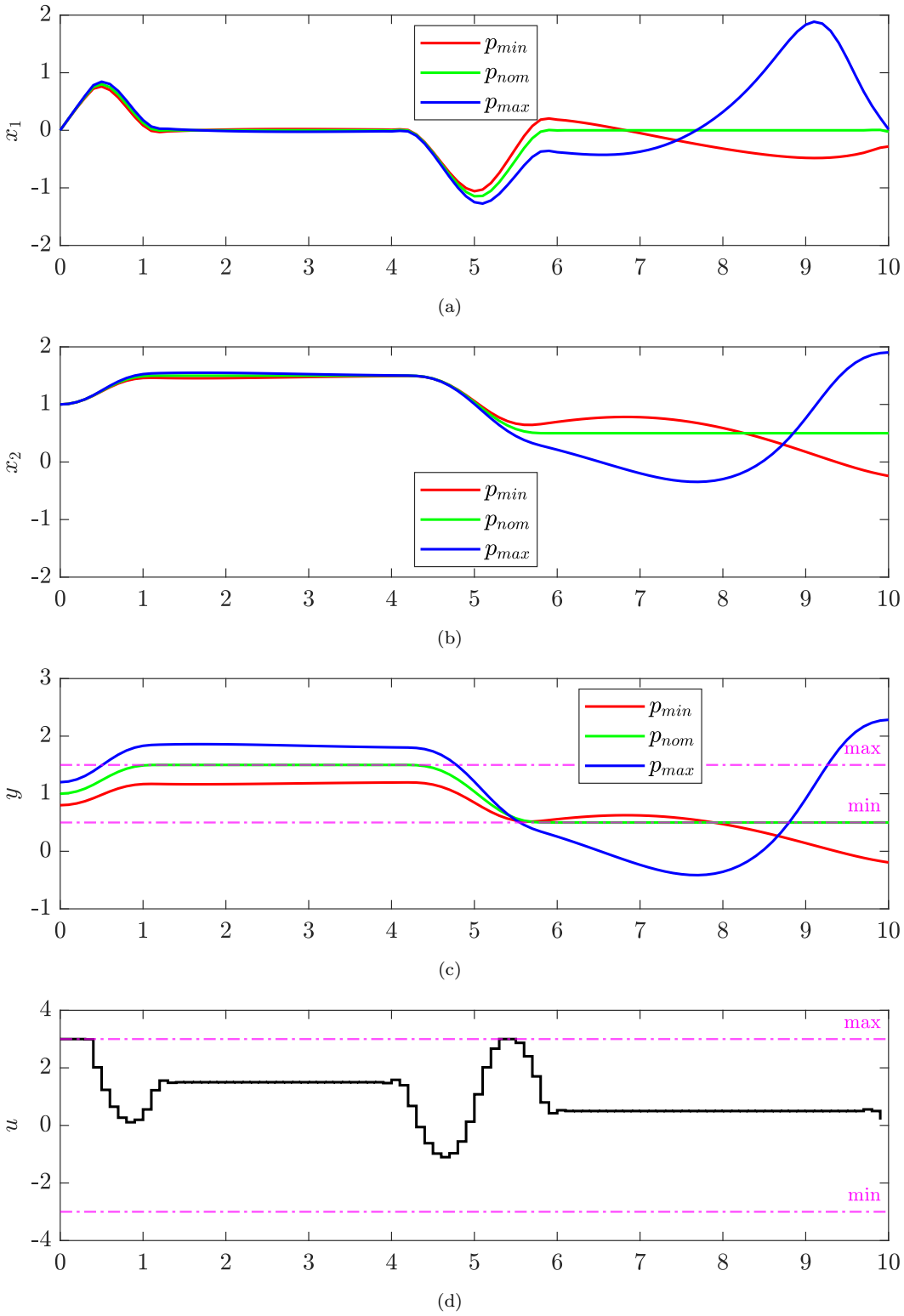

Figure C.2: Optimal control problem applied to the plant with three realizations of uncertainty.

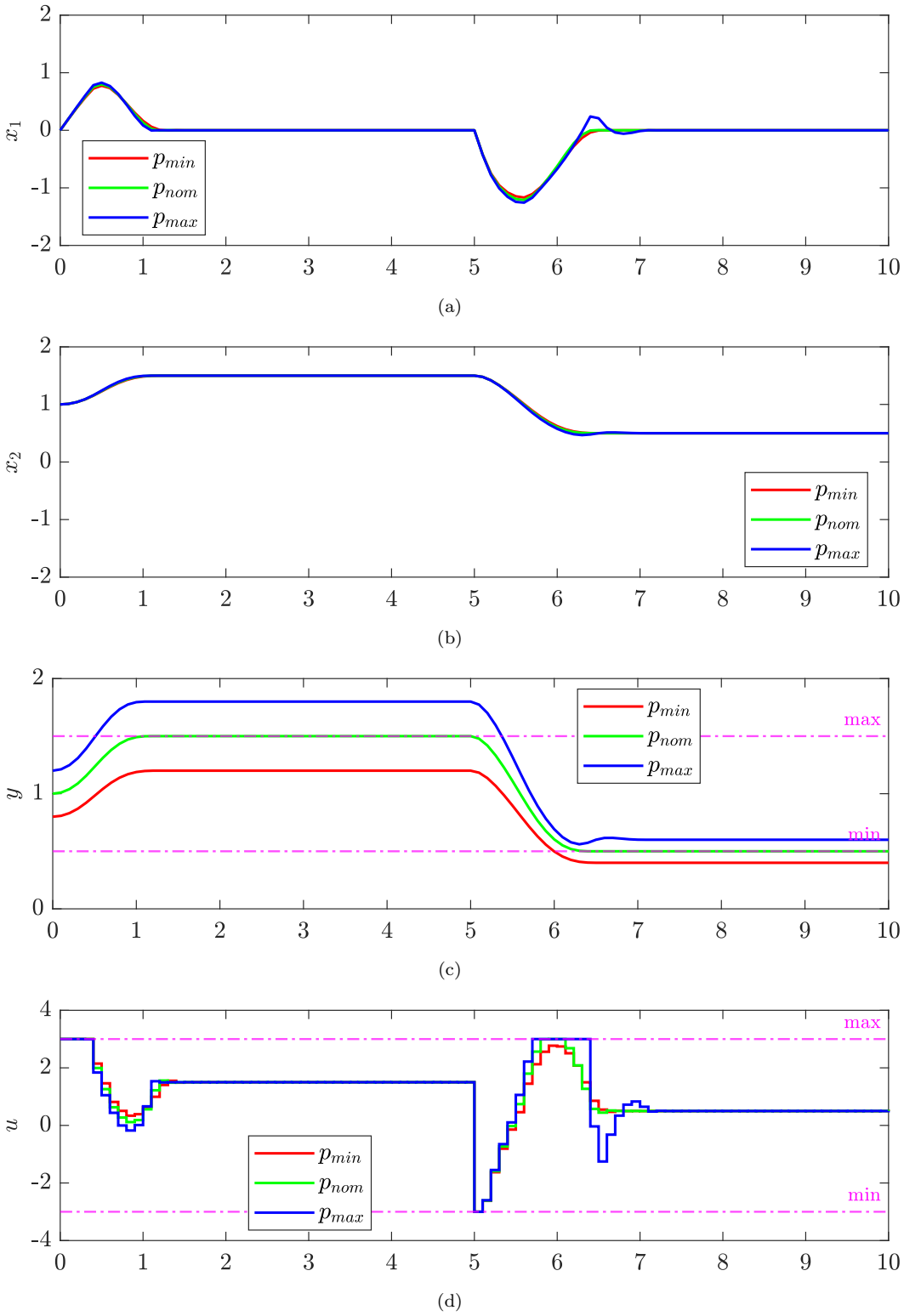

Figure C.3: Model Predictive Control applied to the plant with three realizations of uncertainty.

Min-Max MPC

The formulation of the nonlinear Min-Max MPC for the bounded uncertainty $p \in \mathcal{P}$ over is defined in (C.5). It should be noted that $y(k)$ in the objective function is replaced by its equivalent $px_2(k)$ to make the uncertainty explicitly visible in the problem formulation. The simulation results are plotted in Figure C.4.

$$\min_{\mathbf{x},\mathbf{u}} \quad \max_{p\in\mathcal{P}} \quad \sum_{k=0}^{N_p-1} \left[-\omega(k)\omega_y p x_2(k) + u^2(k)\right] - \omega(N)\omega_y p x_2(N) \tag{C.5a}$$

$$\text{s.t.} \quad x(0) = x_0 \tag{C.5b}$$

$$x(k+1) = f(x(k), u(k), p), \qquad \forall p \in \mathcal{P}, k = 0, 1, \ldots, N_p - 1 \tag{C.5c}$$

$$x_1^{min} \leq x_1(k) \leq x_1^{max}, \qquad \forall p \in \mathcal{P}, k = 0, 1, \ldots, N_p \tag{C.5d}$$

$$x_2^{min} \leq x_2(k) \leq x_2^{max}, \qquad \forall p \in \mathcal{P}, k = 0, 1, \ldots, N_p \tag{C.5e}$$

$$y^{min} \leq y(k) \leq y^{max}, \qquad \forall p \in \mathcal{P}, k = 0, 1, \ldots, N_p \tag{C.5f}$$

$$u^{min} \leq u(k) \leq u^{max}, \qquad \forall p \in \mathcal{P}, k = 0, 1, \ldots, N_p - 1 \tag{C.5g}$$

Multistage MPC

Constructing a scenario tree is the first step in formulating the multistage MPC. For this particular example, three realizations are considered for uncertainty and the branching is continued two sampling times, meaning the robust horizon is considered to be $N_r = 2$. As a result, the number of scenarios would become equal to $N_s = 9$, as demonstrated in Figure C.5. Four sets of non-anticipativity constraints exist in the problem, which are implemented as the equality constraints (C.6h) to (C.6k) in the problem formulation. Each set is exhibited with a different color in Figure C.5. The weights of the scenarios are considered to be equal ω^j for all the scenarios, meaning that all the scenarios are equally likely to occur. The simulation results for multistage MPC are plotted in Figure C.6.

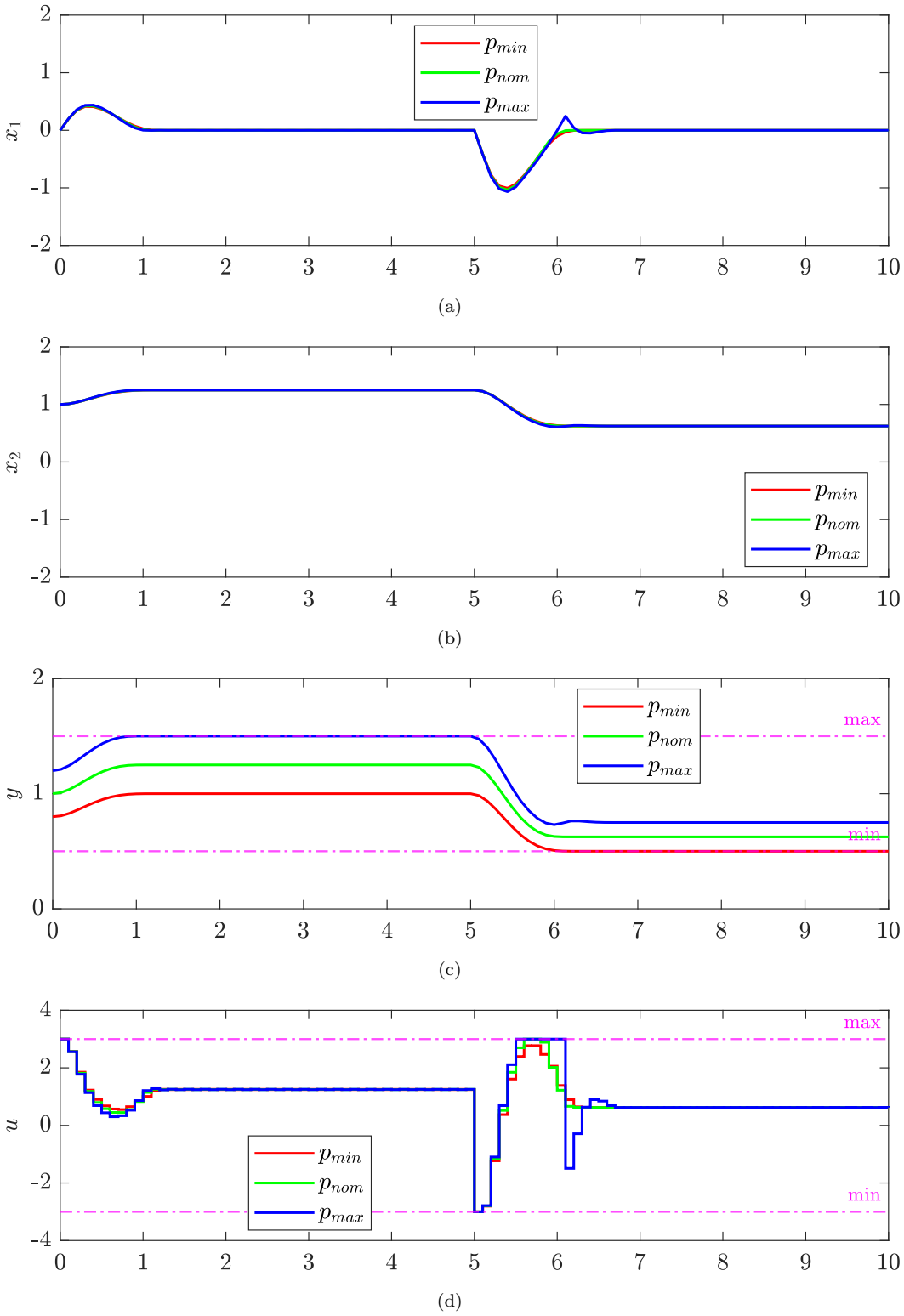

Figure C.4: Min-Max MPC applied to the plant with three realizations of uncertainty.

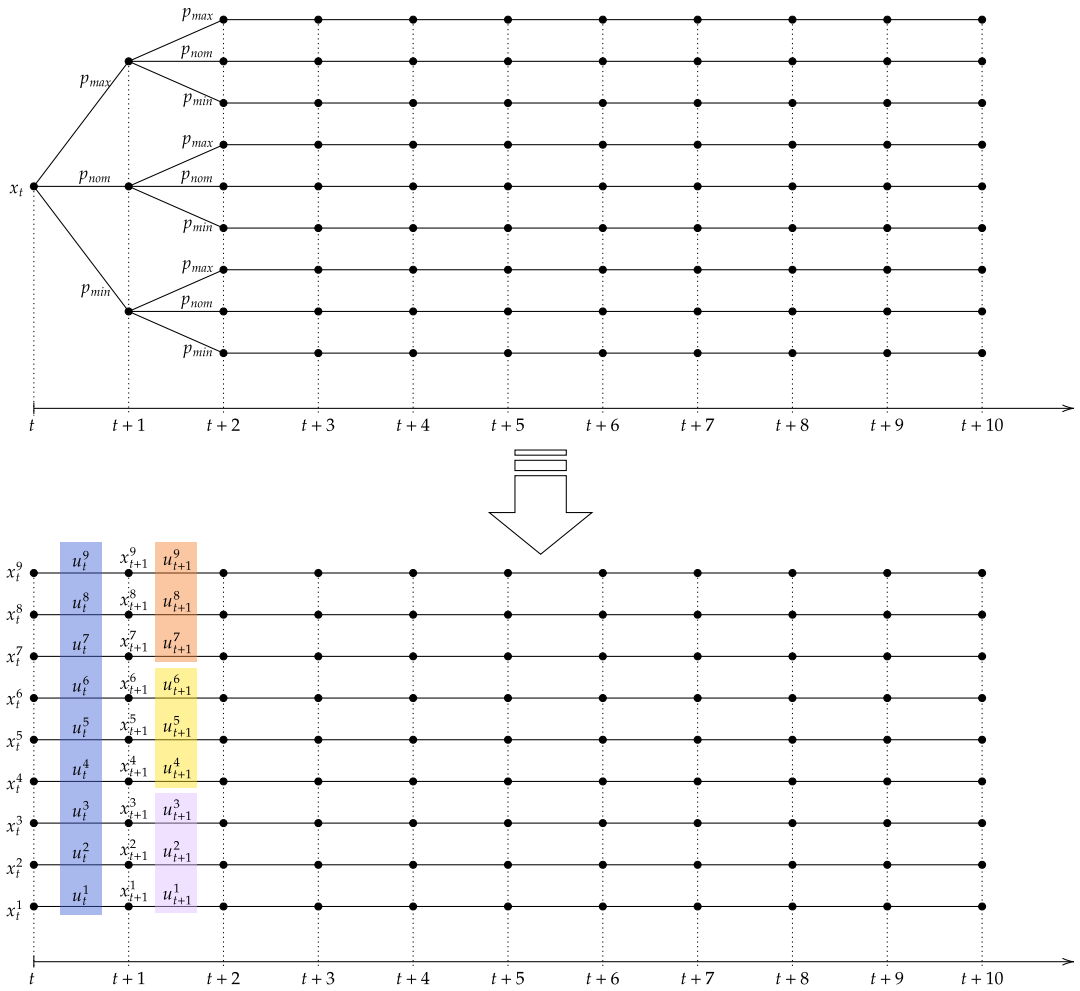

Figure C.5: Scenario tree with three realizations of uncertainty $\mathcal{P} = \{p_{min}, p_{nom}, p_{max}\}$ and robust horizon $N_r = 2$ over a prediction horizon with the length $N_p = 10$.

$$\min_{\mathbf{x},\mathbf{u}} \quad \sum_{j=1}^{N_s} \omega^j \sum_{k=0}^{N_p-1} \left[-\omega(k)\omega_y y^j(k) + {u^j}^2(k) \right] - \omega(N)\omega_y y^j(N) \tag{C.6a}$$

$$\text{s.t.} \quad x^j(0) = x_0, \qquad \forall j \in \mathcal{S} \tag{C.6b}$$

$$x^j(k+1) = f(x^j(k), u^j(k), p^j(k)), \qquad \forall j \in \mathcal{S}, k = 0, 1, \ldots, N_p - 1 \tag{C.6c}$$

$$x_1^{min} \leq x_1^j(k) \leq x_1^{max}, \qquad \forall j \in \mathcal{S}, k = 0, 1, \ldots, N_p \tag{C.6d}$$

$$x_2^{min} \leq x_2^j(k) \leq x_2^{max}, \qquad \forall j \in \mathcal{S}, k = 0, 1, \ldots, N_p \tag{C.6e}$$

$$y^{min} \leq y^j(k) \leq y^{max}, \qquad \forall j \in \mathcal{S}, k = 0, 1, \ldots, N_p \tag{C.6f}$$

$$u^{min} \leq u^j(k) \leq u^{max}, \qquad \forall j \in \mathcal{S}, k = 0, 1, \ldots, N_p - 1 \tag{C.6g}$$

$$u^j(0) = u^l(0), \qquad \forall j, l \in \mathcal{S} \tag{C.6h}$$

$$u^1(1) = u^2(1) = u^3(1) \tag{C.6i}$$

$$u^4(1) = u^5(1) = u^6(1) \tag{C.6j}$$

$$u^7(1) = u^8(1) = u^9(1) \tag{C.6k}$$

Min-Max MPC with Constraint Modification

The formulation of the problem is similar to the standard min-max MPC defined in (C.5). However, the constraint bounds are modified using the modification term as defined at each time instance $k = 0$ in (C.7).

$$\delta y_{\mathrm{L}} = \min(y^c(k)) - y^m(k) \tag{C.7a}$$
$$\delta y_{\mathrm{U}} = \max(y^c(k)) - y^m(k) \tag{C.7b}$$

Therefore, the optimization problem can be modified as:

$$\min_{\mathbf{x},\mathbf{u}} \quad \max_{p\in\mathcal{P}} \quad \sum_{k=0}^{N_p-1} \left[-\omega(k)\omega_y p x_2(k) + u^2(k)\right] - \omega(N)\omega_y p x_2(N) \tag{C.8a}$$
$$\text{s.t.} \quad x(0) = x_0 \tag{C.8b}$$
$$x(k+1) = f(x(k), u(k), p), \qquad \forall p \in \mathcal{P}, k = 0, 1, \ldots, N_p - 1 \tag{C.8c}$$
$$x_1^{min} \leq x_1(k) \leq x_1^{max}, \qquad \forall p \in \mathcal{P}, k = 0, 1, \ldots, N_p \tag{C.8d}$$
$$x_2^{min} \leq x_2(k) \leq x_2^{max}, \qquad \forall p \in \mathcal{P}, k = 0, 1, \ldots, N_p \tag{C.8e}$$
$$y^{min} + \delta y_{\mathrm{L}} \leq y(k) \leq y^{max} + \delta y_{\mathrm{U}}, \quad \forall p \in \mathcal{P}, k = 0, 1, \ldots, N_p \tag{C.8f}$$
$$u^{min} \leq u(k) \leq u^{max}, \qquad \forall p \in \mathcal{P}, k = 0, 1, \ldots, N_p - 1 \tag{C.8g}$$

The simulation results are plotted in Figure C.7.

Adaptive MPC with MHE

The adaptive approach is similar to deterministic MPC, while the parameter and initial states are the estimated values. Therefore Adaptive MPC for can be defined as:

$$\min_{\mathbf{x},\mathbf{u}} \quad \sum_{k=0}^{N_p-1} \left[-\omega(k)\omega_y \hat{p} x_2(k) + u^2(k)\right] - \omega(N)\omega_y \hat{p} x_2(N) \tag{C.9a}$$
$$\text{s.t.} \quad x(0) = \hat{x}_0 \tag{C.9b}$$
$$x(k+1) = f(x(k), u(k), \hat{p}), \qquad k = 0, 1, \ldots, N_p - 1 \tag{C.9c}$$
$$x_1^{min} \leq x_1(k) \leq x_1^{max}, \qquad k = 0, 1, \ldots, N_p \tag{C.9d}$$
$$x_2^{min} \leq x_2(k) \leq x_2^{max}, \qquad k = 0, 1, \ldots, N_p \tag{C.9e}$$
$$y^{min} \leq y(k) \leq y^{max}, \qquad k = 0, 1, \ldots, N_p \tag{C.9f}$$
$$u^{min} \leq u(k) \leq u^{max}, \qquad k = 0, 1, \ldots, N_p - 1 \tag{C.9g}$$

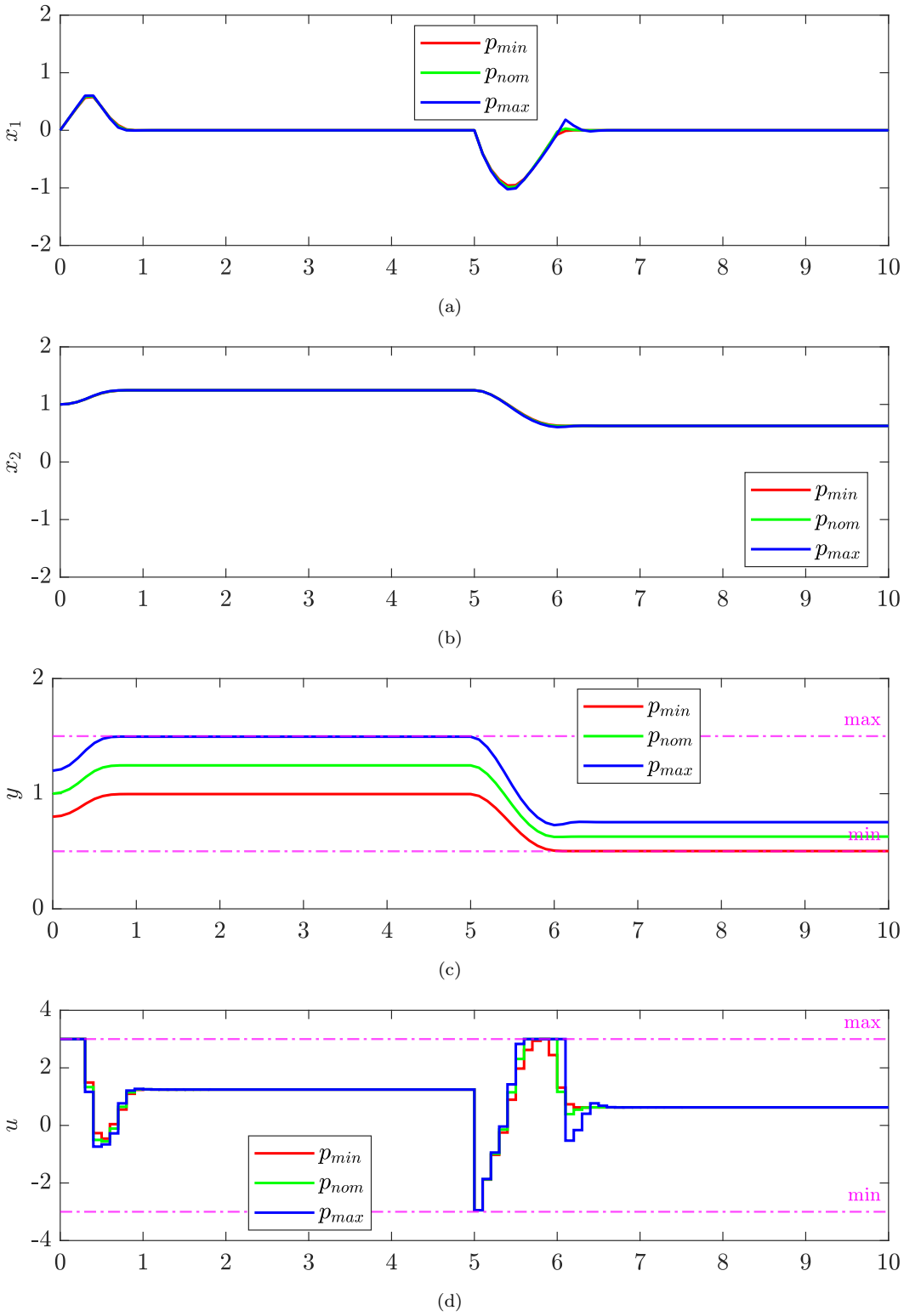

Figure C.6: Multistage MPC applied to the plant with three realizations of uncertainty.

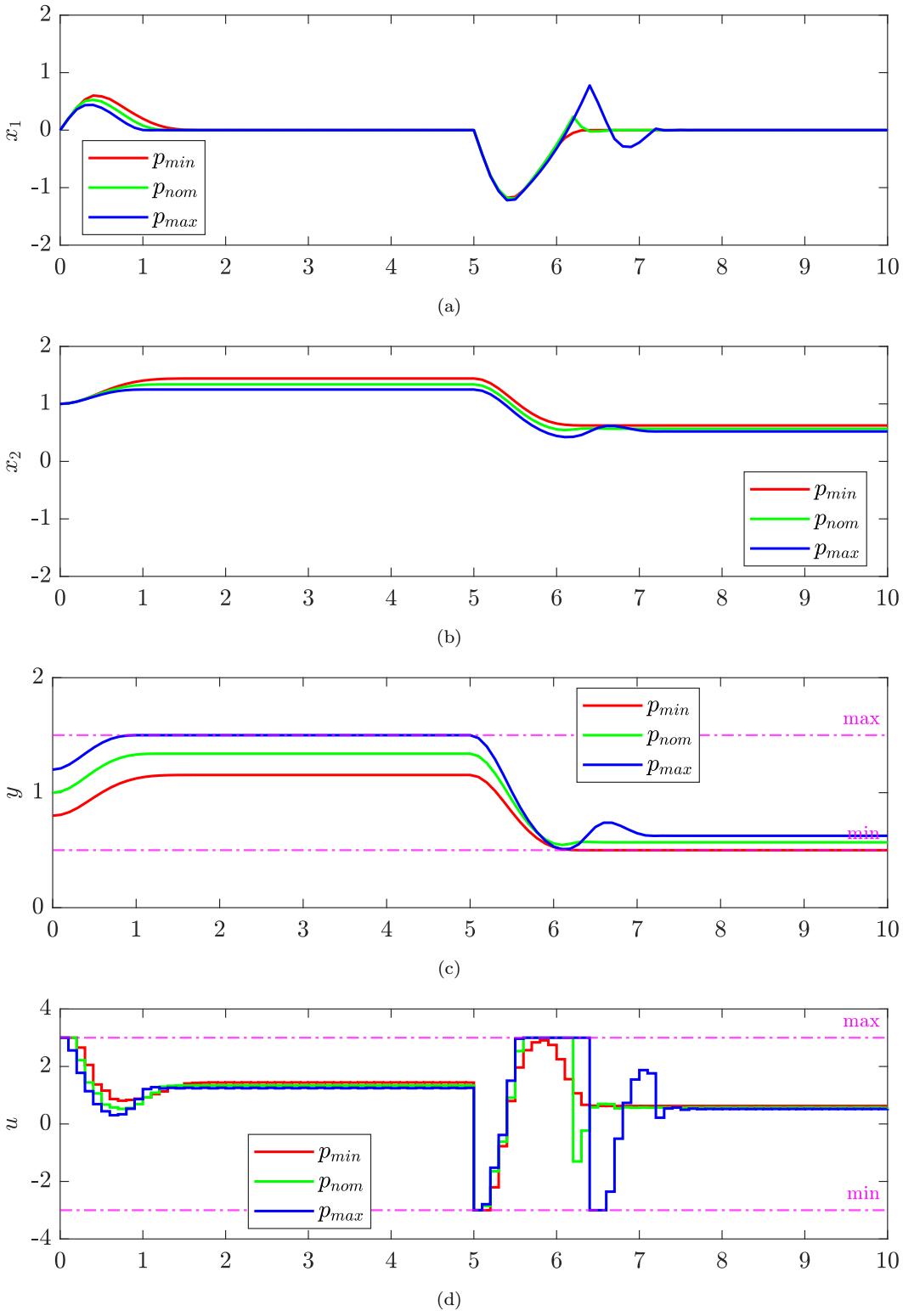

Figure C.7: Min-Max MPC with modification applied to the plant with three realizations of uncertainty.

The estimated parameter and states are the solution to an optimization problem as defined in (C.10). The length of the estimation horizon is ten sampling times $N_{MHE} = 10$, and the weighting matrices in the cost function are considered to be identity matrices with suitable dimensions, $P_x = I_2$, $P_p = 1$, and $P_y = 1$.

$$\begin{aligned}
&\min_{\hat{\mathrm{x}},\hat{p}} \quad 1/2\|\hat{x}(0) - x_a\|^2_{P_x} + 1/2\|\hat{p} - p_{\mathrm{prev}}\|^2_{P_p} \\
&+ 1/2 \sum_{k=0}^{N_{\mathrm{MHE}}-1} \|y^m(k)) - \hat{p}\hat{x}_2(k)\|^2_{P_y} && \text{(C.10a)} \\
\text{s.t.} \quad &\hat{x}(k+1) = f\left(\hat{x}(k), u(k), \hat{p}\right), \quad k = 0, ..., N_{\mathrm{MHE}} - 1 && \text{(C.10b)} \\
&x_1^{min} \leq \hat{x}_1(k) \leq x_1^{max}, \quad k = 0, ..., N_{\mathrm{MHE}} - 1 && \text{(C.10c)} \\
&x_2^{min} \leq \hat{x}_2(k) \leq x_2^{max}, \quad k = 0, ..., N_{\mathrm{MHE}} - 1 && \text{(C.10d)} \\
&0.01 \leq \hat{p} \leq 10 && \text{(C.10e)}
\end{aligned}$$

The simulation results for the adaptive MPC are plotted in Figure C.8. The estimated parameters ans states and their real values are also plotted in Figure C.9

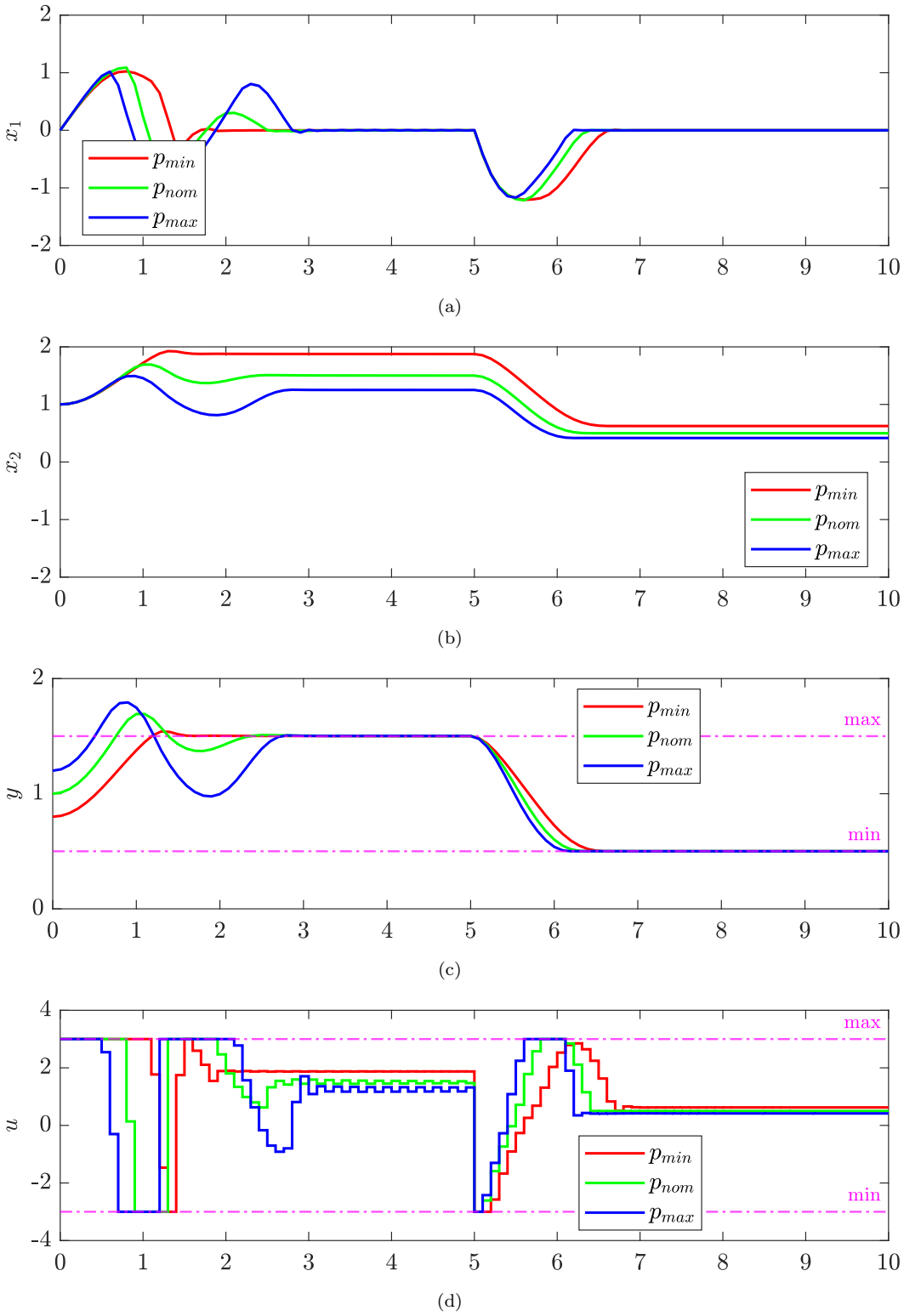

Figure C.8: Adaptive MPC applied to the plant with three realizations of uncertainty.

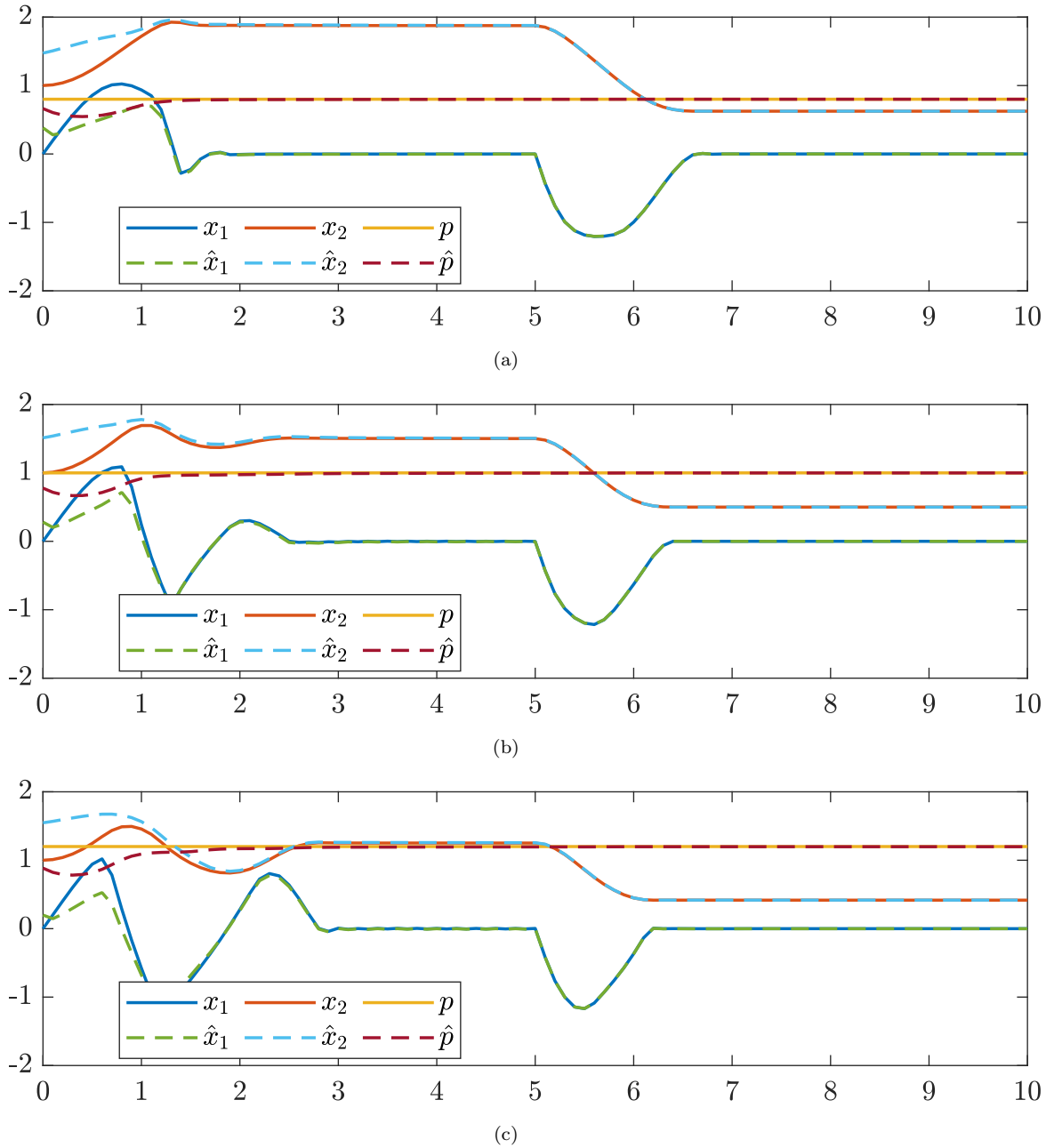

Figure C.9: Estimated parameters and states for three cases: (a) $p = p_{min}$, (b) $p = p_{nom}$, (c) $p = p_{max}$.

Part II
Scientific Papers

Paper A
Model based control and analysis of gas lifted oil field for optimal operation

Published in the *Proceeding of The First SIMS EUROSIM Conference on Modelling and Simulation, SIMS EUROSIM 2021, and 62nd International Conference of Scandinavian Simulation Society, SIMS 2021*, September 21-23, Virtual Conference, Finland, 2021.
Paper presented by Nima Janatian.
Authors: Nima Janatian, Kushila Jayamanne, and Roshan Sharma.
Authors' roles in the article:
Nima Janatian: Main ideas, implementation, and writing.
Kushila Jayamanne: Implementation
Roshan Sharma (Supervisor): Discussions, comments, and proofreading.

Model Based Control and Analysis of Gas Lifted Oil Field for Optimal Operation

Nima Janatian Kushila Jayamanne Roshan Sharma

Department of Electrical Engineering, IT and Cybernetics, University of South-Eastern Norway, Norway,
{Nima.Janatianghadikolaei,Kushila.R.Jayamanne,Roshan.Sharma}@usn.no

Abstract

This paper describes mathematical modeling, optimization, and analysis of a gas lift oil field with five wells. A global sensitivity analysis using the variance-based method is performed to classify the parameters, which are highly sensitive and uncertain simultaneously. An improved model is further used to design a model-based predictive controller to optimally distribute a limited supply of lift gas among the oil wells. Several simulation cases showed an increase in the total oil production, and all the constraints were fully satisfied when the deterministic NMPC was applied to the nominal model. The effect of parametric uncertainty is studied by applying the deterministic NMPC to the plant model containing the uncertain parameters. It has been shown that under the presence of uncertainty, robust constraint satisfaction is not guaranteed with some constraints not being satisfied, leading to unachievable and unrealistic lift gas distribution.

Keywords: Gas Lifted Oil Wells, Model Predictive Control, Global Sensitivity Analysis, Dynamic Modeling and Simulation, Parametric Uncertainty

1 Introduction

It is always of interest to manage and plan resources efficiently to obtain profit as much as possible from a given resource. In this sense, the oil and gas industry is not an exception. Hence, the optimal distribution of available gas is crucial to maximizing total oil production in a gas-lifted oil field where the multiple oil wells share the lift gas supplied by a common source.

In a gas lifted oil field, an artificial external mechanism is exploited to bring the dead wells back to life or increase the production rates from the naturally flowing wells. A continuous flow gas lifted oil field normally consists of multiple gas lift oil wells sharing lift gas from a common supply pipeline. A single gas lifted oil well is shown in Figure 1.In this system which is mostly used to extract the lighter crude oils, the high-pressurized natural gas is continuously injected into the annulus of the well through the gas lift choke valve. The injected gas finds its way into tubing at some points located at proper depths and mixes with the multiphase fluid from the reservoir. As a result of this mixing, the density of the fluid in the tubing will be reduced, which means that the flowing pressure losses in the tubing reduce. Consequently, the reservoir pressure will be able to overcome the flowing resistance in the well and push the reservoir fluid to the surface.

Each well has its own inflow characteristics. For example, two oil wells in the same field may produce different amount of oil even when the same amount of lift gas is injected into them. In other words, there is no rule of thumb on how to distribute the available lift gas among the oil wells to obtain the maximum possible oil production from the field. For optimal distribution of lift gas among the wells, model based real-time optimizer (RTO) can be used. For this an accurate mechanistic model of the process, which should be simultaneously simple enough to be used for real-time optimization and control purposes should be used.

Modeling and control of gas lifted oil field has been studied before in (Sharma et al., 2011), where some simplifying assumptions were made that may not reflect reality. For example, the fluid that comes out of the reservoir was assumed to be pure oil (without gas coming from the reservoir) and all the well parameters were assumed to be deterministic. This model had been used further in optimization of lift gas allocation as nonlinear optimization in (Sharma et al., 2012). This model has been improved in (Krishnamoorthy et al., 2016) by considering the gas to oil ratio. The long term production optimization under uncertainty has been studied in (Capolei et al., 2015; Hanssen et al., 2017) using economic MPC. But when it comes to the short-term optimization, most of the works either consider a deterministic model, which means they simply disregard uncertainty, or they limit the research scope to steady-state optimization using a very simplified linear model (Hanssen and Foss, 2015). Recently, a few papers have been published on real-time process optimization under the presence of uncertainty (Krishnamoorthy et al., 2019) to address the challenges in this area.

The first purpose of this paper is to improve the existing mathematical model of gas lifted oil fields with more realistic assumptions. To achieve this goal, the fluid that comes out of the reservoir is considered to be a mixture of oil, water, and gas. Furthermore, parametric uncertainties are considered for some parameters such as gas to oil ratio and productivity index. The second aim of the paper is to classify parameters that are both highly sensitive and uncertain simultaneously. Therefore, a global sensi-

tivity analysis is performed to study how the uncertainty in output (total oil production from the field) can be apportioned to different sources of uncertainty in the model parameters. The first order and total-effect sensitivity indices are calculated using the variance-based method due to its valuable features, such as the inclusion of interaction effects among input factors (Saltelli et al., 2008). The third goal is to study the effect of parametric uncertainty on lift gas distribution optimization problem. Considering the operational constraints of the process and the inherent robustness (to a certain extent) of the receding horizon strategy, a deterministic nonlinear model based predictive controller is designed based on the nominal plant model to optimally distribute a limited supply of lift gas being shared to several oil wells in the field. Several simulation cases are performed to study the performance of the optimal controller under varying operational scenarios. Simulation results show that the total oil production will be increased and all the constraints will be satisfied when the deterministic NMPC is applied to the nominal model. The effect of parametric uncertainty is shown by applying the deterministic NMPC to the plant model containing uncertain parameters and it has been shown that some constraints will be violated which suggests that the uncertainties should be considered explicitly in the optimal control problem.

The rest of the paper is organized as follows. Section 2 describes mathematical modeling of the gas lifted oil field system, openloop simulation results and the sensitivity analysis. Standard nonlinear model predictive control design, simulation results and stochastic analysis are presented in Section 3 before concluding in Section 4.

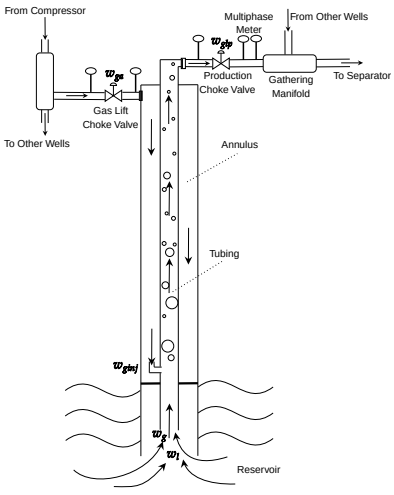

Figure 1. Schematic diagram of a single gas lift oil well

2 Modeling and Sensitivity Analysis

The considered gas lifted oil field of this paper consists of five oil wells that share a common gas distribution pipeline and common gathering manifold. A compressor discharges highly pressurized lift gas into the common gas distribution pipeline where it should be distributed among the oil wells. Considering a single oil well, the lift gas mass flow rate from the common distribution manifold into the well's annulus is denoted by w^i_{ga} where the superscript i refers to the i^{th} oil well. Then, the high pressure lift gas is injected from annulus into tubing (w^i_{ginj}) at a proper depth through the gas injection valve which is always open and only passes the flow in one direction. The injected gas mixes with the multiphase fluid (mixture of oil, water, and the gas from the reservoir) and reduces its density. This causes the hydrostatic pressure of the fluid column in tubing above the injection point and consequently the bottom hole pressure to drop. As a result, the differential pressure between the reservoir and the bottom hole pressure will increase and pushes the liquid column to flows upward to the surface. The produced mixture flows out through all the production choke valves (w^i_{glp}) is collected in the common gathering manifold and finally transported to the separator where they are separated into their corresponding compartments. The gas is then sent back to the compressor system and recycled to be used for lifting purposes.

Friction losses in the pipelines have not been taken into account since it might not be important for the sole purpose of control. All phases of the multiphase fluid are assumed to be evenly distributed with no slugging. The temperature of lift gas and the multiphase fluid is assumed to be constant at 280 K at all sections of the pipelines and the reservoir pressure is assumed to be constant at 150 bar. All the assumption are based on expert knowledge from Equinor ASA.

2.1 Model Description

The model is developed considering all the components of a typical gas lifted oil well as shown in Figure 1. The differential equations in model are obtained from the mass balances of each compartment. The algebraic equations are mostly density models, pressure models, flow models, and so on, which are obtained from equations of states, valve equations, and first principal modeling techniques.

Considering the mass of lift gas in annulus m^i_{ga}, mass of the gas in the tubing above the injection point m^i_{gt}, and mass of the liquid (mixture of oil and water) in the tubing above the injection point m^i_{lt} as three states and applying the mass balance, three corresponding differential equations are given by:

$$\dot{m}^i_{\mathrm{ga}} = w^i_{\mathrm{ga}} - w^i_{\mathrm{ginj}} \tag{1}$$

$$\dot{m}^i_{\mathrm{gt}} = w^i_{\mathrm{ginj}} + w^i_{\mathrm{g}} - w^i_{\mathrm{gp}} \tag{2}$$

$$\dot{m}^i_{\mathrm{lt}} = w^i_{\mathrm{l}} - w^i_{\mathrm{lp}} \tag{3}$$

w^i_{ga} is the mass flow rate of the injected lift gas into each well from the gas lift choke valve (system input), w^i_{ginj} is the mass flow rate of the gas injection from the annulus into the tubing, w^i_{gp} and w^i_{lp} are the produced gas and

liquid phase mass flow rates from the production choke valve, respectively, and w_{g}^{i} and w_{l}^{i} are the gas and liquid mass flow rates from the reservoir into the well. w_{glp}^{i} is the total mass flow rate of all phases from the production choke valve and w_{op}^{i} is the oil compartment of the w_{lp}^{i}. All the flow equations are given by:

$$w_{\mathrm{ginj}}^{i} = K^{i} Y_{2}^{i} \sqrt{\rho_{\mathrm{ga}}^{i} \max(P_{\mathrm{ainj}}^{i} - P_{\mathrm{tinj}}^{i}, 0)} \tag{4}$$

$$w_{\mathrm{gp}}^{i} = \frac{m_{\mathrm{gt}}^{i}}{m_{\mathrm{gt}}^{i} + m_{\mathrm{lt}}^{i}} w_{\mathrm{glp}}^{i} \tag{5}$$

$$w_{\mathrm{lp}}^{i} = \frac{m_{\mathrm{lt}}^{i}}{m_{\mathrm{gt}}^{i} + m_{\mathrm{lt}}^{i}} w_{\mathrm{glp}}^{i} \tag{6}$$

$$w_{\mathrm{l}}^{i} = PI^{i} \max(P_{r} - P_{\mathrm{wf}}^{i}) \tag{7}$$

$$w_{\mathrm{g}}^{i} = GOR^{i} w_{\mathrm{l}}^{i} \tag{8}$$

$$w_{\mathrm{glp}}^{i} = C_{v}(u_{2}^{i}) Y_{3}^{i} \sqrt{\rho_{\mathrm{m}}^{i} \max(P_{\mathrm{wh}}^{i} - P_{s}, 0)} \tag{9}$$

$$w_{\mathrm{op}}^{i} = \frac{\rho_{o}}{\rho_{w}} (1 - WC^{i}) w_{\mathrm{lp}}^{i} \tag{10}$$

P_{a}^{i} is the pressure of lift gas in annulus downstream the gas lift choke valve, P_{ainj}^{i} is the pressure upstream the gas injection valve in the annulus and P_{tinj}^{i} is the pressure downstream the gas injection valve in the tubing, and P_{wh}^{i} and P_{wf}^{i} are the well head and bottom hole pressure respectively. All the pressures are given by:

$$P_{\mathrm{a}}^{i} = \frac{z m_{\mathrm{ga}}^{i} R T_{\mathrm{a}}^{i}}{M A_{\mathrm{a}}^{i} L_{\mathrm{a\_tl}}^{i}} \tag{11}$$

$$P_{\mathrm{ainj}}^{i} = P_{\mathrm{a}}^{i} + \frac{m_{\mathrm{ga}}^{i}}{A_{\mathrm{a}}^{i} L_{\mathrm{a\_tl}}^{i}} g L_{\mathrm{a\_vl}}^{i} \tag{12}$$

$$P_{\mathrm{tinj}}^{i} = \frac{z m_{\mathrm{gt}}^{i} R T_{\mathrm{t}}^{i}}{M V_{G}^{i}} + \frac{\rho_{\mathrm{m}}^{i} g L_{\mathrm{t\_vl}}^{i}}{2} \tag{13}$$

$$P_{\mathrm{wh}}^{i} = \frac{z m_{\mathrm{gt}}^{i} R T_{\mathrm{t}}^{i}}{M V_{G}^{i}} - \frac{\rho_{\mathrm{m}}^{i} g L_{\mathrm{t\_vl}}^{i}}{2} \tag{14}$$

$$P_{\mathrm{wf}}^{i} = P_{\mathrm{tinj}}^{i} + \rho_{\mathrm{l}}^{i} g L_{\mathrm{r\_vl}}^{i} \tag{15}$$

ρ_{ga}^{i} is the average density of gas in the annulus. ρ_{gl}^{i} is the density of liquid phase (oil and water mixture), ρ_{m}^{i} is the average density of multiphase mixture in tubing above the injection point. Y_{2}^{i} and Y_{3}^{i} are the gas expandability factor for the gas that passes through gas injection valve and production choke valve, respectively. V_{G}^{i} is the volume of gas present in the tubing above the gas injection point, and $C_{v}(u_{2}^{i})$ is the production choke valve characteristics as its opening. All the densities and other variables are given by:

$$\rho_{\mathrm{ga}}^{i} = \frac{M(P_{\mathrm{a}}^{i} + P_{\mathrm{ainj}}^{i})}{2 z R T_{\mathrm{a}}^{i}} \tag{16}$$

$$\rho_{\mathrm{l}}^{i} = \rho_{w} WC^{i} + \rho_{o}(1 - WC^{i}) \tag{17}$$

$$\rho_{\mathrm{m}}^{i} = \frac{m_{\mathrm{gt}}^{i} + m_{\mathrm{lt}}^{i}}{A_{\mathrm{t}}^{i} L_{\mathrm{t\_tl}}^{i}} \tag{18}$$

$$Y_{2}^{i} = 1 - \alpha_{\mathrm{Y}} \frac{P_{\mathrm{ainj}}^{i} - P_{\mathrm{tinj}}^{i}}{\max(P_{\mathrm{ainj}}^{i}, P_{\mathrm{ainj}}^{\min})} \tag{19}$$

$$Y_{3}^{i} = 1 - \alpha_{\mathrm{Y}} \frac{P_{\mathrm{wh}}^{i} - P_{s}}{\max(P_{\mathrm{wh}}^{i}, P_{\mathrm{wh}}^{\min})} \tag{20}$$

$$V_{G}^{i} = A_{\mathrm{t}}^{i} L_{\mathrm{t\_tl}}^{i} - \frac{m_{\mathrm{lt}}^{i}}{\rho_{\mathrm{l}}^{i}} \tag{21}$$

$$C_{v}(u_{2}^{i}) = \begin{cases} 0 & \text{if } u_{2}^{i} < 5 \\ 30.303 u_{2}^{i} - 151.788 & \text{if } 5 < u_{2}^{i} < 50 \\ 136.5 u_{2}^{i} - 5460 & \text{if } 50 < u_{2}^{i} \end{cases} \tag{22}$$

Note that the dynamic model 1 to 22 could be written as an explicit ODE (ordinary differential equations) by simply eliminating the algebraic variables. So the model in compact form is given by:

$$\dot{x} = f(x, u) \tag{23}$$

$$y_{1} = h_{1}(x, u) \tag{24}$$

$$y_{2} = h_{2}(x, u) \tag{25}$$

where x and u are the states and system inputs, and y_1 and y_2 are two desired outputs

$$x = \begin{bmatrix} m_{\mathrm{ga}}^{1} & \dots & m_{\mathrm{ga}}^{5} & m_{\mathrm{gt}}^{1} & \dots & m_{\mathrm{gt}}^{5} & m_{\mathrm{lt}}^{1} & \dots & m_{\mathrm{lt}}^{5} \end{bmatrix}^{T} \tag{26}$$

$$u = \begin{bmatrix} w_{\mathrm{ga}}^{1} & w_{\mathrm{ga}}^{2} & w_{\mathrm{ga}}^{3} & w_{\mathrm{ga}}^{4} & w_{\mathrm{ga}}^{5} \end{bmatrix}^{T} \tag{27}$$

$$y_{1} = \sum_{i=1}^{5} w_{\mathrm{op}}^{i} \tag{28}$$

$$y_{2} = \sum_{i=1}^{5} w_{\mathrm{glp}}^{i} \tag{29}$$

2.2 Uncertainties

In this work, the productivity index PI which is a mathematical means of expressing the reservoir's ability to deliver fluids to the wellbore, gas to oil ratio GOR which is defined as the mass ratio of produced gas to produced liquid (oil and water), and water cut WC which is defined as the volumetric flow rate of water to the total produced liquid, are considered to be constant but unknown parameters. Considering the five oil wells, there exist fifteen uncertain parameters in the system that makes it visually impossible to show the uncertainty region. Nevertheless, the uncertainty region of one well is shown in Figure 2 as

an example. All the uncertain parameters of all the five wells in this paper are assumed to have the same ±20% deviation from their nominal values and uniform distribution. The reason of choosing uniform distribution is to challenge the controller.

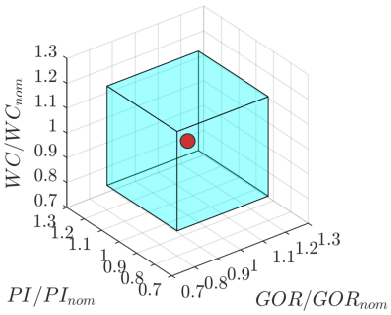

Figure 2. Unceratainty region with ±20% deviation.

2.3 Open Loop Simulation

The system is simulated in open loop using the nominal values of parameters provided in Table 1 and P_r and P_s are assumed to be 150 and 30 bar, respectively. The presented results in Figure 3 show that a decrease in the injected lift gas flow rates causes an increase in bottom hole pressures, and consequently, the oil production flows decrease. This means that the model is capable of showing all the necessary dynamics of gas lifted oil field and will be used further to perform sensitivity analysis and to design nonlinear model predictive control.

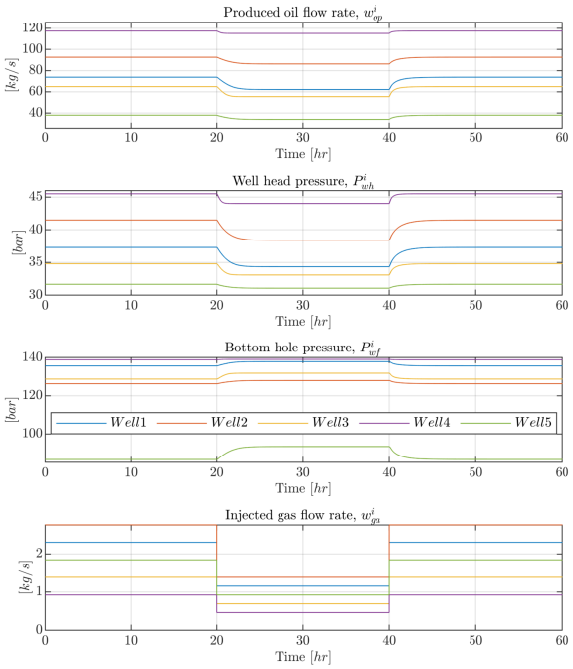

Figure 3. Open loop simulations of the nominal model

2.4 Global Sensitivity Analysis

It is useful to figure out which parameters have a strong/weak influence on the model output, especially under the presence of uncertainties, because the model based control design will be more problematic and needs more care if the uncertain parameters are sensitive as well. Variance based global sensitivity analysis method is selected due to its valuable features such as model independence, capacity to capture the influence of the full range of variation of each input factor, and appreciation of interaction effects among input factors.

The first order and total sensitivity indices are calculated using the variance based method introduced in (Saltelli et al., 2008) which is an improved extension of the original approach provided by (Sobol, 1993) and (Homma and Saltelli, 1996). Here only the results are presented and the readers are referred to the main reference for more information about the method due to the word limitation.

A number of 136000 Monte Carlo simulations have been done to calculate the sensitivity indices. Both sensitivity indices presented in Figure 4 show that for the considered uncertainty region introduced in Figure 2, gas to oil ratio is the most sensitive/influential parameter and productivity index and water cut are at the second and third place, respectively. In other words, the standard controller based on the nominal model will be more robust to deviation in water cut. On the other hand, a slight deviation in the gas to oil ratio leads to a severe mismatch between the nominal and uncertain model, therefore, poor performance is expected. These interpretations will be verified by stochastic analysis results in the following section.

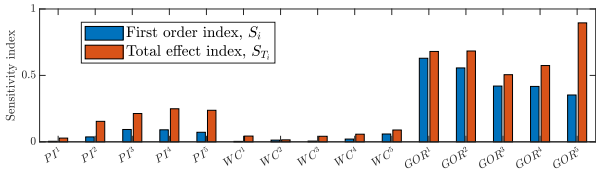

Figure 4. Sensitivity indices

3 Standard NMPC and Stochastic Analysis

3.1 Design of deterministic standard NMPC

The primary control objective is to maximize the total oil production of the field (output y_1) by manipulating the injected lift gas (u). Additionally, u and Δu are introduced to penalize excessive lift-gas utilization and large fluctuations in the control signals. Apart from the model equations, which obviously should be satisfied, the process is subjected to operational constraints. For example, the total injected lift gas should be equal to or less than the total available lift gas ($W_{\text{gc}}^{\max}$) and the total produced fluid should not exceed the maximum capacity of the separator ($W_{\text{s}}^{\max}$). There are also upper and lower bounds on control

Table 1. Nominal values of well parameters used for simulation.

Parameter	*Well1*	*Well2*	*Well3*	*Well4*	*Well5*	*Unit*
K	68.43	67.82	67.82	69.26	66.22	$[\frac{\sqrt{\frac{\text{kgm}^3}{\text{bar}}}}{\text{hr}}]$
PI(1.0e+4)	2.51	1.63	1.62	4.75	0.232	$\frac{\text{kg/hr}}{\text{bar}}$
GOR	0.05	0.07	0.03	0.04	0.06	$[\text{kg}/\text{kg}]$
WC	0.20	0.10	0.25	0.15	0.05	$[\text{m}^3/\text{m}^3]$
$L_{\text{a\_tl}}/L_{\text{t\_tl}}$	2758	2559	2677	2382	2454	$[\text{m}]$
$L_{\text{a\_vl}}/L_{\text{t\_vl}}$	2271	2344	1863	1793	1789	$[\text{m}]$
A_{a}	0.0174	0.0174	0.0174	0.0174	0.0174	$[\text{m}^2]$
A_{t}	0.0194	0.0194	0.0194	0.0194	0.0194	$[\text{m}^2]$
$L_{\text{r\_vl}}$	114	67	61	97	146	$[\text{m}]$

inputs and change of control due to the physical limitation of the actuators (valves). Therefore, the optimal control problem formulation is given by:

$$\min_{x,u} \quad \sum_{k=0}^{N-1}\left(-Q(y_{1,k})^2 + R\sum_{i=1}^{5} u_k^{i^2} + S\sum_{i=1}^{5}\Delta u_k^{i^2}\right) \tag{30}$$

$$\text{s.t.} \quad x_{k+1} = f\left(x_k, u_k, \theta_k\right) \tag{31}$$

$$\sum_{i=1}^{5} u_k^i \leq W_{\text{gc,k}}^{\max} \tag{32}$$

$$y_{2,k} \leq W_s^{\max} \tag{33}$$

$$u_{\text{LB}} \leq u_k^i \leq u_{\text{UB}} \tag{34}$$

$$\Delta u_{\text{LB}} \leq \Delta u_k^i \leq \Delta u_{\text{UB}} \tag{35}$$

where Q, R, and S are tuning weights and are chosen to be 1, 0.5, and 50, respectively. The total available lift gas $W_{\text{gc}}^{\max} = 9.22$[kg/s] and the maximum capacity of the separator $W_{\text{s}}^{\max} = 520$[kg/s]. The lower and upper bounds on the control signal are 0.323 and 11.66[kg/s]. Change of control also is limited between ± 0.15[kg/s]. A sampling time of 10 seconds and a prediction horizon of 25 timesteps (4.1 min) is used. These values are maintained constant throughout this paper.

3.2 Stochastic analysis of parametric uncertainty

In the first scenario, the deterministic NMPC was applied to the nominal model. As shown in Figure 5, open loop simulation started within the feasible region and the controller activated after 1 hour. The simulation results show a 12% increased in the total oil production from the field while all the constraints on the total available lift gas, capacity of separator and actuator limitations are fully satisfied.

In the other scenarios, the same controller is applied to the models containing uncertainties to see whether the controller can cope with the uncertainties in the model. For the extreme cases where the uncertain parameters take their maximums and minimums in the uncertainty region, severe oscillations were observed that led to instability.

Figure 6 shows the result of applying the nominal controller to the plant that only has -10% deviations in water cut, while the gas to oil ratio and productivity index are equal to their nominal values. It can be seen that the total oil production has been increased while the constraint on the maximum capacity of separator is violated. Although this case is not practically implementable, it worth to be noted that the same, or even smaller deviation (about 4%) in gas to oil ratio and productivity index leads to instability. This observation is consistent with the outcome from the sensitivity analysis that says the model is less sensitive to water cut rather than either gas to oil ratio or productivity index.

Figure 7 is the last scenario with -5, 8, and -2 percent deviations in productivity index, water cut, and gas to oil ratio, respectively, from their nominal values. The mismatch between the nominal and uncertain models can be observed from the total fluid production graph. In essence, it can be concluded that the deterministic NMPC is not sufficient for the gas lifted oil field model with uncertain parameters.

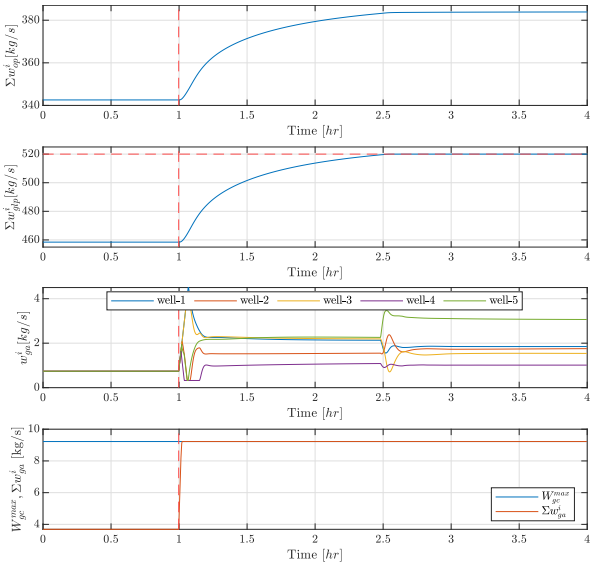

Figure 5. Performance of standard NMPC when it is applied to the nominal model.

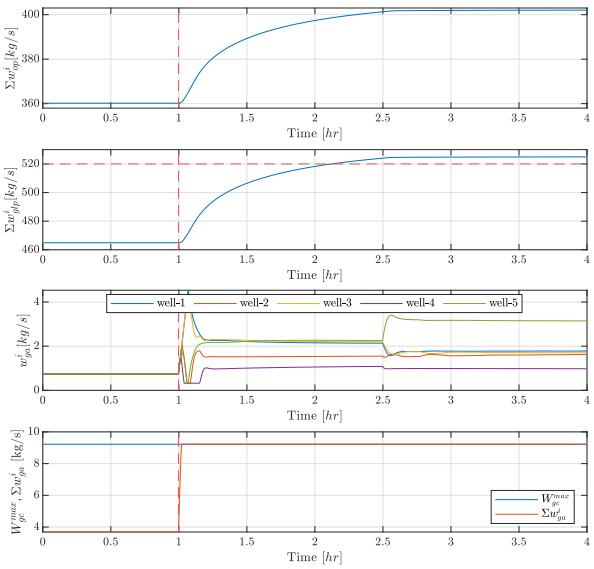

Figure 6. Performance of standard NMPC when it is applied to the uncertain model.

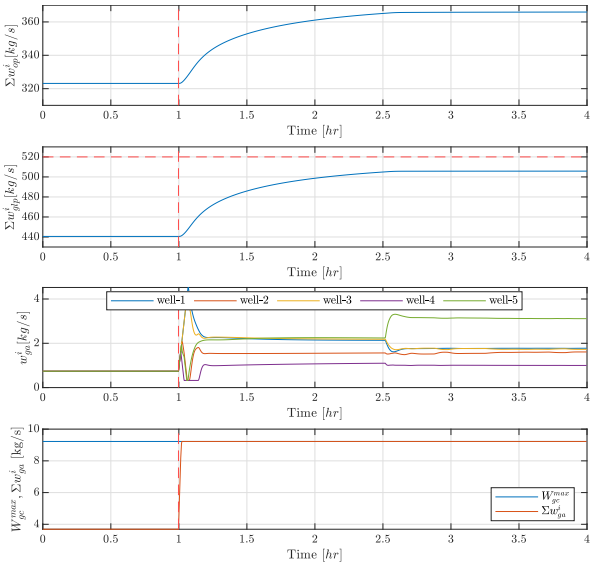

Figure 7. Performance of standard NMPC when it is applied to the uncertain model.

4 Conclusion

This paper presented a modeling framework for the gas lifted well system and total oil production maximization as a dynamic optimization control problem. The simulation results showed that the deterministic NMPC based on nominal model is capable of maximizing the total oil production of the nominal model while fulfills all the operational constraints subjected to the process; however, when the deterministic NMPC is applied to the model contains uncertainties, simulation results showed some constraints violations. This means that a deterministic NMPC is not sufficient to handle parametric uncertainties for this problem. Feasibility issues showed that the uncertainties need to be considered explicitly inside the optimization problem using robust or stochastic model predictive control. The future work includes using such advanced control methods to maximize total oil production while ensuring robust constraint satisfaction for all possible values of the uncertainties.

Acknowledgments

We gratefully acknowledge the economic support from The Research Council of Norway and Equinor ASA through Research Council project “308817 - Digital wells for optimal production and drainage” (DigiWell).

References

Andrea Capolei, Bjarne Foss, and John B. Jørgensen. Profit and risk measures in oil production optimization. *IFAC-PapersOnLine*, 48(6):214–220, 2015. doi:10.1016/j.ifacol.2015.08.034.

Kristian G. Hanssen and Bjarne Foss. Production optimization under uncertainty - applied to petroleum production. *IFAC-PapersOnLine*, 48(8):217–222, 2015. doi:10.1016/j.ifacol.2015.08.184.

Kristian G. Hanssen, Andrés Codas, and Bjarne Foss. Closed-loop predictions in reservoir management under uncertainty. *SPE Journal*, 22(5):1585–1595, 2017. doi:10.2118/185956-PA.

Toshimitsu Homma and Andrea Saltelli. Importance measures in global sensitivity analysis of nonlinear models. *Reliability Engineering & System Safety*, 52(1):1–17, 1996. doi:10.1016/0951-8320(96)00002-6.

Dinesh Krishnamoorthy, Bjarne Foss, and Sigurd Skogestad. Real-time optimization under uncertainty applied to a gas lifted well network. *Processes*, 52(4), 2016. doi:10.3390/pr4040052.

Dinesh Krishnamoorthy, Sigurd Skogestad, and Johannes Jäschke. Multistage model predictive control with online scenario tree update using recursive bayesian weighting. *18th European Control Conference (ECC)*, pages 1443–1448, 2019. doi:10.23919/ECC.2019.8795839.

Andrea Saltelli, Marco Ratto, Terry Andres, Francesca Campolongo, Jessica Cariboni, Debora Gatelli, Michaela Saisana, and Stefano Tarantola. *Global Sensitivity Analysis: The Primer*. John Wiley & Sons, 2008. ISBN 978-0-470-72517-7.

Roshan Sharma, Kjetil Fjalestad, and Bjørn Glemmestad. Modeling and control of gas lifted oil field with five oil wells. *the 52nd International Conference of Scandinavian Simulation Society*, pages 47–59, 2011.

Roshan Sharma, Kjetil Fjalestad, and Bjørn Glemmestad. Optimization of lift gas allocation in a gas lifted oil field as nonlinear optimization problem. *Modeling, Identification and Control*, 33(1):13–25, 2012.

Ilya M. Sobol. Sensitivity analysis for non-linear mathematical models. *Mathematical modelling and computational experiment*, 1:407–414, 1993.

Paper B
Multi-stage scenario-based MPC for short term oil production optimization under the presence of uncertainty

Published in *Journal of Process Control*, Volume 118, October 2022.
Authors: Nima Janatian and Roshan Sharma.
Authors' roles in the article:
Nima Janatian: Main ideas, implementation, and writing.
Roshan Sharma (Supervisor): Discussions, comments, and proofreading.

Journal of Process Control 118 (2022) 95–105

Contents lists available at ScienceDirect

Journal of Process Control

journal homepage: www.elsevier.com/locate/jprocont

Multi-stage scenario-based MPC for short term oil production optimization under the presence of uncertainty

Nima Janatian *, Roshan Sharma

Department of Electrical engineering, Information Technology and Cybernetics, University of South-Eastern Norway, Campus Porsgrunn, Norway

ARTICLE INFO

Article history:
Received 25 January 2022
Received in revised form 21 August 2022
Accepted 23 August 2022
Available online 5 September 2022

Keywords:
Multi-stage stochastic model predictive control
Real-time optimization
Parametric uncertainty
Scenario tree
Gas lift oil wells

ABSTRACT

This paper considers the problem of daily production optimization for a gas lift oil network under the presence of parametric uncertainty. The objective is to find the optimal distribution of injected lift gas to maximize total oil production from an oil network that contains parametric uncertainties subject to some constraints. Typically, the model-based optimization methods in such processes overlook uncertainty and go along with the optimal solution based on the nominal model. Nevertheless, the effect of uncertainty may lead to infeasibility when implemented in real applications. The proposed scenario-based optimization framework in this paper ensures robust feasibility compared to deterministic optimization. Additionally, the superiority of the method has been illustrated in comparison with the other robust optimization counterparts such as Min–Max NMPC in terms of conservativeness and execution time. The simulation results of the nominal, min–max, and scenario-based optimization are compared and discussed.

1. Introduction

Model Predictive Control (MPC) has received considerable attention in process control due to its significant features. It can be used for multiple-input multiple-output systems and it also facilitates the handling of the constraints, either they are on the states, control inputs, or the outputs. Despite its promising features, like every other model-based control method, its performance profoundly depends on the quality of the used model. From a practical point of view, when some uncertainties are present in the system being controlled, then the situation becomes even more challenging, especially if there are hard constraints in the problem that should be satisfied at all times.

Gas lift is a standard artificial lift method of producing oil, where natural gas from an external source is exploited to either increase the production of a flowing well or bring back a dead oil well into production. To maximize the short-term oil production in a field where multiple oil wells share a common lift gas source, the optimal distribution of a given amount of lift gas is an important task. Model predictive control can be used as a real-time optimizer (RTO) for the optimal distribution of a limited amount of total lift gas available for injection. A standard MPC algorithm uses the model of the process to predict the future dynamics of the process and optimizes the desired objective. However, the unmodeled dynamics, the uncertainty in measurements, and parametric uncertainty introduce some mismatch between the model's prediction and what happens in reality. So, considering the dependence of control performance on the quality of the model on the one hand and the fact that no model is totally perfect on the other hand, it becomes inevitable to deal with the robustness when the MPC is applied in reality.

Mathematical modeling of gas-lifted oil fields has been studied before for different purposes such as flow stabilization in [1,2] and production optimization in [3,4]. Despite some minor differences in the assumptions, such as the inflow performance of oil wells and ingredients of the fluid in the reservoir, all the models are derived based on mass conservation of different fluid phases in the tubing and annulus. It has been shown in [5] that these first principle models are sufficient to capture the essential dynamic behavior of the process for control purposes.

The long-term production optimization under uncertainty has been studied extensively in [6,7] using economic MPC, in [8] using multi-objective optimization, and in [9] using Artificial Intelligence. However, most of the works for short-term production optimization consider a deterministic model, see for example [10], which means the uncertainty is neglected. Alternatively, some others included the uncertainty while they limited their scope to steady-state optimization using a very simplified linear model such as in [11].

Recently, real-time process optimization under the presence of uncertainty has been studied in [12] to address the challenges in this area. However, the gas to oil ratio is the only uncertain

* Corresponding author.
E-mail addresses: nima.janatianghadikolaei@usn.no (N. Janatian), roshan.sharma@usn.no (R. Sharma).

https://doi.org/10.1016/j.jprocont.2022.08.012

parameter considered in this work. The other parameters such as water cut and productivity index are assumed to be deterministic, while the water cut is the most varying (uncertain) parameter in the field. So, neglecting the water in the reservoir makes the model unrealistic. Stochastic analysis of the deterministic nonlinear MPC in [13] has shown that the deterministic NMPC may not be sufficient to cope with the parametric uncertainties for the problem of oil production maximization. Thus, the uncertainties need to be considered explicitly inside the optimization problem.

Only a handful of literature is available for the short-term oil production optimization under uncertainty which highlights the fact that it still is an active and ongoing topic for research. Therefore, the first objective of this paper is to develop a control framework for the short-term optimization of a gas lifted oil system that can assure robust performance under the presence of parametric uncertainties in the gas to oil ratio, productivity index, and water cut. A multi-stage scenario-based nonlinear model predictive control method is used to achieve this goal. The developed controller aimed to cope with all the plant realizations within the uncertainty region and never violate the constraints.

The multi-stage scenario-based stochastic optimization method has been used in the context of model predictive control to distribute the lift gas between two oil wells optimally. This method was introduced in [14]. Although, its roots point back to [15], where the notion of feedback in the optimization problem was introduced for the first time. In this method, the uncertainty region is discretized according to a scenario tree, and then the evolution of the plant is taken into account for each scenario. The scenario tree formulation makes it possible to consider that in the future sampling time, the new measurements will be available; hence, future decisions can depend on future information. This approach increases the degree of freedom of the optimization problem and reduces conservativeness.

However, robustness is not free. Conservativeness is the price that one should pay to accomplish robust constraints fulfillment. It means the controller sacrifices the optimality compared to the case everything was precisely known to ensure that the constraints will be appropriately satisfied for all the realizations of uncertain parameters. Hence, the other goal of this paper is to show the superiority of the developed framework compared with the other robust counterparts such as Min–Max NMPC [16] in terms of conservativeness and execution time. The worst-case scenario or min–max NMPC is designed in both open loop and closed-loop optimization fashion for the sake of comparison, and the simulation results have demonstrated that the multi-stage stochastic NMPC has a better performance in terms of conservativeness compared with open loop min–max MPC and execution time compared with closed-loop min–max MPC.

The rest of the paper is organized as follows. Section 2 briefly describes mathematical modeling of the gas lifted oil field system. Multi-stage nonlinear model predictive control design and simulation results are presented in Section 3 and Section 4, respectively before concluding in Section 5.

2. Model of the oil field and uncertainty description

A schematic illustration of a single oil well is demonstrated in Fig. 1. The principle behind the gas lift method is to reduce the density of the fluid mixture in the well's tubing. This density reduction happens by continuous injection of a high-pressurized natural gas into the well's annulus through the gas lift choke valve. The injected gas finds its way into the tubing at some points located at proper depths and mixes with the multi-phase fluid from the reservoir. As a result of this mixing, the fluid density in the tubing will be reduced, which means that the hydrostatic pressure and the flowing pressure losses in the tubing

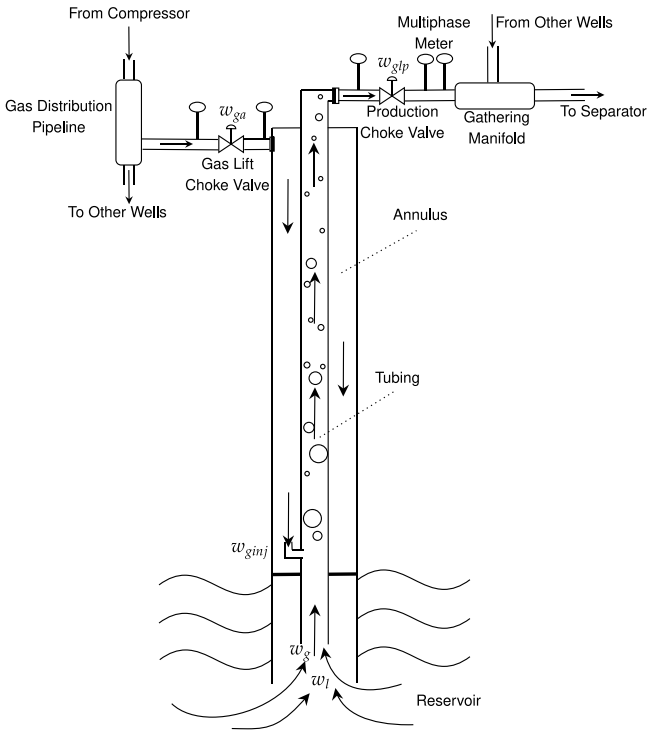

Fig. 1. Schematic diagram of a single gas lift oil well.

will be reduced. Consequently, the reservoir pressure will be able to overcome the flowing resistance in the well and push the reservoir fluid to the surface. Since mathematical modeling is not the main focus of this paper, the model description is only presented briefly in this section. The readers are referred to [3,17] for the full detailed explanation.

The gas lifted oil field studied in this paper consists of two oil wells with a shared gas distribution pipeline and a common gathering manifold. The superscript i refers to the ith oil well. Three considered states for each well are namely, the mass of lift gas in annulus m^i_{ga}, the mass of gas phase in the tubing above the injection point m^i_{gt}, and the mass of liquid phase (mixture of oil and water) in the tubing above the injection point m^i_{lt}. Three corresponding differential equations derived using the law of mass balance are given by:

$$\dot{m}^i_{ga} = w^i_{ga} - w^i_{ginj} \tag{1}$$

$$\dot{m}^i_{gt} = w^i_{ginj} + w^i_g - w^i_{gp} \tag{2}$$

$$\dot{m}^i_{lt} = w^i_l - w^i_{lp} \tag{3}$$

w^i_{ga} is the mass flow rate of the injected lift gas into each well from the gas lift choke valve (system input). w^i_{ginj} is the mass flow rate of the gas injection from the annulus into the tubing. w^i_{gp} and w^i_{lp} are the mass flow rates of the produced gas and liquid phase fluid from the production choke valve, respectively. w^i_g and w^i_l are the gas and liquid mass flow rates from the reservoir into the well. w^i_{glp} is the total mass flow rate of all phases from the production choke valve, and w^i_{op} is the oil compartment of the w^i_{lp}. All the flow equations are given by:

$$w^i_{ginj} = K^i Y^i_2 \sqrt{\rho^i_{ga} \max(P^i_{ainj} - P^i_{tinj}, 0)} \tag{4}$$

$$w^i_{gp} = \frac{m^i_{gt}}{m^i_{gt} + m^i_{lt}} w^i_{glp} \tag{5}$$

$$w_{lp}^i = \frac{m_{lt}^i}{m_{gt}^i + m_{lt}^i} w_{glp}^i \tag{6}$$

$$w_l^i = PI^i \max(P_r - P_{wf}^i) \tag{7}$$

$$w_o^i = \frac{\rho_o}{\rho_w}(1 - WC^i) w_l^i \tag{8}$$

$$w_g^i = GOR^i w_o^i \tag{9}$$

$$w_{glp}^i = C_v Y_3^i \sqrt{\rho_m^i \max(P_{wh}^i - P_s, 0)} \tag{10}$$

$$w_{op}^i = \frac{\rho_o}{\rho_w}(1 - WC^i) w_{lp}^i \tag{11}$$

P_a^i is the pressure of lift gas in the annulus downstream the gas lift choke valve. P_{ainj}^i is the pressure upstream of the gas injection valve in the annulus. P_{tinj}^i denotes the pressure downstream the gas injection valve in the tubing. P_{wh}^i and P_{wf}^i are the wellhead and bottom hole pressure, respectively. All the pressures are given by:

$$P_a^i = \frac{z m_{ga}^i R T_a^i}{M A_a^i L_{a\_tl}^i} \tag{12}$$

$$P_{ainj}^i = P_a^i + \frac{m_{ga}^i}{A_a^i L_{a\_tl}^i} g L_{a\_vl}^i \tag{13}$$

$$P_{tinj}^i = \frac{z m_{gt}^i R T_t^i}{M V_G^i} + \frac{\rho_m^i g L_{t\_vl}^i}{2} \tag{14}$$

$$P_{wh}^i = \frac{z m_{gt}^i R T_t^i}{M V_G^i} - \frac{\rho_m^i g L_{t\_vl}^i}{2} \tag{15}$$

$$P_{wf}^i = P_{tinj}^i + \rho_l^i g L_{r\_vl}^i \tag{16}$$

ρ_{ga}^i is the average density of gas in the annulus. ρ_{gl}^i is the density of the liquid phase (mixture of the oil and water). ρ_m^i denotes the average density of the multi-phase mixture in the tubing above the injection point. Y_2^i and Y_3^i are the gas expandability factors for the gas that passes through the gas injection valve and production choke valve, respectively. V_G^i is the volume of gas present in the tubing above the gas injection point, and C_v is the production choke valve characteristics. All the densities and other algebraic variables are given by:

$$\rho_{ga}^i = \frac{M(P_a^i + P_{ainj}^i)}{2 z R T_a^i} \tag{17}$$

$$\rho_l^i = \rho_w WC^i + \rho_o(1 - WC^i) \tag{18}$$

$$\rho_m^i = \frac{m_{gt}^i + m_{lt}^i}{A_t^i L_{t\_tl}^i} \tag{19}$$

$$Y_2^i = 1 - \alpha_Y \frac{P_{ainj}^i - P_{tinj}^i}{\max(P_{ainj}^i, P_{ainj}^{\min})} \tag{20}$$

$$Y_3^i = 1 - \alpha_Y \frac{P_{wh}^i - P_s}{\max(P_{wh}^i, P_{wh}^{\min})} \tag{21}$$

$$V_G^i = A_t^i L_{t\_tl}^i - \frac{m_{lt}^i}{\rho_l^i} \tag{22}$$

Note that the dynamic model in Eqs. (1) to (22) could be written as an explicit set of ordinary differential equations (ODE) by simply eliminating the algebraic variables. So the model in compact form is given by:

$$\dot{x} = f(x, u, \theta) \tag{23}$$

$$y_1 = h_1(x, \theta) \tag{24}$$

$$y_2 = h_2(x, \theta) \tag{25}$$

where $x \in \mathbb{R}^6$ and $u \in \mathbb{R}^2$ are the states and system inputs. $y_1 \in \mathbb{R}$ and $y_2 \in \mathbb{R}$ are two desired outputs, and $\theta \in \mathbb{R}^6$ is the vector of the uncertain parameters of the process.

$$x = \begin{bmatrix} m_{ga}^1 & m_{ga}^2 & m_{gt}^1 & m_{gt}^2 & m_{lt}^1 & m_{lt}^2 \end{bmatrix}^T \tag{26}$$

$$u = \begin{bmatrix} w_{ga}^1 & w_{ga}^2 \end{bmatrix}^T \tag{27}$$

$$y_1 = \sum_{i=1}^{2} w_{op}^i \tag{28}$$

$$y_2 = \sum_{i=1}^{2} w_{glp}^i \tag{29}$$

$$\theta = \begin{bmatrix} PI^1 & PI^2 & GOR^1 & GOR^2 & WC^1 & WC^2 \end{bmatrix}^T \tag{30}$$

In this study, the productivity index PI which is a mathematical means of expressing the reservoir's ability to deliver fluids to the wellbore, gas to oil ratio GOR which is defined as the mass ratio of produced gas to produced oil, and water cut WC which is defined as the volumetric flow rate of water to the total produced liquid, are considered to be constant but unknown parameters. For a network with two oil wells, there exist six uncertain parameters in the problem that makes it visually impossible to show the uncertainty region in a six dimensional parameter space. However, these uncertain parameters are upper and lower bounded and can take any value within their bounds. For PI, GOR, and WC of each oil well, a deviation of $\pm 10\%$, $\pm 5\%$, and $\pm 15\%$ from their nominal values (as provided in Table 1) are considered respectively based on expert knowledge. A uniform distribution is selected to challenge the control task since the uniform distribution implies that all the values in the uncertainty region are equally likely to occur. Thus, it would be more challenging for the controller to cope with such uncertainty.

3. Multi-stage stochastic MPC

For this production field with two oil wells, the primary objective is to find the optimal distribution of lift gas that maximizes the total oil production from the field. There is a constraint on the total amount of fluid (mixture of oil, water and gas) that can be produced from the field due to the separator capacity. There is another constraint on the maximum available lift gas for injection. Additionally, the injected lift gas and its rate of change can be incorporated into the objective function using proper tuning weights to penalize excessive lift gas utilization and fluctuations in the control signal. Hence for $k \in \{0, 1, \ldots, N-1\}$ where N is the length of the prediction horizon and Q, R and S denote the tuning weights, the objective function is given by:

$$J = \sum_{k=0}^{N-1} \left(-Q(y_{1,k})^2 + R \sum_{i=1}^{2} u_k(i)^2 + S \sum_{i=1}^{2} \Delta u_k(i)^2 \right) \tag{31}$$

And the optimal control problem formulation is given by:

$$\min_{x,u} \quad J \tag{32}$$

$$\text{s.t.} \quad x_{k+1} = f(x_k, u_k, \theta_k) \tag{33}$$

$$\sum_{i=1}^{2} u_k(i) \le W_{gc,k}^{\max} \tag{34}$$

$$y_{2,k} \le W_s^{\max} \tag{35}$$

$$u_{LB} \le u_k \le u_{UB} \tag{36}$$

$$\Delta u_{LB} \le \Delta u_k \le \Delta u_{UB} \tag{37}$$

The discretized dynamic model is implemented as state constraints in (33). The constraint on the used lift gas is denoted in (34) where $W_{gc,k}^{\max}$ represents the total available lift gas. The constraint on the total produced fluid is enforced in (35), where

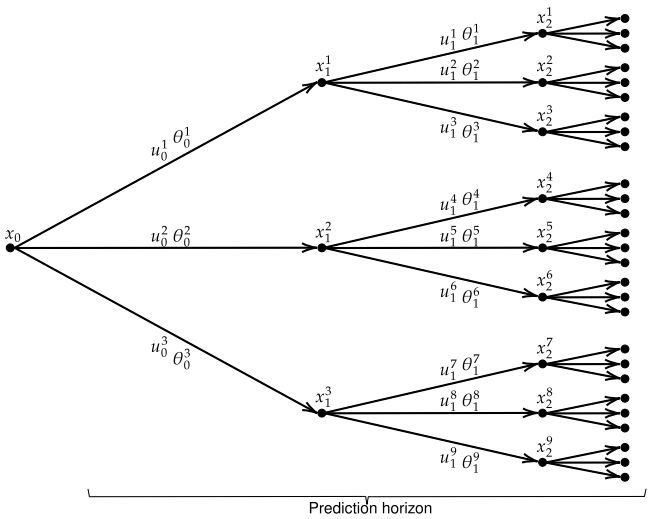

Fig. 2. Illustration of a scenario tree that represents the evolution of states with three models/branches and three future time steps. The total number of scenarios is equal to $3^3 = 27$.

$W_s^{\max}$ stands for the maximum capacity of the separator. The lower and upper bounds on the control signal and the rate of change of control inputs are also implemented in (36) and (37) respectively.

The robust optimization methods propose that the uncertain parameters should be assumed to take their worst-case realization to ensure robust performance. Otherwise, the constraints possibly will be violated. Although the robust optimization, also known as worst-case optimization, ensures the constraints fulfillment, it will be overly conservative since it does not count on the fact that the new information will be received in the future sampling times. The problem of conservativeness is addressed in [15] by introducing the notion of feedback in the optimization problem, which means the optimization problem should be solved over different control policies rather than a single control trajectory. However, doing so would be computationally challenging and intractable due to the infinite dimension of the problem.

Alternatively, in the multi-stage nonlinear model predictive control approach, as introduced in [14], the uncertainty region is discretized into distinct possible realizations for the uncertain parameters. Then, the evolution of the system is considered based on a scenario tree. In other words, a finite number of parameter realizations are considered like separate models, and the plant can evolve into different trajectories depending on which realization/model occurs in reality. A simple scenario tree has been illustrated in Fig. 2 as an example, where three models (possible realization of the plant) are considered. Each path from the root node to leaf is called a scenario; thus, the method is also known as scenario-based optimization. It should be noted that this formulation imposes an extra constraint which is known as a non-anticipativity constraint. This constraint arises from the fact that in real-time decision making, the controller is not able to anticipate the future realization of the uncertainty. Therefore, all the controls that branch from a parent node are equal. For example, in Fig. 2 some of the non-anticipativity constraints are $u_0^1 = u_0^2 = u_0^3$, $u_1^1 = u_1^2 = u_1^3$, $u_1^7 = u_1^8 = u_1^9$, and so on.

The downside of this method is that the number of scenarios grows exponentially with the number of considered models and as the prediction horizon becomes longer. However, this problem is solved by stopping the branching after a certain number of samples. This gives rise to the concept of robust horizon. The robust horizon is usually much shorter than the prediction horizon. It makes sense that the far future uncertainty does not need to be represented precisely because, in any case, the corresponding control variables and state trajectories will be recalculated and refined in future sampling times.

Once the scenario tree and its prerequisites have been defined, the optimization problem can be formulated over all the discrete scenarios of the scenario set $\mathcal{S} = \{1, \ldots, S\}$ throughout the prediction horizon $\mathcal{K} = \{0, \ldots, N-1\}$. It should be noted that the scenario tree enables the inclusion of the feedback in the problem as a closed-loop optimization. In other words, the optimization is formulated over different sets of control inputs rather than a single sequence of control actions. Therefore, for $\forall j \in \mathcal{S}$ and $\forall k \in \mathcal{K}$ and the tuning weights ω_j, that reflect the relative likelihood of occurring each scenario, the multi-stage nonlinear model predictive control is formulated as,

$$\min_{\mathrm{x,u}} \quad \sum_{j=1}^{S} \omega_j J_j \tag{38}$$

$$\text{s.t.} \quad x_{k+1}^j = f\left(x_k^{p(j)}, u_k^j, \theta_k^{r(j)}\right) \tag{39}$$

$$\sum_{i=1}^{2} u_k^j(i) \le W_{gc,k}^{\max} \tag{40}$$

$$y_{2,k}^j \le W_s^{\max} \tag{41}$$

$$u_{LB} \le u_k^j \le u_{UB} \tag{42}$$

$$\Delta u_{LB} \le \Delta u_k^j \le \Delta u_{UB} \tag{43}$$

$$u_k^j = u_k^l \quad \text{if} \quad x_k^{p(j)} = x_k^{p(l)}, \quad \forall j \& l \in \mathcal{S} \tag{44}$$

where the J_j in (38) is the objective function for scenario j. (39) denotes the equation of the states. It means that the states at time $t = k+1$ in scenario j are a function of their parental state $x_k^{p(j)}$ and the corresponding control u_k^j and uncertainty realization $\theta_k^{r(j)}$. For instance according to Fig. 2, $x_2^6 = f\left(x_1^2, u_1^6, \theta_1^6\right)$. The non-anticipativity constraints introduced in (44) reflects the fact that at each time instance k, controls u_k^j and x_k^j from scenarios j and l with the same parental state $x_k^{p(j)} = x_k^{p(l)}$ have to be the equal. For example in Fig. 2, $u_0^1 = u_0^2 = u_0^3$ is one (but not the only) set of non-anticipativity constraints, since all these controls are branched from the same parental node x_0. It is worthwhile to mention that according to the receding horizon strategy, this first control action is the one that will be implemented in real system and the non-anticipativity constraint guarantees that this value is unique.

4. Simulation and results

4.1. Simulation setup

In this study, with two oil wells and six uncertain parameters, 65 possible realizations for uncertainties or models/branches are considered, including all the combinations of boundary values and the nominal case. The robust horizon is chosen to be $N_r = 1$ as exhibited in Fig. 3. If the branching continues two or three timesteps, the number of scenarios grows to 4225 and 274 625 scenarios, respectively, making the problem practically difficult to solve in real-time. It should be noted that since branching has been done only for the first sampling time, $u_0^1 = u_0^2 = \cdots = u_0^{64} = u_0^{65}$ is the only set of non-anticipativity constraints in the problem and this is the control action that is implemented in the real-time.

Tuning wights Q, R, and S that reflect the importance of each term in the objective function are chosen to be 1, 0.5, and 50, respectively. All the sixty-five weights ω_j for sixty-five scenarios are considered to be equal since a uniform distribution function

Table 1
List of the parameters and their corresponding nominal values.

Parameter	Well 1	Well 2	Units	Comments
PI	2.51	1.63	[kg/s bar]	Nominal productivity index
GOR	0.08	0.07	[kg/kg]	Nominal gas to oil ratio
WC	0.15	0.15	[m^3/m^3]	Nominal water cut
L_{a_tl}/L_{t_tl}	2758	2559	[m]	Total length above injection point
L_{a_vl}/L_{t_vl}	2271	2344	[m]	Vertical length above injection point
L_{r_vl}	114	67	[m]	Vertical length below injection point
A_t	0.0194	0.0194	[m^2]	Tubing cross section area
A_a	0.0174	0.0174	[m^2]	Annulus cross section area
K	68.43	67.82	$[\frac{\sqrt{\frac{kg\ m^3}{bar}}}{h}]$	Gas injection valve constant
T_a/T_t	280	280	[K]	Annulus/tubing temperature
P_r	150	150	[bar]	Reservoir pressure
P_s	30	30	[bar]	Separator pressure
α_γ	0.66	0.066	–	Constant
C_v	8190	8190	–	Valve characteristics
ρ_o	800	800	[kg/m^3]	Density of oil
ρ_w	1000	1000	[kg/m^3]	Density of water
M	0.020	0.020	[kg/mol]	Molar mass
z	1.3	1.3	[−]	Compressibility factor

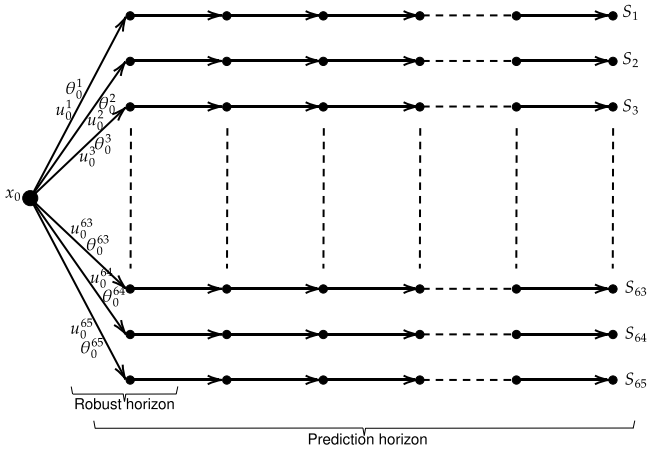

Fig. 3. Scenario tree representation of the uncertainties considered in this study with 65 branches. The prediction horizon length is $N = 25$ and the robust horizon is $N_r = 1$. The total number of scenarios is equal to $65^1 = 65$.

is chosen for the parameters; hence all the scenarios are equally likely to occur.

The total available lift gas $W_{gc}^{\max}$ varied during simulation to indicate the change in operational condition, while the constraint on the maximum capacity of separator assumed to be constant $W_s^{\max} = 175$ [kg/s]. The lower and upper bounds of the gas injection flow rates (control signal) are 0.323 and 11.66[kg/s]. The rate of change of control also is limited between ±0.15 [kg/s]. A sampling time of 20 s and a prediction horizon with 25 sampling times (≈8.3 min) is used. The first control input is applied to the plant in a receding horizon manner. The other parameters related to the gas lift system are presented in Table 1.

The dynamic optimization problem is discretized using the direct multiple shooting method in CasADi v.3.5.5, an open-source tool for nonlinear optimization and algorithmic differentiation [18]. The simulations were implemented in MATLAB R2020b, using a 1.8 GHz laptop with 16 GB memory. The IPOPT v.3.14.1 solver has been used to solve the problem [19].

4.2. Robust performance

In the first simulation case, the performance of the multi-stage NMPC is investigated within the uncertainty region. Accordingly, the proposed multi-stage NMPC is applied to a plant with varying values of uncertain parameters. For this case study, it is known apriori that the worst-case occurs when the productivity index and gas to oil ratio take their maximum possible values, and the water cut takes its minimum value. So, the parameters of the plant are deliberately changed in a way to push the system towards the boundary of constraints to show the robustness of the system. The simulation result is presented in Fig. 4, and the start of optimization is denoted by a vertical red dashed line. It demonstrates that the constraints on the separator capacity and available lift gas will never be violated. In other words, the controller is able to cope with any realization of the uncertain parameters within the uncertainty range. It also can be seen from the last plot of Fig. 4 how the uncertain parameters were changed into their extreme values. It should be noted that the parameters are independent, and they are chosen to vary in a random order.

The robustness is also demonstrated in a comparison between the proposed multi-stage controller and a deterministic standard NMPC. To this end, a deterministic NMPC controller is also designed using the same tuning parameters Q, R, S, and the same constraints on the separator capacity and available lift gas. The only difference with multi-stage NMPC is that the deterministic NMPC neglected the sixty-five scenarios and considered only the nominal realization of uncertain parameters.

The deterministic NMPC is applied to the plant with nominal parameters, and the simulation result is plotted in Fig. 5. The solid dark blue lines in the first and second subplots depict the response of the nominal plant. On the other hand, the light blue dots present the possible reaction of the plant in the case that the parameters take other different values in the uncertainty region. All these light blue dots create an uncertainty bound around the nominal trajectory. Fig. 5 demonstrates that when the deterministic NMPC is applied to the nominal plant, the constraint on the maximum produced fluid (separator capacity) is appropriately satisfied. In contrast, if some other realization of the parameters occurs, the constraint is violated. In other words, the deterministic NMPC is not sufficient to handle the uncertainty in the system.

The same simulation setup is performed for multi-stage NMPC, and the result is presented in Fig. 6. The robust analysis in Fig. 6 demonstrates that the multi-stage NMPC is able to fulfill the constraint for all the realizations of parameters within the uncertainty region.

The comparison of the total produced oil in Figs. 5 and 6 illustrates an essential point which is the effect of uncertainty on the conservativeness. It seems as though the total oil production

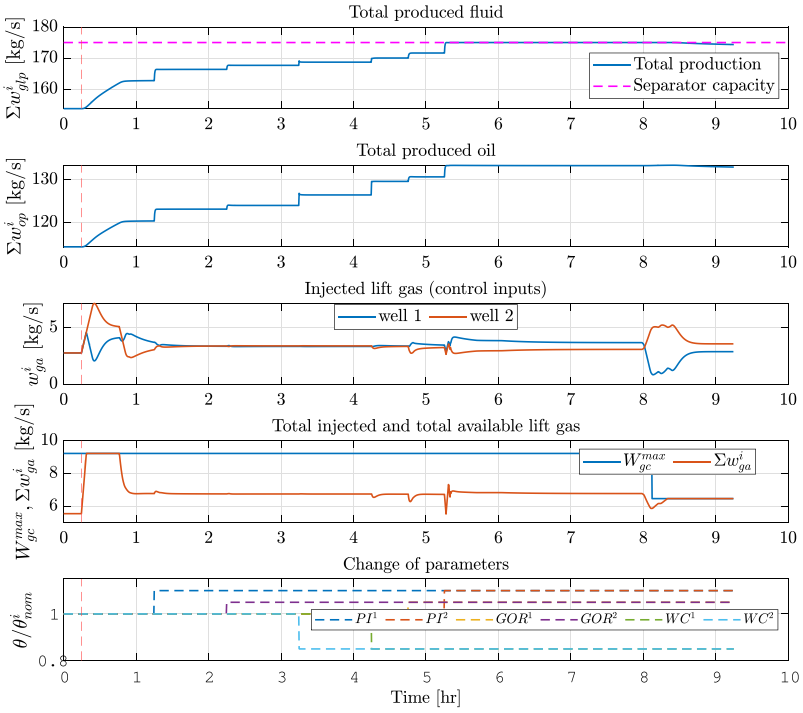

Fig. 4. Simulation result for the multi-stage NMPC applied to a model with varying values of uncertain parameters within the uncertainty boundaries.

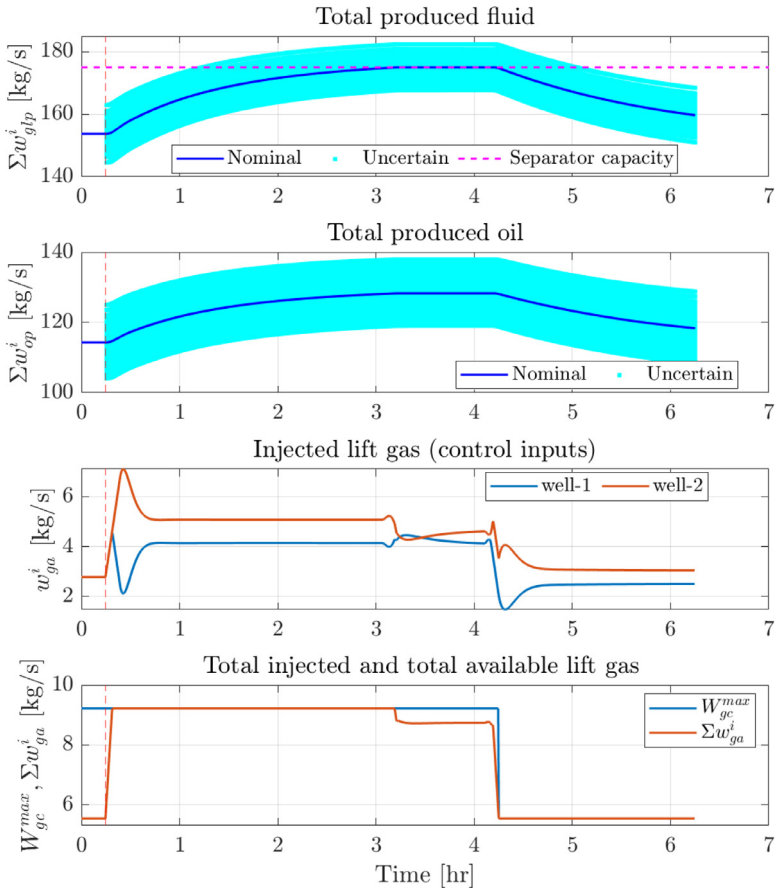

Fig. 5. Robust analysis of the deterministic NMPC.

using the deterministic NMPC is greater than the total oil production using the multi-stage NMPC. However, this decrease in production with the multi-stage NMPC is the price that should be paid to ensure robust feasibility even in the presence of uncertainties in the system. In fact, conservativeness is a compromise between optimality and robustness. There is no other way to

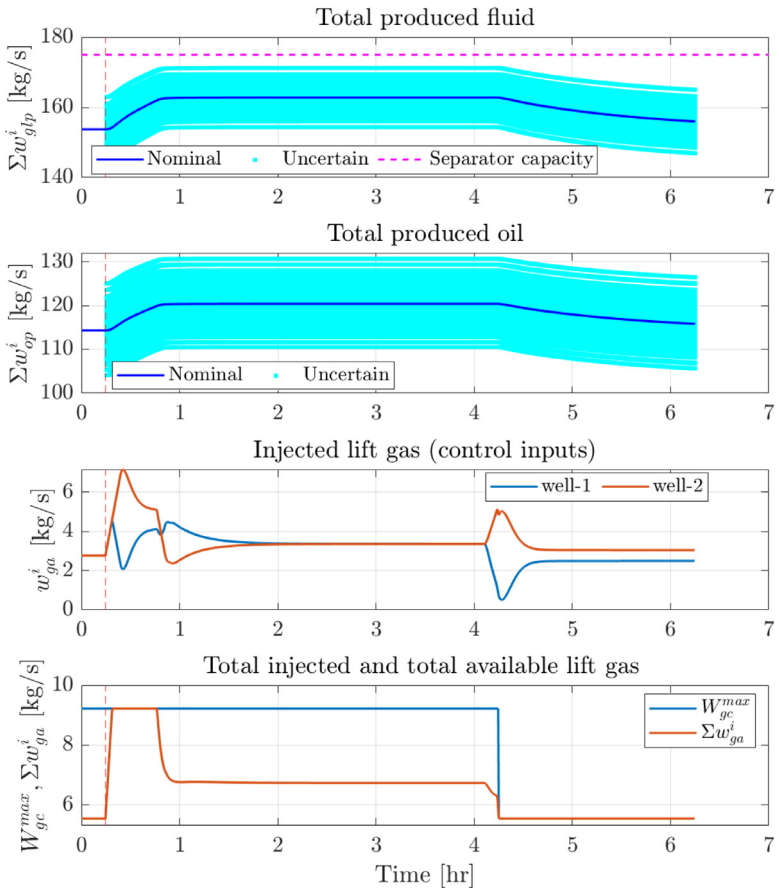

Fig. 6. Robust analysis of the multi-stage NMPC.

achieve robustness rather than to sacrifice some optimality. The light blue shade around the nominal trajectory is a good representation of this inevitable cost of robust feasibility. To reduce the conservativeness, one should narrow down this blue shade by either decreasing the uncertainty range or incorporating more apriori information in the optimization problem.

4.3. Conservativeness and execution time

The superiority of the multi-stage NMPC in terms of conservativeness compared to the other robust methods is elaborated in another simulation case. Accordingly, a min–max NMPC is designed based on the worst-case scenario open-loop optimization [15], which means the notion of feedback is not considered in the optimization problem, and a single control trajectory is used to calculate the objective function for all the possible scenarios.

For a fair comparison, the tuning weights Q, R, S, and all ω_j are all considered to be the same as before. However, the optimization problem defined in (38) changes accordingly to minimize the worst-case (maximum) objective function among the scenarios.

$$\min_{x,u} \max_{j} \omega_j J_j \tag{45}$$

The other difference is that the optimization problem is solved in an open loop fashion, which means there is only a single control trajectory. Therefore the non-anticipativity constraints in (44) are not relevant anymore. The simulations are arranged in two separate cases. In the first case, the varying values of the uncertain parameters are changed in a way to push the plant towards the worst-case operational condition, and the results are presented in Fig. 7. The total produced fluid is plotted because of the constraint on the separator capacity, and the total produced oil is plotted because this is the output of interest. It can be observed that the multi-stage NMPC has the ability to produce more fluid than the min–max NMPC. In other words, the multi-stage NMPC framework is less conservative compared to the min–max NMPC. This is due to the fact that multi-stage NMPC solves the optimization problem over different control trajectories, while the open-loop min–max NMPC considers a single sequence of controls.

In the second case, the varying uncertain parameter values are changed to push the plant away from the worst-case operational condition. The results are plotted in Fig. 8. It illustrates that the multi-stage NMPC framework is less conservative and that the difference between the two controllers is even more noticeable. The reason is that there is no mismatch between the considered model and the reality when the worst-case controller is applied to the plant with the worst-case parameter realization.

The superiority of the multi-stage NMPC in terms of execution time is also investigated in comparison with another robust counterpart. To do so, a min–max NMPC is designed in a closed-loop optimization fashion [15] to have the same level of conservativeness as the multi-stage NMPC has. One might note that when the optimization problem is solved in a closed-loop fashion over different control trajectories (control policies), the incorporation of non-anticipativity constraints is necessary. Therefore, the only difference between the following closed-loop min–max NMPC and the multi-stage NMPC is that the objective function in (38) has been changed to (45). In other words, the maximum objective function among all scenarios is chosen instead of a weighted sum of the objective functions over all possible scenarios.

As presented in Table 2, the mean and maximum execution times of iterations for the multi-stage NMPC are 3.03 and 8.16 s,

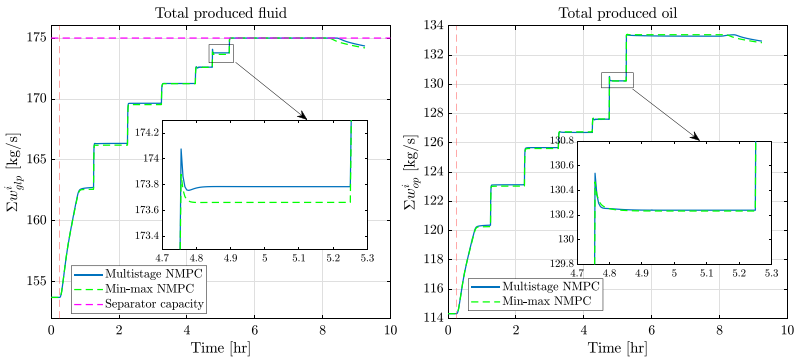

Fig. 7. Comparison between multi-stage and open-loop min–max NMPC in a worst-case operational condition.

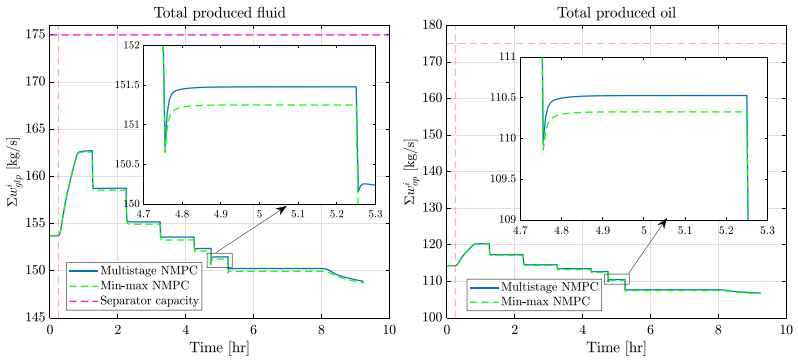

Fig. 8. Comparison between multi-stage and open-loop min–max NMPC far from the worst-case operational condition.

respectively, whereas the closed-loop min–max NMPC could not be solved in real-time. This comparison demonstrates that multi-stage NMPC is considerably faster than closed-loop min–max NMPC, especially for large-scale problems such as this case with 65 scenarios.

The size of the problem was reduced to study the execution time of the methods further. Accordingly, the uncertainty in gas to oil ratio and water cut was neglected for both oil wells. In other words, gas to oil ratios and water cuts of both oil wells were assumed to take their nominal values. Therefore, the number of uncertain parameters was reduced from six to two. Consequently, the number of scenarios was decreased from 65 to 5. The mean execution time of iterations for these new cases shows that in a small-scale problem, the multi-stage NMPC is almost six times faster than closed-loop min–max NMPC.

All the execution times, provided in Table 2, clearly show the superiority of multi-stage NMPC over the other closed-loop optimization method. This advantage can be explained by the difference in the problem formulations. Both the methods need to calculate the objective functions over the possible scenarios, however, the key difference is that multi-stage method picks the weighted sum of all the objective functions of scenarios while the min–max picks the maximum one. In other words, multi-stage NMPC relies on simple addition/multiplication operations whereas the min–max relies on logical operations (max function) which is considerably slower specially when the problem is implemented in a symbolic environment such as CasADi.

Table 2
The mean and maximum execution time of iterations for different methods.

Method	Mean iteration time [s]	Max. Iteration time [s]
Multi-stage (65 scenarios)	3.03	8.16
Closed-loop Min–Max (65 scenarios)	–	–
Multi-stage (5 scenarios)	0.15	1.38
Closed-loop Min–Max (5 scenarios)	0.99	3.90

4.4. The effect of uncertainty description

The last simulation setup is arranged to investigate the effect of uncertainty description where a truncated range of uncertainty is used for control design, and the control performance is compared with the previous standard case. The motivation for such a simulation case is to demonstrate the shortcomings of the method and the opportunities for future improvement.

Since the multi-stage NMPC considers only some finite discrete realizations of uncertainties, normally the bounds and nominal values, the basic idea is that, the bounds can be chosen wisely if a more informative uncertainty description is available. With the intention of doing so, it has been assumed that all the uncertain parameters are normally distributed within the same range with a probability of 99.7%. In other words, the standard deviations of the uncertain parameters are considered in a way that with a normal distribution, 99.7% of the data lie within the same range as before. Then, a truncated range of uncertainty with the probability of 95.4%, as shown in Fig. 9, is used in the control design. It should be noted that the problem formulation in (38) remains the same, and the probability distribution function is not used to propagate the uncertainties into the outputs; however, it has been used to truncate the uncertainty bounds used in making the scenario tree.

The comparison between the truncated and standard design is performed in both nominal and worst-case operational conditions of the plant, as plotted in Figs. 10 and 11 respectively. Fig. 10 illustrates that the controller based on a truncated uncertainty reduces the conservativeness in the nominal operational condition of the plant. Therefore, model identification techniques might be helpful to incorporate more apriori information and

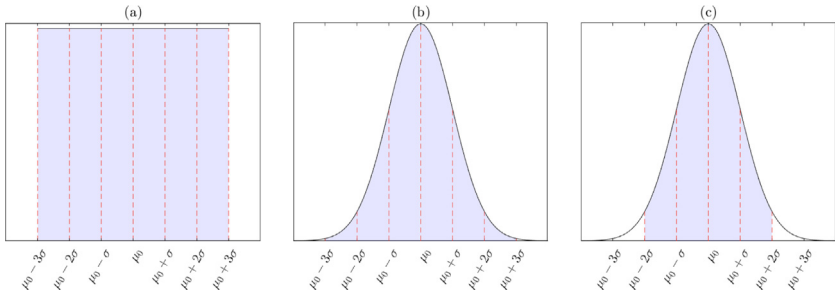

Fig. 9. The probability distribution function of the uncertain parameters: (a) Standard uniform distribution, (b) Normal distribution with the probability of 99.7% within the same range, (c) Truncated normal distribution function with the probability of 95.4% used in control design.

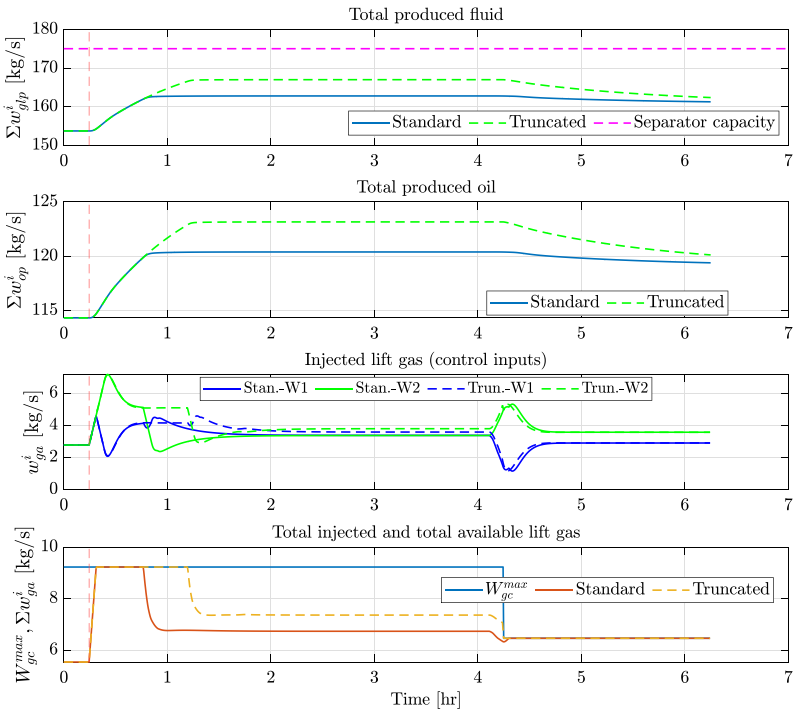

Fig. 10. Comparison between the controllers based on standard and truncated uncertainty applied to the plant at the nominal operational condition.

improve the method's performance. However, as demonstrated in Fig. 11 it is not robust for all the possible realizations of the plant. Therefore, the controller fails to cope with the uncertainty if the rare parameter realization occurs.

It should be noted again that the scenario-based optimization presented in this paper is based on the uniform distribution of the uncertain parameters that leads to equal weights for all the different considered scenarios. Although this is a viable approach if no information about the uncertainty is known, future measurements will reveal more information about the actual uncertainty in the system. Hence, updating the weights for the different scenarios based on the measurements could perhaps improve the performance of scenario-based optimization compared to the worst-case optimization even more.

5. Conclusion

This paper presented a multi-stage nonlinear model predictive framework for the gas lifted well system and total oil production maximization as a dynamic optimization control problem under the presence of parametric uncertainty. The performance of the proposed framework is evaluated through several simulation cases.

The simulation results of the comparison between multi-stage and deterministic NMPC illustrated that uncertainty in parameters influences the constrained dynamic optimization and can make it practically infeasible due to the constraint violations. In other words, the parametric uncertainties should be explicitly handled inside the optimization problem if there are hard constraints in the problem that should be satisfied all the time. However, the optimality has to be sacrificed to achieve this robustness.

The superiority of the multi-stage NMPC has also been shown in comparison with the worst-case scenario min–max MPC. It has been demonstrated that the multi-stage scenario-based NMPC is closer to the optimal condition in terms of conservativeness, and it is faster in terms of execution time.

The uncertainty description also was investigated through simulation cases where different ranges and distributions for the uncertain parameters were considered in the control design. It has been shown that using a truncated uncertainty description in control design improves the conservativeness of working in nominal operational condition, while the controller loses its robustness for the worst-case operational condition.

To summarize the outcomes, the developed multi-stage scenario-based MPC showed promising results. The main goal was achieved, i.e., the controller could prevent any constraint

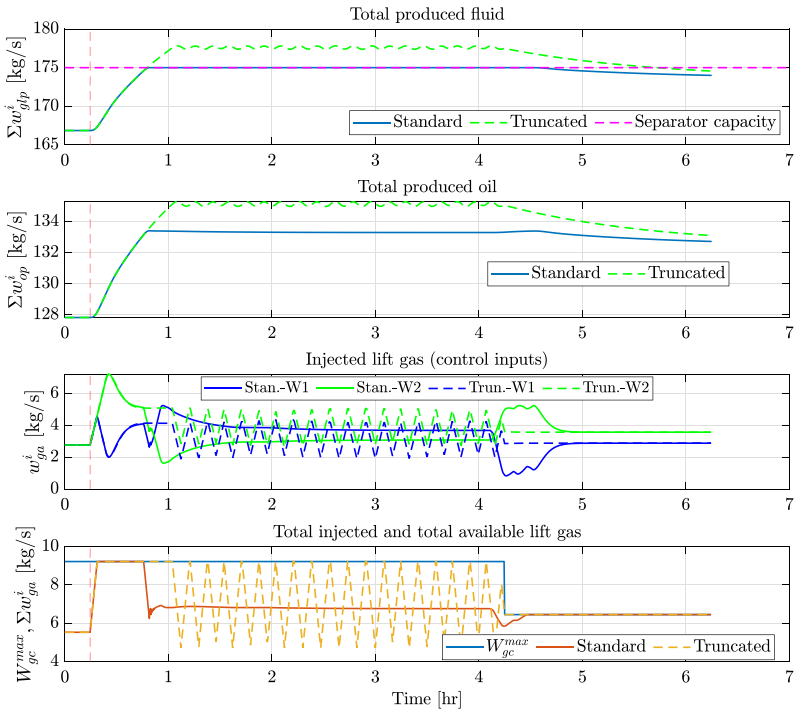

Fig. 11. Comparison between the controllers based on standard and truncated uncertainty applied to the plant at the worst-case operational condition.

violations while the deterministic NMPC failed to fulfill the constraints for all the possible realization of uncertain parameters. Considering the evolution of the system in different scenarios based on a scenario tree allows us to consider the notion of feedback explicitly in the optimization problem. In other words, the future inputs could depend on the future measurements. So this extra degree of freedom relaxed the optimization problem and consequently reduced the conservativeness. The reduction in conservativeness means that the real power of control has been exploited, and the solution is closer to the optimal condition.

Despite the significant advantages of the method, there are opportunities for further improvement in future works. First, the computational cost for a more significant number of uncertain parameters is still a complex challenge to be addressed.

It has been observed that for a smaller range of uncertainty, the conservativeness will be reduced. However, the controller would not be able to cope with the uncertainty beyond the considered boundaries. Hence, the other direction is to work on the uncertainty description and incorporate more information apriori. For example, the weight of each scenario can be improved using more informative distribution functions for uncertain parameters.

Additionally, the scenario tree can be updated after a particular sampling time to reflect the evolution of uncertainties more realistically. Therefore, future work will be focused on reducing the computational burden and improving the prior information to make multi-stage NMPC more applicable in industrial cases.

CRediT authorship contribution statement

Nima Janatian: Conceptualization, Methodology, Software, Writing – original draft. **Roshan Sharma:** Conceptualization, Supervision, Writing – review & editing.

Declaration of competing interest

The authors declare that they have no known competing financial interests or personal relationships that could have appeared to influence the work reported in this paper.

Acknowledgments

We gratefully acknowledge the economic support from The Research Council of Norway and Equinor ASA through Research Council project “308817 - Digital wells for optimal production and drainage” (DigiWell).

References

[1] G.O. Eikrem, L. Imsland, B. Foss, Stabilization of gas lifted wells based on state estimation, IFAC Proc. 37 (1) (2004) 323–328, http://dx.doi.org/10.1016/S1474-6670(17)38752-9.

[2] F.C. Diehl, C.S. Almeida, T.K. Anzai, G. Gerevini, S.S. Neto, O.F. Von Meien, M.C. Campos, M. Farenzena, J.O. Trierweiler, Oil production increase in unstable gas lift systems through nonlinear model predictive control, J. Process Control 69 (1) (2018) 58–69, http://dx.doi.org/10.1016/j.jprocont.2018.07.009.

[3] R. Sharma, K. Fjalestad, B. Glemmestad, Modeling and control of gas liftedoil field with five oil wells, in: The 52nd International Conference of Scandi-Navian Simulation Society, Västerås, Sweden, 2011, pp. 47–59.

[4] A.J. Peixoto, D. Pereira-Dias, A.F. Xaud, A.R. Secchi, Modelling and extremum seeking control of gas lifted oil wells, IFAC-Papers OnLine 48 (6) (2015) 21–26, http://dx.doi.org/10.1016/j.ifacol.2015.08.004.

[5] E. Jahanshahi, S. Skogestad, Simplified dynamic models for control of riser slugging in offshore oil production, Oil Gas Facil. 3 (6) (2014) 080–088, http://dx.doi.org/10.2118/172998-PA.

[6] A. Capolei, B. Foss, J.B. Jørgensen, Profit and risk measures in oilproduction optimization, IFAC-Papers OnLine 48 (6) (2015) 214–220, http://dx.doi.org/10.1016/j.ifacol.2015.08.034.

[7] K.G. Hanssen, A. Codas, B. Foss, Closed-loop predictions in reservoir management under uncertainty, SPE J. 22 (5) (2017) 1585–1595, http://dx.doi.org/10.2118/185956-PA.

[8] B. Chen, R.-M. Fonseca, O. Leeuwenburgh, A.C. Reynolds, Minimizing the risk in the robust life-cycle production optimization using stochastic simplex approximate gradient, J. Pet. Sci. Eng. 153 (1) (2017) 331–344, http://dx.doi.org/10.1016/j.petrol.2017.04.001.

[9] Z. Guo, A.C. Reynolds, Robust life-cycle production optimization with a support-vector-regression proxy, SPE J. 23 (06) (2018) 2409–2427, http://dx.doi.org/10.2118/191378-PA.

[10] R. Sharma, K. Fjalestad, B. Glemmestad, Optimization of lift gas allocation in a gas lifted oil field as non-linear optimization problem, Model. Identif. Control 33 (1) (2012) 13–25, http://dx.doi.org/10.4173/mic.2012.1.2.

[11] K.G. Hanssen, B. Foss, Production optimization under uncertainty- applied to petroleum production, IFAC-Papers OnLine 48 (8) (2015) 217–222, http://dx.doi.org/10.1016/j.ifacol.2015.08.184.

[12] D. Krishnamoorthy, S. Skogestad, J. Jaschke, Multistage model predictive control with online scenario tree update using recursive bayesian weighting, in: 18th European Control Conference (ECC), IEEE, 2019, pp. 3021–3025, http://dx.doi.org/10.23919/ECC.2019.8795839.
[13] N. Janatian, K. Jayamanne, R. Sharma, Model based control and analysis of gas lifted oil field for optimal operation, Scand. Simul. Soc. (2022) 241–246.
[14] S. Lucia, T. Finkler, S. Engell, Multi-stage nonlinear model predictive control applied to a semi-batch polymerization reactor un-der uncertainty, J. Process Control 23 (9) (2013) 1306–1319, http://dx.doi.org/10.1016/j.jprocont.2013.08.008.
[15] P.O. Scokaert, D.Q. Mayne, Min–max feedback model predictive control forconstrained linear systems, IEEE Trans. Automat. Control 43 (8) (1998) 1136–1142, http://dx.doi.org/10.1109/9.704989.
[16] P.J. Campo, M. Morari, Robust model predictive control, in: 1987 American Control Conference, IEEE, 1987, pp. 1021–1026, http://dx.doi.org/10.23919/ACC.1987.4789462.
[17] D. Krishnamoorthy, B. Foss, S. Skogestad, Real-time optimization under uncertainty applied to a gas lifted well network, Processes 52 (4) (2016) 192–208, http://dx.doi.org/10.3390/pr4040052.
[18] J.A. Andersson, J. Gillis, G. Horn, J.B. Rawlings, M. Diehl, CasADi - A software framework for nonlinear optimization and optimal control, Math. Program. Comput. 11 (1) (2019) 1–36, http://dx.doi.org/10.1007/s12532-018-0139-4.
[19] A. Wachter, L.T. Biegler, On the implementation of an interior-point filter line search algorithm for large-scale nonlinear programming, Math. Program. 106 (1) (2006) 25–57, http://dx.doi.org/10.1007/s10107-004-0559-y.

Paper C
A reactive approach for real-time optimization of oil production under uncertainty

Published in the *Proceeding of 2023 American Control Conference (ACC)*, May 31 - June 2, San Diego, CA, USA, 2023.
Paper presented by Nima Janatian.
Authors: Nima Janatian and Roshan Sharma.
Authors' roles in the article:
Nima Janatian: Main ideas, implementation, and writing.
Roshan Sharma (Supervisor): Discussions, comments, and proofreading.

Paper D
A robust model predictive control with constraint modification for gas lift allocation optimization

Published in *Journal of Process Control*, Volume 128, August 2023.
Authors: Nima Janatian and Roshan Sharma.
Authors' roles in the article:
Nima Janatian: Main ideas, implementation, and writing.
Roshan Sharma (Supervisor): Discussions, comments, and proofreading.

Journal of Process Control 128 (2023) 102996

Contents lists available at ScienceDirect

Journal of Process Control

journal homepage: www.elsevier.com/locate/jprocont

A robust model predictive control with constraint modification for gas lift allocation optimization

Nima Janatian *, Roshan Sharma

Department of Electrical Engineering, Information Technology and Cybernetics, University of South-Eastern Norway, Campus Porsgrunn, Norway

ARTICLE INFO

Article history:
Received 13 January 2023
Received in revised form 11 April 2023
Accepted 11 May 2023
Available online 6 June 2023

Keywords:
Robust model predictive control
Real-time optimization
Parametric uncertainty
Gas lift oil wells

ABSTRACT

This paper presents a novel approach for implementing a robust real-time optimization framework under the presence of parametric uncertainty. Conservativeness is an inevitable drawback of a robust control approach. Therefore we aimed to provide a simple and efficient method to mitigate the conservativeness while the robust fulfillment of the constraints is still preserved. The proposed method in this paper is based on the worst-case realization of the uncertainties, however, with constraint modification. The mismatch between measured and predicted output is used directly to modify the active constraint in the optimization problem. The superiority of the method in terms of conservativeness and computational time has been demonstrated in comparison with the other robust optimization counterparts, such as traditional min–max and multi-stage MPC. The promising advantage of the proposed method is that not only it reduces the conservativeness significantly, but also the computational price for this achievement is considerably cheaper than closed-loop optimization methods such as multi-stage MPC.

1. Introduction

Model Predictive Control (MPC) is an advanced optimization strategy with remarkable merits that has received a great deal of attention, especially in the process control community. It is a convenient tool for dealing with multiple-input multiple-output processes. Moreover, it is capable of handling the constraints directly, whether they are on the states, control actions, or outputs. However, the fact that it uses a mathematical model to forecast the future behavior of the process can make it susceptible to poorer performance in practical applications since a perfect mathematical model simply does not exist in most cases.

Parametric uncertainty, unmodeled dynamics, exogenous disturbances, measurement noise, etc., are some well-known sources of uncertainty that introduce a mismatch between the model and the actual process. This mismatch can deteriorate the prediction part of MPC and consequently lead to poor performance. This situation becomes even more challenging when there are hard constraints that should strictly be satisfied throughout the operation. Therefore it is almost inevitable to consider the effect of uncertainty in practical applications.

A conventional remedy to mitigate the effect of uncertainty is the robust approach, where the uncertainty is assumed to belong to a bounded set, and the controller is designed to guarantee robust requirements for the worst-case situation. This ensures that if any other realization within the bounded uncertainty region happens, the controller is able to handle it. The worst-case formulation, which is also known as the min–max formulation, was originally proposed in [1] and later in the context of MPC in [2]. Traditional min–max MPC formulation as well as standard MPC are open-loop optimizations in the sense that they solve an open-loop optimal control problem at each sampling time. An open-loop optimization fashion does not take into account the explicit notion of feedback in the formulation of the optimization problem, although the new information will be available in the next time instance. The main drawback of open-loop optimization is that it leads to an overly conservative solution; therefore, the controller will be significantly sub-optimal, and all resources available in the process may not be fully utilized.

To address the problem of conservativeness, the notion of feedback has been explicitly introduced in the closed-loop min–max framework as in [3,4]. This means that the optimization will be solved over control policies rather than a single control sequence. This allows the future decisions to depend directly on the future measurements. In other words, it introduces some extra degrees of freedom to the optimization problem that reduces the conservativeness. However, the general formulation which leads to dynamic programming suffers from the curse of dimensionality and will not be practically implementable. Hence, optimization over state feedback policies [5], affine policies parameterized on

* Corresponding author.
E-mail addresses: nima.janatianghadikolaei@usn.no (N. Janatian), roshan.sharma@usn.no (R. Sharma).

https://doi.org/10.1016/j.jprocont.2023.102996

the uncertainty [6,7], and deep neural network [8] have been proposed to approximate the general problem.

Tube-based MPC method is another alternative in the framework of robust approach for both linear [9] and nonlinear systems [10]. The basic idea of this method is to split the control problem into two parts. First is an ancillary controller, which is responsible for maintaining the real uncertain system within an invariant set around the nominal trajectory. Second, a deterministic standard MPC with tightened constraints based on the nominal trajectory which steers the bundle of trajectories (known as tube) to the desired state. Since the invariant set can be designed offline, the method does not impose too much extra online computational cost. However, constructing such an invariant set might not be simple, especially for complicated nonlinear systems. Different modifications of the method have been presented in [11–14].

Another possibility to implement closed-loop optimization in the framework of robust MPC is to use multi-stage MPC [15]. This method approximates the general formulation of dynamic programming by considering only a finite realization of the uncertainty, which is represented by a scenario tree. The scenario tree makes it possible to solve the optimization problem over different control trajectories; hence it will reduce the conservativeness. However, the computational cost is still expensive because the number of scenarios and consequently the size of the problem grows exponentially with the length of the prediction horizon and the number of uncertainty realizations considered. Therefore applicability of the method is still limited.

The main challenge in this regard is that the robust methods are inherently conservative, and the existing methods to reduce the conservativeness are either computationally heavy or they deteriorate the robust performance [16]. Therefore, this paper aims to address the problem of conservativeness, particularly by looking into a case study to maximize the oil production from a gas-lifted oil network under the presence of parametric uncertainty. Previous studies [17,18] have shown that parametric uncertainties must be considered in the optimization problem; otherwise, the constraints would be violated. It has also been shown that robust formulations are overly conservative or computationally expensive. Conservativeness, which in this case can be interpreted as an unexploited possibility for more production, is an inevitable price that should be paid to ensure robust performance. However, this paper aims to provide a simple and efficient method to mitigate conservativeness while the robust fulfillment of the constraints is preserved.

The proposed method in this paper is based on the worst-case realization of the uncertainties with constraint modification. More specifically, the mismatch between measured and predicted output is used directly to modify the active constraint in the optimization problem. Since the design is based on the worst-case situation, there will be no mismatch between the prediction and measurement when the worst-case realization of the uncertainty occurs. Under such conditions, the method reduces to traditional min–max MPC. However, for the other realizations of uncertainty, the constraint modification leads to a higher production rate and thus results in a less conservative operation.

Although the output error was employed in the early versions of predictive control [19] and later in more recent versions of adaptive model predictive control [20,21], the fundamental distinction between the proposed method of this paper and previous works lies in the role of measurements. Despite the adaptive approach, which makes use of output error to estimate the uncertainty and utilizes the estimated values of uncertainty in the optimization problem, in the proposed method of this paper, the output error is used directly to reconstruct the boundary on constraints in the optimization problem, meaning the method does not contain any estimation algorithm. It is well known that in an adaptive approach, the constraints can be violated dynamically during the transient periods due to the lag in the parameter estimation step [16]. However, the proposed method of this paper does not estimate the parameters. Instead, the measurement is used to modify the constraint boundaries directly. The second major difference is that contrary to the adaptive approach, the optimization problem in the proposed method is based on the worst-case realization of the uncertainty, which enables this method to fulfill the constraints robustly for all the realizations of uncertainty within the considered bounded set.

Although the proposed method has been developed based on special features of gas-lifted oil fields, it can be generalized to be applicable to a class of systems with the same features. The superiority of the method in terms of conservativeness and computational time has been demonstrated in comparison with the other robust optimization counterparts, such as traditional min–max and multi-stage MPC. The main contribution of this work is that it not only significantly reduces conservatism but also the price for such achievement is considerably cheaper than closed-loop optimization methods such as multi-stage MPC. This puts the proposed method superior to the original min–max MPC since the proposed method is less conservative with the same level of complexity and robustness. The advantage of the proposed method over multi-stage MPC is that it is simpler and computationally more efficient, and it reduces the conservativeness even better than multi-stage MPC.

The rest of the paper is organized as follows. Section 2 briefly describes mathematical modeling of the gas-lifted oil field system. The control design and simulation results are presented in Sections 3 and 4, respectively before concluding in Section 5.

2. Mathematical model of gas-lifted oil field

2.1. Process description

The gas lift mechanism is a well-known artificial lifting method to increase or revive the production from oil fields by reducing the fluid mixture density in the well's tubing. A gas-lifted oil field consists of multiple oil wells that share a common lift gas source. Different components of a single oil well have been shown schematically in Fig. 1. A gas-lifted oil well simply works by injecting high-pressurized natural gas into the well's annulus. For each well, a gas lift choke valve controls the gas flow rate from the common gas distribution pipeline into the annulus. The injected gas finds its way towards the tubing at some points located at proper depths and mixes with the multiphase fluid from the reservoir. As a result, the density of the mixture in the tubing will be reduced. Consequently, the hydrostatic pressure of the column of fluid above the injection point and the flowing pressure losses in the tubing will be reduced. Therefore, the pressure gradient between the reservoir and top side will be sufficient to overcome the resistance in the well and pushes the reservoir fluid to the surface.

First principle modeling of gas-lifted oil fields has been investigated for flow stabilization [22–24], control and production optimization purposes [17,18,25]. All these models are derived based on the mass balance of different fluid phases in the tubing and annulus. It has been shown that the first principle models based on mass conservation are accurate enough to be used for control purposes [26].

2.2. Governing equations

In this section, we only briefly present the governing equations of the process as derived in [18] because mathematical modeling is not the objective of this paper. The readers are also referred to [17,25] for further details. We considered a gas-lifted oil field

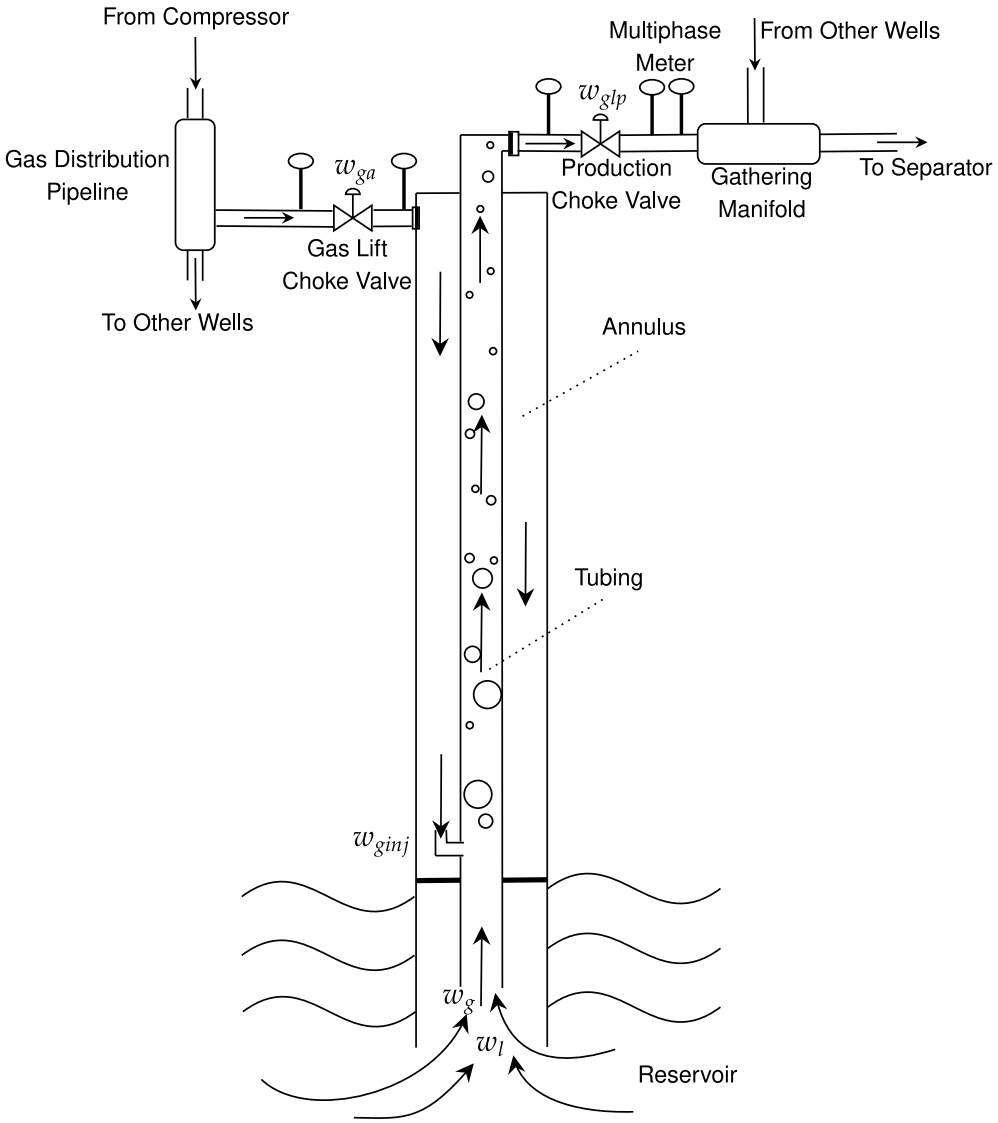

Fig. 1. Schematic diagram of a single gas lift oil well.

with two oil wells that share a gas distribution pipeline and a gathering manifold. The superscript i refers to the ith oil well. Three states are considered for each well, namely, the mass of lift gas in annulus m^i_{ga}, the mass of gas phase in the tubing above the injection point m^i_{gt}, and the mass of liquid phase (mixture of oil and water) in the tubing above the injection point m^i_{lt}. Three corresponding differential equations derived using the law of mass balance are given by:

$$\dot{m}^i_{ga} = w^i_{ga} - w^i_{ginj} \tag{1}$$

$$\dot{m}^i_{gt} = w^i_{ginj} + w^i_{gr} - w^i_{gp} \tag{2}$$

$$\dot{m}^i_{lt} = w^i_{lr} - w^i_{lp} \tag{3}$$

w^i_{ga} is the mass flow rate of the injected lift gas into each well from the gas lift choke valve (control input). w^i_{ginj} is the mass flow rate of the gas injection from the annulus into the tubing. w^i_{gp} and w^i_{lp} are the mass flow rates of the produced gas and liquid phase fluid from the production choke valve, respectively. w^i_{gr} and w^i_{lr} are the gas and liquid mass flow rates from the reservoir into the well. w^i_{glp} is the total mass flow rate of all phases from the production choke valve, and w^i_{op} is the oil compartment of the w^i_{lp}. All the flow equations are given by:

$$w^i_{ginj} = K^i Y^i_2 \sqrt{\rho^i_{ga} \max(P^i_{ainj} - P^i_{tinj}, 0)} \tag{4}$$

$$w^i_{gp} = \frac{m^i_{gt}}{m^i_{gt} + m^i_{lt}} w^i_{glp} \tag{5}$$

$$w^i_{lp} = \frac{m^i_{lt}}{m^i_{gt} + m^i_{lt}} w^i_{glp} \tag{6}$$

$$w^i_{lr} = PI^i \max(P_r - P^i_{wf}) \tag{7}$$

$$w^i_{or} = \frac{\rho_o}{\rho_w}(1 - WC^i) w^i_{lr} \tag{8}$$

$$w^i_{gr} = GOR^i w^i_{or} \tag{9}$$

$$w^i_{glp} = C_v Y^i_3 \sqrt{\rho^i_m \max(P^i_{wh} - P_s, 0)} \tag{10}$$

$$w^i_{op} = \frac{\rho_o}{\rho_w}(1 - WC^i) w^i_{lp} \tag{11}$$

P^i_a is the pressure of lift gas in the annulus downstream of the gas lift choke valve. P^i_{ainj} is the pressure upstream of the gas injection valve in the annulus. P^i_{tinj} denotes the pressure

downstream the gas injection valve in the tubing. P^i_{wh} and P^i_{wf} are the wellhead and bottom hole pressure, respectively. All the pressures are given by:

$$P^i_a = \frac{zm^i_{ga} RT^i_a}{MA^i_a L^i_{a\_tl}} \tag{12}$$

$$P^i_{ainj} = P^i_a + \frac{m^i_{ga}}{A^i_a L^i_{a\_tl}} g L^i_{a\_vl} \tag{13}$$

$$P^i_{tinj} = \frac{zm^i_{gt} RT^i_t}{MV^i_G} + \frac{\rho^i_m g L^i_{t\_vl}}{2} \tag{14}$$

$$P^i_{wh} = \frac{zm^i_{gt} RT^i_t}{MV^i_G} - \frac{\rho^i_m g L^i_{t\_vl}}{2} \tag{15}$$

$$P^i_{wf} = P^i_{tinj} + \rho^i_l g L^i_{r\_vl} \tag{16}$$

ρ^i_{ga} is the average density of gas in the annulus. ρ^i_{gl} is the density of the liquid phase (mixture of the oil and water). ρ^i_m denotes the average density of the multi-phase mixture (oil, water, and gas) in the tubing above the injection point. Y^i_2 and Y^i_3 are the gas expandability factors for the gas that passes through the gas injection valve and production choke valve, respectively. V^i_G is the volume of gas present in the tubing above the gas injection point, and C_v is the production choke valve characteristics. All the densities and other algebraic variables are given by:

$$\rho^i_{ga} = \frac{M(P^i_a + P^i_{ainj})}{2zRT^i_a} \tag{17}$$

$$\rho^i_l = \rho_w WC^i + \rho_o(1 - WC^i) \tag{18}$$

$$\rho^i_m = \frac{m^i_{gt} + m^i_{lt}}{A^i_t L^i_{t\_tl}} \tag{19}$$

$$Y^i_2 = 1 - \alpha_Y \frac{P^i_{ainj} - P^i_{tinj}}{\max(P^i_{ainj}, P^{\min}_{ainj})} \tag{20}$$

$$Y^i_3 = 1 - \alpha_Y \frac{P^i_{wh} - P_s}{\max(P^i_{wh}, P^{\min}_{wh})} \tag{21}$$

$$V^i_G = A^i_t L^i_{t\_tl} - \frac{m^i_{lt}}{\rho^i_l} \tag{22}$$

It should be noted that the algebraic variables given by the Eqs. (4) to (22) can be eliminated by substitution. So the explicit set of ordinary differential equations (ODE) in compact form can be written as:

$$\dot{x} = f(x, u, \theta) \tag{23a}$$

$$y_1 = h_1(x, \theta) \tag{23b}$$

$$y_2 = h_2(x, \theta) \tag{23c}$$

$x \in \mathbb{X} \subset \mathbb{R}^6$ and $u \in \mathbb{U} \subset \mathbb{R}^2$ are the states and control inputs as shown in Eqs. (24) and (25). $y_1 \in \mathbb{Y}_1 \subset \mathbb{R}$ and $y_2 \in \mathbb{Y}_2 \subset \mathbb{R}$ in Eqs. (26) and (27) are two desired outputs denoting total produced oil and total produced fluid respectively. Finally, $\theta \in \Theta \subset \mathbb{R}^6$ in Eq. (28) is the vector of uncertain parameters of the process that includes productivity index, gas to oil ratio, and water cut of each well.

$$x = \begin{bmatrix} m^1_{ga} & m^2_{ga} & m^1_{gt} & m^2_{gt} & m^1_{lt} & m^2_{lt} \end{bmatrix}^{\mathrm{T}} \tag{24}$$

$$u = \begin{bmatrix} w^1_{ga} & w^2_{ga} \end{bmatrix}^{\mathrm{T}} \tag{25}$$

$$y_1 = \sum_{i=1}^{2} w^i_{op} \tag{26}$$

$$y_2 = \sum_{i=1}^{2} w^i_{glp} \tag{27}$$

$$\theta = \begin{bmatrix} PI^1 & PI^2 & GOR^1 & GOR^2 & WC^1 & WC^2 \end{bmatrix}^{\mathrm{T}} \tag{28}$$

2.3. Uncertainty description

According to the sensitivity analysis in [18] three uncertain parameter has been considered for each well. Productivity index *PI* denotes the reservoir's ability to deliver fluids to the wellbore. The gas to oil ratio *GOR* is defined as the mass ratio of produced gas to produced oil, and the water cut *WC* is defined as the volumetric flow rate of water to the total produced liquid. These uncertain parameters are upper and lower bounded and can take any value within their bounds.

$$\theta_i = \theta^{nom}_i \pm \theta^{dev}_i, \qquad i = 1, 2, \ldots, 6 \tag{29}$$

For *PI*, *GOR*, and *WC* of each oil well, a deviation of 10%, 5%, and 15% from their nominal values are considered, respectively, based on expert knowledge. The nominal values of the uncertain parameters and all the other parameters are provided in Table 1.

3. Controller design

3.1. Classical min-max MPC

In this section, the original formulation of open-loop min–max MPC will be presented. The design procedure assumes the uncertain parameters are constant and bounded, as described in Section 2.3. Nevertheless, the controllers are also tested against time-varying parameters to show the capability of handling any parameter change within the uncertainty region. The primary objective is to find the optimal distribution of lift gas between two wells that maximizes the total oil production (output y_1 from Eq. (26)) from the field, subject to some operational constraints. Therefore the objective function includes the total oil production from the field y_1 with the negative sign to pose it as a minimization problem. Additionally, the injected lift gas u and its rate of change Δu can be incorporated into the objective function to penalize excessive lift gas utilization and fluctuations in the control signal. Hence for $k \in \{0, 1, \ldots, N-1\}$ where N is the length of the prediction horizon and Q, R, and S denote proper tuning weights, the objective function is given by:

$$J(x, u, \theta) = \sum_{k=0}^{N-1} \left(-Q(y_{1,k})^2 + R \sum_{i=1}^{2} u_k(i)^2 + S \sum_{i=1}^{2} \Delta u_k(i)^2 \right) \tag{30}$$

The most important operational constraints in the problem arise from separator capacity and the total available lift gas. In particular, the total amount of produced fluid (mixture of oil, water, and gas) should be less than the separator capacity, and the total gas needed for injection should not exceed the total available lift gas. So, the optimal control problem formulation throughout the prediction horizon $\mathcal{K} = \{0, \ldots, N-1\}$ is given by:

$$\min_{x,u} \quad J(x, u, \theta) \tag{31a}$$

$$\text{s.t.} \quad x_{k+1} = f(x_k, u_k, \theta), \qquad k \in \mathcal{K} \tag{31b}$$

$$\sum_{i=1}^{2} u_k(i) \le W^{\max}_{gc,k}, \qquad k \in \mathcal{K} \tag{31c}$$

$$y_{2,k} \le W^{\max}_s, \qquad k \in \mathcal{K} \tag{31d}$$

$$u_{LB} \le u_k \le u_{UB}, \qquad k \in \mathcal{K} \tag{31e}$$

$$\Delta u_{LB} \le \Delta u_k \le \Delta u_{UB}, \qquad k \in \mathcal{K} \tag{31f}$$

Eq. (31b) denotes the discretized dynamic model and is imposed as state continuity constraint. The constraint on the used lift gas is denoted in (31c) where $W^{\max}_{gc,k}$ represents the total

Table 1
List of the parameters and their corresponding nominal values.

Parameter	Well 1	Well 2	Units	Comments
PI^{nom}	2.51	1.63	[kg/s bar]	Nominal productivity index
GOR^{nom}	0.08	0.07	[kg/kg]	Nominal gas to oil ratio
WC^{nom}	0.15	0.15	[m^3/m^3]	Nominal water cut
L_{a_tl}, L_{t_tl}	2758	2559	[m]	Total length above injection point
L_{a_vl}, L_{t_vl}	2271	2344	[m]	Vertical length above injection point
L_{r_vl}	114	67	[m]	Vertical length below injection point
A_t	0.0194	0.0194	[m^2]	Tubing cross section area
A_a	0.0174	0.0174	[m^2]	Annulus cross section area
K	68.43	67.82	$[\frac{\sqrt{\frac{kgm^3}{bar}}}{hr}]$	Gas injection valve constant
T_a, T_t	280	280	[K]	Annulus/tubing temperature
P_r	150	150	[bar]	Reservoir pressure
P_s	30	30	[bar]	Separator pressure
α_Y	0.66	0.066	–	Constant
C_v	8190	8190	–	Valve characteristics
ρ_o	800	800	[kg/m^3]	Density of oil
ρ_w	1000	1000	[kg/m^3]	Density of water
M	0.020	0.020	[kg/mol]	Molar mass
z	1.3	1.3	[–]	Compressibility factor

available lift gas. The constraint on the total produced fluid is enforced in (31d), where y_2 comes from Eq. (27) and $W_s^{\max}$ stands for the maximum capacity of the separator. The lower and upper bounds on the control signal and the rate of change of control inputs are also implemented in (31e) and (31f), respectively.

Due to the uncertainty in the parameters, the problem defined in (31) cannot be solved directly. However, classical open-loop min–max formulation considers the worst-case realization of the uncertainty. In other words, it finds the appropriate decision variables that minimize the maximum of objective functions over all the possible realizations of θ. Classical open-loop min–max MPC formulation is given by:

$$\min_{x,u} \quad \max_{\theta} \quad J(x,u,\theta) \tag{32a}$$

$$\text{s.t.} \quad x_{k+1} = f(x_k, u_k, \theta), \qquad k \in \mathcal{K}, \forall \theta \in \Theta \tag{32b}$$

$$\sum_{i=1}^{2} u_k(i) \le W_{gc,k}^{\max}, \qquad k \in \mathcal{K}, \forall \theta \in \Theta \tag{32c}$$

$$y_{2,k} \le W_s^{\max}, \qquad k \in \mathcal{K}, \forall \theta \in \Theta \tag{32d}$$

$$u_{LB} \le u_k \le u_{UB}, \qquad k \in \mathcal{K}, \forall \theta \in \Theta \tag{32e}$$

$$\Delta u_{LB} \le \Delta u_k \le \Delta u_{UB}, \qquad k \in \mathcal{K}, \forall \theta \in \Theta \tag{32f}$$

Solving the original problem defined in (32) is not always straightforward since the worst-case realization of the uncertainty is not trivial. However, for the application considered in the paper, it is well known that the worst-case scenario occurs when the *PI* and *GOR* of all the wells take their maximum realization and the *WC* of all wells take their minimum realization, simultaneously [17]. Therefore we can simply take the a-priori computed worst-case values of all parameters, and the optimization problem reduces to:

$$\min_{x,u} \quad J(x,u,\theta_w) \tag{33a}$$

$$\text{s.t.} \quad x_{k+1} = f(x_k, u_k, \theta_w), \qquad k \in \mathcal{K} \tag{33b}$$

$$\sum_{i=1}^{2} u_k(i) \le W_{gc,k}^{\max}, \qquad k \in \mathcal{K} \tag{33c}$$

$$y_{2,k} \le W_s^{\max}, \qquad k \in \mathcal{K} \tag{33d}$$

$$u_{LB} \le u_k \le u_{UB}, \qquad k \in \mathcal{K} \tag{33e}$$

$$\Delta u_{LB} \le \Delta u_k \le \Delta u_{UB}, \qquad k \in \mathcal{K} \tag{33f}$$

θ_w in (33) stands for the worst-case realization of uncertainty, and it is equal to the maximum values of all *PI*s and *GOR*s and minimum values for all *WC*s.

3.2. Proposed constraint modification

The proposed method in this section is a modified version of the original min–max MPC to reduce the conservativeness of the classical open-loop min–max in a computationally efficient manner. Since the proposed method does not solve the optimization problem over control policies, it does not increase the computational costs; however, it decreases the conservativeness even better than the closed-loop optimization techniques. The main idea behind this novel method relies on the fact that the output constraint is upper bounded, and the conservativeness arises from overestimating outputs in the prediction part. Therefore a simple innovative method has been developed to compensate for this overestimation by modifying the active output constraint. The most important requirement of the method is that the output (constraint) should be directly measurable, which is an admissible requirement for several chemical processes since the constraints are mostly on pressures or temperatures or flows. Therefore, the method can be generalized to be applicable to a class of systems where this requirement is fulfilled, although it has been developed based on a gas-lifted oil field as the case study.

Since the design is based on robust worst-case optimization like (33), while the active constraint will be modified using measurements, the new method can be formulated as:

$$\min_{x,u} \quad J(x,u,\theta_w) \tag{34a}$$

$$\text{s.t.} \quad x_{k+1} = f(x_k, u_k, \theta_w), \qquad k \in \mathcal{K} \tag{34b}$$

$$\sum_{i=1}^{2} u_k(i) \le W_{gc,k}^{\max}, \qquad k \in \mathcal{K} \tag{34c}$$

$$y_{2,k} \le W_s^{\max} + \delta W, \qquad k \in \mathcal{K} \tag{34d}$$

$$u_{LB} \le u_k \le u_{UB}, \qquad k \in \mathcal{K} \tag{34e}$$

$$\Delta u_{LB} \le \Delta u_k \le \Delta u_{UB}, \qquad k \in \mathcal{K} \tag{34f}$$

The correction factor δW in (34d) reduces the conservativeness by modifying the constraint. It should be emphasized that δW is not a slack variable which is calculated by the optimizer.

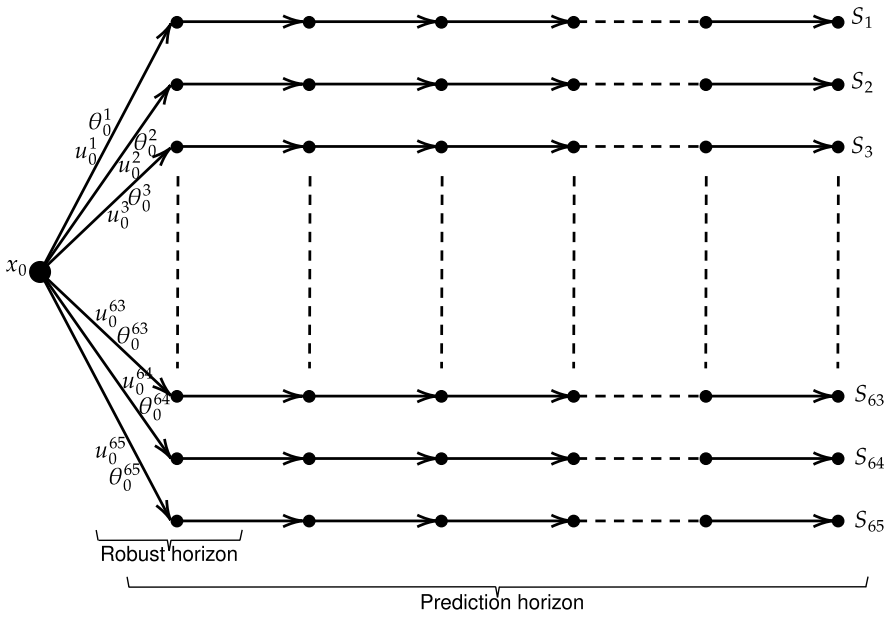

Fig. 2. Scenario tree representation of the uncertainties considered in this study with 65 scenarios and the robust horizon equals 1.

However, it represents how much mismatch exists between the forecast model in the controller and the real process, and it can be calculated by subtracting the measured output (constraint) from the predicted output (constraint) at the current time ($k = 0$) as:

$$\delta W = y_2(x_k, \theta_w) - y_{2,k}^{meas} \tag{35}$$

where $y_2(x_k, \theta_w)$ is the calculated total produced fluid based on the worst-case realization of the parameters and $y_{2,k}^{meas}$ is the measured total produced fluid at the current time $k = 0$. When the parameters of the actual process take their worst-case realization, there will be no mismatch between the prediction and measurement; therefore, the method would be equivalent to a min–max MPC applied in the worst-case situation of the process. Otherwise, the mismatch between the prediction and measurement modifies the upper bound of the constraint and decreases the conservativeness.

3.3. Multi-stage MPC

Multi-stage MPC is used in this paper as a competing alternative to demonstrate the promising features of the novel method presented in this paper. The method behind multi-stage MPC is well documented in the literature [15,27]; therefore, only a condensed explanation of what has been used in this work is presented, and the readers are referred to [28] for more details on the multi-stage MPC for gas-lifted oil network.

Considering the boundaries of six uncertain parameters, there are 2^6 combinations of uncertainty realizations (branch) that adds up to 65 with nominal values. However, since the number of scenarios grows exponentially with the number of branches and time steps, the robust horizon is chosen to be 1. Therefore branching stops after the first node, as shown in Fig. 2 and 65 distinct scenarios are considered overall.

The optimization problem should be formulated over all the discrete scenarios of the scenario set $\mathcal{S} = \{1, \ldots, S\}$ throughout the prediction horizon $\mathcal{K} = \{0, \ldots, N-1\}$. Therefore, for $\forall j \in \mathcal{S}$, and $\forall k \in \mathcal{K}$ and the tuning weights ω_j, the multi-stage MPC is formulated as:

$$\min_{\mathbf{x},\mathbf{u}} \quad \sum_{j=1}^{S} \omega_j J_j \tag{36a}$$

$$\text{s.t.} \quad x_{k+1}^j = f\left(x_k^{p(j)}, u_k^j, \theta_k^{r(j)}\right), \qquad j \in \mathcal{S}, k \in \mathcal{K} \tag{36b}$$

$$\sum_{i=1}^{2} u_k^j(i) \le W_{gc,k}^{\max}, \qquad j \in \mathcal{S}, k \in \mathcal{K} \tag{36c}$$

$$y_{2,k}^j \le W_s^{\max}, \qquad j \in \mathcal{S}, k \in \mathcal{K} \tag{36d}$$

$$u_{LB} \le u_k^j \le u_{UB}, \qquad j \in \mathcal{S}, k \in \mathcal{K} \tag{36e}$$

$$\Delta u_{LB} \le \Delta u_k^j \le \Delta u_{UB}, \qquad j \in \mathcal{S}, k \in \mathcal{K} \tag{36f}$$

$$u_k^j = u_k^l \quad \text{if} \quad x_k^{p(j)} = x_k^{p(l)}, \qquad \forall j \& l \in \mathcal{S}, k \in \mathcal{K} \tag{36g}$$

J_j in (36a) denotes the objective function for scenario j. Tuning weights ω_j represent the relative likelihood of occurring each scenario. The constraint (36b) denotes the equation of the states. It means that the states at time $t = k+1$ in scenario j are a function of their parental state $x_k^{p(j)}$ and the corresponding control u_k^j and uncertainty realization $\theta_k^{r(j)}$. The non-anticipativity constraints introduced in (36g) reflects the fact that at each time instance k, controls u_k^j and x_k^l from scenarios j and l with the same parental state $x_k^{p(j)} = x_k^{p(l)}$ have to be the equal. In our case, branching happens only once; therefore, $u_0^1 = u_0^2 = \cdots = u_0^{65}$ is the only set of non-anticipativity constraints because all these controls are branched from the same parental node x_0 as shown in Fig. 2. According to the receding horizon strategy, this first control action is the one that will be applied to the target system, and the non-anticipativity constraint guarantees that this value is unique.

4. Results and discussion

4.1. Simulation setup

The proposed novel method of this paper, classical min–max MPC, and multi-stage MPC method, have been applied to a gas lifted field with two oil wells. All the parameters of the wells are presented in Table 1. For all three methods, the tuning wights Q, R, and S that reflect the importance of each term in the objective function (30) are chosen to be 1, 0.5, and 50, respectively. All the sixty-five weights ω_j for sixty-five scenarios in the multi-stage method (36) are considered to be equally one because all the scenarios are equally likely to occur.

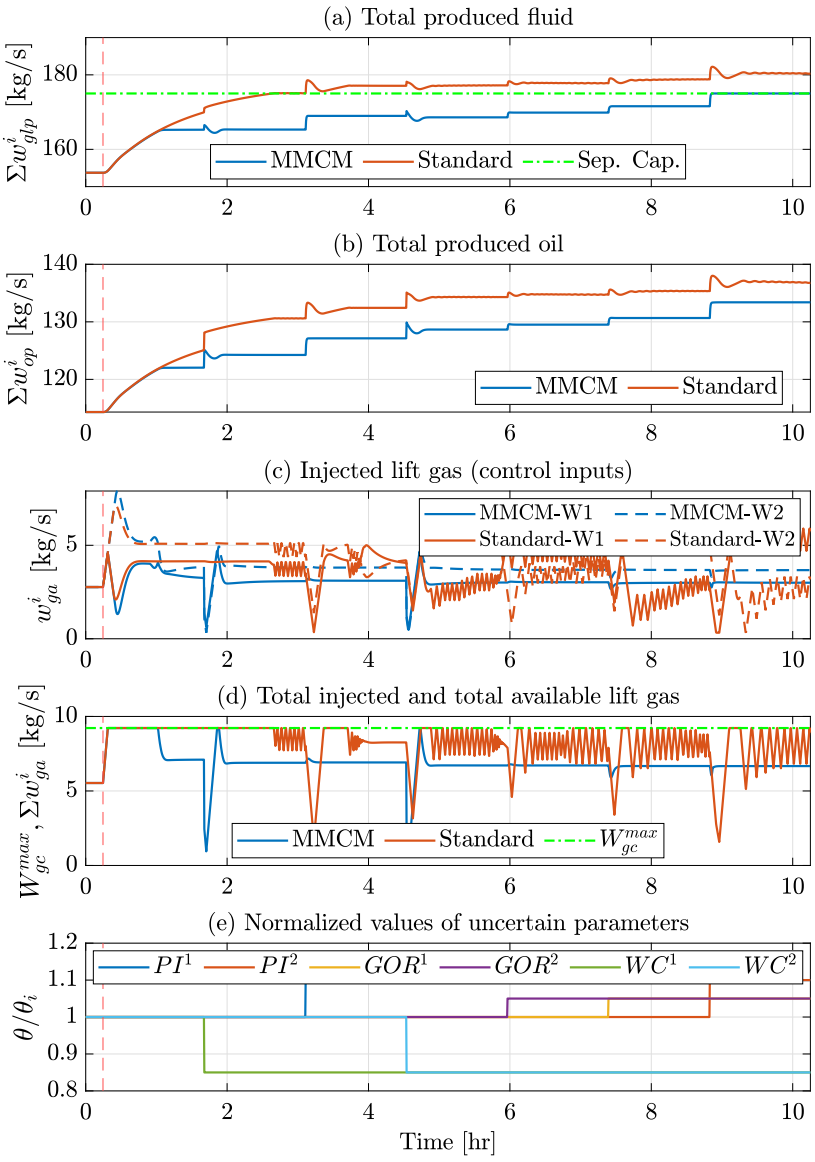

Fig. 3. Total produced fluid, total produced oil, injected lift gas, and normalized values of the uncertain parameters when the proposed method i.e. min–max with constraint modification (MMCM) and standard MPC based on the nominal model, are applied to the plant with varying parameters.

Classical min–max MPC is implemented by solving the optimization problem in (33) in a receding horizon fashion. The proposed method and multi-stage MPC are implemented respectively by solving optimization problems in (34) and (36). In all simulations, the total available lift gas $W^{\max}_{gc}$ varies during simulation to indicate the change in operational condition, while the constraint on the maximum capacity of the separator is assumed to be constant with $W^{\max}_{s} = 175$ [kg/s]. The lower and upper bounds of the gas injection flow rates (control signal) are 0.323 and 11.66 [kg/s]. The rate of control change is limited between ± 0.15 [kg/s]. A sampling time of 20 s and a prediction horizon with 25 sampling times ($\approx$8.3 min) is used for all methods.

The dynamic optimization problem is discretized using the direct multiple shooting method in CasADi v.3.5.5, an open-source tool for nonlinear optimization and algorithmic differentiation [29]. The simulations were implemented in MATLAB R2022b, using a 1.8 GHz laptop with 16 GB memory. The IPOPT v.3.14.1 solver has been used to solve the problem [30].

4.2. Simulation results

The applicability of the proposed approach is demonstrated and compared to competing approaches such as classical min–max and multi-stage MPC in terms of conservativeness and execution time.

The first simulation case has been conducted to show the robustness of the proposed method and the shortcoming of standard MPC in compensating for the parametric uncertainty. To do so, the proposed method and a standard MPC based on nominal values of parameters have been applied to the process with varying parameters. The result is plotted in Fig. 3. The first subplot (a) demonstrates the total produced fluid from the field and its upper bound. The second subplot (b) shows the total produced oil. Control inputs (injected lift gas) are shown in the third subplot (c). The fourth subplot (d) depicts the total lift gas used and its upper bound. And the last subplot (e) shows the uncertain parameters, which are normalized with their nominal values.

In all the subplots, a vertical dashed red line shows the time when the real-time optimizer is activated. It can be seen that the uncertain parameters take their nominal values at the beginning, and then they change to their worst-case realization in random order.

Subplot (a) in Fig. 3 demonstrates that standard MPC based on the nominal model is not able to fulfill the constraint and the total produced fluid exceeds its upper bound. However, this constraint is robustly respected by our method all the time, even in the presence of sudden changes in parameters. It should be noted that the constraint on the output (separator capacity) becomes active only at the end of the simulation time when all the parameters have taken their worst-case realization. However, at other times when at least some of the parameters are not taking their worst-case realization, the controller prefers not to use all the available lift gas even though the constraint on the separator part is not active and even when there is a possibility of higher production. This price that has to be paid to guarantee robust satisfaction of the constraint is typically known as conservativeness.

In the subsequent three simulation cases, it has been shown that the proposed method is superior to the traditional min–max and multi-stage MPC in terms of conservativeness. In other words, the proposed method has the same performance in the worst-case situation, while it is considerably less conservative at other times.

In case (I), all three methods, namely traditional min–max MPC (MM), multi-stage MPC (MS), and the proposed min–max with constraint modification method (MMCM), are applied to the plant with the worst-case realization of uncertain parameters. Total produced fluid and the corresponding constraint, the total produced oil, injected lift gas to each well, and the total injected and available lift gas are plotted in Fig. 4 for all three methods. The first and fourth subplots show that the production will be increased by utilizing all the available gas in the beginning until the constraint on the separator side becomes active. Then the controller decreases the amount of injected lift gas since it has been penalized in the objective function. After almost four hours, all three controllers decreased the total used lift gas even further to respect the constraint on the amount of available gas. The simulation shows that all three competing methods are able to cope with the worst-case realization of the uncertainty; therefore, they are robust.

In case (II), all three methods are applied to the plant with the nominal realization of uncertain parameters to investigate the conservativeness of the methods. The results are plotted in Fig. 5 for comparison. As expected, all three methods are conservative to some extent in the sense that they do not utilize all the available lift gas to increase production. However, the maximum production rate is not touched yet. Nevertheless, their level of conservativeness is not the same. The traditional min–max MPC as an open-loop optimization method is the most conservative one. Multi-stage MPC as a closed-loop optimization method increases the oil production by around 0.1%, which is justifiable considering six uncertain parameters in the process. The proposed novel method is the least conservative method among these three competitors. It increases the oil production by 1.46% with respect to standard min–max MPC, while it does not increase the complexity of the problem compared with open-loop min–max MPC.

The third and last case is case (III), where the three methods are applied to the process in which the *PI* and *GOR* of all the wells take their minimum realization and the *WC* of all wells take their maximum realization, simultaneously. The special fact about the considered case is that all the parameter realizations are exactly the opposite with respect to the worst-case realization. This means if the constraint was lower bounded as well (which

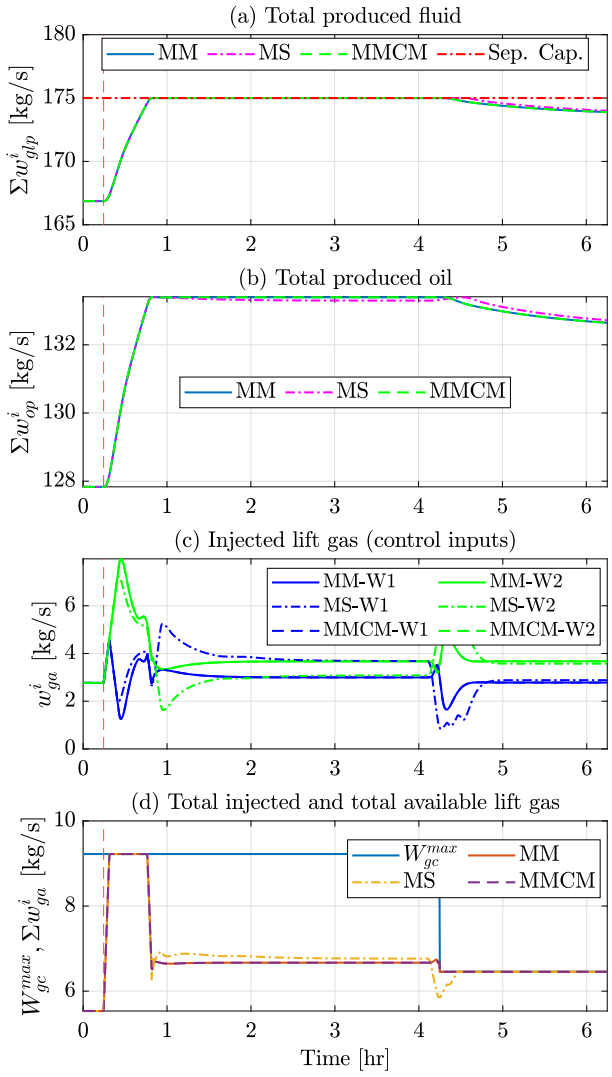

Fig. 4. Case (I): Applying standard min–max MPC (MM), multi-stage MPC (MS), and the proposed method i.e. min–max with constraint modification (MMCM) to the plant with the worst-case realization of uncertain parameters.

is not the case in our process), this combination of uncertain parameters would be the worst-case realization corresponding to the lower bound of the constraint. In other words, this case is the farthest distance to the worst-case realization of uncertainties; therefore, it is preferred to call it the safe case. All the other realizations of parameters within the uncertainty range put the process between these two extremes. The simulation result for case (III) is presented in Fig. 6. It can be seen that the improvement made by the proposed novel method is more significant. The method increases the oil production by 3.44% with respect to standard min–max MPC, while multi-stage MPC increases the production only by 0.2%.

The other advantage of the method proposed is low computational costs. In contrast to multi-stage MPC, which reduces the conservativeness by solving the optimization problem over control policies, the proposed novel method is still an open-loop optimization method. Therefore, its computational cost remains at the same level as open-loop min–max MPC. This has been validated by comparing the execution time of the methods for the three discussed cases. The execution time for each iteration

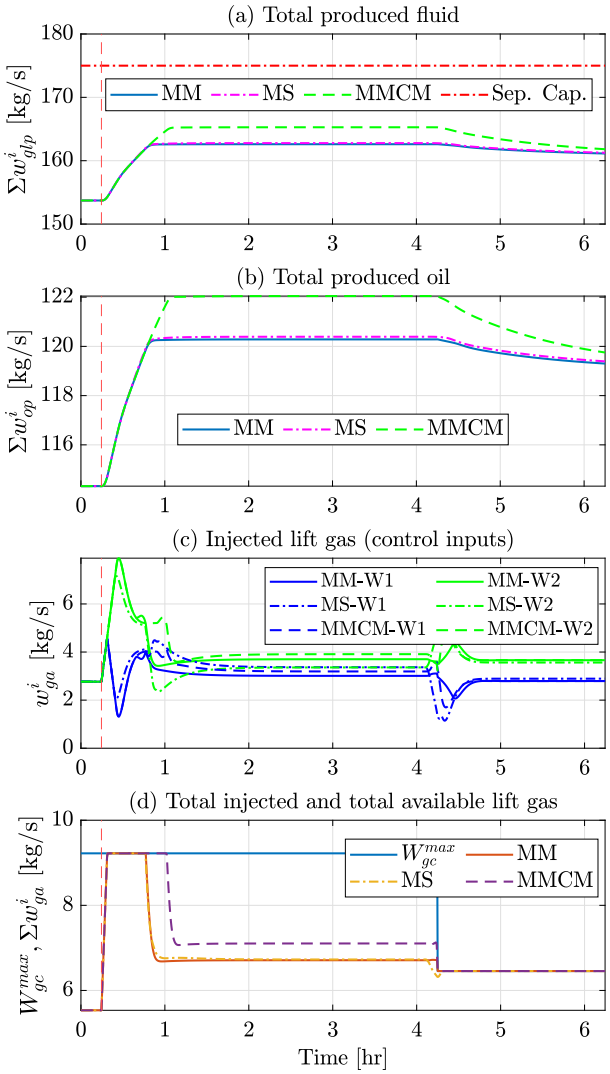

Fig. 5. Case (II): Applying standard min–max MPC (MM), multi-stage MPC (MS), and the proposed method min–max with constraint modification (MMCM) to the plant with the nominal realization of uncertain parameters.

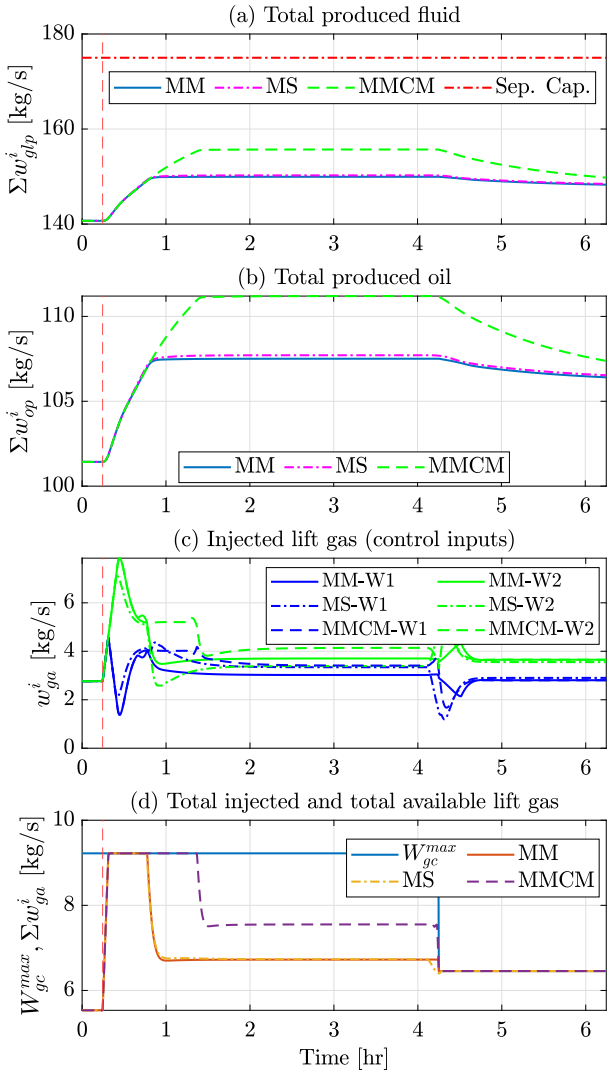

Fig. 6. Case (III): Applying standard min–max MPC (MM), multi-stage MPC (MS), and the proposed method min–max with constraint modification (MMCM) to the plant with the safe realization of uncertain parameters.

Table 2
The mean execution time of iterations for three cases (I), (II), and (II).

	Min–max	Multi-stage	Proposed novel method
Case (I)	0.030	3.01	0.029
Case (II)	0.042	2.85	0.038
Case (III)	0.037	3.38	0.029

has been plotted in Fig. 7. It shows that the computational costs for min–max MPC and the proposed novel method are more or less the same; however, the multi-stage MPC is computationally expensive. The average execution time for each method is also presented in Table 2 and reflects the same fact. Table 2 apparently shows that the proposed novel method is approximately 100 times faster than multi-stage MPC, yet it is less conservative.

5. Conclusion

All the robust methods are inherently conservative when the uncertainties take other values rather than their worst-case realization. Therefore, an efficient, robust nonlinear model predictive framework, particularly for real-time production maximization of the gas lifted well network under the presence of parametric uncertainty was presented in this paper to mitigate the problem of conservativeness. The conservativeness in our problem can be interpreted as the unutilized resources to increase production. So, the performance of the proposed framework is evaluated in this regard through several simulation cases.

The proposed optimal control framework of this paper consists of traditional open-loop min–max MPC with constraint modification. In particular, the error between measured and predicted output is used as a correction factor to modify the upper bound of the constraint. The design is based on the worst-case realization of the uncertainty; therefore, when the parameters take their worst-case realization, the error between measurement and prediction is zero, which means that the formulation reduces to a standard min–max MPC. Otherwise, the error term modifies the constraint that, consequently, leads to a reduction in conservativeness.

Several simulation cases have been conducted to demonstrate the promising advantages of the proposed novel method over open-loop min–max MPC and multi-stage MPC. All the competing methods are applied to a gas-lifted oil field with two oil wells in three simulation cases. It has been shown that when the uncertain parameters of the process take their worst-case

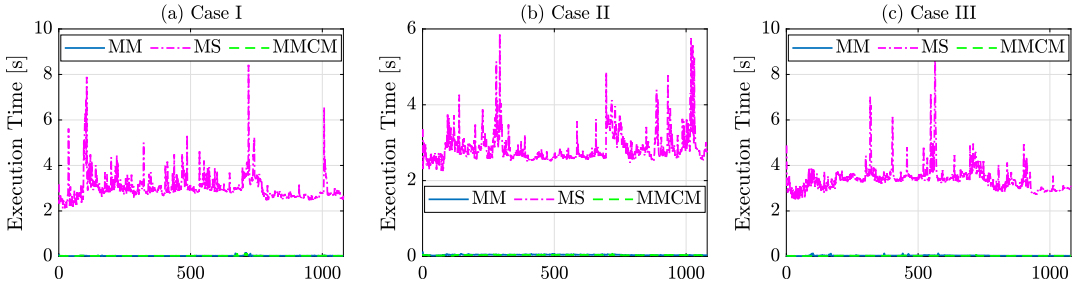

Fig. 7. Execution time for three cases. Case(I): worst-case realization of uncertainty, Case(II): nominal realization of uncertainty, Case(III): safe case realization of uncertainty.

realizations, all three methods are able to satisfy the constraints, i.e., all methods are robust within the uncertainty region. However, when the uncertain parameters take other realizations, the proposed method is significantly less conservative than min–max and multistage methods; therefore, the proposed method is superior to both min–max and multistage methods because it preserves the robust performance and reduces the conservativeness significantly. The method's superiority in terms of complexity is also investigated by comparing the execution times. It has been shown that the complexity of the method is at the level of min–max MPC, and it is considerably more straightforward and more efficient than multistage MPC.

Despite the significant benefits of the developed method, there are some limitations that give rise to further improvement in future works. First, some a priori knowledge about the process has been used to simplify the min–max MPC; however, the worst-case realization of the parameter might not be known a priori for other processes. Although this is a valid argument, it should be noted that the method at least does not impose any further complexity on the original min–max formulation. While on the contrary, multi-stage MPC introduces too much complexity with less reward in terms of conservativeness.

The next and most critical limitation which should be addressed in future works is that the method needs the active constraints to be directly measurable. The future direction in this regard is to generalize this work for the cases where constraints are not directly measurable by using other outputs/measurements to modify the constraints.

In fact, this method falls somewhere between the adaptive and robust methods. This is because, in the adaptive approach, the measurements are used to estimate the uncertain parameters, and then the estimated parameters will be used in a certainty equivalence deterministic MPC. However, the measurements in our method are used to directly modify the active constraints.

CRediT authorship contribution statement

Nima Janatian: Conceptualization, Methodology, Software, Writing – original draft. **Roshan Sharma:** Conceptualization, Supervision, Writing – review & editing.

Declaration of competing interest

The authors declare that they have no known competing financial interests or personal relationships that could have appeared to influence the work reported in this paper.

Data availability

No data was used for the research described in the article.

Acknowledgments

We gratefully acknowledge the economic support from The Research Council of Norway and Equinor ASA through Research Council project "308817 - Digital wells for optimal production and drainage" (DigiWell). All authors approved the version of the manuscript to be published.

References

[1] H. Witsenhausen, A minimax control problem for sampled linear systems, IEEE Trans. Automat. Control 13 (1) (1968) 5–21.
[2] P.J. Campo, M. Morari, Robust model predictive control, in: 1987 American Control Conference, IEEE, 1987, pp. 1021–1026.
[3] J.H. Lee, Z. Yu, Worst-case formulations of model predictive control for systems with bounded parameters, Automatica 33 (5) (1997) 763–781.
[4] P.O. Scokaert, D.Q. Mayne, Min–max feedback model predictive control for constrained linear systems, IEEE Trans. Automat. Control 43 (8) (1998) 1136–1142.
[5] A. Bemporad, Reducing conservativeness in predictive control of constrained systems with disturbances, in: Proceedings of the 37th IEEE Conference on Decision and Control (Cat. No. 98CH36171), IEEE, 1998, pp. 1384–1389.
[6] J. Lofberg, Approximations of closed-loop minimax MPC, in: 42nd IEEE International Conference on Decision and Control (IEEE Cat. No. 03CH37475), IEEE, 2003, pp. 1438–1442.
[7] P.J. Goulart, E.C. Kerrigan, J.M. Maciejowski, Optimization over state feedback policies for robust control with constraints, Automatica 42 (4) (2006) 523–533.
[8] J.A. Paulson, A. Mesbah, Approximate closed-loop robust model predictive control with guaranteed stability and constraint satisfaction, IEEE Control Syst. Lett. 4 (3) (2020) 719–724.
[9] D.Q. Mayne, M.M. Seron, S. Raković, Robust model predictive control of constrained linear systems with bounded disturbances, Automatica 41 (2) (2005) 219–224.
[10] D.Q. Mayne, E.C. Kerrigan, E. Van Wyk, P. Falugi, Tube-based robust nonlinear model predictive control, Internat. J. Robust Nonlinear Control 21 (11) (2011) 1341–1353.
[11] P. Falugi, D.Q. Mayne, Getting robustness against unstructured uncertainty: a tube-based MPC approach, IEEE Trans. Automat. Control 59 (5) (2013) 1290–1295.
[12] S. Raković, W.S. Levine, B. Açikmese, Elastic tube model predictive control, in: 2016 American Control Conference, ACC, IEEE, 2016, pp. 3594–3599.
[13] X. Lu, M. Cannon, Robust adaptive tube model predictive control, in: 2019 American Control Conference, ACC, IEEE, 2019, pp. 3695–3701.
[14] J. Köhler, R. Soloperto, M.A. Müller, F. Allgöwer, A computationally efficient robust model predictive control framework for uncertain nonlinear systems, IEEE Trans. Automat. Control 66 (2) (2020) 794–801.
[15] S. Lucia, T. Finkler, S. Engell, Multi-stage nonlinear model predictive control applied to a semi-batch polymerization reactor under uncertainty, J. Process Control 23 (9) (2013) 1306–1319.
[16] D. Krishnamoorthy, B. Foss, S. Skogestad, Steady-state real-time optimization using transient measurements, Comput. Chem. Eng. 115 (2018) 34–45.

[17] D. Krishnamoorthy, B. Foss, S. Skogestad, Real-time optimization under uncertainty applied to a gas lifted well network, Processes 4 (4) (2016) 52.
[18] N. Janatian, K. Jayamanne, R. Sharma, Model based control and analysis of gas lifted oil field for optimal operation, in: The First SIMS EUROSIM Conference on Modelling and Simulation, SIMS EUROSIM 2021, and 62nd International Conference of Scandinavian Simulation Society, SIMS 2021, Linköping Electronic Conference Proceedings, 2022, pp. 241–246.
[19] C.E. Garcia, A.M. Morshedi, Quadratic programming solution of dynamic matrix control (QDMC), Chem. Eng. Commun. 46 (1–3) (1986) 73–87.
[20] D.A. Copp, T.A. Nguyen, R.H. Byrne, Adaptive model predictive control for real-time dispatch of energy storage systems, in: 2019 American Control Conference, ACC, IEEE, 2019, pp. 3611–3616.
[21] P.A. Delou, J.P.A. de Azevedo, D. Krishnamoorthy, M.B. de Souza Jr., A.R. Secchi, Model predictive control with adaptive strategy applied to an electric submersible pump in a subsea environment, IFAC-PapersOnLine 52 (1) (2019) 784–789.
[22] G.O. Eikrem, O.M. Aamo, H. Siahaan, B. Foss, Anti-slug control of gas-lift wells-experimental results, IFAC Proc. Vol. 37 (13) (2004) 799–804.
[23] O.M. Aamo, G.O. Eikrem, H.B. Siahaan, B. Foss, Observer design for multiphase flow in vertical pipes with gas-lift—theory and experiments, J. Process Control 15 (3) (2005) 247–257.
[24] L. Sinegre, N. Petit, P. Menegatti, Predicting instabilities in gas-lifted wells simulation, in: 2006 American Control Conference, ACC, IEEE, 2006, pp. 5530–5537.
[25] R. Sharma, K. Fjalestad, B. Glemmestad, Modeling and control of gas lifted oil field with five oil wells, in: 52nd International Conference of Scandinavian Simulation Society, SIMS, 2011, pp. 47–59.
[26] E. Jahanshahi, S. Skogestad, Simplified dynamic models for control of riser slugging in offshore oil production, Oil Gas Facil. 3 (6) (2014) 80–88.
[27] R. Marti, S. Lucia, D. Sarabia, R. Paulen, S. Engell, C. de Prada, Improving scenario decomposition algorithms for robust nonlinear model predictive control, Comput. Chem. Eng. 79 (2015) 30–45.
[28] N. Janatian, R. Sharma, Multi-stage scenario-based MPC for short term oil production optimization under the presence of uncertainty, J. Process Control 118 (2022) 95–105.
[29] J.A. Andersson, J. Gillis, G. Horn, J.B. Rawlings, M. Diehl, CasADi – A software framework for nonlinear optimization and optimal control, Math. Program. Comput. 11 (1) (2019) 1–36, http://dx.doi.org/10.1007/s12532-018-0139-4.
[30] A. Wächter, L.T. Biegler, On the implementation of an interior-point filter line-search algorithm for large-scale nonlinear programming, Math. Program. 106 (1) (2006) 25–57, http://dx.doi.org/10.1007/s10107-004-0559-y.

Paper E
Short-term production optimization for Electric Submersible Pump lifted oil field with parametric uncertainty

Published in *IEEE Access*, Volume 11, September 2023.
Authors: Nima Janatian and Roshan Sharma.
Authors' roles in the article:
Nima Janatian: Main ideas, implementation, and writing.
Roshan Sharma (Supervisor): Discussions, comments, and proofreading.

IEEE Access
Multidisciplinary ⋮ Rapid Review ⋮ Open Access Journal

Received 16 August 2023, accepted 1 September 2023, date of publication 5 September 2023,
date of current version 11 September 2023.

Digital Object Identifier 10.1109/ACCESS.2023.3312169

RESEARCH ARTICLE

Short-Term Production Optimization for Electric Submersible Pump Lifted Oil Field With Parametric Uncertainty

NIMA JANATIAN AND ROSHAN SHARMA
Department of Electrical Engineering, Information Technology and Cybernetics, University of South-Eastern Norway, 3918 Porsgrunn, Norway
Corresponding author: Nima Janatian (nima.janatianghadikolaei@usn.no)

This work was supported by the Research Council of Norway and Equinor ASA through Research Council Project "Digital Wells for Optimal Production and Drainage" (DigiWell) under project number 308817.

ABSTRACT This paper uses a scenario-based optimization method to address the Daily Production Optimization from an Electric Submersible Pump lifted oil field under the presence of uncertainty. The primary contribution of this work lies in addressing the presence of uncertainty in short-term production optimization of the oil industry, a significant aspect that is frequently overlooked. It has been shown that using the dynamic model of the plant in the optimization problem is too computationally expensive, even in a deterministic case. Therefore, the steady-state model of the system has been used in a robust optimization framework. The necessity of considering uncertainty in the optimization problem and the promising results of the proposed robust method is compared with the deterministic optimization counterpart. An additional novelty of this study involves the utilization of a scenario-based optimization framework to explore various forms of uncertainty, including uncertainty in well flow parameters and oil price. It has been shown that the uncertainty in oil price does not affect the optimal solution during normal operation, at least in short-term optimization such as Daily Production Optimization. On the contrary, the uncertainty in the well parameters is important to be considered since well flow parameters influence the optimizer in preferring one well over the other. Consequently, the economic objective for the lucrative business of the oil industry will be translated into production maximization, and the optimizer's task involves allocating the total production capacity among the different wells to maximize the proportion of the oil to water in the produced fluid.

INDEX TERMS Constrained optimization under uncertainty, electric submersible pump lifted oil well, parametric uncertainty, scenario-based robust optimization, short-term production optimization.

I. INTRODUCTION

The cost and revenue from an oil and gas production unit are typically affected by decisions that are required to be taken at different time scales. The planning horizon for these decisions ranges from seconds to the entire lifetime of the field, depending on the objectives. Daily Production Optimization (DPO), which is equivalent to Real-Time Optimization (RTO) from a process systems perspective, corresponds to the decisions and plans that are taken in the time scale of a few hours to a couple of days to maximize the daily operating revenue of the production unit. Typical decisions in this scope involve selecting the choke opening of the different wells or allocating shared resources such as electric power and available lift gas in order to maximize the daily operational profit and ensure that the process and operating constraints are satisfied [1].

Daily production optimization has been reported to increase production by 1-4% [2], [3]. These improvements are even more pronounced for fields in the late plateau and decline phases than earlier phases [4]. On the other hand, it is well known that the presence of uncertainty may jeopardize the real-life application of constrained optimization since it is reasonably possible that the mismatch introduced

The associate editor coordinating the review of this manuscript and approving it for publication was Zhiwu Li.

due to uncertainty may make an optimal solution practically infeasible. Thus, this paper will investigate the daily production optimization problem for an Electric Submersible Pump (ESP) lifted oil field under the presence of uncertainty.

A mathematical model for a single ESP oil well was developed in [5], and a linear Model Predictive Control (MPC) was designed in the Statoil Estimation and Prediction Tool for Identification and Control (SEPTIC) based on the step response model of the process. This controller was later implemented on a Programmable Logic Controller (PLC) in [6]. A Moving Horizon Estimator (MHE) was successfully implemented in [7] using the same model to estimate the flow rate and the productivity index of the well and the viscosity of the produced fluid.

A similar first principle model was derived in [8] for multiple ESP wells that share a common production manifold. The steady-state version of this model was used in [9] to develop a nonlinear optimization based on Sequential Quadratic Programming (SQP) for two optimal control strategies. The authors demonstrated that the production choke valve for each oil well has to be fully open during normal operation to maintain the optimal fluid flow rate and minimize electrical power. The same authors formulated a Mixed Integer Nonlinear Programming problem (MINLP) in [10] to calculate and identify the number of oil wells that should be used for special cases with low production demand. The dynamic version of the model was also used in [11], where the nonlinear model predictive control framework was implemented as an economic optimizer for maximizing profit. Even though the controls in this work were assumed constant throughout the prediction horizon, the length of the prediction horizon was limited to one second due to the fast dynamics of ESP and the high computational cost of a longer prediction horizon.

The research based on the model developed in [5] was pursued further, and it was shown in [12] that the linear model of an ESP lifted well varies significantly depending on the choke opening. Therefore, a model adaptation based on the homotopic transition between models was proposed in [13], where an adaptive linear MPC strategy was implemented as a Quadratic Dynamic Matrix Control (QDMC) algorithm in order to control the pump inlet pressure, minimizing the pump power and respecting the variable's constraints. An adaptive infinite horizon MPC strategy was also implemented in [14], where the proposed control law used successive linearization of the dynamic model in [5] to update the model internally. The ESP model was used in [15] to investigate the implementation aspects of measured disturbances in MPC. The main control objective in this work was to sustain a given production rate from the well while maintaining acceptable operating conditions for the pump.

A different approach was proposed in [1], translating the optimization objectives into control objectives to avoid solving a numerical optimization problem. The proposed method was applied to a single ESP lifted well successfully to track the inlet pressure of ESP subject to constraints. Nevertheless, the method violated the constraints dynamically. Recently a high-fidelity model of a single ESP well was proposed in [16] to be used as a surrogate model for the real plant. This model was used in [17] to propose an economic-oriented MPC autotuning strategy with a flexible structure able to enclose different MPC formulations, different tuning requirements, online implementation, and process attributes. An Echo State Neural Network was trained in [18] to capture the dynamic model of ESP well. The trained neural network was used for two nonlinear model predictive controllers that aimed to track the bottom-hole pressure subject to constraints on control inputs, bottom-hole and well-head pressures, and liquid flows.

The literature, as mentioned earlier, clearly shows two neglected aspects that are required to be addressed for the DPO problem for an ESP oil field:

- **Problem Formulation:** The control presented in [5] and almost all its successors aimed to track a certain set point (mostly bottom-hole pressure). This type of objective corresponds to the lower layer (Control and Automation layer as described in [4]) in the multilevel control hierarchy, where the set points to be tracked are determined by the higher-level optimizer called Production Optimization. Therefore, none of these works have answered the main question of DPO, which is: *How much should be produced from each well to maximize the economic objective?*
- **Parametric Uncertainty:** The other research works that started from [8] have considered multiple wells in a field, and the optimization problem is formulated to produce the optimal amount of fluid from each well to maximize the overall economic objective. Nevertheless, the composition of the produced fluid is considered constant over time, meaning the uncertainty in the real value of the well flow parameters like water cut or change in the water cut is neglected, while it is well known that the uncertainty in the parameter can make the optimal solution practically infeasible due to the mismatch between the prediction model and the real process [19], [20].

Therefore this paper aims to address these two knowledge gaps by investigating the daily production optimization from an ESP oil field with multiple oil wells considering the parameter uncertainty.

Scenario-based optimization method provides a versatile framework for robust optimization under uncertainty with improved conservativeness. The key feature of the method is the inclusion of finite realization of uncertainty represented by a scenario tree. The method was incorporated into a nonlinear model predictive control scheme in [21] for dynamic optimization of a semi-batch polymerization reactor under uncertainty. The method has been widely utilized across various applications. For instance, it has been applied to allocate pumped-storage hydropower units, as described in [22]. It was also used in the domain of oil production to optimally allocate a limited amount of available lift gas between multiple wells in a gas-lifted oil field [20], [23], [24]. However, using the dynamic model of ESP for DPO becomes problematic since the fast dynamics of the pumps require a

short sampling time, and the number of decision variables over a relatively long prediction horizon, such as in DPO, becomes intractable.

In order to address this problem, the piecewise steady operation of the plant is assumed throughout the prediction horizon. In particular, the fairly long prediction horizon of DPO is divided into segments, and the plant is considered to operate at a possibly new steady-state over each segment. Therefore, the steady-state model of the plant is used as the prediction model to determine the future of the system over each segment. This assumption is admissible not only because it is in line with the major conclusion of [4], which states that successive static optimization suffices in most relevant DPO cases, but also because the open loop simulation of the process demonstrates that the system is sufficiently fast that the transition between steady-states is negligible with respect to the length of the prediction horizon and can be overlooked.

Accordingly, the steady-state version of the model provided by [8] is used in this paper, supplemented by fairly subtle realistic assumptions and parametric uncertainty in various forms. The daily production optimization is formulated as successive scenario-based optimization problems in a receding horizon fashion to address the constraint fulfillment under the presence of uncertainty. In other words, only the first optimal decision is implemented in the plant, and the whole optimization process will be repeated at each time step. The main contribution of this work is threefold:

- Formulating the daily production optimization for an ESP-lifted oil field with a fairly more realistic objective function that includes the income from selling oil and the costs due to the electric power consumption, water treatment, and petroleum taxation.
- Considering the parametric uncertainty in DPO and using the scenario-based optimization framework to satisfy the fulfillment of the constraints robustly.
- Investigating the various forms of uncertainty, such as the uncertainty in oil price and the characteristics of the wells.

The rest of the paper is organized as follows. Section II briefly describes the mathematical modeling of the ESP oil field unit. The justification for preferring a steady-state model over a dynamic model is presented in Section III. Scenario-based optimization for DPO is presented in Section IV. The different aspects of the uncertainty, such as uncertainty in oil price and well parameters, are investigated in Section V before concluding in section VI.

II. MATHEMATICAL MODEL OF ESP-LIFTED OIL FIELD

A. PROCESS DESCRIPTION

An Electric Submersible Pump lifted oil well is an artificial lifting system where a submersible multistage centrifugal pump is installed at the bottom of the wellbore [8] to produce the pressure gradient needed for flowing the fluid to the surface. ESP lifting method is well suited for producing high volumes of heavy liquid [25]. Fig. 1 demonstrates the

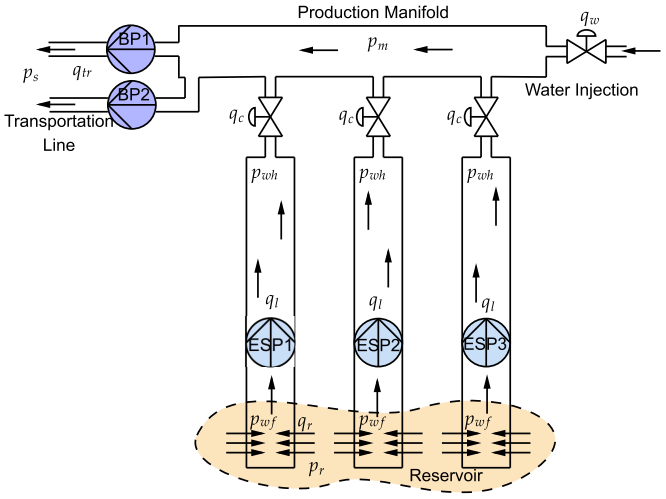

FIGURE 1. Schematic diagram of the production network with three ESP lifted oil wells and two identical transportation lines.

schematic diagram of the considered production network in this paper with three oil wells. Each well is equipped with an ESP unit at the bottom hole and a production chock valve at the wellhead. The amount of fluid produced from each well can be controlled by manipulating the speed of the pump. The oil produced from each well is collected together in a common production manifold. The reservoir is assumed to contain two-phase fluid, including crude oil with higher viscosity and water with no gas flow. The viscosity of the fluid produced from the wells is reduced by adding water to the production manifold from one end using a water injection valve to ease the transportation of the highly viscous fluid over a long distance. Two identical transportation lines are used to transport the gathered fluid from the production manifold to the separator located on the topside facility. Each transportation line is fitted with a booster pump which is used to increase the pressure to overcome the sum of flowing pressure losses in the transportation line.

Simple mechanistic models of ESP-lifted oil wells are developed in [5] and [8] for optimization and control purposes. Both models are derived based on mass and momentum balance in the pipes and manifolds. The considered mathematical model of this paper is adopted from [8] with subtle modifications on assumptions:

- Modeling the electrical motors subsystem is neglected due to the fast response of electrical systems.
- Assumption of constant water cut in the production manifold is substituted by a more realistic one. Therefore, instead of injecting water to keep the water cut constant, which needs a perfect controller, a constant flow of water is injected into the manifold. Accordingly, the water cut of the liquid phase within the manifold is varying and depends on the proportion of fluid produced from production chock valves.
- Water cuts of the wells are considered to be different to draw a meaningful optimization problem.

B. GOVERNING EQUATIONS

This section only briefly presents the governing equations of the process since modeling is not the main focus and contribution of this work. However, the readers are referred to [8] for a more detailed explanation of the modeling.

The process is described by three states for each well, namely, the pressure at the bottom hole p_b^i, the pressure at the wellhead p_h^i, and the average volumetric flow rate of the well q_l^i, where the superscript i refers to the i^{th} oil well. The remaining states are the pressure in the production manifold p_m and the average volumetric flow rate of the j^{th} transportation line q_{tr}^j. The corresponding differential equations are given by:

$$\dot{p}_b^i = \frac{\beta}{A_r^i L_r^i}\left[q_r^i - q_l^i\right] \tag{1}$$

$$\dot{p}_h^i = \frac{\beta}{A_t^i L_t^i}\left[q_l^i - q_c^i\right] \tag{2}$$

$$\dot{q}_l^i = \frac{A_t^i}{\rho_l^i\left(L_r^i + L_t^i\right)}\Big[p_b^i - p_h^i + \rho_l^i g H_{esp}^i(q_l^i, f^i) - \rho_l^i g(L_r^i + L_t^i) - \Delta p_{f,t}^i - \Delta p_{f,r}^i\Big] \tag{3}$$

$$\dot{p}_m = \frac{\beta}{A_m L_m}\left[\sum_{i=1}^{3} q_c^i - \sum_{j=1}^{2} q_{tr}^j + q_w^{inj}\right] \tag{4}$$

$$\dot{q}_{tr}^j = \frac{A_{tr}^j}{\rho_{tr}^j L_{tr}^j}\left[p_m - p_s + \Delta p_{bp}^j - \Delta p_{f,tr}^j\right] \tag{5}$$

And the set of algebraic equations is given by:

$$q_r^i = \text{PI}^i\left(p_r - p_b^i\right) \tag{6}$$

$$q_c^i = C_v^i\sqrt{\frac{\max(p_h^i - p_m, 0)}{\rho_l^i}} \tag{7}$$

$$\Delta p_f^i = \frac{f_D L \rho \upsilon^2}{2D_h} \tag{8}$$

$$H_{esp}^i(Q,f) = \frac{\bar{a}_0^i}{f_0^2}f^2 + \frac{\bar{a}_1^i}{f_0}fQ(f) + \bar{a}_2^i Q^2(f) + \frac{\bar{a}_3^i}{f}f_0 Q^3(f) \tag{9}$$

$$\text{BHP}_{esp}^i(Q,f) = \frac{\hat{a}_0^i}{f_0^3}f^3 + \frac{\hat{a}_1^i}{f_0^2}f^2 Q(f) + \frac{\hat{a}_2^i}{f_0}fQ^2(f) + \hat{a}_3^i Q^3(f) + \frac{\hat{a}_4^i}{f}f_0 Q^4(f) \tag{10}$$

$$\rho_l^i = \text{WC}^i\rho_w + (1 - \text{WC}^i)\rho_o \tag{11}$$

$$\text{WC}_{tr} = \frac{q_w^{inj} + \sum_{i=1}^{3}\text{WC}^i q_c^i}{q_w^{inj} + \sum_{i=1}^{3} q_c^i} \tag{12}$$

$$q_o = \sum_{j=1}^{2}(1 - \text{WC}_{tr})q_{tr}^j \tag{13}$$

$$q_w = \sum_{j=1}^{2}\text{WC}_{tr}q_{tr}^j \tag{14}$$

$$Q_{\min}^i(f) = \frac{f}{f_0}Q_{f_0,\min}^i \tag{15}$$

$$Q_{\max}^i(f) = \frac{f}{f_0}Q_{f_0,\max}^i \tag{16}$$

TABLE 1. List of the algebraic variables and parameters.

Variable	Description
q_r	Volumetric flow rate from reservoir into well
q_c	Volumetric flow rate through production choke valve
ρ_l	Density of the fluid in the well
H_{esp}	Head developed by ESP
BHP_{esp}	ESP brake horsepower
Δp_f	Frictional pressure drop in the pipe
WC_{tr}	Water cut in transportation line
WC	Water cut of the well
PI	Productivity index of the well
q_o	Total produced oil
q_w	Total produced water
$Q_{\min}$	Minimum flow through the ESP
$Q_{\max}$	Maximum flow through the ESP

TABLE 2. List of the parameters and their corresponding values.

Parameter	Value	Unit	Comments
L_{tr}	4000	[m]	Length of transportation line
L_m	500	[m]	Length of production manifold
L_t	2000	[m]	Length of well above ESP
L_r	100	[m]	Length of well below ESP
D	0.1569	[m]	Diameter of all pipelines
A	0.0193	[m^2]	Cross section area of all pipelines
β	1.5e9	[N/m^2]	Bulk modulus of the reservoir fluid
ρ_o	900	[kg/m^3]	Density of water
ρ_w	1000	[kg/m^3]	Density of oil
p_r	220	[bar]	Pressure of the reservoir
p_s	30	[bar]	Pressure of the separator
C_v	0.2275	$[\sqrt{\frac{\text{kgm}^3}{\text{s}^2\text{bar}}}]$	Valve opening characteristic
μ_o	100e-6	[m^2/s]	Kinematic viscosity of oil
μ_w	1e-6	[m^2/s]	Kinematic viscosity of pure water
Δp_{bp}	10	[bar]	Pressure gradient by booster pump
f_0	60	[Hz]	ESP characteristics ref. freq.
$Q_{f_0,\min}$	228.648	[gpm]	ESP minimum flow at ref. freq.
$Q_{f_0,\max}$	400.111	[gpm]	ESP maximum flow at ref. freq.

All the algebraic variables of the model are introduced in Table 1, and the model parameter values are presented in Table 2. The Darcy friction factor f_D in (8) can be evaluated using Serghides' explicit approximation to Colebrook-White equation [26]. The polynomial coefficients of ESP in (9) and (10) are also presented in Table 3.

Note that the algebraic variables can be easily substituted in the differential equations of the model presented in (1) to (5) to obtain an explicit set of ordinary differential

TABLE 3. Polynomial coefficients of ESP.

	$\bar{a}_0\backslash\hat{a}_0$	$\bar{a}_1\backslash\hat{a}_1$	$\bar{a}_2\backslash\hat{a}_2$	$\bar{a}_3\backslash\hat{a}_3$	$\bar{a}_4\backslash\hat{a}_4$
H_{esp}	3.9719e3	-9.4149	4.5285e-2	-8.6465e-5	0
BHP_{esp}	2.2498e2	7.3984e-1	-6.8839e-4	2.1777e-6	-5.4696e-9

TABLE 4. Nominal values of uncertain parameters.

Parameter	Well 1	Well 2	Well 3	Unit
PI_{nom}	4.5e-4	5.4e-4	4.1e-4	$[\frac{m^3}{bar.s}]$
WC_{nom}	0.23	0.05	0.67	-

equations (ODE) in a compact form as:

$$\dot{x} = f\,(x, u, d) \tag{17}$$

where $x \in \mathbb{R}^{12}$ and $u \in \mathbb{R}^3$ are the states and system inputs, and $d \in \mathbb{R}^6$ is the vector of the uncertain parameters of the process as given by:

$$\begin{bmatrix}\mathbf{p_b} & \mathbf{p_h} & \mathbf{q_l} & \mathbf{p_m} & \mathbf{q_{tr}}\end{bmatrix} \tag{18}$$

$$\begin{bmatrix}f^1 & f^2 & f^3\end{bmatrix} \tag{19}$$

$$\begin{bmatrix}\mathrm{PI}^1 & \mathrm{PI}^2 & \mathrm{PI}^3 & \mathrm{WC}^1 & \mathrm{WC}^2 & \mathrm{WC}^3\end{bmatrix} \tag{20}$$

C. UNCERTAINTY DESCRIPTION

The uncertainty in the productivity index and water cut of the wells are considered in this study. The productivity index PI represents the reservoir's ability to deliver fluids to the wellbore, and the water cut WC is defined as the volumetric flow rate of water to the total produced liquid. For a network with three oil wells, there exist six uncertain parameters in the problem. Amongst specialists in the field, it is widely acknowledged that the water cut is more prone to experiencing abrupt changes, whereas alterations in the productivity index occur in a smoother manner. Hence, it is reasonable to suppose that the quantification of uncertainty in the water cut is greater than the uncertainty in the productivity index. As a result, a deviation of $\pm 10\%$ and $\pm 30\%$ from their nominal values are considered for PI and WC of each oil well, respectively, and the parameters can take any value within their bounds. No specific distribution of the parameters is selected to challenge the controller; thus, all the values in the uncertainty region are equally likely to occur. The nominal values of the parameters and their upper and lower bounds are presented in Table 4.

III. DYNAMIC VERSUS STEADY-STATE OPTIMIZATION

Although it has been argued in [4] that repetitive static optimization formulation suffices in most relevant DPO cases, some effort has been made to integrate the DPO layer into the Control and Automation layer using multistage nonlinear model predictive control with economic objective function as a dynamic optimizer in [20], [23], and [24]. Accordingly, this section intends to illustrate why the same approach is not applicable, particularly to the ESP lifted oil field described in Section II.

To do so, a deterministic nonlinear MPC is considered with an economic objective function to maximize the profit from the field. The primary objective is to adjust the pump frequencies in order to produce an optimal amount of fluid from each well for a given separator capacity. Therefore, the objective function includes the total income from selling the produced oil with a negative sign to pose it as a minimization problem. Additionally, the costs due to electric power consumption of the ESPs, water treatment, and carbon taxation are incorporated into the objective function. Hence over the prediction horizon with the length N_p the objective function is given by:

$$J_{eco} = \sum_{k=1}^{N_p}\left(-c_o q_o^k + c_e \sum_{i=1}^{3} \mathrm{BHP}_{esp}^{i,k} + c_s q_w^k + c_t q_o^k\right) \tag{21}$$

where c_o, c_e, c_s, and c_t denote the price of oil, electricity, water treatment, and carbon taxation, respectively. Their values are presented in Table 5.

The most important operational constraints in the problem arise from separator capacity and the ESP operating envelope. In particular, the magnitude of produced fluid (mixture of oil and water) should be equal to or less than the separator handling capacity, and the ESP pumps need to be kept within a safe operating window to avoid mechanical failure. Thus, the optimal control problem formulation over the prediction horizon is given by:

$$\min_{\mathrm{x,u}} J_{eco}(\mathrm{x, u, d}) \tag{22a}$$

$$\text{s.t. } x_k = f\,(x_{k-1}, u_{k-1}, d)\,, \quad k = 1, \ldots, N_p \tag{22b}$$

$$\sum_{i=1}^{2} q_{tr}^{i,k} \le Q_{\mathrm{sep}}^k, \quad k = 1, \ldots, N_p \tag{22c}$$

$$Q_{\min}^{i,k} \le q_l^{i,k} \le Q_{\max}^{i,k}, \quad k = 1, \ldots, N_p \tag{22d}$$

$$u_{LB} \le u_k \le u_{UB}, \quad k = 0, \ldots, N_p - 1 \tag{22e}$$

$$\Delta u_{LB} \le \Delta u_k \le \Delta u_{UB}, \quad k = 0, \ldots, N_p - 1 \tag{22f}$$

Equation (22b) denotes the discretized dynamic model and is imposed as a state continuity constraint. The constraint on the total produced fluid is enforced in (22c), where Q_{sep}^k stands for the maximum handling capacity of the separator. The safe operation of the ESP pumps within the pump envelope is denoted in (22d) by maintaining the pump flow between the minimum and maximum allowed flow which is provided by (15) and (16). The lower and upper bounds on the control signal (pump frequency) and the rate of change of control inputs are also implemented in (22e) and (22f), respectively.

The optimal control problem in (22) is solved in a receding horizon fashion using the nominal value of the parameters provided in Table 2 and Table 3. A sampling time of 0.3 seconds and a prediction horizon of 25 time steps (7.5 s) is used. The separator capacity is considered to be 8500 [m^3/d]. The lower bound and upper bound for pump frequency is 45 and 80 [Hz]. The rate of change in pump frequency has to be maintained between -1 and 1 [Hz/s]. The prices in the objective function are presented in Table 5. The dynamic optimization problem is discretized using the direct multiple shooting method in CasADi v.3.5.5. The simulations are implemented in MATLAB R2022b, and IPOPT v.3.14.1 solver has been used to solve the optimization problems.

TABLE 5. Prices.

Price	Value	Unit	Comments
c_o	75	[$/bbl]	Price of oil per barrel
c_e	15	[$/kWh]	Price of electricity per unit of energy
c_s	2	[$/bbl]	Cost of water treatment per barrel
c_t	30	[$/bbl]	Carbon taxation per barrel

The simulation result is presented in Fig. 2. All the constraints on the control input, separator capacity, and pump envelope are respected successfully, as demonstrated in subplots (a), (b), and (e). However, the execution time remains the main challenge for dynamic optimization. The execution time, which is shown in subplot (d), has an average of 0.15 s and peaks up to 0.2 s at some points. This simply means that the method is barely implementable even in a deterministic case since the computations should be executed during one sampling time (0.3 s). It is also worth mentioning that the uncertainty is not considered yet, and the prediction horizon is relatively short. Considering uncertainty with scenario-based dynamic optimization problem increases the execution time significantly and may become intractable if more oil wells are considered in the field, as observed in [20], [23], and [24]. Therefore, using a steady-state model is unavoidable for DPO under uncertainty, and it is in line with the claim in [4], which states that a steady-state model typically suffices for DPO.

IV. SCENARIO-BASED OPTIMIZATION USING STEADY-STATE MODEL

According to the scenario-based optimization approach, the uncertainty region is discretized into finite distinct possible realizations, and the system's evolution is evaluated based on a scenario tree. This means that the future evolution of the plant is branched into different trajectories depending on which realization of the uncertainty occurs in reality. Nevertheless, the computations may become intractable since the number of scenarios grows exponentially with the number of considered uncertainty and the length of the prediction horizon. The solution to this drawback gives rise to a concept named robust horizon. The robust horizon means the branching is continued for only a certain number of samples which is typically one or two samples ahead in time. The justification for a robust horizon arises from the fact that the corresponding control variables and state trajectories will be recalculated and refined in future sampling times; hence, the far future uncertainty does not need to be represented precisely.

Considering the maximum and minimum values of the six uncertain parameters and the nominal case, $N_s = 2^6 + 1 = 65$ possible realizations for uncertainties or branches are considered in this paper, including all the combinations of boundary values and the nominal case. The scenario tree with the robust horizon $N_r = 1$ is exhibited in Fig. 3. Each path from the root node to the leaf is called a scenario; thus, the method is also known as scenario-based optimization.

It is worthwhile to mention that this formulation imposes an extra constraint which is known as a non-anticipativity constraint. This constraint represents the fact that in real-time decision-making, the controller can not anticipate the future realization of the uncertainty. Therefore, all the controls that branch from a parent node are made equal using the non-anticipativity constraint.

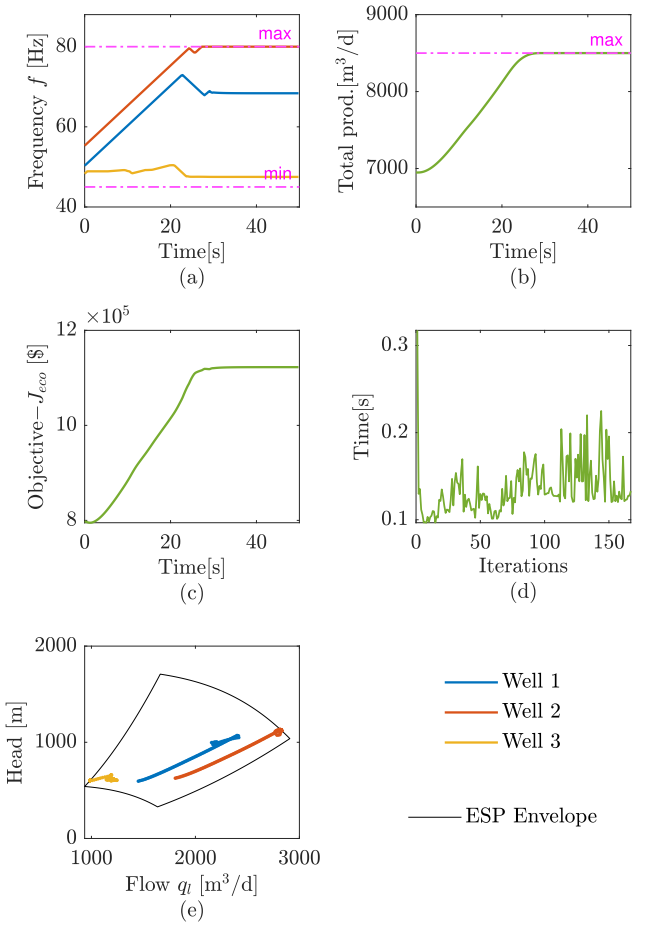

FIGURE 2. Dynamic optimization using standard deterministic Nonlinear Model Predictive Control: (a) Pump frequency, (b) Total produced fluid, (c) Negative of the objective function, (d) Execution time, (e) ESP operating envelope.

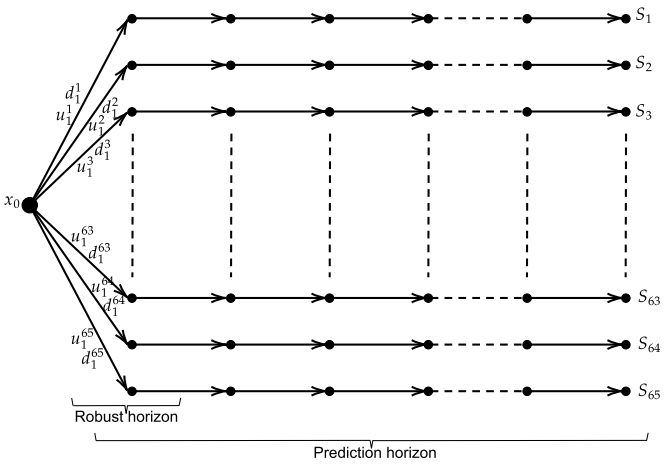

FIGURE 3. Scenario tree with $N_s = 65$ scenarios and robust horizon $N_r = 1$.

Once the scenario tree and its prerequisites have been defined, the objective function of each scenario j can be calculated as:

$$J^j_{eco} = \sum_{k=1}^{N_p} \left(-c_o q_o^{k,j} + c_e \sum_{i=1}^{3} \mathrm{BHP}^{i,k,j}_{esp} + c_s q_w^{k,j} + c_t q_o^{k,j} \right) \tag{23}$$

Accordingly, the optimization problem can be formulated over all the discrete scenarios of the scenario set $\mathcal{S} = \{1, \ldots, N_s\}$, throughout the prediction horizon $\mathcal{K} = \{1, \ldots, N_p\}$ as follows:

$$\min_{\mathrm{x,u}} \sum_{j=1}^{N_s} \omega_j J^j_{eco} \tag{24a}$$

$$\text{s.t.} f\left(x^j_k, u^j_k, d^j_k\right) = 0, \ \forall k \in \mathcal{K}, \ \forall j \in \mathcal{S} \tag{24b}$$

$$\sum_{i=1}^{2} q^{i,k,j}_{tr} \leq Q^k_{\mathrm{sep}}, \ \forall k \in \mathcal{K}, \ \forall j \in \mathcal{S} \tag{24c}$$

$$Q^{i,k,j}_{\min} \leq q^{i,k,j}_{l} \leq Q^{i,k,j}_{\max}, \ \forall k \in \mathcal{K}, \ \forall j \in \mathcal{S} \tag{24d}$$

$$u_{LB} \leq u^j_k \leq u_{UB}, \ \forall k \in \mathcal{K}, \ \forall j \in \mathcal{S} \tag{24e}$$

$$u^j_k = u^l_k \quad \text{if} \quad x^{p(j)}_k = x^{p(l)}_k, \ \forall k \in \mathcal{K}, \ \forall j \& l \in \mathcal{S} \tag{24f}$$

where J^j_{eco} is the objective function of the j^{th} scenario and ω_j is the corresponding tuning weight that reflects the relative likelihood of occurring j^{th} scenario. The steady-state condition of the system is implemented as a constraint in (24b). It ensures that the states at every time $k \in \mathcal{K}$ from scenario j are at a steady condition which is a function of their corresponding control u^j_k and uncertainty realization d^j_k. The constraints on the separator capacity, pump envelope, and frequency are imposed in (24c), (22d), and (24e), respectively. It should be noted that the constraint on the change of control input is not relevant anymore since the transition between the steady-states is neglected. Instead, the non-anticipativity constraint is introduced in (24f), which reflects the fact that at each time step k, controls u^j_k and x^l_k from scenarios j and l with the same parental node $x^{p(j)}_k = x^{p(l)}_k$ have to be equal. In other words, all the controls that are branched from the same parental node are equal. It should be noted that, as shown in Fig. 3, branching has been done only for the first sampling time. Therefore, $u^1_1 = u^2_1 = \ldots = u^{64}_1 = u^{65}_1$ is the only set of non-anticipativity constraints in the problem, and according to the receding horizon strategy, this first control action is the one that will be applied to the real system. Hence, the non-anticipativity constraint guarantees that this value is unique.

A comparison between the proposed scenario-based optimization method and a deterministic standard optimization is conducted to demonstrate the capability of the method to handle uncertainty. To this end, a deterministic nonlinear MPC controller is also designed based on the steady-state model with nominal values of uncertain parameters. The formulation is not duplicated since it can be considered as a special case of the optimization problem in (24) with only one nominal scenario.

A prediction horizon of two days with a sampling time of six hours is chosen for the controller. The plant containing well flow characteristic uncertainty is simulated using both deterministic and scenario-based methods. The simulation results are presented in Fig. 4 and Fig. 5. Subplots (b) and (c) in Fig. 4 demonstrate that for some realizations of uncertainty, the constraints on separator capacity and pump envelope will be violated. This means the lower-level controller will be requested to track infeasible set points due to neglecting the uncertainty in the optimization problem. On the other hand, the scenario-based method, as can be seen from subplots (b) and (c) in Fig. 5, successfully satisfies all the constraints for all realization of the uncertainty within the considered uncertainty range. Two important points should be noted. First, like any other robust method, the scenario-based method is not able to cope with uncertainty beyond the considered range of uncertainty. Second, the capability of compensation for uncertainty is not free. The price that should be paid to gain this robustness is sacrificing optimality to some extent. In this sense, the sacrifice means that the optimizer decides to produce less than the maximum allowed production, shown in a thick red line in subplot (b), to ensure that the upper bound of constraint will be respected for all uncertainty realizations. It should be noted that the execution times for both cases, as presented in Table 6, are in the order of seconds, which means using the steady-state model allowed the computations to be executed safely within the sampling time (six hours). Hence, the solution can be implemented easily.

V. VARIOUS FORMS OF UNCERTAINTY

Using scenario-based optimization with the steady-state version of the model for prediction provides the possibility to consider different types of uncertainty in the optimization problem. Consequently, this section investigates how uncertainty in oil price and well characteristics affects daily production optimization problems.

A. UNCERTAINTY IN OIL PRICE

Two simulation cases are proposed to study the effect of uncertainty on the oil price. In the first case, the optimization problem defined in (24) is solved and applied to a plant considering the oil price is constant at 75 [$/bbl], as presented in Table 5. For the second simulation case, the oil price is assumed to fall drastically from almost 110 [$/bbl] to 60 [$/bbl] as shown in subplot (f) in Fig. 6. In this case, the average of maximum and minimum oil prices shown by the black line (real price) in subplot (f) is considered to calculate the objective function.

The simulation results for both cases are plotted in Fig. 6. The optimal frequency of the pumps for both constant and varying scenarios are demonstrated in subplots (a) and (b), respectively. It can be seen that despite the difference between oil prices, the optimal frequencies for the two cases are the same. As a result, the total produced fluid for both cases

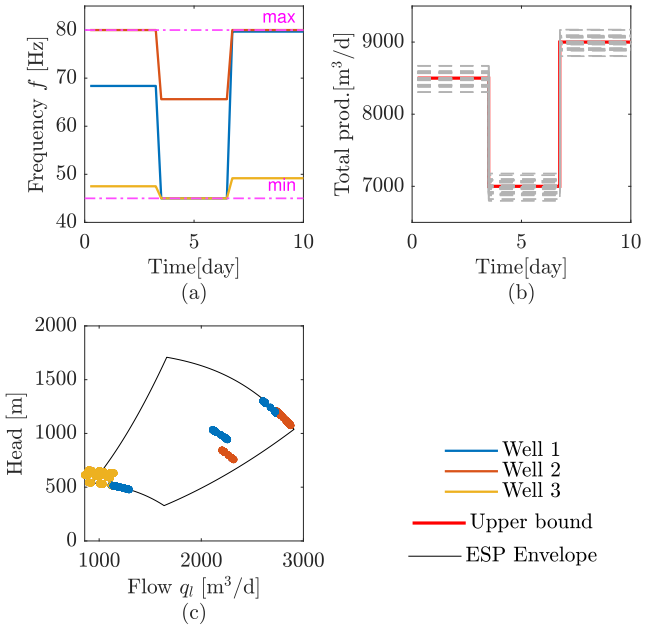

FIGURE 4. Deterministic DPO based on nominal values of the parameters applied to the uncertain model: (a) Pump frequency, (b) Total produced fluid, (c) ESP operating envelope.

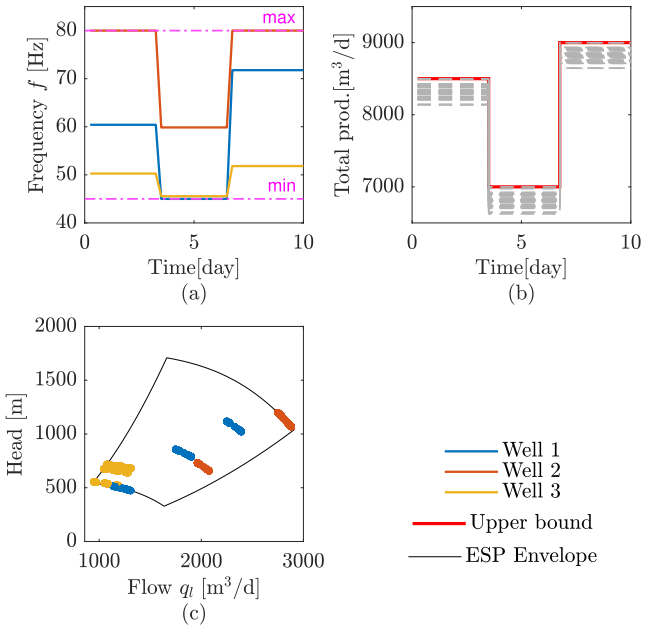

FIGURE 5. Scenario-based DPO based on scenario tree applied to the uncertain model: (a) Pump frequency, (b) Total produced fluid, (c) ESP operating envelope.

is the same, as presented in subplot(c), together with the separator capacity for handling the production in a solid red line. However, the absolute values of the objective functions, as depicted in subplot (e), are different due to the difference between oil prices in the two cases. This implies that the optimal solution for both cases is identical. In other words, although the absolute values of the objective functions are different, the uncertainty in oil price does not influence the optimal solution itself. Hence, the uncertainty in oil price

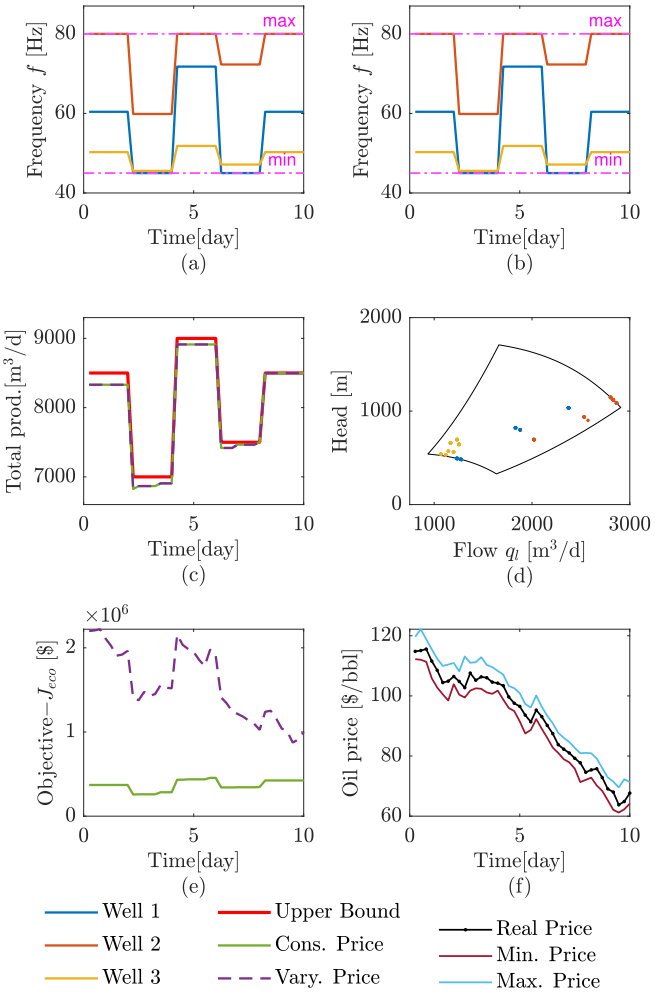

FIGURE 6. Scenario-based DPO based on constant and varying oil price: (a) Pump frequency for constant oil price case, (b) Pump frequency for varying oil price case, (c) Total produced fluid for both cases, (d) ESP operating envelope for both cases, (e) Negative value of the objective functions for both cases, (f) Variation of the oil price for the varying price case.

does not affect the short-term optimization from ESP lifted field.

Another case study is conducted where the oil price drops even more to almost 20 [$/bbl] to demonstrate that the economic optimizer works appropriately. The simulation result is presented in Fig. 7. Subplot (b) clearly shows that in the beginning, the optimizer tries to produce as much as possible while respecting the upper bound of the production constraint. However, after 7.75 days, it decides to decrease the production rate. The reason can be explained by taking a closer look at the negative value of the objective function and the oil price in subplots (c) and (d). It can be seen that after 7.75 days, when the oil price drops approximately from 37 [$/bbl] to 34 [$/bbl], the objective function changes sign. In other words, production from the field is not profitable anymore. As a result, the optimizer decides to set the frequency of all pumps to the minimum value, as shown in subplot (a), to decrease production and financial loss.

Furthermore, it is important to mention that the execution times for all cases, as shown in Table 6, are in the range of

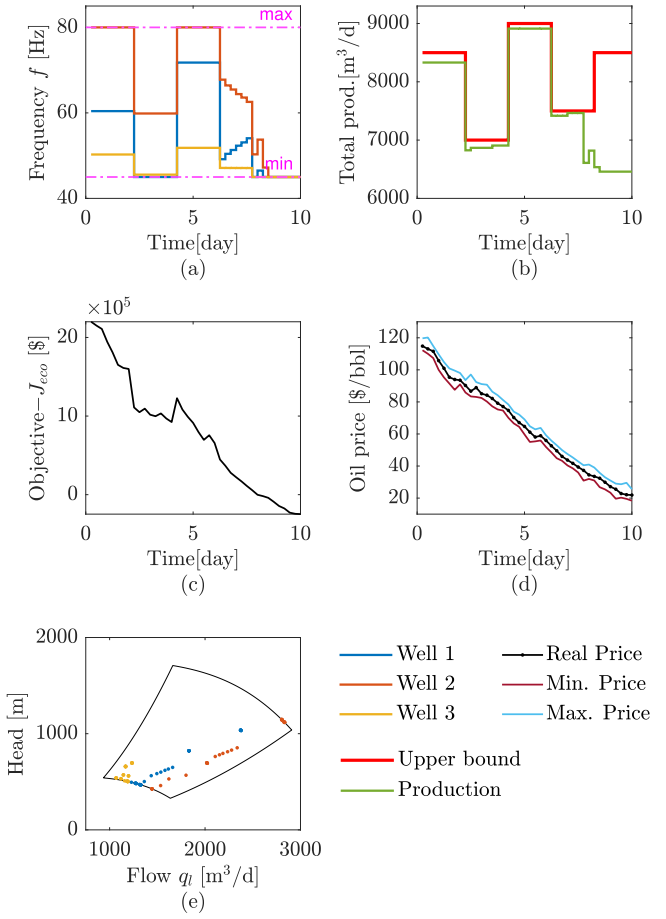

FIGURE 7. Scenario-based DPO for significantly low oil price: (a) Pump frequency, (b) Total produced fluid and maximum allowed production, (c) Negative value of the objective function, (d) Variation of the oil price, (e) ESP operating envelope.

seconds, and implementing the solution should be straightforward.

B. UNCERTAINTY IN WELL CHARACTERISTICS

An additional prospect worth exploring is how the variation in uncertainty range can be exploited to decrease the conservativeness of the method. To illustrate it more, consider a single bounded slightly varying uncertain parameter over the prediction horizon as shown in Fig. 8. The idea is to exploit the fact that uncertainty grows in the future to decrease the conservativeness of the method. In other words, although the uncertain parameter can take an extreme value in the future, this extreme value necessarily does not occur at the moment. This is the case, especially for the daily production optimization of an ESP network. For example, the uncertainty in the water cut of oil well over the prediction horizon with a length of 2 days and a sampling time of 6 hours. The water cut may increase or decrease by 50% over the course of two days; however, this change may not occur at once. Therefore it makes sense to assume that uncertainty during the next six hours is limited to ±15% of nominal value, and it increases gradually to ±50%.

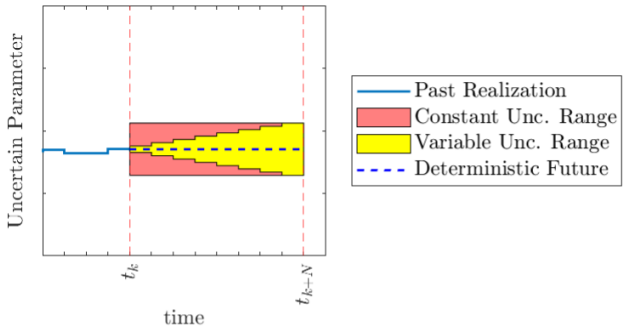

FIGURE 8. Schematic illustration of the constant and varying range of uncertainty for an uncertain parameter over the prediction horizon.

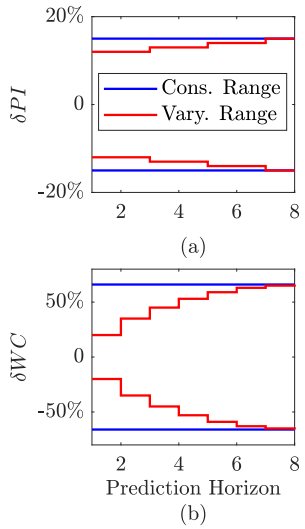

FIGURE 9. The constant and varying range of the uncertainty considered for all the wells: (a) Productivity index, (b) Water cut.

TABLE 6. Execution time of different simulation cases.

Simulation case	mean [s]	max [s]	Corresponding Fig.
Deterministic MPC	0.0122	0.0278	Fig. 4
Multistage MPC	1.0494	2.0635	Fig. 5
Varying price scenario	1.0026	1.8021	Fig. 6
Constant price scenario	0.8918	1.5027	Fig. 6
Low price scenario	1.3749	2.3056	Fig. 7
Constant uncertainty range	0.9805	1.9656	Fig. 10
Varying uncertainty range	1.1156	2.0350	Fig. 10

Two simulation cases have been considered to demonstrate the concept. In the first case, namely the constant range scenario, there is a constant ±15% and ±65% uncertainty in the productivity index and water cut of all wells, respectively, throughout the prediction horizon. However, in the varying range scenario, as shown in Fig. 9, it has been assumed that the uncertainty in the productivity index grows gradually from ±12% to ±15% and uncertainty in the water cut grows gradually from ±20% to ±65%. The simulation result for two cases is presented in Fig. 10. For both cases, the pump frequency of the three pumps is demonstrated in subplots (a), (b), and (c), respectively. It can be seen from subplot (d) that the difference between frequencies resulted in a higher production rate for the varying range scenario, which is

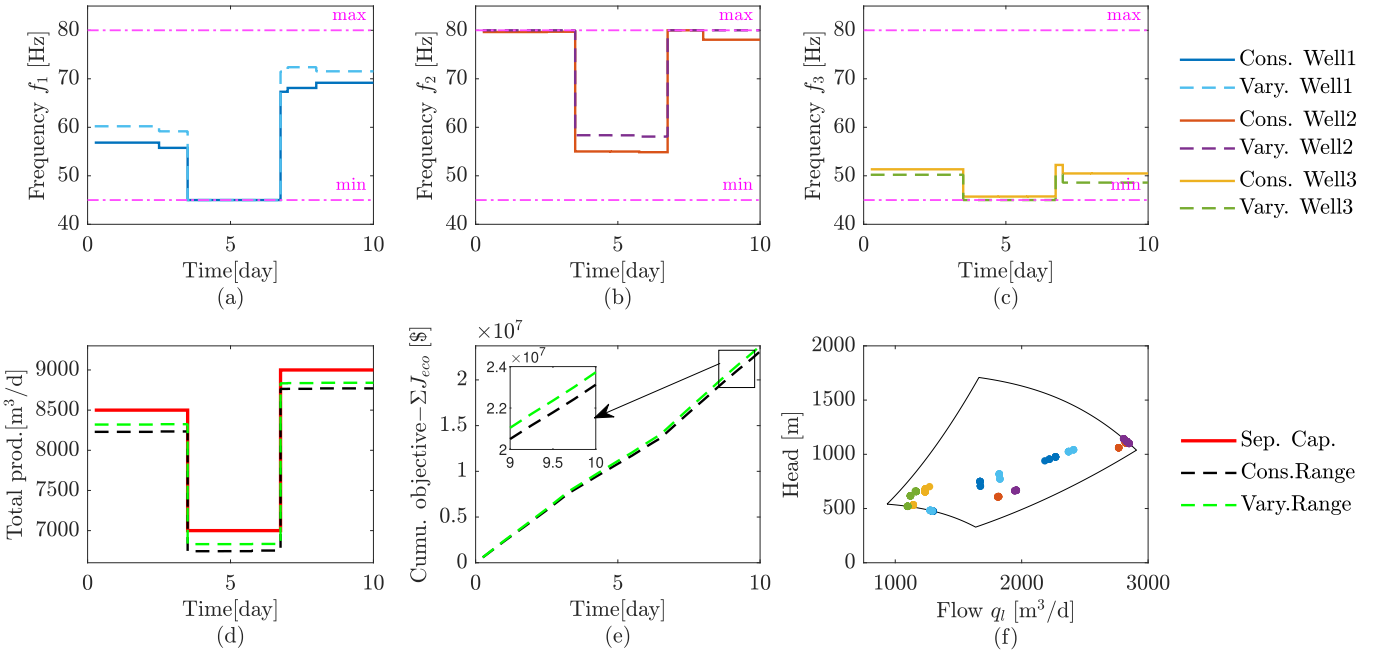

FIGURE 10. Scenario-based DPO based on the constant and varying range of uncertainty in the well parameters: (a) Pump frequency of ESP1, (b) Pump frequency of ESP2, (c) Pump frequency of ESP3, (d) Total produced fluid, (e) Negative value of the cumulative objective function, (f) ESP operating envelope for both cases.

equivalent to a 2.58% increase in the cumulative objective function, as shown in subplot (e). Additionally, as presented in Table 6, the execution times are not more than two seconds, which means the solution is implementable.

VI. CONCLUSION

This paper exploited the scenario-based optimization method to address the Daily Production Optimization for an ESP lifted oil field under parametric uncertainty. It was shown that using a steady-state model in the context of DPO for an ESP lifted oil field is tractable and has a huge potential to be used in a real oil field.

The accomplishment of the proposed method and the necessity of considering uncertainty is demonstrated by a comparison between the deterministic optimization based on a nominal model and the scenario-based optimization applied to a plant containing uncertainty. It has been shown that scenario-based optimization for DPO yields a robust solution, and safe operation of the ESP pump as well as robust satisfaction of the operational constraints, are guaranteed.

The potentials provided by representing the uncertainty with a scenario tree were exploited to investigate the different forms of uncertainty. It has been shown that the uncertainty in the oil price does not affect the short-term optimal production, at least during the normal operation of the market. Additionally, it has been demonstrated that for the DPO solution to be affected by the oil price, there has to be an extremely low price for the oil, which is not impossible but relatively rare during normal operation. Nevertheless, if such a rare occasion occurs, DPO can handle the situation by minimizing production from the field. This implies an intuitive and yet interesting conclusion, that is, the economic objective would be translated to achieving either maximum or minimum production, depending on whether the production is profitable or not.

On the other hand, the investigation on the range of considered uncertainty in well flow parameters revealed that contrary to the oil price, the uncertainty related to the well characteristics is significantly important, and the net profit from a field can be increased by reducing the uncertainty in well flow parameters. This observation can be easily explained by considering that during the regular operation of a lucrative business such as oil production, the economic objective is typically equivalent to maximizing the total production from the field. Consequently, the daily production optimization seeks to allocate this total production among the different wells in a way that maximizes the proportion of the oil to water in the total produced fluid, which is a direct outcome of the well parameters.

In summary, this research yields two key findings. Firstly, utilizing scenario-based optimization effectively manages uncertainty in daily production optimization. This is crucial because deviating from optimal pump operation reduces their lifespan and entails costly repairs. Secondly, while price uncertainty can be disregarded in short-term optimization, it is vital to account for uncertainties in well characteristics.

Although this paper discusses several useful outcomes of the proposed method, there are potential opportunities for further improvement yet to be explored. First, the dynamic measurements that are being obtained continuously in a real-time application can be used together with estimation algorithms to truncate the range of uncertainty and potentially

improve the method in terms of conservatives. Second, the method can be extended using Mixed Integer Optimization, which makes it possible to shut down the wells, if it is necessary, in a more complex network with more oil wells.

REFERENCES

[1] D. Krishnamoorthy, K. Fjalestad, and S. Skogestad, "Optimal operation of oil and gas production using simple feedback control structures," *Control Eng. Pract.*, vol. 91, Oct. 2019, Art. no. 104107, doi: 10.1016/j.conengprac.2019.104107.

[2] B. Stenhouse, M. Woodman, and P. Griffiths, "Model based operational support—Adding assurance to operational decision making," presented at the SPE Intell. Energy Conf. Exhib., Mar. 2010, Paper no. SPE-128694-MS, doi: 10.2118/128694-MS.

[3] A. F. Teixeira, M. C. M. M. de Campos, F. P. Barreto, A. S. Stender, F. F. Arraes, and V. R. Rosa, "Model based production optimization applied to offshore fields," presented at the OTC Brasil, Rio de Janeiro, Brazil, Oct. 2013, Paper no. OTC-24301-MS, doi: 10.4043/24301-MS.

[4] B. Foss, B. R. Knudsen, and B. Grimstad, "Petroleum production optimization—A static or dynamic problem?" *Comput. Chem. Eng.*, vol. 114, pp. 245–253, Jun. 2018, doi: 10.1016/j.compchemeng.2017.10.009.

[5] A. Pavlov, D. Krishnamoorthy, K. Fjalestad, E. Aske, and M. Fredriksen, "Modelling and model predictive control of oil wells with electric submersible pumps," in *Proc. IEEE Conf. Control Appl. (CCA)*, Juan Les Antibes, France, Oct. 2014, pp. 586–592.

[6] B. J. T. Binder, D. K. M. Kufoalor, A. Pavlov, and T. A. Johansen, "Embedded model predictive control for an electric submersible pump on a programmable logic controller," in *Proc. IEEE Conf. Control Appl. (CCA)*, Juan Les Antibes, France, Oct. 2014, pp. 579–585.

[7] B. J. T. Binder, A. Pavlov, and T. A. Johansen, "Estimation of flow rate and viscosity in a well with an Electric Submersible Pump using Moving Horizon Estimation," *IFAC-PapersOnLine*, vol. 48, no. 6, pp. 140–146, Jul. 2015, doi: 10.1016/j.ifacol.2015.08.022.

[8] R. Sharma and B. Glemmestad, "Modeling and simulation of an electric submersible pump lifted oil field," *Int. J. Petroleum Sci. Technol.*, vol. 8, no. 1, pp. 39–68, 2014.

[9] R. Sharma and B. Glemmestad, "Optimal control strategies with nonlinear optimization for an electric submersible pump lifted oil field," *Model., Identificat. Control*, vol. 34, no. 2, pp. 55–67, 2013, doi: 10.4173/mic.2013.2.2.

[10] R. Sharma and S. Glemmestad, "Mixed integer nonlinear optimization for ESP lifted oil field and improved operation through production valve choking," *Int. J. Model. Optim.*, vol. 4, no. 6, pp. 465–475, Dec. 2014, doi: 10.7763/IJMO.2014.V4.419.

[11] R. Sharma and B. Glemmestad, "Nonlinear model predictive control for optimal operation of electric submersible pump lifted oil field," in *Proc. Model., Identificat. Control*, Innsbruck, Austria, 2014, pp. 229–236.

[12] D. Krishnamoorthy, E. M. Bergheim, A. Pavlov, M. Fredriksen, and K. Fjalestad, "Modelling and robustness analysis of model predictive control for electrical submersible pump lifted heavy oil wells," *IFAC-PapersOnLine*, vol. 49, no. 7, pp. 544–549, 2016, doi: 10.1016/j.ifacol.2016.07.399.

[13] P. D. A. Delou, J. P. A. de Azevedo, D. Krishnamoorthy, M. B. de Souza, and A. R. Secchi, "Model predictive control with adaptive strategy applied to an Electric Submersible Pump in a subsea environment," *IFAC-PapersOnLine*, vol. 52, no. 1, pp. 784–789, 2019, doi: 10.1016/j.ifacol.2019.06.157.

[14] B. A. Santana, R. M. Fontes, L. Schnitman, and M. A. F. Martins, "An adaptive infinite horizon model predictive control strategy applied to an ESP-lifted oil well system," *IFAC-PapersOnLine*, vol. 54, no. 3, pp. 176–181, 2021, doi: 10.1016/j.ifacol.2021.08.238.

[15] B. J. T. Binder, T. A. Johansen, and L. Imsland, "Improved predictions from measured disturbances in linear model predictive control," *J. Process Control*, vol. 75, pp. 86–106, Mar. 2019, doi: 10.1016/j.jprocont.2019.01.007.

[16] E. A. Costa, O. S. L. D. Abreu, T. D. O. Silva, M. P. Ribeiro, and L. Schnitman, "A Bayesian approach to the dynamic modeling of ESP-lifted oil well systems: An experimental validation on an ESP prototype," *J. Petroleum Sci. Eng.*, vol. 205, Oct. 2021, Art. no. 108880, doi: 10.1016/j.petrol.2021.108880.

[17] R. M. Fontes, D. D. Santana, and M. A. F. Martins, "An MPC autotuning framework for tracking economic goals of an ESP-lifted oil well," *J. Petroleum Sci. Eng.*, vol. 217, Oct. 2022, Art. no. 110867, doi: 10.1016/j.petrol.2022.110867.

[18] J. P. Jordanou, I. Osnes, S. B. Hernes, E. Camponogara, E. A. Antonelo, and L. Imsland, "Nonlinear model predictive control of electrical submersible pumps based on echo state networks," *Adv. Eng. Informat.*, vol. 52, Apr. 2022, Art. no. 101553, doi: 10.1016/j.aei.2022.101553.

[19] N. Janatian, K. Jayamanne, and R. Sharma, "Model based control and analysis of gas lifted oil field for optimal operation," in *Proc. 1st SIMS EUROSIM Conf. Model. Simulation*, Mar. 2022, pp. 241–246.

[20] N. Janatian and R. Sharma, "Multi-stage scenario-based MPC for short term oil production optimization under the presence of uncertainty," *J. Process Control*, vol. 118, pp. 95–105, Oct. 2022, doi: 10.1016/j.jprocont.2022.08.012.

[21] S. Lucia, T. Finkler, and S. Engell, "Multi-stage nonlinear model predictive control applied to a semi-batch polymerization reactor under uncertainty," *J. Process Control*, vol. 23, no. 9, pp. 1306–1319, Oct. 2013, doi: 10.1016/j.jprocont.2013.08.008.

[22] M. A. Nasab, M. Zand, S. Padmanaban, M. S. Bhaskar, and J. M. Guerrero, "An efficient, robust optimization model for the unit commitment considering renewable uncertainty and pumped-storage hydropower," *Comput. Electr. Eng.*, vol. 100, May 2022, Art. no. 107846, doi: 10.1016/j.compeleceng.2022.107846.

[23] D. Krishnamoorthy, B. Foss, and S. Skogestad, "Real-time optimization under uncertainty applied to a gas lifted well network," *Processes*, vol. 4, no. 4, p. 52, Dec. 2016, doi: 10.3390/pr4040052.

[24] N. Janatian, and R. Sharma, "A robust model predictive control with constraint modification for gas lift allocation optimization," *J. Process Control*, vol. 128, Aug. 2023, Art. no. 102996, doi: 10.1016/j.jprocont.2023.102996.

[25] G. Takacs, *Electrical Submersible Pumps Manual: Design, Operations, and Maintenance* Cambridge, MA, USA: Gulf, 2017, pp. 11–52.

[26] T. Serghides, "Estimate friction factor accurately," *Chem. Eng. J.*, vol. 91, no. 5, pp. 63–64, 1984.

NIMA JANATIAN received the B.S. and M.S. degrees in mechanical engineering from the Amirkabir University of Technology, Tehran, in 2013 and 2016, respectively. He is currently pursuing the Ph.D. degree in process energy and automation engineering with the University of South-Eastern Norway, Porsgrunn. His research interests include advanced model-based control, robust model predictive control, and real-time optimization under uncertainty with application to energy systems.

ROSHAN SHARMA received the B.S. degree in engineering from Tribhuvan University, Kirtipur, in 2007, and the M.S. degree in systems and control engineering and the Ph.D. degree in process, energy and automation engineering from the Telemark University College, Norway, in 2011 and 2014, respectively. After about two years of academic experience as an assistant lecturer, he received his M.S. and Ph.D. degrees. He is currently an Associate Professor with the University of South-Eastern Norway, Porsgrunn. His research interests include advanced process control and optimization.

Paper F
Investigating the performance of robust daily production optimization against a combined well–reservoir model

Submitted to *Modeling, Identification and Control*, October 2023.
Authors: Nima Janatian, Stein Krogstad, and Roshan Sharma.
Authors' roles in the article:
Nima Janatian: Main ideas, implementation, and writing.
Stein Krogstad: Discussions, comments, and proofreading.
Roshan Sharma (Supervisor): Discussions, comments, and proofreading.

Investigating the Performance of Robust Daily Production Optimization Against a Combined Well–Reservoir Model

Nima Janatian[a,*], Stein Krogstad[b], Roshan Sharma[a]

[a]Department of Electrical Engineering, Information Technology and Cybernetics, University of South-Eastern Norway, Porsgrunn, Norway
[b]Department of Mathematics and Cybernetics, SINTEF Digital, Oslo, Norway

Abstract

This paper presents a scenario-based optimization framework applied to Daily Production Optimization (DPO) for an Electric Submersible Pump lifted oil field under parametric uncertainty. The study also develops a simplified combined well–reservoir model, which is used solely to assess the performance of the methods in a more realistic setting. The combined model consists of the steady-state model of wells combined with the reservoir model through bottom hole pressure and well flow. Moreover, it successfully represents the change in uncertain parameters based on reservoir dynamics rather than random variations. The superiority of scenario-based DPO and the importance of considering uncertainty are demonstrated through extensive comparisons between deterministic and robust methods. The comparisons show that the deterministic DPO fails to satisfy output constraints, leading to violations, particularly in wellhead pressure. Conversely, the scenario-based DPO exhibits significant potential for real oil field application, effectively respecting all input and output constraints. Nevertheless, this safety comes at the cost of sacrificing net profit to some extent. The research emphasizes the importance of considering uncertainty in DPO for oil field operations, providing valuable insights for achieving robustness and operational safety.

Keywords: ESP Lifted Oil Well, Scenario-based Robust Optimization, Constrained Optimization under Uncertainty, The MATLAB Reservoir Simulation Toolbox (MRST), Coupled Well–Reservoir Model

1. Introduction

Decisions made at various time scales have a significant impact on the cost and revenue of an oil and gas production unit. Depending on the goals, these decisions can span from immediate choices made in seconds to long-term plans encompassing the entire lifespan of the field. Daily Production Optimization (DPO), also known as Real-Time Optimization (RTO) in the context of process systems, corresponds to the

*Corresponding author
Email addresses: nima.janatianghadikolaei@usn.no (Nima Janatian), stein.krogstad@sintef.no (Stein Krogstad), roshan.sharma@usn.no (Roshan Sharma)

decisions and plans that are taken within a timeframe ranging from a few hours to a couple of days to maximize the daily operating revenue from the production unit. Typical decisions in this area involve selecting the choke opening of the different wells or allocating shared resources such as available electric power and lift gas. These decisions aim to maximize the daily operational profit while simultaneously ensuring the fulfillment of process and operating constraints [1]. Studies have reported the advantageous impact of daily production optimization, resulting in an increase in production within the range of 1-4% [2, 3]. These improvements are even more pronounced for fields in the late plateau and decline phases than earlier phases [4]. On the other hand, it is widely acknowledged that real-life implementations of constrained optimization may be jeopardized by the presence of uncertainty as the mismatch introduced due to uncertainty may potentially lead to constraint violation and make an optimal solution practically infeasible [5, 6]. Thus, this paper aims to extend the current boundaries of daily production optimization under uncertainty one step further by investigating the daily production optimization problem for an Electric Submersible Pump (ESP) lifted oil field under the presence of uncertainty to bring it closer to practical implementation in real-world scenarios.

Mathematical modeling of a single ESP oil well was proposed in [7]. Furthermore, a linear model predictive control (MPC) was designed in the Statoil Estimation and Prediction Tool for Identification and Control (SEPTIC) based on the step response model of the process, which was later implemented on a Programmable Logic Controller (PLC) in [8]. It was shown in [9] that the linear model of an ESP lifted well varies significantly depending on the choke opening. Therefore, a model adaptation based on the homotopic transition between models was proposed in [10], where an adaptive linear MPC strategy was implemented as a Quadratic Dynamic Matrix Control (QDMC) algorithm in order to control the pump inlet pressure, minimizing the pump power and respecting the variable's constraints. An adaptive infinite horizon MPC strategy was also implemented in [11], where the proposed control law used successive linearization of the dynamic model of ESP to update the model internally. The ESP model was used in [12] to investigate the implementation aspects of measured disturbances in MPC. The main control objective in this work was to sustain a given production rate from the well while maintaining acceptable operating conditions for the pump. Recently, an Echo State Neural Network was trained in [13] to capture the dynamic model of ESP well. The trained neural network was used for two nonlinear model predictive controllers that aimed to track the bottom-hole pressure subject to constraints on control inputs, bottom-hole and well-head pressures, and liquid flows. Nevertheless, the control presented in the aforementioned studies aimed to track a certain set point (mostly bottom-hole pressure). This type of objective corresponds to the lower layer (Control and Automation layer as described in [14]) in the multilevel control hierarchy, where the set points are determined by the higher level called Production Optimization to be tracked. Therefore, none of these works have answered the principal question of DPO, which is: What is the optimal production allocation from each well to maximize the overall economic objective?

A similar first principle model was developed in [15] for multiple ESP wells that share a common production manifold. The steady-state version of this model was used in [16] to develop a nonlinear optimization based on Sequential Quadratic Programming (SQP) for two optimal control strategies. The same model was used later in [17] to calculate and identify the number of oil wells that should be used for special cases with low production demand by formulating a Mixed Integer Nonlinear Programming problem (MINLP).

The dynamic version of the model was also exploited in [18], where the nonlinear model predictive control framework was implemented as an economic optimizer for maximizing profit. Despite assuming constant controls throughout the prediction horizon, the length of the prediction horizon was restricted to one second due to the fast dynamics of ESP and the significant computational expenses associated with a longer prediction horizon. Furthermore, the uncertainty was neglected, while it is well known that the uncertainty in the parameters can make the optimal solution practically infeasible due to the mismatch between the prediction model and the real process [19].

In spite of the numerous studies on daily production optimization, such as [20, 21, 22, 23, 24] to name a few, the uncertainty has rarely been taken into account in the optimization problem explicitly. Therefore this paper aims to fill this knowledge gap by extending our previous research work presented in [25] by incorporating a more sophisticated representation of the actual plant in order to facilitate the implementation of the method in real-life application. To accomplish this objective, the scenario-based optimization framework has been used in this paper for robust optimization under uncertainty. The Principal aspect of the method involves incorporating a scenario tree to represent finite realizations of uncertainty. The method was integrated into a nonlinear model predictive control scheme in [26] for dynamic optimization of semi-batch polymerization reactor under uncertainty. It was also used in the domain of oil production to optimally allocate a limited amount of available lift gas between multiple wells in a gas-lifted oil field [27, 28]. However, using the dynamic model of ESP for DPO becomes problematic since the fast dynamics of the pumps require a short sampling time, and the number of decision variables over a relatively long horizon, such as in DPO, becomes intractable. Accordingly, the piecewise steady operation of the plant is assumed throughout the prediction horizon. More specifically, the prediction horizon of DPO is divided into segments, and the plant is considered to operate at a possibly new steady state over each segment. Therefore, the steady-state model of the plant is used as the prediction model to determine the future of the system over each segment. The authenticity of this assumption is discussed thoroughly in [4, 25], which state that successive static optimization suffices in most relevant DPO cases and the ESP system is sufficiently fast that the transition between steady states is negligible and can be disregarded. As a result, the daily production optimization is formulated as successive scenario-based optimization problems in a receding horizon fashion to address the constraint fulfillment under the presence of uncertainty. In other words, only the first optimal decision is implemented in the plant, and the whole optimization process will be repeated at each time step.

Although both the current and previous work in [25] make use of a simple linear well flow model with productivity index and water cut in the optimization problem, the distinction between the two works lies in the inclusion of a more advanced plant model in this work to accurately portray the actual process. To this end, a reservoir model is coupled in a simple and efficient way to represent the real process. Particularly, instead of testing the optimization algorithm against the same linear model with different parameters, a coupled well-reservoir model is tailored to evaluate the performance of the optimization algorithm. Thus, this work contributes to two major aspects:

- First, incorporating the explicit notion of uncertainty in DPO as a short-term production optimization.
- Second, investigating the performance of the method against a more sophisticated

representation of the real process.

The rest of the paper is organized as follows. Section 2 describes the process, including the mathematical modeling of the ESP oil wells and the coupled well–reservoir model. The problem formulations for both standard deterministic DPO and robust scenario-based DPO are presented in Section 3. The considered case study and the simulation setup are presented in Section 4. The simulation results are presented and discussed in Section 5 before concluding in Section 6.

2. Process Description

2.1. ESP Lifting Method

ESP lifting method is an ideal artificial lifting method for producing substantial quantities of dense and viscous hydrocarbons [29]. In this method, an electrical submersible multistage centrifugal pump is installed at the bottom of the wellbore [15] to produce the required pressure gradient for bringing the fluid to the surface. A schematic diagram of ESP lifted production unit with three oil wells is presented in Figure 1. Each well, as demonstrated in Figure 1, is equipped with a separate ESP unit at the bottom hole and a production chock valve at the wellhead. During normal operation, the volumetric production rate of individual wells can be regulated by adjusting the pump speed, as it is more beneficial to maintain the production choke valves in a fully open position. Eventually, the oil produced from each well is routed through the top-side network toward the separator for further processing.

Simple mechanistic models of ESP-lifted oil wells are developed in [7, 15] for optimization and control purposes. Both models are derived by applying the mass and momentum balance principles to the pipelines. This paper considered a similar mathematical model adopted from [15] with minor adjustments made to certain assumptions:

- Modeling the electrical motors subsystem is neglected due to the fast response of electrical systems.
- Water cuts of the wells are considered to be different to draw a meaningful optimization problem.
- Modeling the common production manifold and transportation lines are neglected, as it is elaborated upon below.

It is worth mentioning that the well model, in a nutshell, is nothing but a flow model through a pipe. And it is typically defined by two boundary pressures, namely the reservoir pressure on one end and the separator or manifold pressure on the other end. However, for the considered model in this paper, the top-side boundary pressure is discarded, and two boundary conditions are considered at the bottom hole, namely the boundary pressure (bottom hole pressure) and boundary flow (reservoir inflow). As a result, the production choke valve is excluded, and the top-side pressure (wellhead pressure) is treated as a free variable. The justification for this assumption is threefold:

- Firstly, the well model is going to be coupled with the reservoir model through the flow and pressure at the bottom hole; therefore, specifying a boundary pressure at the top side of the well model results in an overdetermined subsystem.

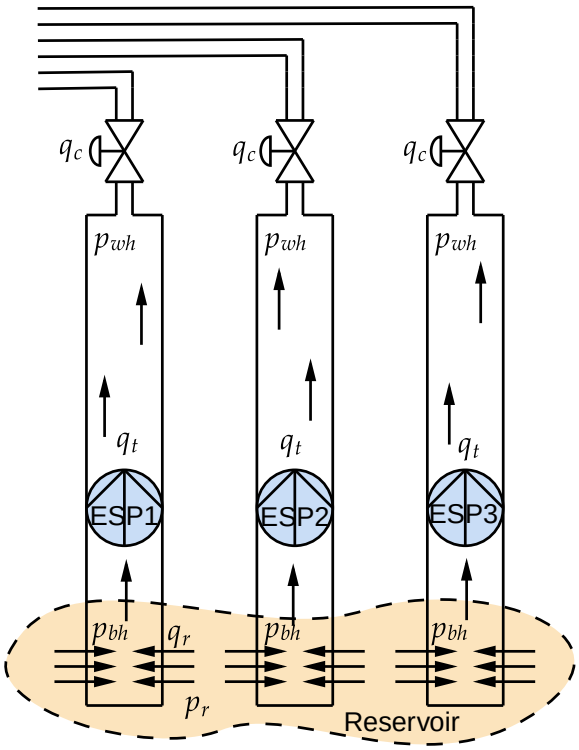

Figure 1: Schematic diagram of three ESP lifted oil wells.

- Secondly, the main objective of this paper is to find the optimal production from each well that maximizes the total economic profit, and routing the produced fluid through the top-side network toward the separator falls out of the scope of this paper. Accordingly, putting constraints on the wellhead pressure is sufficient to address the top-side operational constraint in this work.
- Finally, although a more sophisticated coupling between the well model and reservoir model could be possible, it requires solving both the reservoir and well model simultaneously. This is computationally expensive and makes the optimization problem intractable.

2.2. Governing Equations

This section only briefly presents the governing equations of the process since modeling is not the main focus and contribution of this work. However, the readers are referred to [15] for a more detailed explanation of the modeling.

The process is described by three states for each well, namely, the pressure at the bottom hole p^i_{bh}, the pressure at the wellhead p^i_{wh}, and the average volumetric flow rate of the well q^i_t, where the superscript i refers to the i^{th} oil well. The corresponding differential equations are given by:

$$\dot{p}^i_{bh} = \frac{\beta}{V^i}\left[q^i_r - q^i_t\right] \tag{1a}$$

$$\dot{p}^i_{wh} = \frac{\beta}{V^i}\left[q^i_t - q^i_c\right] \tag{1b}$$

$$\dot{q}^i_t = \frac{A^i}{\rho^i_l L^i}\left[p^i_{bh} - p^i_{wh} + \rho^i_l g H^i_{esp} - \rho^i_l g L^i - \Delta p^i_f\right] \tag{1c}$$

The steady-state equations of the model can simply be determined by setting the right-hand side of differential equations (1) to zero.

$$q^i_r - q^i_t = 0 \tag{2a}$$

$$q^i_t - q^i_c = 0 \tag{2b}$$

$$p^i_{bh} - p^i_{wh} + \rho^i_l g H^i_{esp}(q^i_t, f^i) - \rho^i_l g L^i - \Delta p^i_f = 0 \tag{2c}$$

And the set of algebraic equations is given by:

$$q^i_r = PI^i\left(p_r - p^i_{bh}\right) \tag{3}$$

$$\Delta p^i_f = \frac{f_D L \rho \upsilon^2}{2D_h} \tag{4}$$

$$H^i_{esp} = \bar{c}_0(\frac{f}{f_0})^2 + \bar{c}_1(\frac{f}{f_0})q^i_t + \bar{c}_2 q^{i2}_t + \bar{c}_3(\frac{f_0}{f})q^{i3}_t \tag{5}$$

$$BHP^i_{esp} = \hat{c}_0(\frac{f}{f_0})^3 + \hat{c}_1(\frac{f}{f_0})^2 q^i_t + \hat{c}_2(\frac{f}{f_0})q^{i2}_t + \hat{c}_3 q^{i3}_t + \hat{c}_4(\frac{f_0}{f})q^{i4}_t \tag{6}$$

$$\rho^i_l = WC^i\rho_w + (1 - WC^i)\rho_o \tag{7}$$

$$q^i_o = (1 - WC^i)q^i_t \tag{8}$$

$$q^i_w = WC^i q^i_t \tag{9}$$

All the algebraic variables of the model are introduced in Table 1. The Darcy friction factor f_D in equation (4) can be evaluated using Serghides' explicit approximation to Colebrook-White equation [30]. The polynomial coefficients of ESP in equations (5) and (6) are also presented in Table 2 and all the numerical values of the parameters are presented in Table 3.

Note that the model is described by a set of algebraic equations presented in (2) to (9), which can be encapsulated in a compact form as:

$$\mathbf{F}(x, u, d) = \mathbf{0} \tag{10}$$

where $x \in \mathbb{R}^{10n_w}$ and $u \in \mathbb{R}^{2n_w}$ are the algebraic variables and system inputs, and $d \in \mathbb{R}^{2n_w}$ is the vector of the uncertain parameters of the process. n_w represents the number of wells, and bold typeface in (11) means the vector that encompasses that variable for all the wells.

$$x = \begin{bmatrix} \mathbf{p_{bh}} & \mathbf{p_{wh}} & \mathbf{q_r} & \mathbf{q_c} & \mathbf{q_o} & \mathbf{q_w} & \mathbf{H_{esp}} & \mathbf{BHP_{esp}} & \rho_\mathbf{l} & \mathbf{\Delta p_f} \end{bmatrix}^T \tag{11a}$$

$$u = \begin{bmatrix} \mathbf{f} & \mathbf{q_t} \end{bmatrix}^T \tag{11b}$$

$$d = \begin{bmatrix} \mathbf{PI} & \mathbf{WC} \end{bmatrix}^T \tag{11c}$$

Table 1: List of the algebraic variables and parameters.

Variable	Description
q_r	Volumetric flow rate from reservoir into well
q_t	Volumetric flow rate through well
q_c	Volumetric flow rate through production choke valve
p_{bh}	Bottom hole pressure
p_{wh}	Wellhead pressure
f	Frequency of ESP
H_{esp}	Head developed by ESP
BHP_{esp}	ESP brake horsepower
ρ_l	Density of the fluid in the well
Δp_f	Frictional pressure drop in the pipe
q_o	Volumetric flow rate of oil
q_w	Volumetric flow rate of water
PI	Productivity index
WC	Water cut

2.3. Well–Reservoir Coupling

The interactions between two main components of the coupled model, namely the reservoir and well models, are demonstrated in the block diagram presented in Figure 2. It can be seen that the ESP frequency and desired production rate are the input to the plant. The production rate is fed into the reservoir model as well controls, while the true response of the reservoir is utilized alongside the pump frequency in the well model

Table 2: Polynomial coefficients of ESP.

	$\bar{c}_0 \backslash \hat{c}_0$	$\bar{c}_1 \backslash \hat{c}_1$	$\bar{c}_2 \backslash \hat{c}_2$	$\bar{c}_3 \backslash \hat{c}_3$	$\bar{c}_4 \backslash \hat{c}_4$
H_{esp}	467.248	10.937	-0.212	7.649e-04	
BHP_{esp}	224.988	0.740	-6.884e-04	2.178e-06	-5.469e-09

Table 3: List of the parameters and their corresponding values.

Parameter	Value	Unit	Comments
L	2100	[m]	Length of well above ESP
D	0.1569	[m]	Diameter of all pipelines
A	0.0193	[m^2]	Cross section area of all pipelines
ρ_o	900	[kg/m^3]	Density of water
ρ_w	1000	[kg/m^3]	Density of oil
p_r	400	[bar]	Pressure of the reservoir
μ_o	100e-6	[m^2/s]	Kinematic viscosity of oil
μ_w	1e-6	[m^2/s]	Kinematic viscosity of pure water
f_0	60	[Hz]	ESP characteristics ref. freq.
$Q_{f_0,\min}$	161.591	[m^3/d]	ESP minimum flow at ref. freq.
$Q_{f_0,\max}$	395.252	[m^3/d]	ESP maximum flow at ref. freq.

to compute the other outputs such as wellhead pressure and head of the pump, etc. Employing this straightforward coupled model instead of a well model with synthetic varying parameters makes it possible to benefit from a more accurate representation of the plant by capturing the variation of uncertainty interactively in accordance with the dynamic of the reservoir and its history.

2.4. Uncertainty Description

Given the fact that the water cut and productivity index are computed at every sampling time, and their values at each sampling time are potentially different from their previous values at the previous sampling time, the uncertainty is inherently incorporated into the plant. However, a deviation of ±10% and ±20% from their actual values are added to them, respectively, as demonstrated in Figure 2, to represent the fact that the actual values of the uncertainties are unknown to the controller.

3. Problem Formulation

3.1. Standard Deterministic DPO

This section presents the standard deterministic optimization using the steady-state model over a finite prediction horizon. The plant is assumed to operate in a piecewise steady manner throughout the prediction horizon. This implies that the prediction horizon of DPO is divided into segments, and the plant is considered to operate at a possibly new steady state over each segment.

The primary objective is to adjust the decision variables, namely pump frequencies and inflow to the wells, in order to produce an optimal amount of fluid from each well

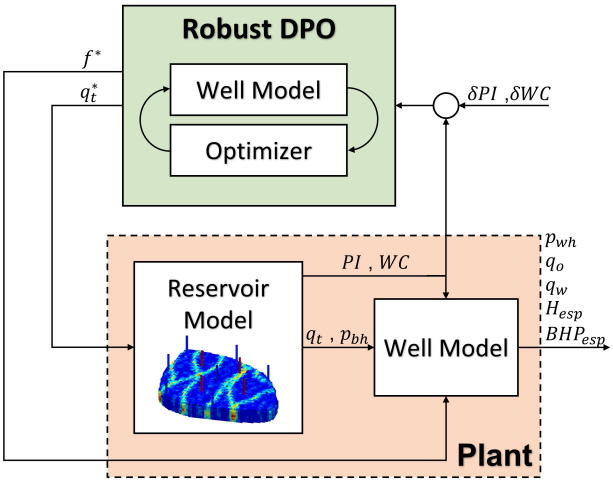

Figure 2: Block diagram of the coupled model and robust optimizer.

which maximizes the total profit from the production and takes into account all the operational constraints. Therefore, the economic objective function includes the total income from selling the produced oil with a negative sign to pose it as a minimization problem. Additionally, the costs associated with electric power consumption of the ESPs and water treatment are incorporated into the objective function. Hence, over the prediction horizon $\mathcal{K} = \{1, ..., N_p\}$ with the length N_p the objective function is given by:

$$J_{eco} = \sum_{k=1}^{N_p} \left(-c_o \sum_{i=1}^{n_w} q_o^{i,k} + c_e \sum_{i=1}^{n_w} BHP_{esp}^{i,k} + c_w \sum_{i=1}^{n_w} q_w^{i,k} \right) \tag{12}$$

where c_o, c_e, and c_w denote the price of oil and costs due to the use of electricity and water treatment, respectively.

The most important operational constraints in the problem arise from separator handling capacity and the ESP operating envelope, and the pressures. In particular, the magnitude of produced fluid (comprising both oil and water) should not exceed the separator capacity, and the ESP pumps need to be maintained within a safe operating window to avoid mechanical failure. Additionally, it is required to keep the bottom hole pressure and wellhead pressure within range to ensure the safe operation of the system.

Thus, the optimal control problem formulation over the prediction horizon is given by:

$$\min_{\mathrm{x,u}} \quad J_{eco}(\mathrm{x},\mathrm{u},\mathrm{d}) \tag{13a}$$

$$\text{s.t.} \quad \mathbf{F}(x_k, u_k, d_k) = \mathbf{0}, \qquad \forall k \in \mathcal{K} \tag{13b}$$

$$\sum_{i=1}^{n_w} q_t^{i,k} \leq Q_{\text{sep}}, \qquad \forall k \in \mathcal{K} \tag{13c}$$

$$Q_{\min}^{i,k} \leq q_t^{i,k} \leq Q_{\max}^{i,k}, \qquad \forall k \in \mathcal{K} \tag{13d}$$

$$p_{bh}^{\min} \leq p_{bh}^{i,k} \leq p_{bh}^{\max}, \qquad \forall k \in \mathcal{K} \tag{13e}$$

$$p_{wh}^{\min} \leq p_{wh}^{i,k} \leq p_{wh}^{\max}, \qquad \forall k \in \mathcal{K} \tag{13f}$$

$$f_{\min} \leq f^{i,k} \leq f_{\max}, \qquad \forall k \in \mathcal{K} \tag{13g}$$

The equality constraint in (13b) denotes the steady state of the system at each segment of the prediction horizon. The constraint on the total produced fluid is enforced in (13c), where Q_{sep} stands for the maximum handling capacity of the separator. The safe operation of the ESP pumps within the pump envelope is denoted in (13d) by maintaining the pump flow between the minimum and maximum allowed flow which is provided by the ESP manufacturer. The lower and upper bounds on bottom hole pressure and wellhead pressure are also implemented in (13e) and (13f), respectively. Finally, (13g) ensures the pump frequency is maintained within the range. The optimization problem should be solved in a receding horizon fashion, meaning only the first control action is implemented, and the optimization problem will be solved again at the next sampling time. It should also be noted that the parameters used in the control design are deviated (uncertain) parameters, as the exact values of the parameter are not known.

3.2. Robust Scenario-based DPO

According to the scenario-based optimization approach, the uncertainty region is discretized into a finite number of distinct possible realizations. These realizations are used to evaluate the system's future by employing a scenario tree. This implies that the future evolution of the plant is split into multiple branches, each representing a different trajectory based on the specific realization of the uncertainty that occurs in reality. Nonetheless, the drawback of the method is that the calculations may become intractable as the number of scenarios grows exponentially with the number of considered uncertainty and the length of the prediction horizon. Accordingly, the concept of robust horizon emerged to address this limitation. The robust horizon means the continuation of branching is limited to only a limited number of samples which is typically one or two sampling times ahead in time. The justification for a robust horizon lies in the fact that the corresponding control variables and state trajectories will be recalculated and refined in future sampling times; hence, the far future uncertainty does not need to be represented precisely.

In this paper, the scenario-based optimization method is employed, considering a total of $N_s = 2^6 + 1 = 65$ possible realizations or branches for uncertainties. These realizations encompass all combinations of the maximum and minimum values of the six uncertain parameters and the nominal case. The scenario tree, depicted in Figure 3, illustrates the branching structure with a robust horizon of $N_r = 1$. Each path from the root node to a

leaf node represents a scenario; hence the term "scenario-based optimization" is used to describe this method.

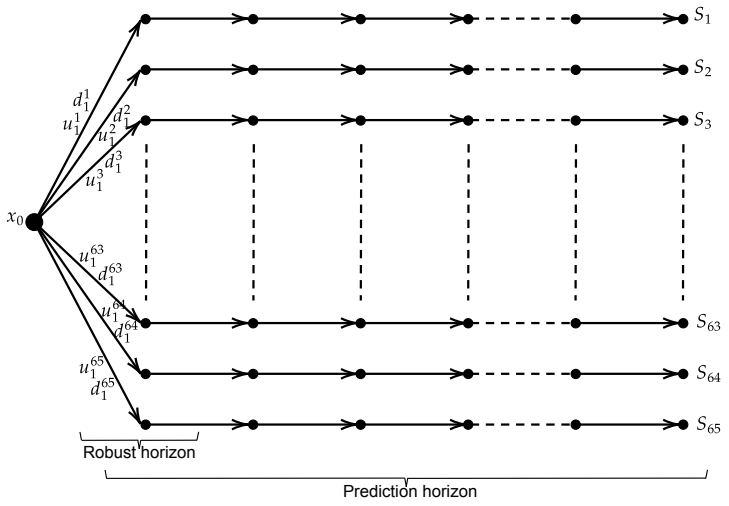

Figure 3: Scenario tree with $N_s = 65$ scenarios and robust horizon $N_r = 1$.

It is worthwhile to mention that this formulation imposes an extra constraint which is known as a non-anticipativity constraint. This constraint represents the fact that in real-time decision-making, the decision-maker is not able to anticipate the future realization of the uncertainty. Therefore, all the decisions that branch from a parent node are equal.

After defining the scenario tree and its prerequisites, the objective function for each scenario j can be computed as follows:

$$J_{eco}^{j} = \sum_{k=1}^{N_p} \left(-c_o \sum_{i=1}^{n_w} q_o^{i,j,k} + c_e \sum_{i=1}^{n_w} BHP_{esp}^{i,j,k} + c_w \sum_{i=1}^{n_w} q_w^{i,j,k} \right) \tag{14}$$

Accordingly, the optimization problem can be formulated over all the discrete scenarios of the scenario set $\mathcal{S} = \{1, ..., N_s\}$, throughout the prediction horizon $\mathcal{K} = \{1, ..., N_p\}$ as follows:

$$\min_{\mathrm{x,u}} \quad \sum_{j=1}^{N_s} \omega_j J_{eco}^j \tag{15a}$$

$$\text{s.t.} \quad \mathbf{F}\left(x_k^j, u_k^j, d_k^j\right) = \mathbf{0}, \qquad \forall k \in \mathcal{K}, \forall j \in \mathcal{S} \tag{15b}$$

$$\sum_{i=1}^{n_w} q_t^{i,j,k} \leq Q_{\text{sep}}^j, \qquad \forall k \in \mathcal{K}, \forall j \in \mathcal{S} \tag{15c}$$

$$Q_{\min}^{i,k} \leq q_t^{i,j,k} \leq Q_{\max}^{i,k}, \qquad \forall k \in \mathcal{K}, \forall j \in \mathcal{S} \tag{15d}$$

$$p_{bh}^{\min} \leq p_{bh}^{i,j,k} \leq p_{bh}^{\max}, \qquad \forall k \in \mathcal{K}, \forall j \in \mathcal{S} \tag{15e}$$

$$p_{wh}^{\min} \leq p_{wh}^{i,j,k} \leq p_{wh}^{\max}, \qquad \forall k \in \mathcal{K}, \forall j \in \mathcal{S} \tag{15f}$$

$$f_{\min} \leq f^{i,j,k} \leq f_{\max}, \qquad \forall k \in \mathcal{K}, \forall j \in \mathcal{S} \tag{15g}$$

$$u_k^j = u_k^l \quad \text{if} \quad x_k^{p(j)} = x_k^{p(l)}, \qquad \forall k \in \mathcal{K}, \forall j \& l \in \mathcal{S} \tag{15h}$$

where J_{eco}^j in (15a) is the objective function of the j^{th} scenario and ω_j is the corresponding tuning weight that reflects the relative likelihood of occurring j^{th} scenario. The steady condition of the system is implemented as a constraint in (15b). It ensures that the states at every time $k \in \mathcal{K}$ from scenario j are at a steady condition which is a function of their corresponding control u_k^j and uncertainty realization d_k^j. The constraints on the separator capacity, pump envelope, and pressures are imposed in (15c), (15d), (15e), and (15f), respectively. And the constraints on the pump frequency are enforced in (15g). Moreover, the non-anticipativity constraint is introduced in (15h), which reflects the fact that at each time step k, controls u_k^j and x_k^l from scenarios j and l with the same parental node $x_k^{p(j)} = x_k^{p(l)}$ have to be equal. In other words, all the controls that are branched from the same parental node are equal. It should be noted that, as shown in Figure 3, branching has been done only for the first sampling time. Therefore, $u_1^1 = u_1^2 = ... = u_1^{64} = u_1^{65}$ is the only set of non-anticipativity constraints in the problem, and according to the receding horizon strategy, this first control action is the one that will be applied to the real system. Hence, the non-anticipativity constraint guarantees that this value is unique.

4. Case Study

4.1. Reservoir Model

The 'Egg Model' is a synthetic reservoir model consisting of an ensemble of 101 relatively small three-dimensional realizations of a channelized oil reservoir produced under water flooding conditions with eight water injectors and four oil producers. The 'standard version' of the model introduced in [31] is used as the case study in this paper. The reservoir is demonstrated in Figure 4. The majority of the characteristics of the reservoir, such as rock properties, geometry, etc., remained unchanged. Nevertheless, there are a few minor modifications to meet our requirements. These modifications include:

- The model originally consisted of four production wells and eight injection wells; however, as demonstrated in Figure 4 only three producers are considered in this study.

- The compressibility of oil is set to 1e-3 in order to avoid an unrealistic response.
- The limits on all producer wells are removed as the controller is responsible for satisfying these constraints.
- The injection rate is scaled up to 112.5 [m^3/d] to be consistent with the top side model and requirements.
- The well control for the producers is changed from bottom hole pressure to total rate, which is provided by the optimizer.

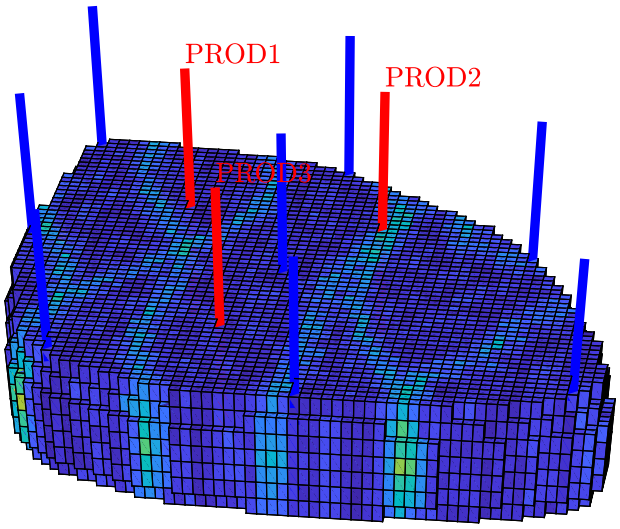

Figure 4: The modified reservoir model with three producers and eight injectors.

4.2. Simulation Setup

The standard deterministic DPO presented in Section 3.1 and the robust scenario-based DPO proposed in Section 3.2 and a third 'No Control' scenario are simulated to investigate the different aspects of the methods. The so-called 'No Control' scenario, as its name suggests, does not involve any production optimization and assumes the separator capacity is shared equally between three producers. More specifically, each producer produces one-third of the separator capacity. All scenarios are tested against the coupled model in a setup demonstrated in the block diagram of Figure 2.

All the parameters of the wells are presented in Table 2 and Table 3. The price of oil and the costs associated with the electricity and water treatment, which are used in equations (12) and (14), are presented in Table 4. All the sixty-five weights ω_j for sixty-five scenarios in the robust method (15a) are considered to be equally one as all the scenarios are equally likely to occur. The other boundaries of the constraints in the optimization problems defined in (13) and (15) are the same. The separator capacity is considered to be Q_{sep} = 900 [m^3/d]. The bottom hole pressures are considered to be limited between $p_{bh}^{\min}$ = 200 [bar] to $p_{bh}^{\max}$ = 400 [bar]. The lower and upper limits

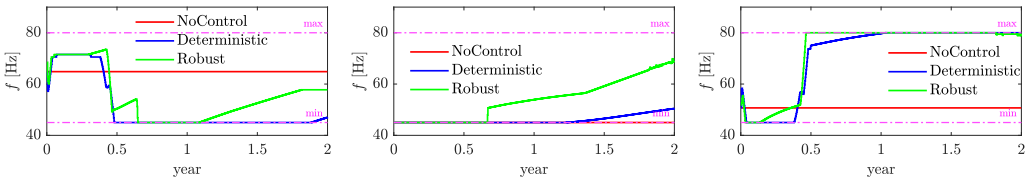

(a) Well 1 (b) Well 2 (c) Well 3

Figure 5: Frequency of ESPs for the production wells.

on the Wellhead pressures are $p_{wh}^{\min}$ = 150 [bar] and $p_{wh}^{\max}$ = 300 [bar], respectively. The production from each well is limited between $Q_{\min}$ = 150 [m^3/d] to $Q_{\max}$ = 500 [m^3/d]. The pump frequencies are maintained between $f_{\min}$ = 45 [Hz] and $f_{\max}$ = 80 [Hz], and the pump envelope at each frequency is computed by the affinity law.

A prediction horizon of three days with a sampling time of one day is used for both optimization problems. The optimization problems are implemented in CasADi v.3.5.5 in MATLAB R2022b. The IPOPT v.3.14.1 solver has been used to solve the problem on a 1.8 GHz laptop with 16 GB memory. The MATLAB Reservoir Simulation Toolbox (MRST) [32] has been used for reservoir simulation.

Table 4: Price of oil, electricity, and water treatment.

Price	Value	Unit
c_o	20.03	[$/bbl]
c_e	0.146	[$/kWh]
c_w	3.02	[$/bbl]

5. Results and Discussion

Two simulation cases are conducted to examine various aspects of the method. The first simulation case presents a comparison among three scenarios: deterministic DPO, robust DPO, and the 'No Control' scenario, which serves as the baseline. The frequency of ESPs for each of these three scenarios is plotted in Figure 5. The other decision variable, which is the production rates, is also Figure 6. It can be seen that all upper and lower bounds are successfully respected, as there is no uncertainty associated with the control inputs. For the same reason, the ESPs for both methods operate within the operating envelope as demonstrated in Figure 7.

However, the other constraint on the outputs, such as the bottom hole and wellhead pressures, may be violated due to the presence of uncertainty. Bottom hole pressures of three scenarios are presented in Figure 8, and the wellhead pressures are presented in Figure 9. The simulation results clearly show that the robust DPO effectively handles the uncertainty, whereas the deterministic DPO leads to constraint violations for a great amount of time.

The subplot (a) in Figure (10) depicts the cumulative profit for each of the three scenarios. In comparison to the baseline scenario, the deterministic DPO shows a total

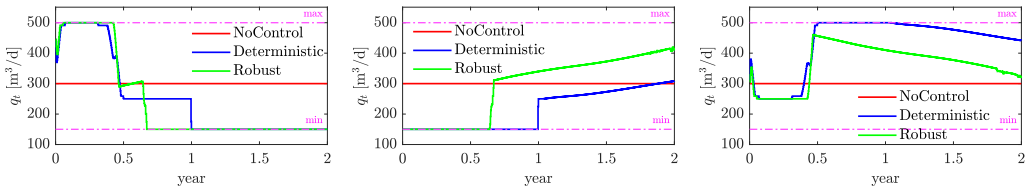

(a) Well 1 (b) Well 2 (c) Well 3

Figure 6: Total fluid flow rates through ESPs in Production wells.

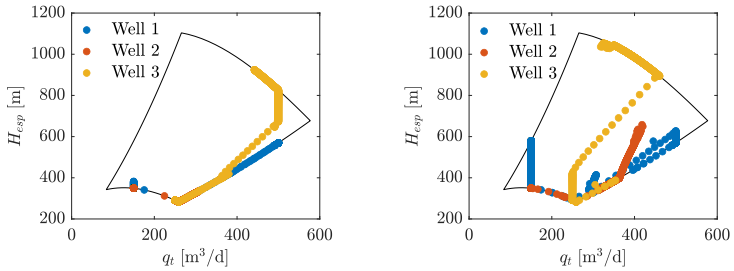

(a) Deterministic DPO (b) Multistage DPO

Figure 7: Operating window of ESPs for different scenarios.

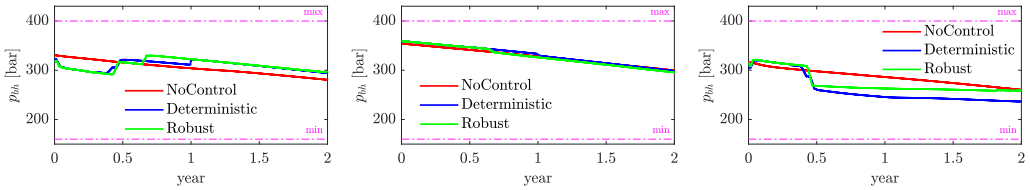

(a) Well 1 (b) Well 2 (c) Well 3

Figure 8: Bottom hole pressure of the production wells.

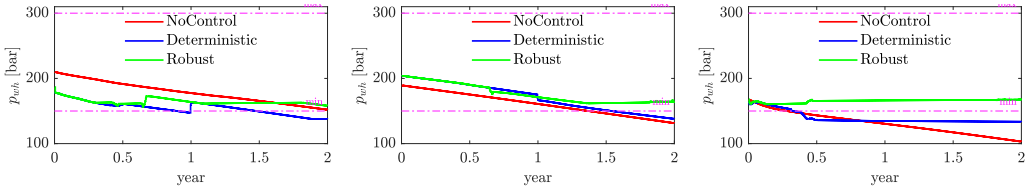

(a) Well 1 (b) Well 2 (c) Well 3

Figure 9: Wellhead pressure of the production wells.

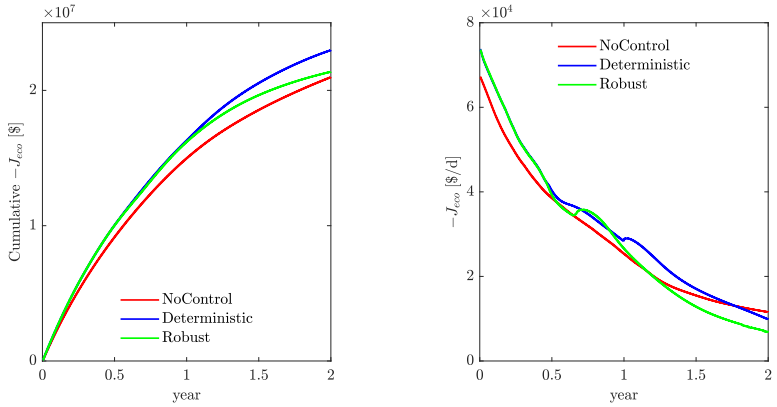

(a) Cumulative profit

(b) Instantaneous profit

Figure 10: Net profit ($-J_{eco}$) from production in three scenarios.

increase of 9.5% in net profit, whereas the robust DPO increases the net profit only by 1.9%. On the other hand, the instantaneous profit from subplot (10b) indicates that both the robust and deterministic DPOs exhibit similar behavior during the initial phases of production. However, as production continues, their divergence becomes more noticeable. Notably, it can be seen from Figure 9 that this differentiation between the two controllers aligns with the constraint violation. In other words, ensuring robust constraint fulfillment comes at a cost, and the price that needs to be paid is to sacrifice potential profit in order to ensure safe and reliable operations.

A second comparison is performed to demonstrate the capability of robust DPO for handling uncertainty. To this end, both methods are tested against the uncertain plant in 20 scenarios with 20 extreme realizations of uncertainty. These uncertainty realizations, as presented in Table 5, are random combinations of the uncertainty bounds. The results of these forty simulations are presented throughout Figure 11 to Figure 15. As depicted in Figure 11 and Figure 12, the frequency and pump flow for both methods remain within the constrained bounds since no uncertainty is associated with the control inputs. Consequently, the pump envelope constraint is successfully fulfilled by both methods, as illustrated in Figure 13. However, the constraint on pressures may be violated. Figure 14 and Figure 15 depict the bottom hole and wellhead pressure, respectively. It can be observed that the constraint on wellhead pressure is violated by deterministic DPO, whereas the robust DPO effectively fulfills the constraint all the time.

6. Conclusion

This paper utilized the scenario-based optimization framework to address the robust fulfillment of the constraint in Daily Production Optimization for an ESP lifted oil field under parametric uncertainty. Additionally, it presented a simple coupled well–reservoir model to analyze the performance of the method in a more realistic setting.

In order to achieve this objective, the steady-state model of the ESP wells was coupled with the reservoir model in a simple and efficient way. As a result, although the optimization algorithms themselves are based on top-side well models, their performance was

Table 5: Twenty random extreme scenarios considered for simulation.

Scenario	δPI^1	δPI^2	δPI^3	δWC^1	δWC^2	δWC^3
1	-10%	-10%	-10%	-20%	20%	-20%
2	10%	10%	-10%	-20%	-20%	-20%
3	10%	-10%	10%	-20%	-20%	-20%
4	10%	-10%	-10%	20%	-20%	-20%
5	-10%	10%	-10%	-20%	20%	-20%
6	-10%	-10%	-10%	20%	-20%	20%
7	10%	10%	10%	-20%	-20%	-20%
8	10%	10%	-10%	20%	-20%	-20%
9	10%	10%	-10%	-20%	20%	-20%
10	10%	-10%	10%	20%	-20%	-20%
11	10%	-10%	10%	-20%	-20%	20%
12	10%	-10%	-10%	20%	-20%	20%
13	-10%	10%	10%	-20%	20%	-20%
14	-10%	10%	-10%	20%	-20%	20%
15	-10%	-10%	10%	20%	-20%	20%
16	10%	10%	10%	20%	-20%	-20%
17	10%	10%	10%	-20%	20%	-20%
18	10%	10%	10%	-20%	-20%	20%
19	10%	10%	-10%	20%	-20%	20%
20	-10%	10%	10%	-20%	20%	20%

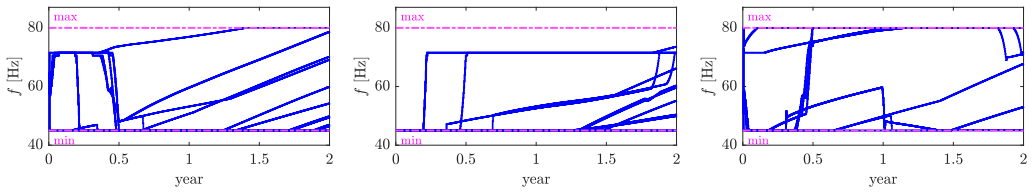

(a) Deterministic - Well 1 (b) Deterministic - Well 2 (c) Deterministic - Well 3

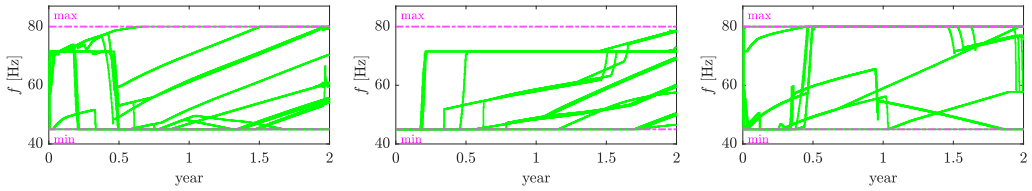

(d) Robust - Well 1 (e) Robust - Well 2 (f) Robust - Well 3

Figure 11: Frequency of ESPs for the production wells.

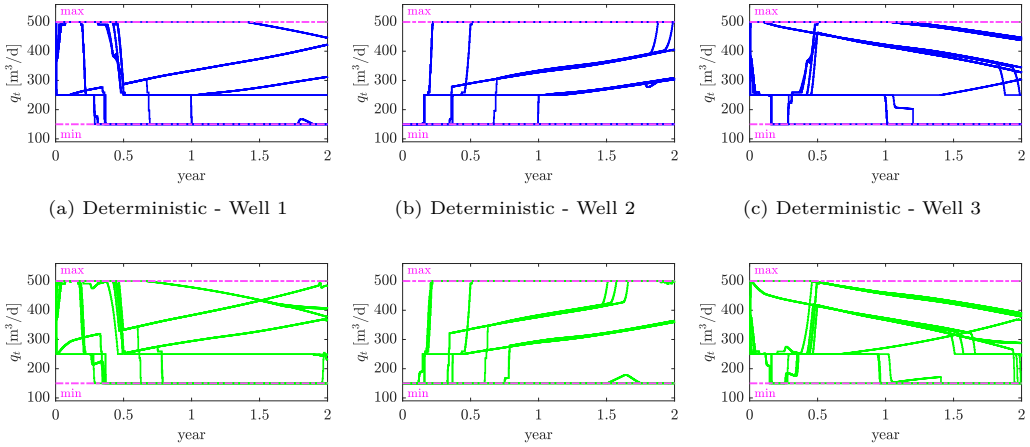

(a) Deterministic - Well 1 (b) Deterministic - Well 2 (c) Deterministic - Well 3

(d) Robust - Well 1 (e) Robust - Well 2 (f) Robust - Well 3

Figure 12: Total fluid flow rates through ESPs in Production wells.

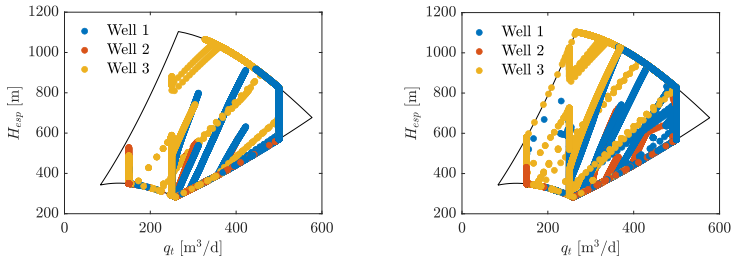

(a) Deterministic DPO (b) Robust DPO

Figure 13: Operating window of ESPs for different scenarios.

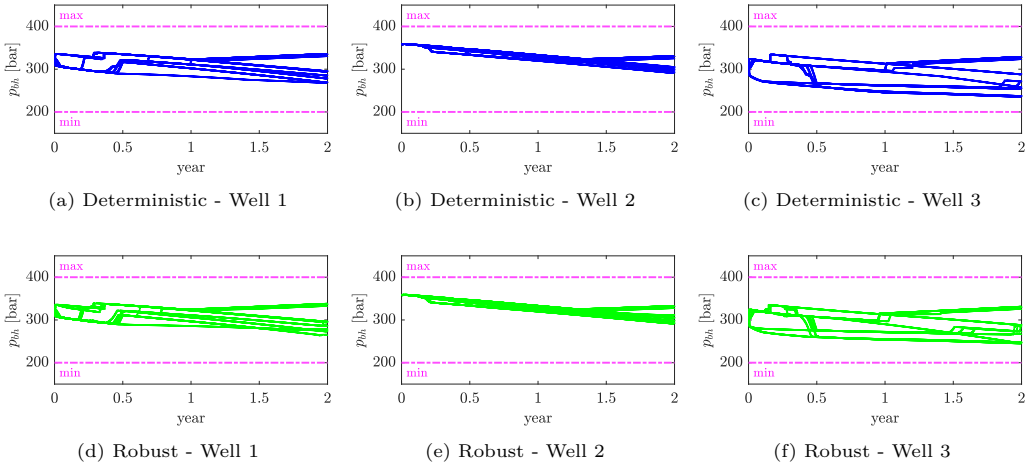

(a) Deterministic - Well 1 (b) Deterministic - Well 2 (c) Deterministic - Well 3

(d) Robust - Well 1 (e) Robust - Well 2 (f) Robust - Well 3

Figure 14: Bottom hole pressure of the production wells.

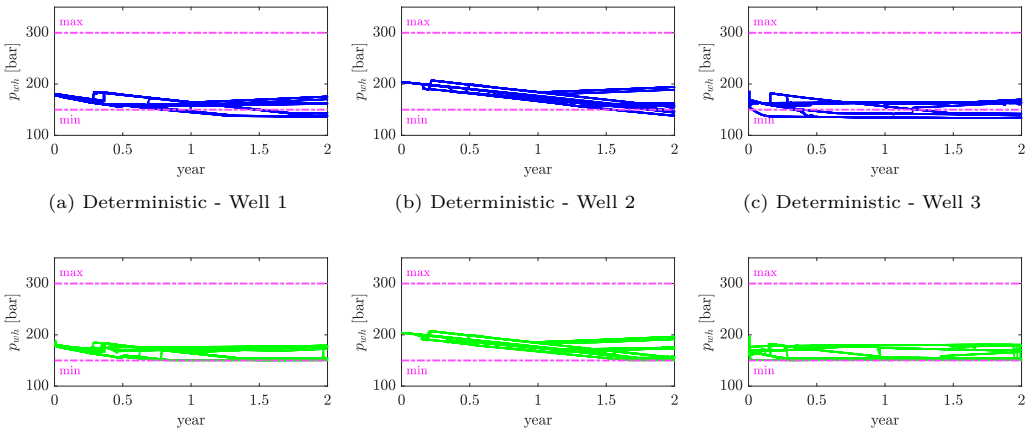

(a) Deterministic - Well 1 (b) Deterministic - Well 2 (c) Deterministic - Well 3

(d) Robust - Well 1 (e) Robust - Well 2 (f) Robust - Well 3

Figure 15: Wellhead pressure of the production wells.

evaluated against a more sophisticated model in which the uncertain parameters change interactively in accordance with the dynamic of the reservoir and its history rather than randomly.

The triumph of the proposed method and the importance of considering uncertainty were highlighted through comprehensive comparisons between deterministic and robust DPO applied to the coupled model in the presence of uncertainty. It has been shown that, contrary to the deterministic method, the scenario-based optimization for DPO yields a safe solution, and robust satisfaction of the operational constraints is guaranteed. More specifically, the constraints on pump frequency and flow were fulfilled by both methods, as no uncertainty was associated with the decision variables. However, the simulation results demonstrated that the deterministic DPO is not sufficient for satisfying the constraints on the outputs, and the constraint bounds on some outputs, such as wellhead pressure, were violated. On the other hand, the scenario-based DPO demonstrated a huge potential to be used in a real oil field by effectively respecting all the constraints on both input and output variables. Nevertheless, this safety is achieved at the cost of sacrificing the net profit to some extent.

Despite the contributions of this work, there are potential opportunities for further improvement yet to be explored. The first future direction that should be pursued is to extend the method using Mixed Integer Optimization, which makes it possible to shut down the wells, if it is necessary, as it is reasonably likely that it may be beneficial to shut down some wells during some periods. Another future direction that is worth exploring is to extend the top-side model and consider a more complex network with more oil wells and transportation lines, and gathering manifolds. By pursuing these future directions, the research can further contribute to the field and offer even more valuable insights and solutions for optimizing oil field operations under uncertainty.

Declaration of Competing Interest

The authors declare that they have no known competing financial interests or personal relationships that could have appeared to influence the work reported in this paper.

Acknowledgments

We gratefully acknowledge the economic support from The Research Council of Norway and Equinor ASA through Research Council project "308817 - Digital wells for optimal production and drainage" (DigiWell).

References

[1] D. Krishnamoorthy, K. Fjalestad, S. Skogestad, Optimal operation of oil and gas production using simple feedback control structures, Control Engineering Practice 91 (2019) 104107.

[2] B. Stenhouse, M. Woodman, P. Griffiths, Model based operational support-adding assurance to operational decision making, in: SPE Intelligent Energy Conference and Exhibition, OnePetro, 2010, pp. –.

[3] A. F. Teixeira, M. de Campos, F. P. Barreto, A. S. Stender, F. F. Arraes, V. R. Rosa, Model based production optimization applied to offshore fields, in: OTC Brasil, OnePetro, 2013, pp. –.

[4] B. Foss, B. R. Knudsen, B. Grimstad, Petroleum production optimization–a static or dynamic problem?, Computers & Chemical Engineering 114 (2018) 245–253.

[5] N. Janatian, R. Sharma, A reactive approach for real-time optimization of oil production under uncertainty, in: 2023 American Control Conference (ACC), IEEE, 2023, pp. 2658–2663.

[6] N. Janatian, K. Jayamanne, R. Sharma, Model based control and analysis of gas lifted oil field for optimal operation, Scandinavian Simulation Society (2022) 241–246.

[7] A. Pavlov, D. Krishnamoorthy, K. Fjalestad, E. Aske, M. Fredriksen, Modelling and model predictive control of oil wells with electric submersible pumps, in: 2014 IEEE Conference on Control Applications (CCA), IEEE, 2014, pp. 586–592.

[8] B. J. T. Binder, D. K. M. Kufoalor, A. Pavlov, T. A. Johansen, Embedded model predictive control for an electric submersible pump on a programmable logic controller, in: 2014 IEEE Conference on Control Applications (CCA), IEEE, 2014, pp. 579–585.

[9] D. Krishnamoorthy, E. M. Bergheim, A. Pavlov, M. Fredriksen, K. Fjalestad, Modelling and robustness analysis of model predictive control for electrical submersible pump lifted heavy oil wells, IFAC-PapersOnLine 49 (7) (2016) 544–549.

[10] P. d. A. Delou, J. P. de Azevedo, D. Krishnamoorthy, M. B. de Souza Jr, A. R. Secchi, Model predictive control with adaptive strategy applied to an electric submersible pump in a subsea environment, IFAC-PapersOnLine 52 (1) (2019) 784–789.

[11] B. A. Santana, R. M. Fontes, L. Schnitman, M. A. Martins, An adaptive infinite horizon model predictive control strategy applied to an esp-lifted oil well system, IFAC-PapersOnLine 54 (3) (2021) 176–181.

[12] B. J. T. Binder, T. A. Johansen, L. Imsland, Improved predictions from measured disturbances in linear model predictive control, Journal of Process Control 75 (2019) 86–106.

[13] J. P. Jordanou, I. Osnes, S. B. Hernes, E. Camponogara, E. A. Antonelo, L. Imsland, Nonlinear model predictive control of electrical submersible pumps based on echo state networks, Advanced Engineering Informatics 52 (2022) 101553.

[14] B. Foss, B. Grimstad, V. Gunnerud, Production optimization–facilitated by divide and conquer strategies, IFAC-PapersOnLine 48 (6) (2015) 1–8.

[15] R. Sharma, B. Glemmestad, Modeling and simulation of an electric submersible pump lifted oil field, International Journal of Petroleum Science and Technology 8 (1) (2014) 39–68.

[16] R. Sharma, B. Glemmestad, Optimal control strategies with nonlinear optimization for an electric submersible pump lifted oil field, Modeling, Identification and Control 34 (2) (2013) 55–67.

[17] R. Sharma, B. Glemmestad, Mixed integer nonlinear optimization for esp lifted oil field and improved operation through production valve choking, International Journal of Modeling and Optimization 4 (6) (2014) 465.

[18] R. Sharma, B. Glemmestad, Nonlinear model predictive control for optimal operation of electric submersible pump lifted oil field, in: Proceedings of the IASTED International Conference on Modelling, Identification and Control, 2014, pp. 229–236.
[19] N. Janatian, R. Sharma, A robust model predictive control with constraint modification for gas lift allocation optimization, Journal of Process Control 128 (2023) 102996.
[20] M. Mohammadzaheri, R. Tafreshi, Z. Khan, M. Franchek, K. Grigoriadis, An intelligent approach to optimize multiphase subsea oil fields lifted by electrical submersible pumps, Journal of Computational Science 15 (2016) 50–59.
[21] J. A. P. Mejía, L. A. Silva, J. A. P. Flórez, Control strategy for oil production wells with electrical submersible pumping based on the nonlinear model-based predictive control technique, in: 2018 IEEE ANDESCON, IEEE, 2018, pp. 1–6.
[22] E. I. Epelle, D. I. Gerogiorgis, Mixed-integer nonlinear programming (minlp) for production optimisation of naturally flowing and artificial lift wells with routing constraints, Chemical Engineering Research and Design 152 (2019) 134–148.
[23] A. Hoffmann, M. Stanko, Short-term model-based production optimization of a surface production network with electric submersible pumps using piecewise-linear functions, Journal of Petroleum Science and Engineering 158 (2017) 570–584.
[24] E. R. Müller, E. Camponogara, L. O. Seman, E. O. Hülse, B. F. Vieira, L. K. Miyatake, A. F. Teixeira, Short-term steady-state production optimization of offshore oil platforms: Wells with dual completion (gas-lift and esp) and flow assurance, Top 30 (1) (2022) 152–180.
[25] N. Janatian, R. Sharma, Short-term production optimization for electric submersible pump lifted oil field with parametric uncertainty, [Submitted to IEEE ACCESS], (July 2023).
[26] S. Lucia, T. Finkler, S. Engell, Multi-stage nonlinear model predictive control applied to a semi-batch polymerization reactor under uncertainty, Journal of process control 23 (9) (2013) 1306–1319.
[27] N. Janatian, R. Sharma, Multi-stage scenario-based mpc for short term oil production optimization under the presence of uncertainty, Journal of Process Control 118 (2022) 95–105.
[28] D. Krishnamoorthy, B. Foss, S. Skogestad, Real-time optimization under uncertainty applied to a gas lifted well network, Processes 4 (4) (2016) 52.
[29] G. Takacs, Electrical submersible pumps manual: design, operations, and maintenance, Gulf professional publishing, 2017.
[30] T. Serghides, Estimate friction factor accurately, Chemical engineering (New York, NY) 91 (5) (1984) 63–64.
[31] J. D. Jansen, R. M. Fonseca, S. Kahrobaei, M. Siraj, G. Van Essen, P. Van den Hof, The egg model–a geological ensemble for reservoir simulation, Geoscience Data Journal 1 (2) (2014) 192–195.
[32] K. A. Lie, O. Møyner, Advanced modelling with the MATLAB reservoir simulation toolbox, Cambridge University Press, 2021.

Real-time Optimization and Control for Oil Production under Uncertainty
Nima Janatian

Doctoral dissertations at the University of South-Eastern Norway no. 179

ISBN: 978-82-7206-822-5 (print)
ISBN: 978-82-7206-823-2 (online)

usn.no